A Method for Interactive Recognition of Three-dimensional Adjacency Patterns in Point Sets, Based on Relative Neighbourhood Graphs

An Archaeological Application

A thesis submitted in
partial fulfilment of the requirements for the degree of
Doctor of Philosophy
by

Diego Jiménez Badillo

University College London

Department of Geomatic Engineering

2004

ProQuest LLC
789 East Eisenhower Parkway
P.O. Box 1346
Ann Arbor, MI 48106-1346

ABSTRACT

This thesis proposes an exploratory method of spatial analysis oriented to the recognition of adjacency patterns in point sets. The underpinning elements of such method are the relative neighbourhood concept, the retrieval of proximity graphs, the measurement of graph-theoretic relational properties, both at global and local levels; and the visualisation of spatial patterns in three dimensions. This is called *Relative Neighbourhood Method of Spatial Analysis*, or *RN-Method*, for short.

The method was specifically designed to analyse a special type of archaeological deposit, which we denominate as 'spatial symbolic contexts.'

Spatial symbolic contexts are artefact arrangements, ordered in such a way that the literal significance of each item acquires a parallel meaning thanks to its spatial associations with other elements of the set.

These appear frequently as a subject of study in archaeology. Unfortunately, before the start of this project, there were not appropriate methods to investigate them. We undertook the challenge of improving such a state of affairs by focusing on the requirements of an interesting study case, namely the Mexica offerings.

The Mexica offerings are archaeological deposits which contain a great diversity of ritual objects. The specific arrangement of the items responded to Aztec religious beliefs, whose decipherement is of great relevance for the understanding of such culture.

The RN-Method provides formal means to explore the topology of such arrangements as a previous step to interpreting the overall meaning of the caches. These include a graph representation of the offerings in which artefacts correspond to vertices and edges model their spatial adjacency. The specific types of graph used in this thesis are the so-called Relative Neighbourhood Graph, Gabriel Graph, Beta-

skeleton, and Limited Neighbourhood Graph. All of them are based on an interesting morphological notion known as relative neighbourhood. This retrieves spatial relations based on the relative position of points, as opposed to their absolute location. In this sense, the concept is different from traditional 'metric' notions such as nearest neighbour.

Two major steps of the RN-Method are the visualisation and quantification of global structure, from which it is possible to identify overall similarities or differences in the offerings layout, as well as to make comparisons accross multiple deposits.

The method also adopts some measures to assess the relative importance of vertices. Applying such measures to the Mexica offerings, we are able to identify objects located in positions of lower and higher control, as well as objects in integrated and segregated places.

In addition, the method includes the application of a visual clustering technique, oriented to the identification of regular combinations of artefacts that may have constituted a 'symbolic theme'.

Finally, we illustrate with three offerings the type of interpretation procedure that can be applied to decipher the meaning of these spatial symbolic contexts.

ACKNOWLEDGEMENTS

The research presented in this thesis was supported by several institutions and individuals which I would like to thank:

Especially useful was the scholarship No. 111159/111354, granted by the Mexican Government through CONACYT (Consejo Nacional para la Cultura y las Artes). Thanks to this generous founding I was able to pay fees and living expenses while studying in University College London.

Equally important was the support from my current employer, the Instituto Nacional de Antropología e Historia, for allowing me to move to a different country while keeping my tenure position as an archaeological researcher at Museo del Templo Mayor.

In the Department of Geomatic Engineering of University College London I was fortunate to interact with many intelligent people, who contributed to my work in many different ways. To mention all of them would require a much larger list. Here, I want to recognise in particular all I have learned from Dave Chapman, who supervised this research with great knowledge, but also with patience and most of all with invaluable encouragement and friendship. My second supervisor Stephen Shennan, from the Institute of Archaeology at UCL, also gave me invaluable feedback.

Encouragement also came from many colleagues and friends. Especial thanks to former director of Museo del Templo Mayor Eduardo Matos, as well as to the current director Juan A. Román Berrelleza.

My friend Jorge Suárez deserves especial acknowledgment for reading the final draft and correcting the grammatical errors, as well as for his constant support.

Finally, I am very grateful to my mother and sisters, as well as to all my friends, but most especially to Michael Barone.

To all, many thanks.

CONTENTS

LIST OF ILLUSTRATIONS

FIGURES

TABLES

1 INTRODUCTION

1.1. THE SUBJECT OF THIS THESIS

This thesis proposes an exploratory method of spatial analysis designed for the recognition of adjacency patterns in point sets. The underpinning elements of such a method are the relative neighbourhood concept, the retrieval of proximity graphs, the measurement of graph-theoretic relational properties among the points, and the visualisation of spatial patterns in three dimensions. This is called the *Relative Neighbourhood Method of Spatial Analysis*, or *RN-Method*, for short.

1.2. THE FIELD OF APPLICATION

The method was developed to discover meaningful regularities in a special type of archaeological deposit, which we identify as 'spatially symbolic contexts.' These are groups of objects whose arrangement and meaning are determined by symbolic ideas expressed through the spatial ordering of different categories of artefacts. In such deposits, the specific location of each object -as well as its spatial association with the rest of the assemblage- creates characteristic

observable 'patterns'. In studying contexts like these, analysts seek to formulate hypotheses about the *logic principles* projected onto each particular object *arrangement*.

1.3. THE CASE STUDY

Spatially symbolic contexts appear frequently in archaeological excavations. Abundant examples have been recorded in sites of ancient Mesoamerica, including Mexico City, the Mayan area, the valley of Oaxaca, etc. In most cases they appear in the form of ritual caches. This thesis demonstrates the usefulness of the RN-Method by focusing on one case of spatial symbolism from that particular region: the so-called Mexica offerings.

Between 1978 and 1982, a team of archaeologists recovered 108 caches composed of a great diversity of items, including artefacts, flora, fauna, and human remains, etc. Such discoveries were made in Mexico City within a zone previously occupied by the *Sacred Precinct of Tenochtitlan*, the most important religious centre for the Mexica, or Aztecs, as they are also known. The caches came either from the main temple or its surroundings and contained nearly 8000 objects. The quantity has grown considerably in recent years with the excavation of further offerings.

Shortly after the first discoveries it became clear that the objects had been carefully placed forming perceivable arrangements. Thus, the interpretation process depended on finding a method of spatial analysis appropriate for these contexts. Some suggested applying standard tests for spatial randomness, like those based on nearest neighbour statistics. It became obvious, however, that the caches could not be treated simply as realisations of a *stochastic process*. The reason for this being that a

symbolic element seemed to be playing a very important role in the location of the artefacts. In fact, a major feature of the caches was the spatial combination of specific categories of objects. Each particular combination suggested the intention to represent a different abstract concept.

This element raised questions among archaeologists about what was the original purpose of the caches. Soon it became clear that they were *ritual offerings*. As many other religious constructs of the Mexica, the offerings appeared to be the outcomes of ritual rules which prescribed how to arrange *specific categories* of objects over space. Therefore, the interpretation process began to be seen as a *decoding* challenge in which spatial relationships, mainly of morphological nature, had to be considered in accordance with the particular symbolism of each class of artefact.

At the time, the analysis of 'spatially symbolic contexts' was one of the less developed areas of archaeology. This situation has endured for nearly twenty years and even today there are very few proposals that specifically target the visualisation, description and interpretation of this type of remains.

Such a lack of methods and tools has forced archaeologists to divert their attention towards other non-spatial types of analysis. One of these is the classification of offerings in terms of their contents in order to identify cache 'families' (i.e. groups) with a maximum degree of similarity. The groups are formed exclusively by coincidences in the presence/absence of objects (López Luján, 1994).

Other approaches focus on analysing a single class of artefact without considering other types (López Luján, 1989; Olmedo y González, 1986; Urueta Flores, 1990, Velázquez Castro, 1999, 2000). Finally, a third approach consists in selecting an individual offering to investigate all its contents

with procedures developed on a case by case basis (Ahuja 1991; Del Olmo Frese, 1999; Schulze 1997). Unfortunately, none of these approaches tries to investigate spatial patterns in a formal way.

1.4. THE RESEARCH QUESTION AND THE PROPOSAL

One goal of this research has been to improve such a state of affairs by providing an answer to the following question:

What kind of spatial analytical approach is needed to explore spatial arrangements of artefacts resulting from spatial symbolism?

Our basic proposal consists in solving the problem by representing each context as a point set, and then exploring topological relationships; in other words, analysing three-dimensional patterns of adjacency among the points, as opposed to focusing on metric or statistical characteristics.

This solution combines concepts and technologies developed in a variety of disciplines. Amongst the most important are an ingenious notion of spatial adjacency known as *relative neighbourhood*, as well as connectivity concepts derived from graph theory, pattern recognition algorithms, and computer visualisation techniques.

We are convinced that the combination of such elements will allow the recognition of meaningful spatial patterns from the Mexica offerings and hopefully from other spatially symbolic contexts as well. For example, given a distribution of artefacts in the caches we may be able to discover whether certain categories of objects are recurrently located in the proximity of some other categories. And if they form some sort of regular arrangement, we may have reasons to consider such pattern as a 'symbolic theme.'

Finally, we may be able to formulate hypotheses about its particular meaning based on other cultural sources, such as iconography and historic texts.

Besides the RN-Method, another product of this research is a computer program called *RNG Explorer*. This provides interactive 3D-visualisation and analysis tools to implement each step of the procedures proposed in this thesis.

1.5. THE INTENDED AUDIENCE

The above explanation helps to understand the long title of the thesis, as well as its intended audience:

The first sentence, "A Method for Interactive Recognition of Three-dimensional Adjacency Patterns in Point Sets, Based on Relative Neighbourhood Graphs," purposely uses general mathematical terms to describe the goal, attribute, analytic units and concepts investigated. In doing so, it appeals to the broad range of spatial analysis experts that may benefit from this research.

The second part, "An Archaeological Application," tries to capture the attention of specialists in the field where the results have been successful.

Therefore, this thesis is about spatial analysis in the sense that involves the acquisition of a method for gaining knowledge about a phenomenon operating in space. However, it is also about archaeology, because it offers a solution to a specific problem and adapts the method to the nature of distinctive archaeological contexts.

1.6. THE ORGANISATION OF THE THESIS

The organisation of the thesis reflects such a dichotomy. Long sections are entirely devoted either to spatial analysis or geometric related concepts, while others contain archaeological data almost exclusively.

Shifting between these two types of information is the most appropriate strategy to communicate the contents of the thesis. An emphasis on spatial analysis appears useful in Chapter 2, where we need to describe standard approaches for studying point-recorded phenomena. The contents include statistical analysis of point distributions (section 2.1), tessellation-based approaches (section 2.2), and network analysis (section 2.3).

The goal of such presentation is to demonstrate that, despite the wide range of available perspectives, the investigation of some intriguing phenomena, such as *spatial symbolism,* demands the development of new ad-hoc procedures.

Following the identification of *spatial symbolism* as a problem that requires new analytical methods, we commit ourselves to providing one solution and chose the Mexica example and its concrete products, the ritual offerings, as a case study to learn the complexities of the problem (section 2.4).

At this point, archaeological information becomes extremely relevant to provide the necessary background about the Mexica culture. We divide such information into two parts: Chapter 3 describes the general principles of the Mexica spatial symbolism, while chapter 4 deals specifically with the ritual offerings, their role in Aztec society, their physical appearance, and the state-of-the-art in this subject of study. A conclusion of those chapters is that morphology and point-topology represent the most appropriate sources of procedures to analyse the Mexica offerings.

This leads to the 'geometry contents' of chapter 5. Here, we describe mathematical structures to reveal the topology of point sets. Such presentation focuses on proximity graphs. These include the Voronoi diagram, the Delaunay Triangulation, and other interesting constructs, such as the Relative Neighbourhood Graph, Gabriel Graph, Beta-skeleton, and Limited Neighbourhood Graph.

Both geometric and archaeological information come together in chapter 6, the most important of the thesis, which uses geometric graphs as the basis for the Relative Neighbourhood Method of Spatial Analysis. The description of each procedure is supported with empirical data from three Mexica offerings.

The discussion of the thesis ends with some concluding remarks presented in chapter 7.

Additionally, the thesis contains two useful appendices dealing with computational issues:

Appendix A explains a simple algorithm to compute adjacency graphs, and shows how to extract Relative Neighbourhood Graphs, Gabriel Graphs, Beta-skeletons, and Limited Neighbourhood Graphs.

Appendix B offers a presentation of RNG Explorer, a software package designed to implement each step of the RN-Method.

There is also a companion CD at the back of the thesis. This includes a copy of RNG Explorer as well as source data.

2 SPATIAL ANALYSIS OF POINT-RECORDED PHENOMENA

We begin this thesis with a description of the most common approaches to spatial analysis. The focus is on perspectives that involve point records as part of their source data. Throughout the text we refer to such records as a *point set.* In Euclidean geometry, this is defined as *a collection of dimensionless mathematical objects, each one specified in some region by two or more spatial coordinates.* We assume that each record represents one of the empirical entities under investigation.

The approaches are divided into:

2.1. Statistical analysis of point distributions
2.2. Analysis based on tessellation
2.3. Network analysis

In the first section a point set is seen as a standalone structure, which means that the analysis only considers point locations. In contrast, the remaining sections deal with point sets as elements of more complex models. Section 2.2 considers point units in relation to surrounding areas, while section 2.3 investigates them in the context of connecting lines.

Such presentation is useful to show that, despite the wide range of existing approaches and applications, there are still some problems that lack appropriate analysis procedures and tools.

One of these is the topic of section 2.4, the last one of this chapter. Here, we identify the phenomenon of spatial symbolism as a subject where available procedures are not applicable. We also argue for the need of developing ad-hoc approaches to investigate such phenomenon, and propose to explore one particular example –the Mexica offerings- by focusing on the topology of point sets, instead of investigating metric or statistical properties.

2.1. STATISTICAL ANALYSIS OF POINT DISTRIBUTIONS

Considerable numbers of events and objects take place at certain points over a study region as a result of natural or social phenomena. In such cases, the driving forces of the phenomenon determine the specific locations of its constitutive events. Therefore, the spatial structure given by the separation or aggregation of those events can be used as a source for inferring both the intensity and dynamics of the generative process.

Given the causal relationship between process and spatial structure, it makes sense to investigate how likely it is that empirical events –marked with point-records- have been caused by a systematic process, as opposed to being generated by 'accident'. Such is precisely the purpose of the spatial analysis approach described in this section. This consists of observing the statistical behaviour of some spatial properties in order to extract a quantitative index, which expresses the degree of randomness or regularity of empirical point distributions (Bailey and Gatrell 1995: Ch. 1-2, 75-139; Boots and Getis 1988; Cressie 1991: Ch. 8; Dacey 1964a,

1964b; Diggle 1983: Ch. 1-5, 2003; Getis and Boots 1978; Ripley 1981, Unwin 1981; Upton and Fingleton 1985).

The statistical analysis of point distributions can be practised at two levels (Unwin 1996):

- The simplest one consists of 'exploring' a point set in order to obtain some quantitative description of its distribution pattern. At this level, analysts make very few *a priori* assumptions about the generative process because their final objectives are precisely (a) to identify it, and (b) to formulate hypothesis about any possible forces influencing the point distribution (Bailey and Gatrell 1995: 23-24; Harvey 1966; Tukey 1977). Archaeological examples of this approach can be found in Kintigh and Ammerman (1982), as well as in Carr (1991).

- A more complex level is formulating a general statistical model of the phenomenon under study. This seeks to *predict* all possible outcomes of the process, and in accordance with such a goal, analysts use all available knowledge about the phenomenon in order to design tests, verify certain hypothesis, and explain statistically why certain point patterns, but no others, must be considered realisations of that specific process.

Both levels of statistical analysis offer numerous applications. In archaeology, for example, scholars may be interested in determining whether the scattering of potsherds and other materials found on certain habitation floor has been caused by post-depositional accidents or by recognisable human activities.

In the latter case, it is expected to observe a systematic distribution of materials, instead of the random dispersion usually produced by post-

depositional accidents (Blankholm 1991; Carr 1985b; Hietala 1984; Hodder and Orton 1976; Whallon 1973, 1974).

In another example, a high number of cases of a disease may happen simultaneously within a short distance from each other and this may arise some of the following questions about the causes of those incidents: Does the disease exhibit an ordered pattern or, instead, do the events appear unrelated?; given the observed pattern, where are the new incidents of the disease more likely to appear?, and so on. (Hills and Alexander 1989; Marshall 1991).

The key principle of statistical spatial analysis is considering the events of interest as the outcome of a stochastic process. By definition, such processes are governed by probability laws. In a spatial context, this implies that the chances for an event occurring "... at each location or area represents a probabilistic (random) selection from some underlying generating distribution" (Unwin 1996: 543).

The most extreme case of spatial stochastic process is *Complete Spatial Randomness* (CSR) (Diggle 1983, 2000). In simple terms, CSR means that any event (i.e. point) has an equal probability of occurring at any location of space. Additionally, it implies that events do not interact with one another, so that the specific location of any event is independent of the location of any other (Bailey and Gatrell 1995: 96; King 1969: 42).

CSR provides a theoretical distribution, or 'benchmark', against which empirical events can be compared in order to determine their degree of randomness.

The first step in such direction consists in calculating a statistical index (e.g. variance/mean ratio) based on some spatial property of the point set under study.

Three of the most frequently examined properties are dispersion, density and inter-point distance. The latter is the only one which can be properly called "point pattern" and it is defined as the "... spatial arrangement of objects given by their spacing in relation to each other" (Unwin 1996: 544; see also Hudson and Fowler 1966). In contrast, dispersion refers to the frequency in the number of points falling in subdivisions (usually squares) of the study region, while density relates to the average number of points per area-unit (Unwin 1996).

In a second step, the observed distance, density or dispersion index is compared with the value expected for a process ruled by complete spatial randomness. The Poisson function, representative of a CSR process, is normally used as theoretical model for such a purpose.

As a result of these steps analysts may conclude that the overall structure of a point distribution exhibits a systematic order; in other words, that events either appear regularly distributed or are found forming clusters. In other situations, the structure may reveal events scattered at random (Bailey and Gatrell 1995: 75). Figure 2.1 shows some typical point distributions: a) perfectly regular; b) regular; c) clustered; and d) random.

Particular interest is devoted to detecting any form of clustering or regularity, because it is assumed that if events are not randomly produced, then some "forces" are actually causing the spatial variation. At the end, knowing about such forces would allow relating the structure of the pattern with its generative process.

Statistically, it is important to distinguish two kinds of forces responsible for the appearance of non-random patterns. They are known in the standard literature as first and second order effects, or alternatively as global and local variations.

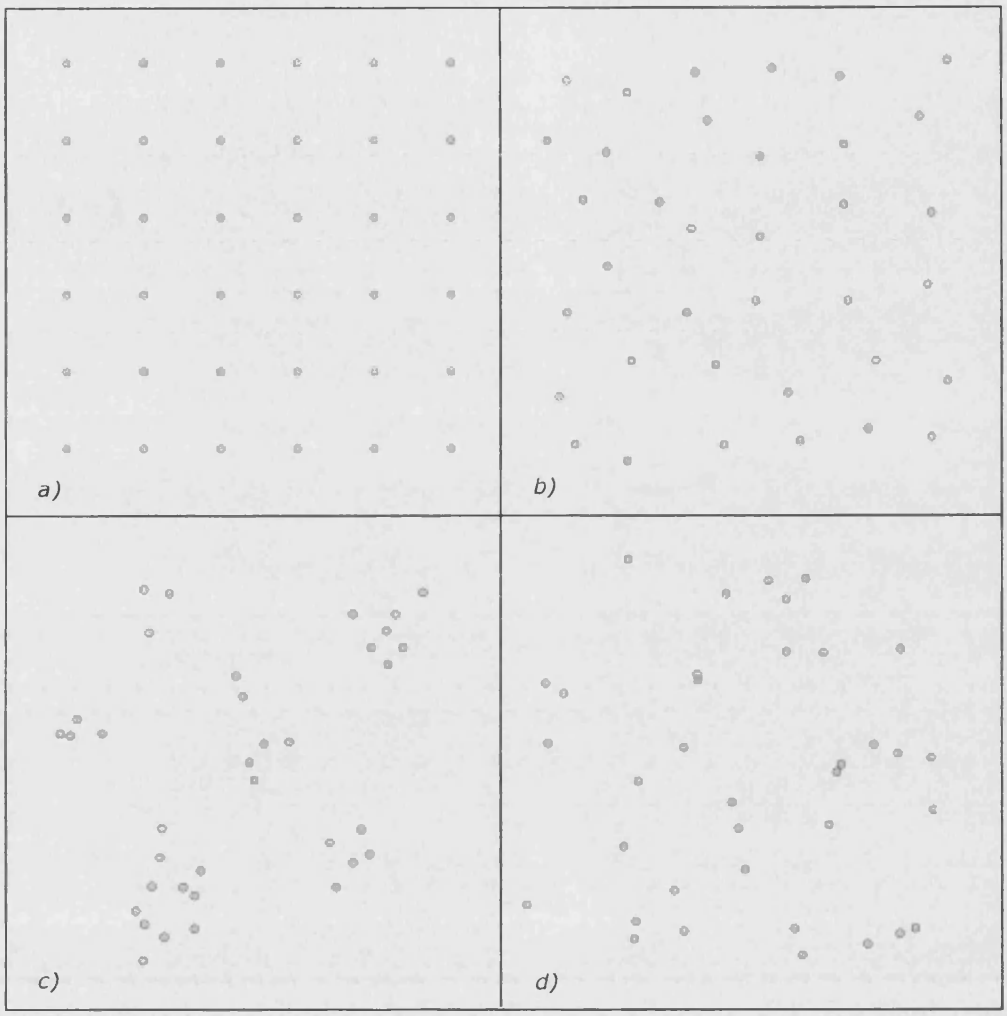

Figure 2.1. Typical distributions of point sets: a) perfectly regular; b) regular; c) clustered; and d) random

2.1.1. FIRST ORDER EFFECTS

First order effects (i.e. global variations) are differences in the concentration of events over the study region which result exclusively from variations in the intensity of the spatial process.

A simple way to detect these effects is calculating the *variance/mean index* of some characteristics like dispersion or inter-point distance. Such a value is then compared with the result obtained from a Poisson distribution with the same intensity (Bailey and Gatrell, 1995: 32).

The dispersion index is easily calculated with the quadrat method. This consists of dividing the entire region under study into zones of equal size and shape (usually squares). The second step is counting frequencies in the number of events observed in each quadrat. The level of randomness of the empirical pattern can then be tested assuming that if such counts follow a Poisson distribution, then we would expect the mean and variance of point frequencies to be equal (i.e. the index of dispersion equals one). In contrast, dispersed or regular patterns have a variance/mean index significantly less than one; and clustered patterns are characterised by index values greater than one. The significance of those numbers is then assessed using the chi-squared function (Bailey and Gatrell, 1995: 97; Boots and Getis 1988; Greig-Smith 1964:63; Thomas 1977).

Alternately, one may prefer to use a distance method. The simplest one is the nearest neighbour index or R-value (Clark and Evans 1954). First, this method calculates the distance from each point in the data set to its nearest neighbour. Secondly, it extracts the mean value of all such distances. Finally, it divides the observed mean value by the one expected from a Poisson process with the same intensity. This would give a ratio indicating the degree of clustering, regularity or randomness of the point set. The R-index for random points is one; clustered patterns have an R significantly less than one, approaching zero in many cases; and for regular distributions the index is greater than one, reaching 2.1491 in the extreme case of a perfectly regular arrangement like the one in figure 2.1a (Boots and Getis 1988; Hodder and Orton 1976: 40). A discussion about archaeological applications can be found in Blankholm 1991; Hodder and Orton (1976), and Whallon (1974).

The quadrat method has been used frequently in archaeology, mainly because it is a natural match for the way information is collected during

field work. However, the index of dispersion is severely affected by the size and shape of the quadrat used (see examples in Grieg-Smith 1952; Kershaw 1964; Hodder and Orton, 1976: 36; Pielou 1957; and Stiteler and Patil 1976).

On the other side, nearest neighbour methods present other specific problems. The main one is related to the size of the area chosen for investigation. Different patterns may emerge depending on how much surrounding area is included in the analysis (Getis 1964, Hodder and Orton 1976, Hsu and Tiedemann 1968; Unwin 1996).

2.1.2. SECOND ORDER EFFECTS

Second order effects are those caused by attraction or repulsion forces among events, that is, by inter-event interactions. The way to detect second order effects consists in estimating the covariance, or correlation structure of the points with respect to each other (Bailey and Gatrell, 1995: 77).

In order to simplify the analysis, most methods assume a *stationary* spatial process. In a stationary process both the mean and variance of the phenomenon remain constant over the whole region (i.e. homogeneous). If such an assumption holds, the second order effects can be discovered by focusing only on the distance and direction between the events, and in some cases only on the distance (in case of isotropic processes), rather than on their absolute locations (Bailey and Gatrell, 1995: 33).

Second order effects are also called second order intensity. Gatrell *et al.* (1996) describe some exploratory methods to identify second order effects. One of them calculates the cumulative probability distribution of event-event distances. This is known as G function, and it is defined as:

G(w) = number of (w_i <= d) / *n*;

> Where w_i is the *ith* nearest neighbour distance; d is a distance parameter used as a threshold to explore the pattern; and *n* equals the number of points in the data set.

A second alternative is to plot the probability function of point-event distances. That is, distances from randomly selected points within the area under study to their nearest events. The latter is known as F function:

F(x) = number of (x_i <= d) / *m*;

> Where x_i is the distance between the *ith* random point and its nearest neighbour; d is a distance parameter used as a threshold to explore the pattern; and *m* is the number of random points sampled.

An additional technique is the so-called Kernel estimation, which investigates the density of the points. A good description can be found in Silverman (1986) and Gatrell (1994).

The statistical methods described above are certainly the most frequently applied within the field of spatial analysis. However, they do not offer solutions to all problems involving point sets. Sometimes, the phenomenon under study raises questions regarding the territoriality of sites. In such cases analysts must widen the focus of their research, and instead of analysing exclusively 'locations' they must include observations of areas around points. We now turn to describing such approach to spatial analysis, which is based on tessellation procedures.

2.2. ANALYSIS BASED ON TESSELLATION

Tessellation is a partition of space into convex polygonal regions, which do not overlap nor leave any gaps. Mathematicians often reserve the term exclusively to divisions of the plane into symmetric shapes, such as

the one in figure 2.2 (Britton 1999, Cundy and Rollet 1989: 60-63; Gardner 1988: 162-176). However, within the fields of spatial analysis and computational geometry it is common to extend the definition so as to include partitions that allow asymmetric and even irregular cells, which in most cases present convex shapes (see fig. 2.3)

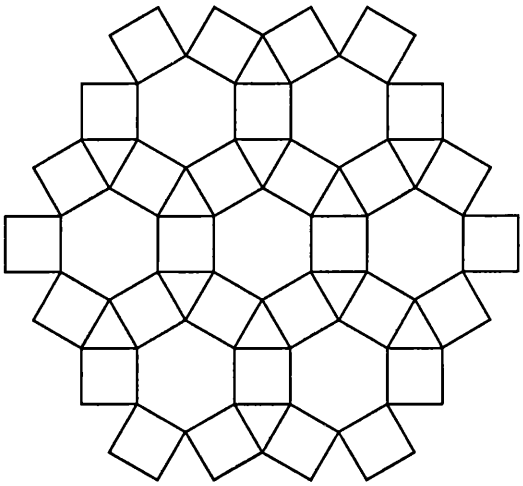

Figure 2.2. An example of symmetric tessellation

The definition of tessellation is also applicable to higher dimensional space. In the latter case the divisions become polyhedrons (3D) or n-polytopes (Okabe *et al.* 1992, 2000; O'Rourke 1994).

One of the most pervasive methods of tessellation produces the so-called Voronoi diagram. This structure, along with its main geometric properties, is described in chapter 5 (section 5.3). Yet, for the purposes of this section we provide in advance the following definition:

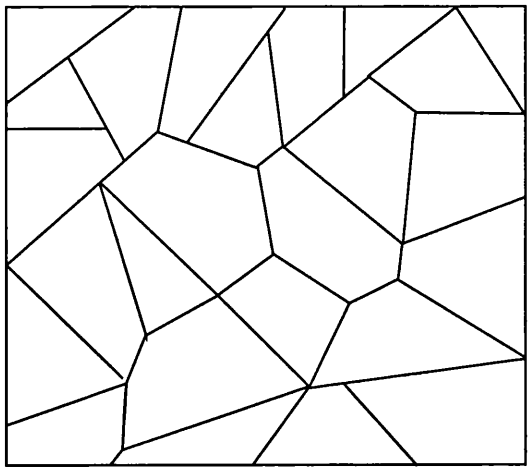

Figure 2.3. An example of asymmetric tessellation

Given a set of n *points, the Voronoi diagram is an exhaustive subdivision of space into* n *cells, each of which represents the region closer to one particular point than to any other.*

The cells resulting from a Voronoi tessellation are called Voronoi cells (or polyhedra in 3D space). They are also known as Thiessen polygons or Dirichlet regions (see fig. 2.4).

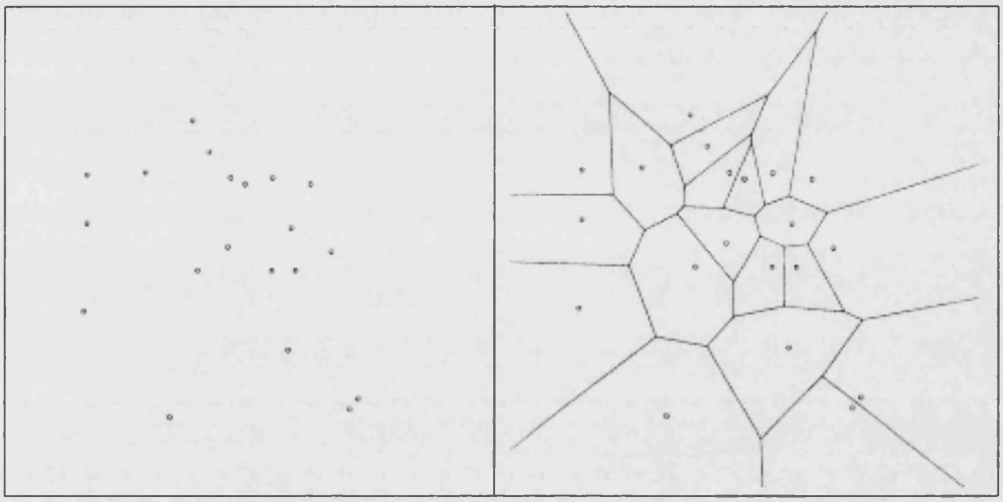

Figure 2.4. A set of points and the corresponding Voronoi diagram. (Source: O'Rourke 1994: Fig. 5.5).

Voronoi diagrams have been applied in statistical approaches to run tests for randomness in point sets (Aurenhammer 1991: 359-360). This gives rise to the so-called "polygonal statistical methods", which measure selected properties of Voronoi cells to reveal the underlying generating process of the point distribution (see Evans 1967; Okabe *et al.* 1992: 405-432). Generally speaking, they follow the same logic described in section 2.1, only this time the properties examined are, among others, the number of egdes intersecting at every Voronoi vertex, the length of Voronoi edges (Boots 1973; Vincent *et al.* 1976, 1977, 1983), as well as the area, perimeter, and internal angles of Voronoi cells (Boots 1974, 1986; Hutchings and Discombe 1986; Kendall 1981, 1990; Mardia 1989).

In this section we concentrate on a different application of Voronoi diagrams, namely the study of organisational structure of point sets, as part of territorial studies.

Voronoi diagrams offer an intuitive solution to identify boundaries around points. It is assumed that the perimeter, area, shape, orientation, etc. of each Voronoi cell is informative of interesting aspects of point-recorded systems (a set of towns belonging to the same economic system, for example).

Basically, the approach consists of comparing the cell shapes of a Voronoi diagram extracted from the empirical points with those foreseen for a regular tessellation. This method would give a sense of how distorted is the layout of the empirical system in relation to the ideal established by the geometric model. Finally, this would indicate how close is a real phenomenon to its optimum organisation. Scholars distinguish three generic situations in which this type of analysis is relevant:

2.2.1. SPACE ASSIGNMENT

This refers to situations where a series of static points (settlements or atoms, for example) coexist within a given space, and it is necessary to identify a boundary around each point. According to the application, the space enclosed by such boundary may represent the region of influence, tributary area, territory, domain, etc., of every point under study (Getis and Boots, 1978:121-144). This concept has important applications in crystallography, solid-state physics, biology, astronomy, physiology, urban economics, archaeology, and many other fields. One area of application is the identification of market areas using weighted Voronoi diagrams. Very similar concepts are used to model trade areas for retail stores (West and Hohenbalken 1984, Jones and Simmons 1987). Voronoi diagrams have also been used to study boundaries between the market areas of two competing centres under various conditions of market prices and transportation costs (Shieh 1985).

2.2.2. SPATIO-TEMPORAL DYNAMICS

This refers to situations in which some point-like objects, retail stores for example, independently move to maximise the area of its Voronoi region (e.g. retail territories). Through such process, the Voronoi diagram of the point set may change over time, or reach a state of equilibrium when there is no incentive for the points to relocate. Hotelling (1929) developed a method to understand the organisation of such systems at each stage and to forecast mathematically the state of equilibrium. Therefore, this process is also known as the *Hotelling problem* (Okabe and Aoyagi 1991; Okabe and Suzuki 1987; Okabe et. al. 1992, 2000).

2.2.3. TWO-SPECIES COMPETITION

This refers to a dynamic situation, in which pairs of point-like objects compete for space over a region. In this case, both objects simultaneously try to maximise their corresponding areas of influence. The geometric properties of the system change with relocation, altering the organisation of the system.

Examples of two-species competition and spatio-temporal problems, along with detailed descriptions of procedures to analyse them, can be found in Okabe at al. (1992, 2000). In this section we restrict ourselves to provide one example of the analysis procedures involved in a case of space assignment. Consider the following example:

We need to explain the organisation of a geographic region, where different settlements coexist as elements of a social and economic system. It is assumed that consumers in certain sites demand goods or services that they do not produce for themselves. Therefore, service centres are needed in the best possible locations so as to minimise the effort and cost of the

exchange of products. Three types of properties are relevant for the study of such systems:

a) The spacing of sites with regard to each other (i.e. distance)

b) The arrangement of sites (i.e. geometric shape of the point set).

c) The rank of different types of settlements, as given by their function, as well as the shape and size of their corresponding *areas of influence*.

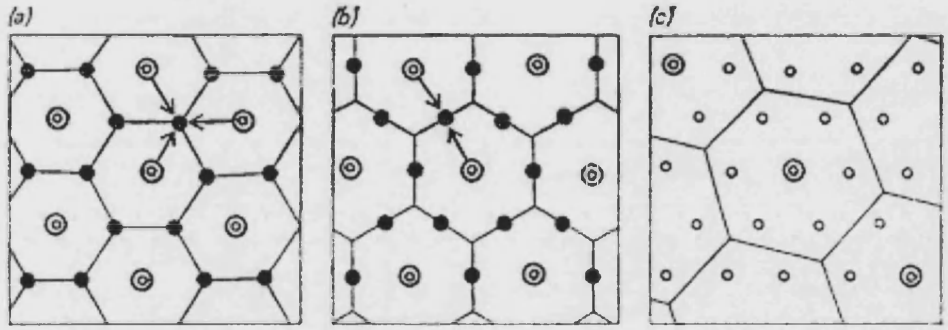

Figure 2.5. Distribution of sites according to a) the market, b) the transport, and c) the administrative models predicted by Central Place Theory. (Source Hodder and Orton 1976: 61, fig. 4.5).

Modelling these properties is the subject of the so-called *Central Place Theory* (Christaller 1933, Dacey 1965; King 1984; Lösch 1936; Mardia *et al.* 1977; Medvedkov 1967). This theory establishes that in any region those towns that concentrate specialised services (i.e. central places) would find an optimal organisation if they were regularly distributed forming a triangular lattice. In such cases, the area of influence for each town (e.g. its trade, administrative and transport territories) presents a hexagonal form, corresponding precisely with the shape of its Voronoi cell. From a mathematical point of view, it has been proven that the hexagon represents the most efficient shape to manage trade, transport and administrative services among settlements of different hierarchy (Haggett 1965) (see fig. 2.5).

Although it is naive to expect that any real region will match this ideal distribution, the theory provides a good geometric model to compare how far an empirical system is from its optimal organisation.[1]

Figure 2.6. Voronoi polygons drawn around Mayan archaeological sites, delineating the territory closest to each site. (Source: Hammond 1974: Fig. 3).

The intertwining of central place theory and Voronoi tessellations has found useful applications in archaeology in building hypothesis about the territorial organisation of ancient societies (Clarke 1972, 1977, 1979; Hodder 1972). Hammond (1972, 1974), for example, has drawn Voronoi polygons around points that represent Mayan archaeological sites (see fig. 2.6). Each polygon defines the *region of control* or *realm* of one particular ceremonial centre. This strategy allows him to appreciate the range of natural resources available within such areas and speculate about the ways in which their distribution affected site location and inter-site trade. As he points out:

> The use of [Voronoi] polygons in defining boundaries is a purely initial one, suggesting where evidence for natural or artificial frontiers may be sought, and their utility in delineating regions of control is also dependent on the assumption that the centres are in a coequal rather than hierarchical relationship; in either case, however, and no matter how small the territory, there is a strong probability that the area of the polygon includes the 'sustaining

[1] Central Place Theory represents a very deterministic approach. A much more natural solution should include some probability functions explaining why actual people don't behave in the well-defined way predicted by the theory.

> area' that provided the basic economic substructure for the ceremonial centre, and the analysis of this is in itself a useful task (Hammond 1974: 316, 322).

Additional applications of central place theory in archaeology can be found in diffusion studies, trade, exchange, migration, etc.

To finalise this section it is worth mentioning that tessellation is not the only means by which we can study organisational aspects of point-recorded systems. Another alternative is explored in the following section, where we offer some examples that involve the study of interaction between localities.

2.3. NETWORK ANALYSIS

Many problems in geography and other sciences require modelling patterns using lines, instead of areas. To address these cases, we use techniques based on network analysis and graph theory (Cliff *et al.* 1979; Haggett and Chorley 1969; Haynes and Fotheringham 1984; Lowe and Moryadis 1975; Tinkler 1977, 1979, Wilson and Bennett 1985:77-83).

We start with a basic definition: *a graph is a diagram containing a finite non-empty collection of points, known as vertices and a set of lines called edges. In this structure, every edge connects exactly two points and two distinct points are connected by at most one edge* (Harary 1969, Hartsfield and Ringel 1994: 7; Wilson 1996: 8).

In some cases, the term graph is replaced by *network* and the words *node* and *link* are used as substitutes for *vertex* and *edge*, respectively. This happens in empirical situations, when it is important to emphasise the physical nature of connectivity or flow-relations between point-like entities. Consider, for example, a system of air links between cities. In

these circumstances we may prefer to talk of a transportation network instead of a graph (see fig. 2.7).

In this thesis *network* will appear when referring to *physical links* (e.g. this section), and *graph* when highlighting *abstract spatial relations* (e.g. chapters 5 and 6).

Graphs and networks are useful representations of many phenomena, including some that do not generate spatial patterns. Obviously, in this thesis we are concerned only with those representing spatial phenomena.

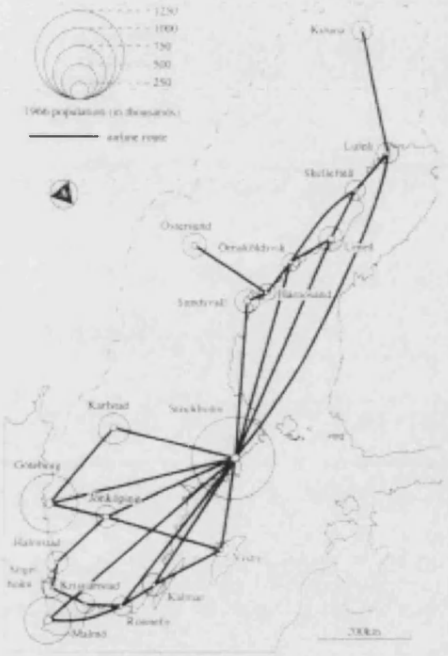

Figure 2.7. Network representation of transport links between Swedish airports circa 1966 (source: Bailey and Gatrell 1995: Fig. 9.1).

Spatial networks are used in finding solutions to optimisation problems, such as location-allocation, spatial interaction and route planning, while spatial graphs are useful representation for analysing abstract relationships associated to the adjacency of point sets.

In this section we concentrate in network analysis and leave graph based analysis for chapter 5 onwards.

2.3.1. SPATIAL INTERACTION MODELLING

Spatial interaction refers to any movement of goods, people and/or information among places in response to levels of supply and demand

existing at certain locations. It is assumed that demand declines over distance. Thus the separation between loci of supply and demand affects the rate of interaction within a particular system. The situation is usually represented with a spatial network, and the problem consists in analysing patterns of flow from those nodes considered as 'origins' (i.e. those representing demand) to the ones defined as 'destinations' (i.e. supply nodes). The objective is to select, from a vast number of possibilities, the flow-paths that better match some predefined optimisation criteria (Bailey and Gatrell 1995:337-382)

In order to make such decision, four types of variables are considered: a) the spatial separation between 'origins' and 'destinations'; b) measures of outflow from each origin; c) measures of inflow arriving at each destination; and d) the cost of flow (*ibid.*). A mathematical function explores the relations between these variables in order to achieve practical benefits such as minimising costs or maximising the volume of flow through the network. The natural fields of application for that kind of analysis are Operations Research and planning. The so-called *transportation problem* offers a typical case. This consists in finding a way to minimise the total cost of transporting products between locations, given defined levels of supply at particular nodes of the network. Additional examples include labour migration (Fik et al. 1992), air travel linkages (Ivy 1995), shopping trips, commuting journeys, telecommunications, etc. The most common solutions to problems of spatial interaction rely strongly on the application of gravity models and entropy maximisation criteria, approaches that have much to do with linear programming and integer linear programming (Bailey and Gatrell 1995: 367, Bell and Lida 1997; Haynes and Fotheringham 1984). However, some recent methods involve other approaches based on genetic algorithms (Buckely and Hayashi 1993; Ishibushi *et al.* 1994; Jiménez and Verdegay 1996; Medina and Yepes 1993).

2.3.2. LOCATION-ALLOCATION

A second category of network analysis addresses a problem involving two main components. One is finding the best locations for a set of server-facilities; the other consists in allocating the demand to those facilities in optimal way. If both demand and facilities are modelled as vertices of a network, then their relative positions and mutual effects can be explored to achieve the best possible solution to an optimisation problem. There are two generic optimisation problems related to location-allocation (Densham and Rushton 1988, 1991; Gosh and Rushton 1987; Klinkenberg 1997; Sanaei-Nejad and Faraji-Sabokbar, unpub.):

a) The first one is to determine the minimum number of facilities that are needed to cover a specified demand given distance or time constraints. For example, we may want to cover the health necessities of a given population by installing the minimum number of hospitals, providing that no one has to travel more than 10 km or spend more than 1 hour on a journey.

a) The second generic problem consists of finding locations for a predetermined number of facilities, in which case it is expected that each facility covers a maximal volume of demand (Lea and Simmons 1995). A retail chain, for instance, may want to open 10 new outlets and needs to locate them in the best possible locations such that each store maximises its share of the potential market.

Besides those generic problems, some specific questions can be answered with location-allocation analysis. These include, among others, how effective is a particular facility within a given network?; why the volume of demand changes at certain points of the network? It is also possible to assess alternative locations of facilities, to forecast the effect of such

changes in the allocation of demand, and to predict the impact on existing facilities in the event that a competitor facility appears.

2.3.3. NETWORK DESIGN

A third category of analysis arises when it is necessary to build a new network or to add a certain number of nodes and links to an existing one. Planning a railway system provides a typical example. In such a case we are confronted with exploring alternative routes between major cities, estimating the effect of connecting or ignoring intermediate towns. A major dilemma is to optimise the relationship between length of railroad (the shorter the better) and the volume of traffic supported by the network (the greater the better). There are two alternative strategies to solve such problem (see Haggett *et al.* 1977: 64-96):

a) The first one is the so-called *positive deviation*, which consists in increasing traffic capacity despite lengthening the route.

a) The second strategy, known as *negative deviation*, is to avoid certain barriers or to minimise the distance travelled between high cost areas, even if that means lowering the volume of flow.

In other network applications the design problem may also include finding the best location for connection points. This is known as the *junction problem*. In the railway example, junctions may represent those places where passengers can change trains. Some applications allow junctions to occur at any location in the plane, which gives rise to the so-called *floating-point problem*. In contrast, there are cases where junctions are confined to predetermined locations (*fixed-point problem*) and the analyst needs to select the best ones according to optimisation criteria (*ibid.*).

2.3.4. ROUTES THROUGH NETWORKS

Finally, network design is closely related to further problems involving *routes through networks*, that is, the analysis of paths or *tours* connecting nodes, which match especial criteria such as being the most efficient encompassing route, or being the shortest path between nodes. In the specialised literature these problems are known as the travelling salesman problem and the shortest spanning tree problem (Haggett et al. 1977: 76-96):

a) The *travelling salesman problem* consists of defining an optimal route through n nodes (e.g. towns) so as to start at node 1, to visit each of the other n-1 nodes only once, and then to return to node 1 (Haggett *et al.* 1977: 76).

a) *Spanning tree problem.* Given a graph with *n* vertices, a *spanning tree* is a set of *n-1* edges joining the *n* vertices, such that any vertex can be reached from any other vertex. The *minimal spanning tree* is the shortest of all such spanning trees (*ibid.*; Bailey and Gatrell 1995: 367) representing a good solution to plan movements through a network, which involves shorter trips among localities.

The methods described so far represent the most typical approaches to point set analysis, showing the diversity of problems that can be solved with these procedures. One particular problem, however, cannot be solved with those general-purpose procedures, and that is the analysis of patterns resulting from certain forms *of spatial symbolism*. In the following section we argue that the analysis of that phenomenon presents especial challenges that can be faced only with custom-designed methods.

2.4. SPATIAL SYMBOLISM AS A SUBJECT OF ANALYSIS

Spatial symbolism refers to the projection of metaphysical ideas onto physical space through the placement of specific categories of objects, architectural features, and/or other material entities, even people, in locations that have special connotations.

The ideas may have roots in systems of abstract thought such as mythology, religion, cosmology and the like, and their realisation in space may serve social, economic or political purposes. On the other side, the objects and other actual elements constitute physical carriers for those ideas; that is, their role is to be material signs for conveying social meanings.

Such a phenomenon produces an arrangement of elements, ordered in such a way that the literal significance of each item acquires a parallel, deeper meaning *thanks to its spatial associations with the rest of the group.* In this thesis we refer to such arrangements as *spatially symbolic contexts.*

Traditional methods are not applicable to decipher the relation between space and meaning encountered in such contexts. For instance, statistical reasoning helps to determine whether or not a point set is randomly distributed, but for the analysis of symbolic contexts it is also necessary to consider spatial relationships among semantic categories of objects. On the other hand, analyses based on tessellation deal with site relationships, though most of those methods are circumscribed to study territorial issues. Finally, traditional network analyses have been mainly designed to solve practical problems, like optimising relationships of *quantitative* properties attached to nodes and edges rather than discovering associations between *abstract semantic categories,* as is required in the case of symbolic contexts.

This emphasises the importance of getting to know the main features of spatially symbolic phenomena in order to find an adequate method of study.

Spatial symbolism is part of the culture of many non-industrialised societies. It appears frequently as a subject of study in archaeology, ethnography, anthropology and architecture. Interesting cases have been documented across continents and historic periods with records covering variable scales, from the organisation of large towns and villages, to the layout of medium-size domestic spaces, to the distribution of objects inside offerings deposited during ritual acts.

The following ethnographic and archaeological information provides concrete examples of the phenomenon:

The Malagasy societies, which include the Merina and Betsileo of Madagascar, invest a great deal of effort to regulate the spatial relationships between people, architectural features, furniture, and activity areas within their households by assigning a meaning to each space according to an elaborate symbolic code. One of the purposes of such a code is sustaining the political order of Malagasy society. As Kus and Raharijaona (1990: 23-24) explain, in Malagasy's worldview:

> Height is perhaps the most obvious spatial dimension to invest with social value and accordingly the Malagasy associate high social status with an elevated position. A second spatial ordering which makes reference to the cardinal directions forms a symbolic set of two contrasting pairs of characteristics. The north is associated with nobility and seniority while the south is associated with things humble and lowly; the east is associated with the sacred and the west with the profane...
>
> In addition to height and a spatial orientation that makes reference to the cardinal directions there exists a third spatial element to the Malagasy conceptual field. This is a calendrical division of the year into twelve months associated with the twelve major *vintana* or "destinies" that can be mapped onto a rectangular space. *In the Merina oral tradition [one of the Malagasy*

> *groups]... height, the cardinal directions and the system of vintana are often seen to play a critical role in the symbolic mappings associated with the political order (Kus 1982). The same spatial elements are also said to have played a role in the traditional layout of the Merina house* (Kus and Raharijaona, 1990: 24, emphasis added).

The projection of the above ideas onto space extends beyond the domestic scale, affecting the use of space throughout the whole of Malagasy villages, tombs, and agricultural fields. Similar phenomena are documented for other ethnic groups, who like the Malagasy create their living spaces based on symbolic codes:

> Indeed, the anthropological literature contains many stunning examples of how metaphysical principles are appropriated somatically and emotionally through the architecture of and the activities contained within the house, Cunnigham (1973) has shown for the Atoni of Indonesian Timor that the structural form of the house and the names assigned to its parts relate to the social and political order of their society. Tambiah (1973) has shown for the Thai that their classification of animals is reflected in the placement of various animals in and under the traditional Thai house. Bourdieu (1973), in his analysis of the Berber house, offers and elegant presentation of how major metaphysical dualities are mapped onto each other in the Kabyle house and thus are interwoven into the fabric of life of this North African group (Kus and Raharijaona, 1990: 23).

In ancient times, other peoples created their own forms of spatial symbolism, leaving behind a great number of archaeological remains that contemporaneous scholars seek to interpret in order to grasp important aspects of those societies (Douglas 1972).

One of these was the Mexica, also known as Aztecs, who inhabited the central part of Mexico from the XIV to the XVI centuries. The Mexica practised a very peculiar religion, which conceived the universe in terms of a geometric model. In such tradition, the entire cosmos was seen as a division of space into vertical and horizontal sections. Each section provided a distinctive scenario for the interaction between human beings and specific combinations of supernatural forces (i.e. god-forces). The Mexica also

believed that their interplay and confrontation with such god-forces could not happen randomly but was meant to occur in specific locations (see chapter 3). Consequently, human beings felt compelled to attract the deities' goodwill -as well as to prevent bad omens- by organising things over space according to an elaborate set of symbolic rules. Such rules prescribe, among many other things, the location and type of objects that should be deposited as offerings to the gods. Regarding the type of objects, the criteria involved the shape, colour and raw material of ritual items (e.g. figurines, deities' paraphernalia, etc.). As for the locational criteria, the rules indicated the position and neighbouring relations of each type of object. During solar rituals, for instance, the figure of the god of fire was usually placed next to other 'hot items' and in opposition to objects symbolically associated with 'humidity' or 'water'. The symbolic code constituted a general framework, which humans applied creatively in each situation according to their specific goals and needs.

This kind of symbolism was responsible not only for the regulation of offerings, but also for the way Aztecs designed their own cities, including the capital Tenochtitlan, as well as for the interior-plan of houses and the space-organisation of many daily activities. We offer a more detailed account of the system in chapters 3 and 4, where we will use the Mexica offerings as a case study to illustrate the application of the spatial analytical method proposed in this thesis.

For the purposes of the current discussion, it suffices to say that the key question in the Aztec and other cases of spatial symbolism is how to unravel the relation between physical patterns and abstract thought, especially when the authors of such systems have long been gone. This has been a major subject of discussion in many fields, particularly in anthropology, archaeology, ethnography, and cultural geography.

Nevertheless, despite the abundance of philosophical and theoretical arguments (Crang and Thrift 2002; Gregory and Urry 1985; Jackson 1989; Lagopolous 1993; Lefebvre 1991; Levi-Strauss 1963; Sack 1980; Simonsen 1991, 1996) very few analytical methods -and even fewer tools- exist today that specifically target the problem from a practical point of view. This is due in part to the fact that the phenomenon of spatial symbolism appears with an unusual variety and diversity, which complicates dealing with the problem from a generic point of view.

Interestingly, some lessons can be extrapolated from fields outside archaeology and anthropology:

From the field of architecture we find useful ideas in the space syntax theory and method proposed by Hillier and Hanson in the book *The Social Logic of Space* (1984). The authors do not target specifically the study of spatially symbolic contexts, but address the more general problem of analysing the *logic* of all forms of architectural space, from building plans to settlement layouts. By 'logic' they mean the dichotomy between "...the social content of spatial patterning and the spatial content of social patterning."

Their approach is based on the reflection that the social organisation of space belongs to a special type of systems that they call morphic languages:

> A morphic language is any set of entities that are ordered into different arrangements [through the application of combinatorial rules] so as to constitute social knowables (Hillier and Hanson, 1984: 48).

Combinatorial rules (or 'syntax', as they call it) necessarily have an abstract cultural referent, but can only operate in the physical world through the use of space. Those rules are the most important property of a morphic language. As they say: "What is knowable about the spatio-temporal

output of a morphic language is its syntax [i.e. combinatorial rules]. Conversely, syntax permits spatio-temporal arrangements to exhibit systematic similarities and differences" (Hillier and Hanson, 1984: 48).

Architectural complexes are not the only example of morphic languages. Kinship systems, modes of production and cooperation, and some products of spatial symbolism can also be seen as systems supported by combinatorial rules.

The ritual offerings examined in this thesis certainly are a product of a *system of relations* governed by combinatorial rules. As we will explain in chapter 3, in the Aztec worldview a rule dictated that those spaces with an excess of 'negative' influences must be filled with objects symbolically associated with 'positive' energies. Another rule indicated that 'feminine' artefacts ought to be balanced with 'masculine' items, and so on (López Austin 1995). The purpose of that kind of rules was to guide the placement of material entities (e.g. artefacts), and more importantly to prescribe the spatial relationships among them.

For example, specific categories of artefacts had to be placed facing cardinal directions, below or above certain boundaries, next to or in opposition to other objects or features, and so on. Such rules created arrangements, whose physical *form* was therefore indicative of its meaning.

This leads to the conclusion that an appropriate approach to the analysis of such contexts must consider not the absolute location of each object but its *relative position* with regard to other items.

In methodological terms, the above conclusion has an important consequence: it means that location and distance -the two underpinning concepts of spatial statistics and other analytic approaches- must be

replaced by the most complex notion of morphology:

> The term morphology comes from classical Greek (*morphe*) and means shape or form. Thus morphology is the study of the shape and arrangement of parts of an object, and how these parts "conform" to create a whole or Gestalt. The "objects" in question can be physical objects (e.g. an organism, an anatomy, a geography or an ecology) or mental objects (e.g. word forms, concepts or systems of ideas) (Ritchey 2003).

The idea of applying morphological concepts as the foundation of spatial analysis methods is not new.[2] In fact, during the 1950's and 1960's scholars like Schaeffer (1953), Bunge (1966), Haggett (1965), and Medvedkov (1967) advocated the investigation of topological and geometric properties to study certain spatial phenomena. They, however, concentrated on solving practical problems rather than on analysing symbolic ones. These included, for example, predicting the development of a group of settlements based on connectivity capabilities of transport networks as given by their topological properties (Bunge 1966; Kansky 1963).

These authors explicitly promoted morphological analysis as an alternative to statistical methods. As Wilson and Bennett (1985:22) point out:

> The proposal was that there are generalities of location which link the uniqueness of *relative position with geometrical and topological regularities* that apply across space in a repetitive and predictable form... Schaeffer's influence,... stimulated an approach to spatial data that primarily emphasized the inductive search for pattern matched against prior theory derived from geometric and topological properties of space [*emphasis added*].

Unfortunately, the 'quantitative revolution' of the 1970's displaced the inductive search for morphological patterns from the main focus of spatial analysis. New interest on topology and morphological arrangements,

[2] Earlier approaches of morphological analysis, in the form of settlement models, appeared since the early XIX and XX centuries with the work of Von Thunen (1826), Weber (1909), Christaller (1933) and Lösch (1936).

however, would certainly expand the capabilities of the field, especially in situations where it is necessary to interpret the arrangement of a set of points in order to make sense of its meaning.

Such a problem is already common in Pattern Recognition, where scientists often need to infer some significant visual pattern out of dots, just like in the children's game of 'finding-the-hidden-figure' (O'Rourke et al. 1987; Toussaint 1980a, 1988). Consider, for example, the dot patterns shown in figure 2.8.

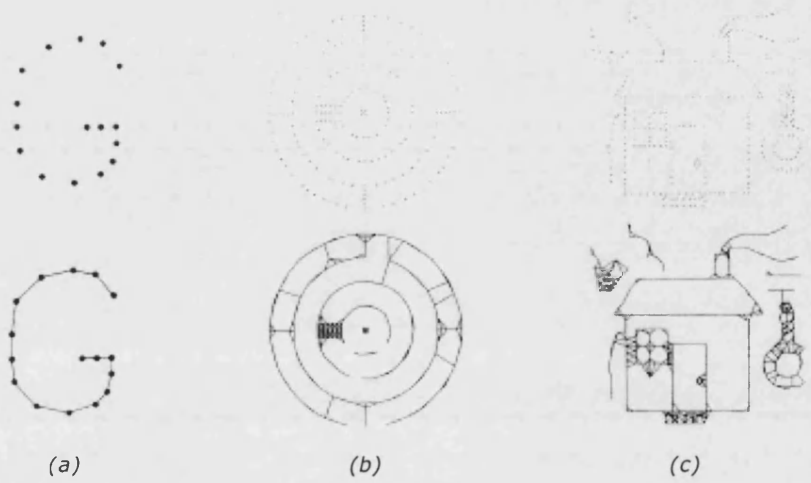

Figure 2.8. Three examples of point sets and their corresponding shapes as determined by Pattern Recognition algorithms: (a) the letter 'G' (source: Toussaint 1980a: Fig. 6); (b) a circular structure (source: Toussaint 1988: Fig. 39); and (c) a house (source: Toussaint 1988: Fig. 40).

A key challenge in Pattern Recognition is to produce mechanisms to retrieve the shape of the points automatically, and then to assess whether they represent (i.e. symbolise) some 'significant' entities, such as the letter 'G' (fig. 2.8a), a circular structure (fig. 2.8b), or a house (fig. 2.8c).

A similar challenge exists in identifying significant patterns from artefact arrangements in spatially symbolic contexts such as the Mexica offerings.

In this particular case, analysts need to get a description of the morphological arrangement (i.e. topological structure) of the objects, in order to assess whether specific classes of artefacts are recurrently associated to certain other classes.

To achieve that goal, in later parts of this thesis we propose to apply the notion of *relative neighbourhood*. This is an ingenious way to detect spatial associations by considering the *relative* position of pairs of points with respect to the *relative* position of any other point in the set. This contrasts with assessing the absolute distance between one single point and the remaining points in a set, which is typical of nearest neighbour approaches.

Before describing any details of the proposal, it is necessary to expand our description of the Mexica spatial symbolism and the archaeological offerings resulting from such phenomenon. These are precisely the topics of the next two chapters.

3 THE MEXICA SPATIAL SYMBOLISM

In accordance with our goal of developing appropriate procedures to analyse spatial symbolic contexts, this chapter introduces some background information, which for all of its complexities illustrates the challenges involved in studying this kind of phenomenon. Here, we refer in general terms to the Mexica spatial symbolism, a system of mythological and religious beliefs rooted in the Mesoamerican cultural tradition.[1] As we will explain, this influenced the use of space and affected many daily activities in Aztec times.

We concentrate only on key features of the system: the idea of god (section 3.1), the geometric model of the Mexica cosmos (section 3.2), and the outcomes of these beliefs, especially those affecting the spatial conceptions of the Mexica (section 3.3). This information will provide the cultural background which is needed to describe the most important archaeological evidence of these beliefs: the ritual offerings, which are described separately in chapter 4.

[1] The cultural region known as Mesoamerica covers a large geographic area whose borders have not been accurately defined yet. It comprises major parts of Mexico, Guatemala, Belize and El Salvador, as well as some portions of Honduras, Nicaragua and Costa Rica. Before the Spanish Conquest the region was inhabited by a variety of ethnic groups (e.g. Zapotec, Maya, Mexica, etc.), which despite local differences shared a common cultural background, especially in terms of religion (Kirchhoff 1967).

3.1. THE CONCEPTION OF DEITY AMONG THE MEXICA

As did many other ancient peoples, the Mesoamericans practiced a polytheistic religion, explaining the universe as a place subjected to the influence of many different gods. The Mexica, in particular, identified deities with different stars and natural phenomena. Thus, it is not rare to find in this tradition references to gods of rain, wind, fire, the sun, the moon, the planet Venus, the Milky Way, etc.

3.1.1. GODS CONCEIVED AS SETS OF FORCES

Gods were conceived as complex entities, which usually exhibited animal or human personality. It was understood, however, that their external features were just a wrapping for the true ingredient of the gods, which was a mixture of energies. Gods were indeed conceived *as aggregations of forces*.

The power of each god derived from his/her individual combination of forces. Some of the constituent energies may harmonise with or complement each other, while others may be contrasting or totally opposite.

Such divine forces appeared in the physical world under a wide range of forms and were found inside things, animals, and people. These entities provide a 'container' for the allocation of such 'god-forces' (López Austin, 1990: 175-176).

An insect called 'uch', for example, was thought to be the container for a devouring god of the same name because the animal was fond of sucking the nourishing properties of food. The same god/force was part of a mammal called *tlacuache*, which was given to consuming grains from the fields (*ibid.*).

3.1.2. GODS CONCEIVED AS CHANGING CHARACTERS

A particular combination of forces gave each god the capacity to influence a life process in specific ways. Gods were also able to reconfigure their sets of energies. This gave them the power to perform extra functions and to participate in additional processes. Even more, some gods merged with one another in order to form new deities. Such dynamism extended beyond the assimilation of forces, thus gods were also capable of dividing their qualities and splitting their powers. These constant transformations -described by an expert as the *fusion* and *fission* of Mesoamerican gods- constituted one of the most important characteristics of Mexica religion (López Austin 1983).

To mention one example, Quetzalcoatl was a masculine god who appeared in different contexts with a distinctive function for each occasion. In his basic role he was a pioneer god, the originator of many inventions. It was believed, for example, that he discovered the ingredients to produce human beings. He also brought the arts to mankind, and taught the principles of the cult of the Sun. A second role of this god was to produce wind just before the starting of the humid season. The Aztecs considered that during that period gusts of air were necessary *to generate* rain (Nicholson 1971: 416, Sahagún 1950-1969, book 1: 3). In other occasions, he transformed himself into the planet Venus, because the emergence of that planet in the sky *preceded* the sunrise.

In each of the above cases the god received a different name. As wind he was called Ehecatl, while Tlahuizcalpantecuhtli designates his appearance as the planet Venus (see fig. 3.1). It is worth noticing, however, that throughout these transformations Quetzalcoatl maintained his common nature as *creator, precursor* or *initiator*.

Figure 3.1. Two representations of the god Quetzalcoatl: Ehecatl, god of wind (left); and Tlahuizcalpantecuhtli, the planet Venus (right). (Source: Codex Borbonicus, reproduced in Mateos Higuera 1993: Fig. 48/1 and 50/1).

When transformations occurred, the gods had to adjust their symbols to reflect their new powers. These mutations help to understand why the images of deities from the Mexica pantheon vary so often. A deity did not always have to bear the same attire or emblems because his/her functions, actions and circumstances changed in different contexts (López Austin 1983). Quetzalcoatl, for example, wore different insignia and symbolic elements to differentiate his role as god of wind from his appearance as the planet Venus (Mateos Higuera 1993) (see fig. 3.2).

The attire and emblems of gods were elements of a very complex symbolic code. Unfortunately, the specific rules of that code are not yet well known and many scholars are still trying to develop means to understand its underlying principles, especially through iconographic studies.

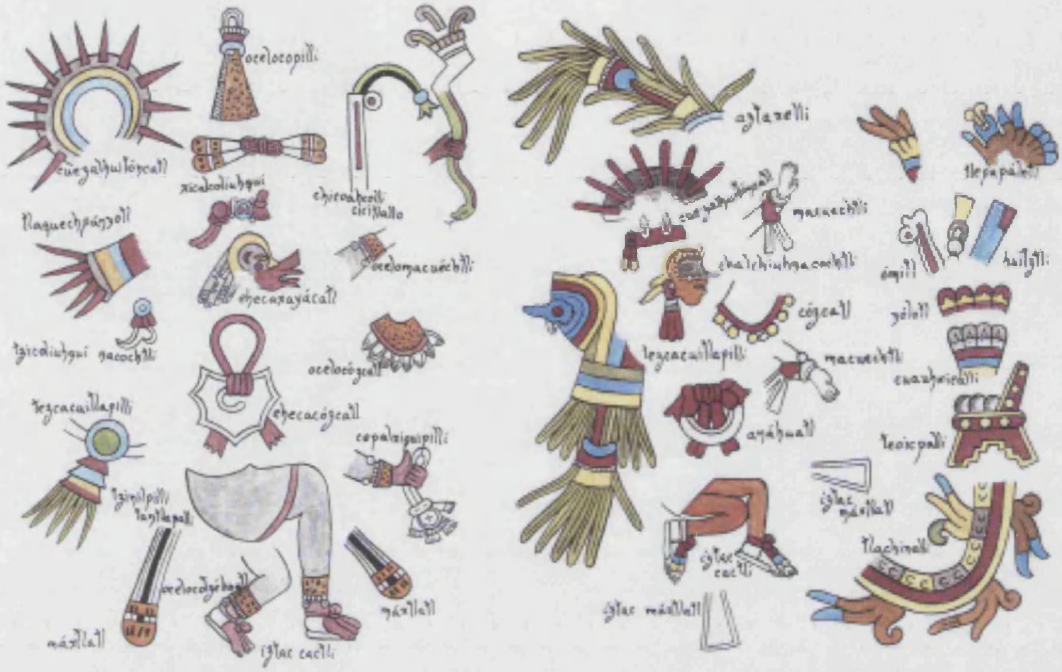

Figure 3.2. Decomposition of Ehecatl (left) and Tlahuizcalpantecuhtli (right) to show their respective attributes. Notice the different attire and symbols that characterise these two representations of Quetzalcoatl (source: Codex Borbonicus, reproduced

Iconography has played a vital role in revealing patterns in the associations between the symbolic elements of the gods (López Austin 1987; Spranz 1973). This has been complemented by analyses of religious ceremonies, which allow identifying the gods worshiped in different rituals and their attached meanings (Graulich 1990, 1999).

Besides those efforts, we consider equally important to analyse the system of spatial symbolism embedded in the Mexica conception of cosmos. This would not only improve our understanding of the abstract principles of the Mexica religious code, but it would also provide a means to interpret many archaeological remains resulting from such conception, especially ritual offerings. Hence, we devote the following section to describe the geometric model of the cosmos adopted by the Mexica people.

Figure 3.3. Cipactli, the marine creature related to the creation of the Cosmos, from a detail of Codex Vaticanus 3773, 'B' (Anders and Jansen 1993).

3.2. THE GEOMETRIC CONCEPTION OF COSMOS

The setting for the action of Mexica gods was a complex universe, partly physical, partly supernatural, in which they exercise both their beneficial and harmful powers. Such a universe was conceived in a geometric fashion, characterised by a vertical division into 22 layers and a horizontal partition into 4 areas plus the centre.

3.2.1. THE VERTICAL SCHEME.

A depiction of the vertical organisation of the cosmos has survived through the narratives of some historic sources. A famous myth, for example, explained the creation of the earth as the division of a monstrous female creature named Cipactli. She was portrayed in many documents as an amphibian or reptilian animal, often resembling a crocodile or a sawfish (see fig. 3.3).

Such animals became very important symbols of the earth. In fact, some Mexica offerings contain remains of crocodile and sawfish as key elements of their contents (see figs. 3.4 and 3.5).

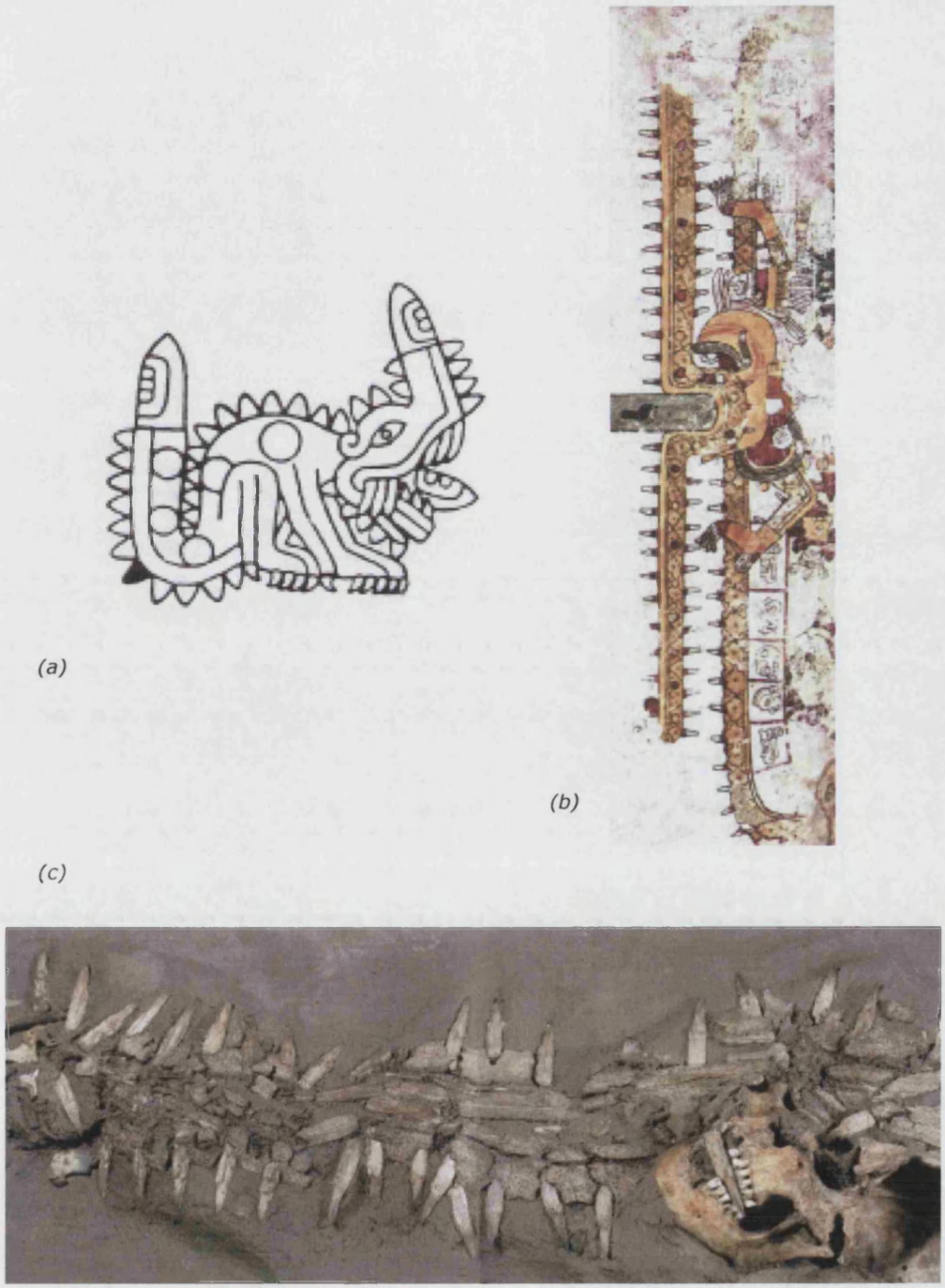

Figure 3.4. Sawfish as symbol of Earth. In Aztec tradition the rostra of this elasmobranch was used to represent the surface of the earth in clear allusion to Cipactli, the mythical monster of Cosmos creation. (a) Cipactli resembles a crocodile/sawfish in a relief carved on an offering box; (b) the Earth Monster represented as a sawfish, from a detail of Codex Borgia (Anders *et al.* 1993); (c) sawfish rostra and human skull found among the contents of Offering 60 in the Great Temple of Tenochtitlan. The latter may be evidence of certain Aztec sacrifices, during which the victim was beheaded with the snout of a sawfish.

Figure 3.5. Crocodile skull found in Offering 61 of the Great Temple of Tenochtitlan. This was an alternative symbol of the earth surface and its remains are not rare among the contents of Mexica offerings.

It was believed that some gods took Cipactli by force and partitioned her body longitudinally into two portions. The upper side produced thirteen layers, nine of which became the heaven, while the remaining four gave origin to the earth. Similarly, the lower part formed another nine layers which constituted the underworld (see fig. 3.6).

The nine upper layers of heaven provided residence for those gods considered as 'givers', whose energies possessed the following characteristics: masculine, hot, dry, vital, luminous, fecund. Sometimes, a flying animal, the eagle, symbolised the heavens.

In contrast, the nine layers of the underworld contained spirits considered as 'takers', who were feminine, cold, humid, deadly, dark, and were symbolised by a terrestrial mammal, the jaguar.

After the splitting of Cipactli four gods were placed in the cardinal directions, between the heaven and the underworld, in order to prevent the reunion of her two components. In other versions of the myth, four trees replaced the gods. According to these accounts, the trunks of the trees provided channels for the circulation of gods and energies from the upper and lower layers (see fig. 3.7a). The energies carried time and destiny, as well as all beneficiary or destructive elements affecting humans (López Austin, 1993: 26).

Gods coming from both ends of the cosmos travelled in contrary directions trough the cosmic channels bringing influences characteristic of their place of origin. They flew in the form of energies interwoven with each other and followed spiral movements until reaching the terrestrial layers (fig. 3.7b,c).

The flow of gods was profusely illustrated in codices, where it adopts forms such as whirlpools, swirls, and so on. It can also be found in artefacts placed in ritual offerings (see figs. 3.7d, 3.7e, and 3.7f).

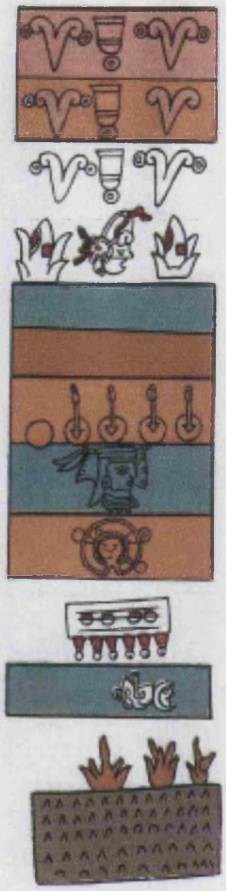

(a)

(b)

Figure 3.6. Aztec glyphs referring to: (a) the upper and (b) lower layers of the universe. The first (i.e. highest) and last (lowest) levels are missing, probably because these layers had no name (Codex Vaticanus 3738 'A', 1979).

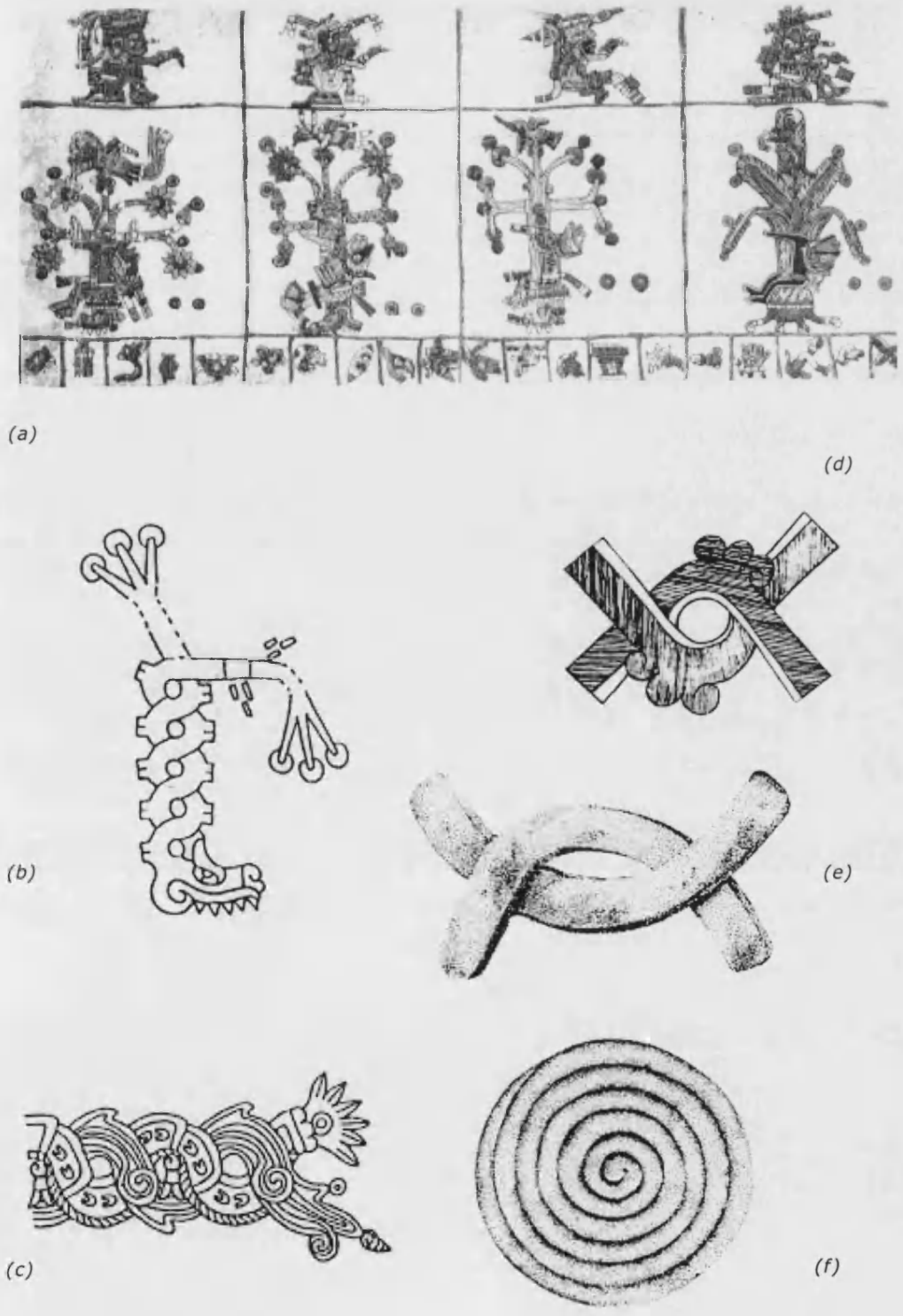

Figure 3.7. Flow of god-forces through the cosmic layers: (a) cosmic trees and deities associated with the four cardinal directions, Codex Vaticanus 3773 'B' (Anders and Jansen 1993); (b) and (c) glyphs representing the flow of energies; (d), (e), and (f) artefacts symbolising cosmic flow, from several offerings in the Great Temple of Tenochtitlan.

Once in the earth, the energies spread out affecting all classes of beings by allocating into them different proportions of contrary substances.

As a result of this process, some entities acquired a major amount of cold, feminine or humid substances, while others received more hot, masculine and dry elements. In this way, the Mexica and other Mesoamerican groups explained the diversity of flora, fauna and the rest of natural resources. (López Austin 1993: 26; López Austin 1995: 438).

Whether hot or cold, masculine or feminine, dry or humid, heavenly or earthly, the differential proportion of energies also affected space and locations. Therefore, in some circumstances it was necessary to bring equilibrium into particular places by attracting certain opposite energy. For example, placing objects of feminine nature would restore stability in a place overflowed with masculine energy.

The same principles applied even for diseases. A person would die unless the correct balance between cold and hot energies prevailed in the body (López Austin, 1988).

3.2.2. THE HORIZONTAL SCHEME.

The principles of binary opposition also help to understand the horizontal organisation of the cosmos. The world was conceived as a big plane segmented into four quadrants. Each section had a distinctive colour and was the territory of specific types of energies and gods (see fig. 3.8).

Some historical sources assign the black colour to the north and relate this sector to the spirit of death. The south was blue and used to represent life. Red was the colour for the east, region of masculine influences. In contrast, the west was white and feminine. Between the collection of symbols associated with the cardinal directions it is important to mention,

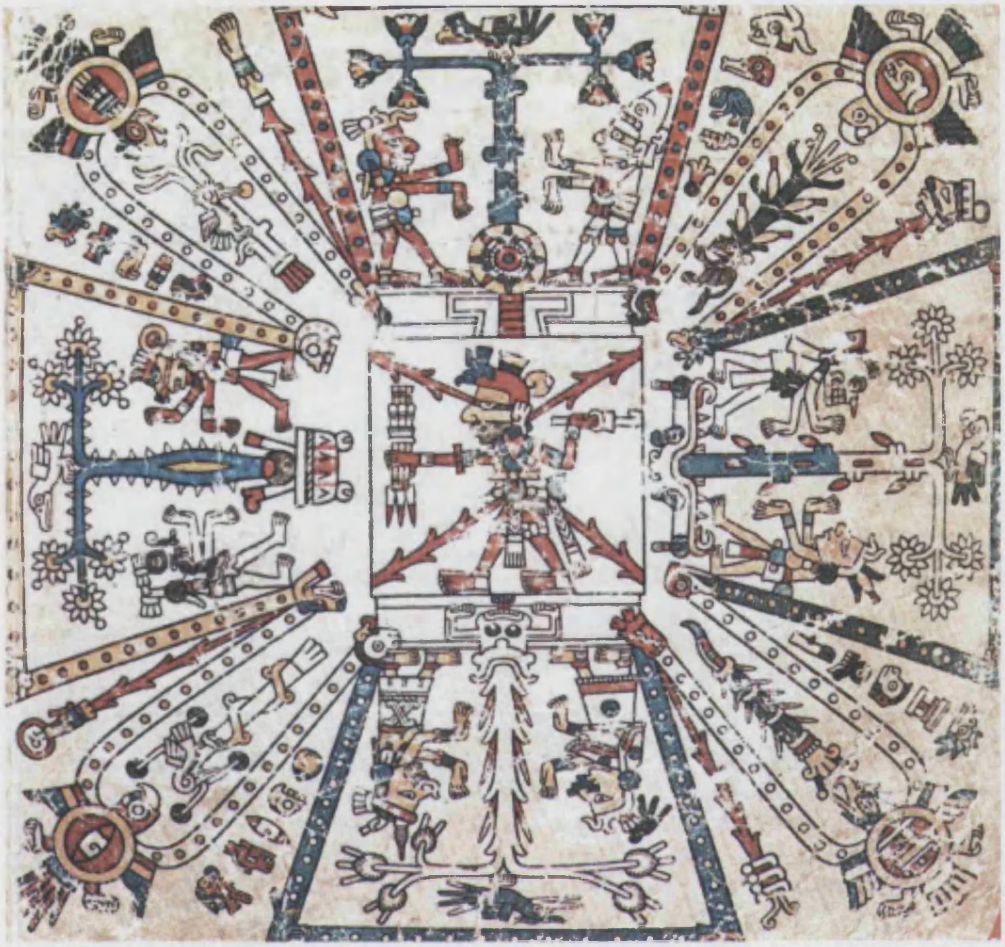

Figure 3.8. The horizontal scheme of the universe according to the Aztec tradition.

for example, that a flint knife was used to symbolise the north (and consequently the dead). A rabbit symbolised the south, a reed denoted the east and a house the west (López Austin 1993: 26).

Additionally, the centre represented the location of perfect equilibrium; the spot where beneficial and destructive forces arriving from the upper and lower levels of the cosmos reached a balance. This was also the spot where spirits from the cardinal directions converged.

Many documents and iconic representations assign the central location to the god of fire, Xiuhtecutli, the oldest and one of the most important deities in ancient Mesoamerica for his symbolic association with the Sun.

3.2.3. THE TIME SCHEME.

The previous section exposes the spatial organisation of the Mesoamerican universe emphasising the appearance of deities on certain locations. However, the material manifestation of each god (and his/her forces) occurred not only in certain spaces but also at specific moments. The orderly succession of different gods on the surface of earth followed a cyclic pattern, which caused the impression of time for the human beings. Thus, time was explained precisely as the sequential appearance of pre-determined gods and influences over the human world.

The passing of months and days degraded the intensity and quality of god/forces and therefore the humans were compelled to revitalise the cycle by offering sacrifices to the gods. This gave rise to a complex system of ritual ceremonies performed at regular intervals according to a complex calendar.

Each ceremony targeted those deities that were likely to affect humans on that particular period of time. The goal of the rituals was to attract their blessings or to avoid harmful effects.

The ritual calendar worked in conjunction with a solar calendar and was extremely important in regulating activities through every season of the year. Particularly important were the ceremonies performed in every temple to mark the beginning and the end of the 18 months of such a calendar. During those ceremonies, the Mexica performed dances, represented mythical episodes and placed offerings to worship the gods who were the patrons during that particular period (Graulich 1999).

3.3. OUTCOMES OF THE MEXICA SPATIAL SYMBOLISM

The ideas concerning the cosmos and deities had an effect on the way Mexica organised space. Such effects can be seen in archaeological remains at different scales. Some interesting examples are the layout of Mexico-Tenochtitlan and the organisation of space within ceremonial complexes such as the Sacred Precinct of Tenochtitlan.

3.3.1. THE LAYOUT OF MEXICO-TENOCHTITLAN

The Mexica capital was originally designed as a squared settlement and special attention was given to orientate buildings towards the cardinal directions. Indeed, four major roads divided the city into four quadrants, which converged at the centre. The neighbours of each district were supposed to live under the tutelage of the god associated with the corresponding cardinal direction. Thus, there was a quadrant in which a northern god was worshipped. In the opposite section of the city a southern god ruled, and so on. The whole city may be thought of as a representation of the horizontal organisation of the cosmos.

3.3.2. THE LAYOUT OF THE SACRED PRECINCT OF TENOCHTITLAN

Even more interesting is the spatial organisation within the so-called Sacred Precinct of Tenochtitlan. This was a stately complex of buildings intended for civic and religious activities, which was built at the centre of the city, precisely where the four main roads and sections intersected.

The plan and boundaries of the precinct are well known thanks to the descriptions of XVI century witnesses as well as to contemporary research. It was laid out as a big square surrounded by walls, which enclosed up to 78 buildings including temples, oratories, altars and administrative premises (see fig. 3.9).

Figure 3.9. View of the numerous buildings inside the Sacred Precinct of Tenochtitlan, according to a reconstruction by Marquina (1960).

The biggest and most important building of the precinct was a pyramidal structure called the Templo Mayor (Great Temple). This was shaped as a great rectangular platform above which four smaller sloping structures were erected. In that way the Mexica tried to replicate the appearance of a mythological mountain in which their guardian gods were supposed to live. In ancient Mesoamerica it was believed that from such pyramids the gods of a particular community would keep in equilibrium the forces of life and death. Such balance would defend people from illnesses, dry seasons, bad harvests, and would provide protection against harmful energies coming from the gods of neighbouring towns (López Austin 1973: 62, 1990: 197, 1993: 23, López Luján 1994: 94).

The top of the pyramid provided space for two shrines or *adoratories* (see fig. 3.10). The one located in the southern half, with red decoration, was dedicated to Huitzilopochtli, the ancestral god of the Mexica, who was symbolically linked to the sky, the sun, the war, and the fire.

Figure 3.10. A detailed view of the Great Temple of Tenochtitlan. Notice the two shrines or adoratories at the top of the pyramid, the one closer to the viewer is the shrine of Huitzilopochtli. At the opposite side, also at the top of the pyramid, there is the shrine devoted to Tlaloc.

The shrine in the north served to the cult of Tlaloc, god of rain and fertility, also associated with the earth (Matos Moctezuma 1986; López Luján 1994: 60)

The importance given to the gods of fertility and war could be easily justified by considering the fact that the Mexica based their sustenance fundamentally on agriculture and obtaining tribute by military means from neighbouring groups (Matos Moctezuma 1986).

The partition of the Templo Mayor into two spatially symbolic sections, however, cannot be explained only on the basis of political and economic factors. As some scholars have pointed out, its dual nature is a consequence of the binary structure of the Mesoamerican cosmic vision, which shows an obsessive tendency to explain the physic-temporal world as a result of the interaction between opposing forces of nature. Such energies were opposed but at the same time they complemented each other and therefore they

existed together. Life and death, for example, were explained as complementary states in the cyclic stream of existence (León Portilla 1978: 45; Broda 1987; Graulich 1987, López Austin 1983, 1994).

As it was said before, in this conception forces and energies were not regarded as physical facts but as attributes of gods that affected the human world. Thus, it is likely that the presence of Huitzilopochtli and Tlaloc at the top of Templo Mayor attempted to symbolise the complementary role of celestial and terrestrial elements.

Additional symbols associated with the same gods reinforced the binary symbolism of Templo Mayor. For example, the dry and rainy seasons, the summer and winter solstices, day and night, as well as the noteworthy symmetry between blood and water, the two most precious liquids in Mexica thought. The next list shows the correspondence of Tlaloc and Huitzilopochtli with these concepts.

Tlaloc	Hutzilopochtli
North location	South location
Terrestial god	Celestial god
Rainy season	Dry season
Winter solstice	Summer solstice
Night	Day
Fertility	Sacrifice
Cold	Hot
Water	Fire

Given the fact that the Templo Mayor was built at the centre of the Sacred Precinct, it is easy to infer its meaning as the centre of the universe. If that were truth, the pyramid would mark the spot where the cosmic levels of heaven, earth and underworld connected with each other

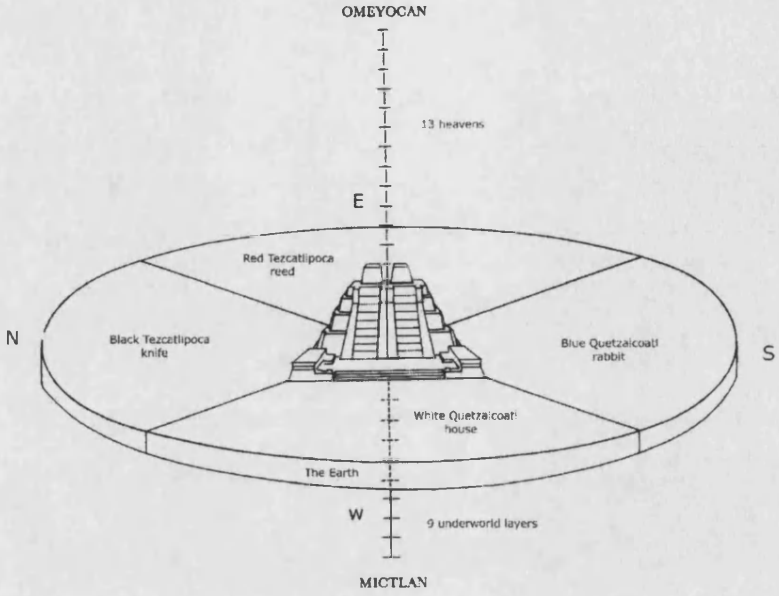

Figure 3.11. Scheme of the Great Temple as the centre of the world. Each cardinal direction was associated with a particular deity, colour and object (Adapted from Matos Moctezuma 2000: 116, fig. 74).

and the point where the four cardinal directions intersected (Carrasco 1987; Matos Moctezuma 1986:32). In fact, the Mexica referred to the temple as 'the navel of the earth', denoting its central position in their spatial conception (Sahagún 1950-1969: vol. 6: 18-19, 42-43, 88-89) (see fig. 3.11).

In accordance with the same criterion, Templo Mayor was the setting par excellence to celebrate both periodic rituals and exceptional festivities, many of them related to the solar calendar (Sahagún 1956).

Many scholars have proven such relation. Tichy (1978, 1981) and Ponce de León (1982), for example, demonstrated that the middle point of the east and west facades of Templo Mayor were carefully orientated to mark the point where the sun would rise and fall on March 4th and October 10th of each year.

On those two occasions, the Mexica celebrated major rituals and deposited numerous offerings in honour of Xiuhtecutli, Huitzilopochtli, and other important deities.

Analysing the spatial features of such offerings provides an opportunity to complement the knowledge about the Mexica symbolism that is normally gathered by other means (e.g. iconography). We devote the next chapter to presenting the major characteristics of such offerings, and then proceed to discuss geometric procedures to identify their spatial features (chapter 5 and chapter 6). In the course of that presentation, the reader may find it useful to keep in mind the following points.

1 The Mesoamerican religion was polytheistic

2 Gods were conceived as sets of forces.

3 Gods were dynamic characters as opposed to inmutable personae; they were subjected to processes of fusion and fission of divine energies.

4 Gods operated in a geometric universe.

5 Each god had particular control over certain places of the universe.

6 Gods travelled to the earth in specific times.

7 Passing of time degraded the nature of gods and therefore human beings were compelled to revitalise the cosmic cycle by performing sacrifices and placing offerings.

8 As each god had particular control over certain places of the universe, it was important to follow strict spatial codes for the allocation of offerings and sacrifices, so the appropriate god received the oblation.

9 The oblation, in the form of sacrifices or offerings, had to contain artefacts that appropriately call upon the god-forces that were necessary in a particular context.

4 THE MEXICA OFFERINGS

The previous chapter showed how important it was for the Mexica to believe in gods who control beneficial and harmful processes through the release of different proportions of supernatural forces. They also believed that such energies lasted only for a limited period of time, after which they started to fade away.

Thus, human beings felt compelled to revitalise the beneficial forces -as well as to avoid the bad ones- by performing sacrifices and oblations to their gods (López Austin 1990: 126, 214; López Luján 1994: 48, 52). These ritual gifts included a variable number of artefacts carefully selected and distributed according to rigorous plans. Their remains appear frequently during archaeological excavations in Mexico.

As we pointed out before, these offerings comply with our definition of spatially symbolic contexts and represent a worthy case study. This chapter explains their role in Aztec society (section 4.1), describes their main features (section 4.2), mentions the relevant factors for the analysis of these contexts (section 4.3), and justifies their interest as a subject of spatial analysis (section 4.4).

Figure 4.1. A Mexica priest in the act of offering. The black circles and bars are numerals, which indicate the quantities of the objects presented (Codex Fejérváry-Mayer, León Portilla 1985).

4.1. THE CULTURAL ROLE OF THE MEXICA OFFERINGS

A key element of the Mexica religion was the idea of restitution. Human beings had to return what they had received from the gods (López Austin, 1994: 204). That explains why so many offerings have been found in Aztec temples. By placing objects appealing to the gods, the Mexica tried to obtain good harvests, military successes, as well as to prevent diseases, stop dry seasons, and keep supernatural forces under control (López Luján 1994).

The placement of such offerings were a significant part of multifaceted rituals, which involved 'theatrical' performances to recreate mythical episodes, as well as processions, dances, chanting of sacred hymns, human sacrifices, etc. Both religious leaders and common people took part on those rites (see fig. 4.1).

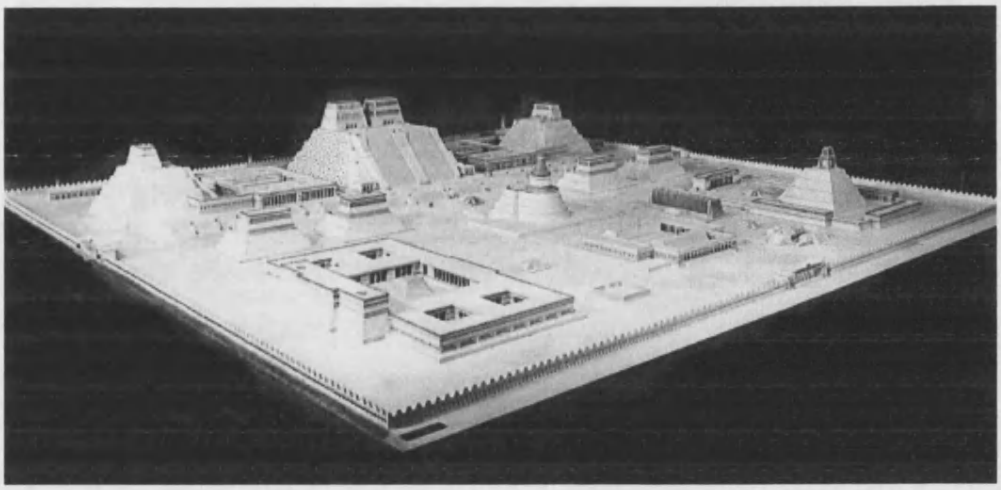

Figure 4.2. A model of the Sacred Precinct of Tenochtitlan. Notice the distribution of buildings and the plaza where most ritual ceremonies occurred.

The ceremonies occurred on a regular basis in the Sacred Precinct of Tenochtitlan, especially in the plaza facing the Great Temple (see fig. 4.2). As we mentioned before, in the Aztec mentality the location of this building marked a point to reach perfect balance of cosmic energies (López Luján 1994: 46, see also chapter 3: fig. 3.11).

Therefore, it is not strange to find remains of numerous offerings in the Sacred Precinct and in the Great Temple itself. The most important occasions for the burial of offerings were:

a) Eighteen festivities synchronised with the solar cycle. These events occurred every 20 days, coinciding with the duration of the Aztec 'month'. According to many scholars, the most spectacular rites were performed during the periods known as Tlacaxipehualiztli, Etzalcualiztli, and Panquetzaliztli (Graulich 1999; López Luján 1994: 97-103).

b) Construction and dedication of new buildings. Laying offerings was equally important to initiate the construction of new buildings or

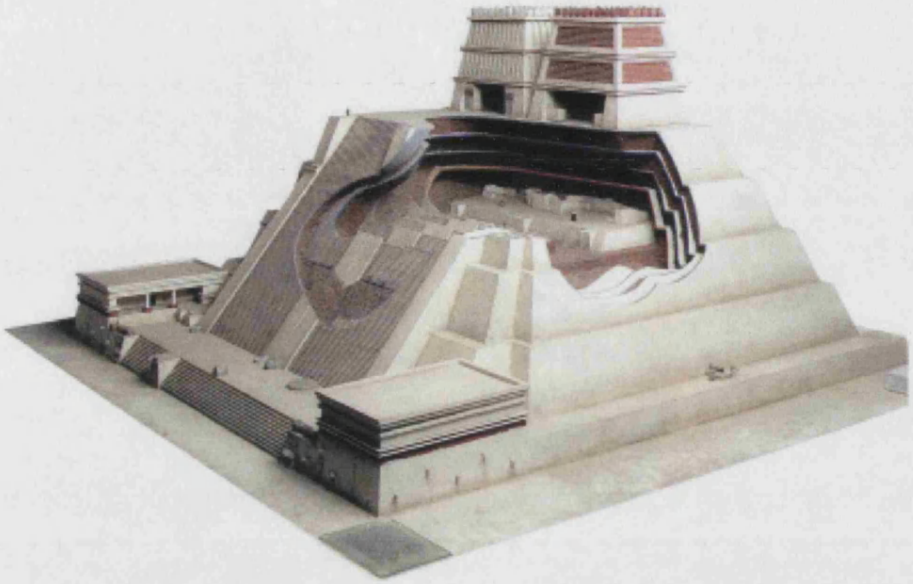

Figure 4.3. A model of the Great Temple of Tenochtitlan showing several construction phases. Mexica rules commissioned the enlargement of the pyramid after successful military campaigns.

to consecrate extensions of previous structures. Recent archaeological excavations, for example, have revealed at least 7 periods of enlargement of the Great Temple (see fig. 4.3). Successive Mexica kings commissioned these projects after major military conquests. The new pyramids covered previous facades without destroying the old ones. In the process, offerings were buried with the purpose to load the appropriate energies into the new buildings and in this way the construction became ready for human occupancy. Archaeologist López Luján (1994: 100) believes that a significant percentage of offerings found in the Great Temple are the result of those rites.

c) Important events in kings' lives. Ceremonies for the coronation of new kings were additional motives for the deposition of offerings.

Those were as important as the ones held in connection with the death of important leaders. The types of caches, however, have not been found so frequently in the Great Temple despite repeated references in historic accounts (Chávez Balderas 2002).

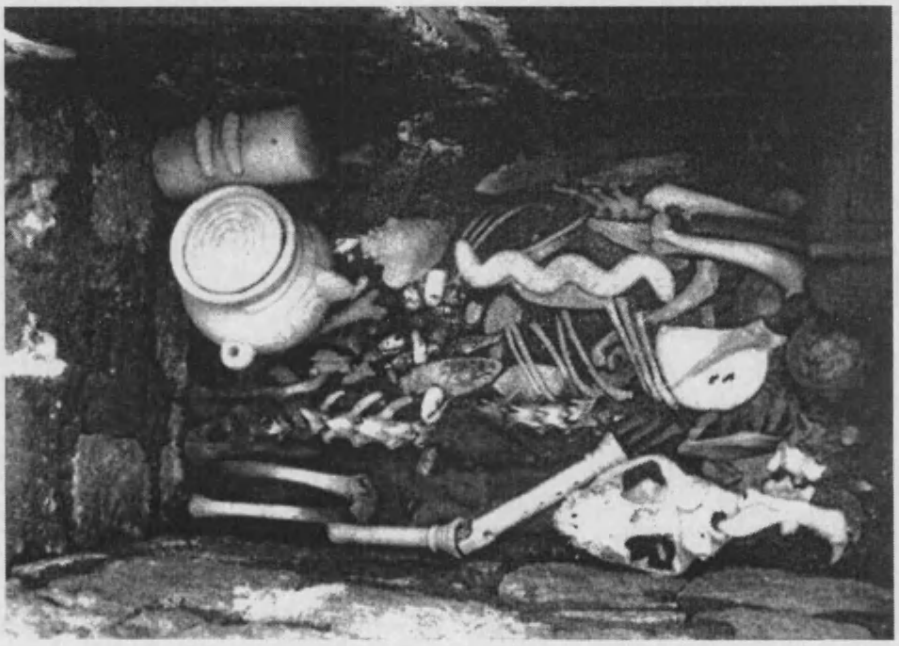

Figure 4.4. Offering H from the Great Temple of Tenochtitlan. This deposit illustrates the type of objects found in archaeological caches; particularly interesting is the serpentiform sceptre in front of the pot, as well as the spiral engraved on the lid of such vessel. Other distinguishable items are a drum, flutes and the skeleton of a jaguar.

4.2. PHYSICAL DESCRIPTION OF THE OFFERINGS

During all these acts of offering, the priests selected items of religious significance and placed them either on the altars of temples or underground. The latter type is precisely the kind of symbolic contexts found in the Sacred Precinct of Tenochtitlan (see fig. 4.4). So far, 128 caches have been recovered, either from the interior of 8 buildings, or from 3 surrounding plazas (López Luján 1994: 111).

The latest discovery (April 2000) is a spectacular offering containing objects of exceptional quality and in excellent state of preservation. The most remarkable of all is a sculpture covered with a paper costume, the first item of this material to survive for 500 years the harsh environmental conditions of Mexico City.

Such discoveries are not circumscribed to Central Mexico. Other regions of Mesoamerica, such as the Maya area, the Valley of Oaxaca, etc., have been equally prolific in caches findings (see fig. 4.5).

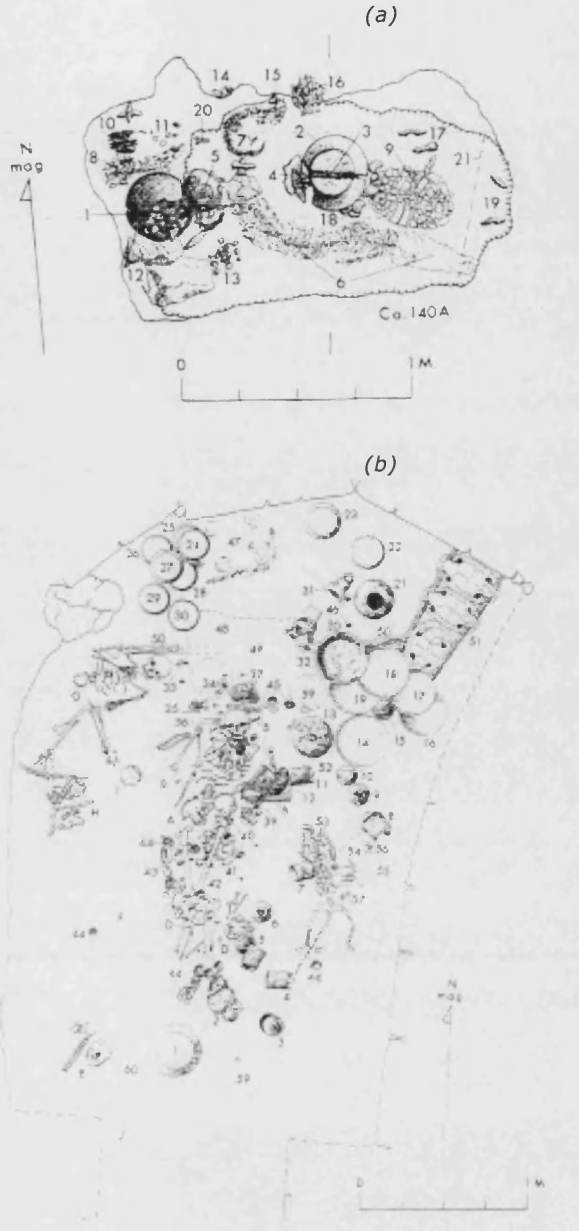

Figure 4.5. Two offerings from Tikal, Guatemala: (a) Cache 140; (b) Tomb 110 (source: Baudez 1999).

In the case of the Mexica offerings the worshipers arranged the objects carefully, either within a stone box (see fig. 4.6), or without receptacle directly under the ground (Matos Moctezuma 1988b). The caches were located inside walls, nearby important sculptures, in courtyards, or even within the fill of constructions (Olmedo and González 1986).

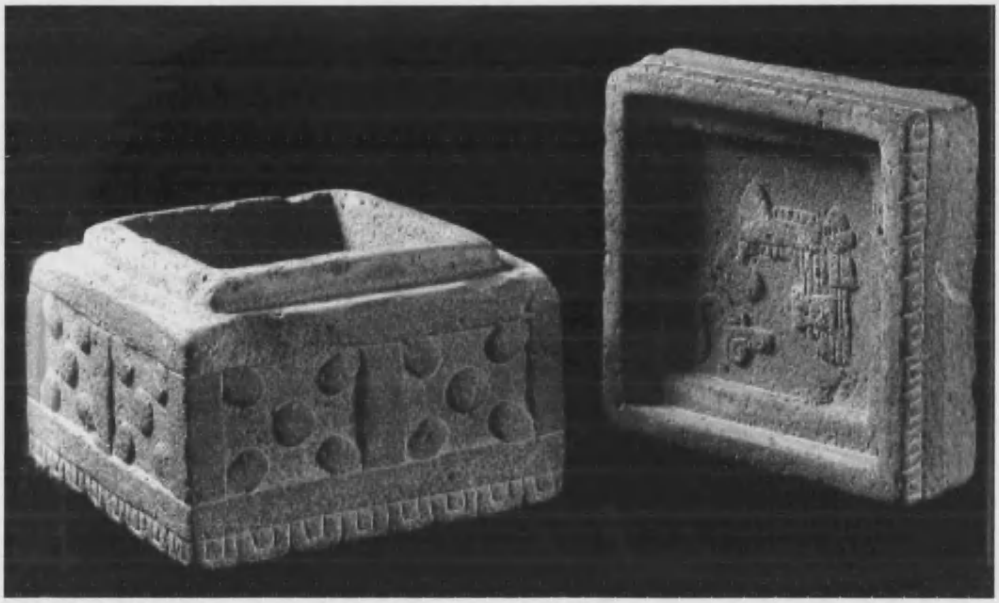

Figure 4.6. An elaborate offering container, provenance unknown, probably from the surroundings of the Great Temple of Tenochtitlan (approximate size 60 x 60 x 60 cm).

Amongst the items recovered are: remains of plants; remains of animals like jaguars, crocodiles, turtle shells, eagles and other kinds of birds, fish, and marine shells; human beings -mainly victims of sacrifice- and a great diversity of ritual implements. Noteworthy objects include medium sized sculptures as well as small figurines portraying diverse gods, also the gods' insignia like sceptres, ear-pools, nose-plugs, breastplates, masks, musical instruments, sacrificial tools (e.g. knives, awls, blades), and many other items (see figs. 4.7, 4.8, 4.9, and 4.10).

The selection of artefacts for a particular oblation responded to specific goals. For example, if the purpose of the offering was to propitiate timely rains, then the priests selected objects suitable for receiving forces from the gods of rain and fertility. The chosen artefacts may be sculptures resembling the gods themselves, their insignia, or items symbolising the region of the cosmos in which they inhabit. Such an offering may also include items intended to keep other forces, like drought and death,

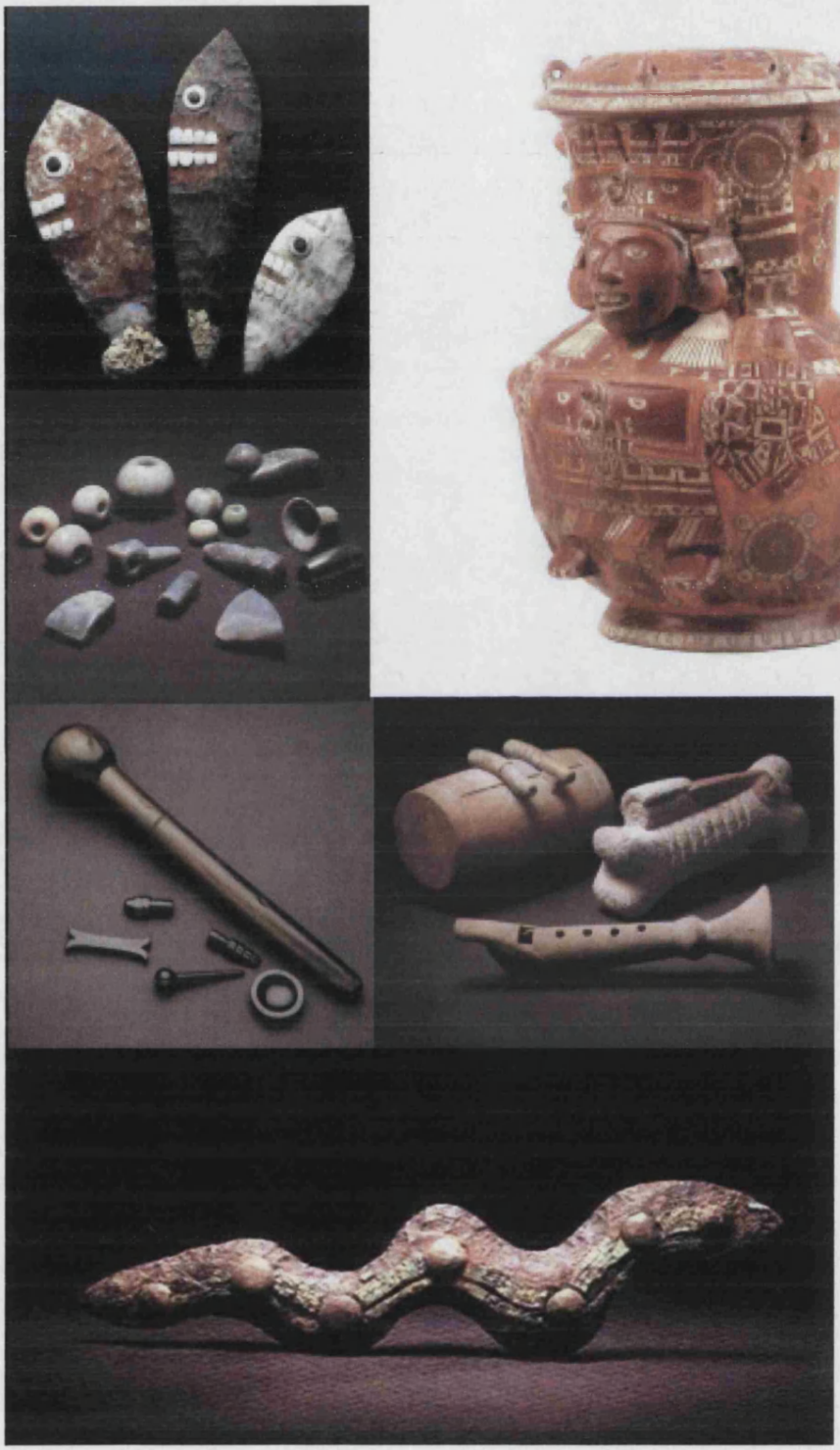

Figure. 4.7. A sample of artefacts found in several offerings of the Great Temple of Tenochtitlan: Pot portraying a fertility goddess, sacrificial knifes, greenstone beads, obsidian artefacts, models of musical intruments, and a serpentiform sceptre (Xiucoatl)

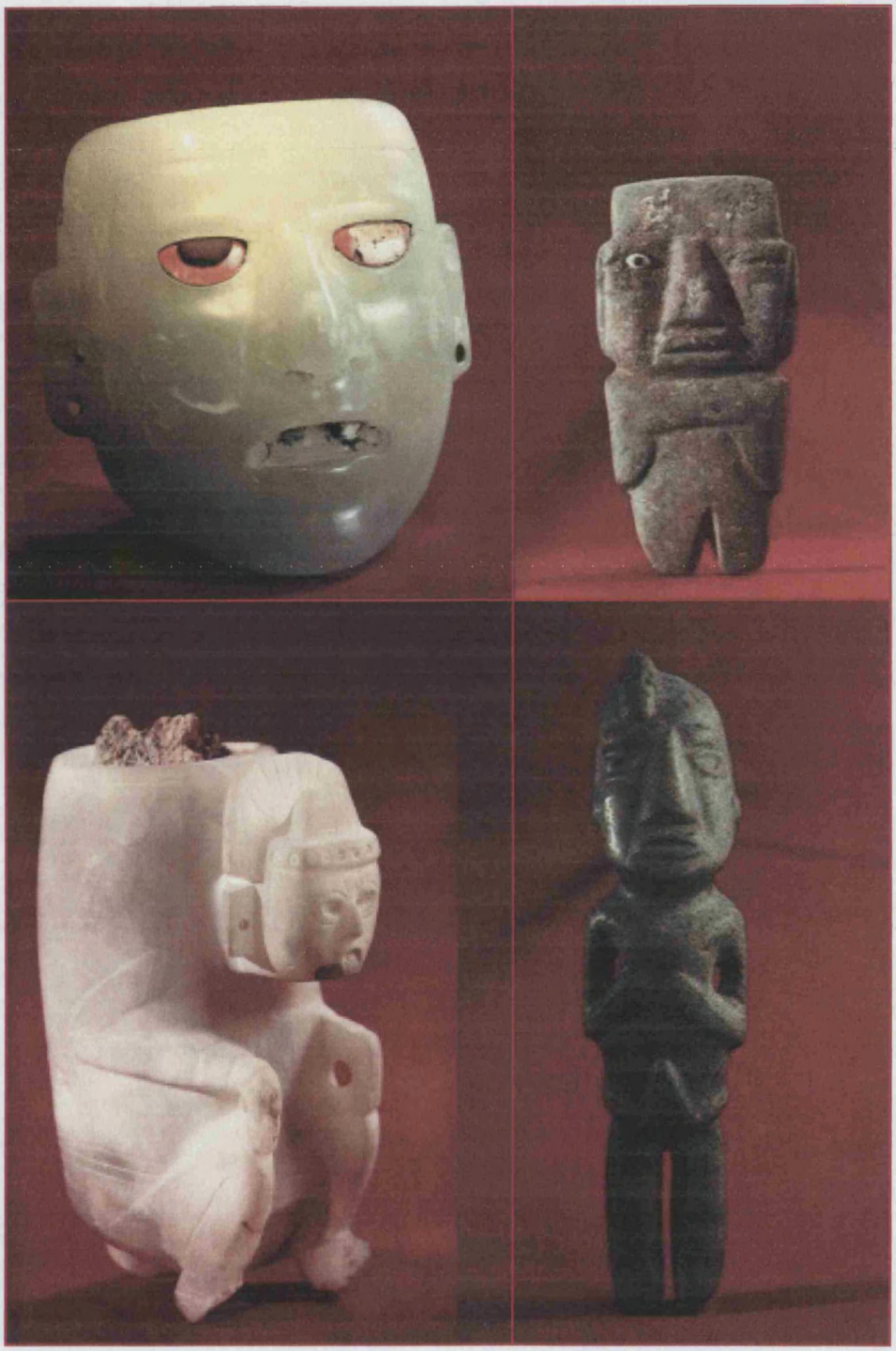

Figure 4.8. Mask and figurines from several offerings of the Great Temple of Tenochtitlan.

Figure 4.9. Skull mask, a fertility goddess, and a pot portraying Tlaloc, the god of rain and fertility.

Figure 4.10. Turtle models, turtle shells and jade plaque from the some Mexica offerings.

under control. Moreover, as each god had power over determined places, it was important to follow strict rules for the allocation of each artefact within the offering, so that the appropriate deity received the oblation.

4.3. FACTORS FOR THE ANALYSIS OF OFFERINGS

The importance of the Mexica offerings lies in the fact that they constitute the major source of evidence about the activities celebrated in the Great Temple. For that reason, they are considered the key to understand the meaning of the whole site.

This explains why the offerings have been the subject of numerous studies. In fact, many scholars in Mexico and abroad are still engaged in solving questions regarding these symbolic contexts. Some have published detailed descriptions of the deposits, while others have gone a step further identifying the more perceptible features of the assemblages or producing explanations of their meaning (Nagao 1985, Matos Moctezuma 1988a, López Luján 1994, Del Olmo Frese 1999; Velázquez Castro 2000). In all those works, the use of two traditional sources of information is pervasive:

4.3.1. HISTORIC DOCUMENTS

The most common sources of data about the offerings are the ritual accounts contained in historic documents. These include narrative manuscripts and pictorial codices written or compiled in the XVI or early XVII centuries. During this time, early historians witnessed the performance of Aztec rituals or retrieved first-hand information from native people. Unfortunately, very few passages mention the placing of offerings and sometimes the information is ambiguous, contradictory, or distorted by the author's cultural views.

Figure 4.11. Chicahuaztli sceptre from the Great Temple and some pictorial representations from Codex Borbonicus. Comparing these images with archaeological examples of this artefact allow formulating hypothesis about its meaning (Source: López Luján 1994: 262, fig. 116).

4.3.2. ICONOGRAPHY

Another source of information is iconography. The graphic record contained in reliefs, sculptures, and codices provide contextual information to learn how ritual artefacts were actually used in Aztec times. Comparisons between these sources and the offering items reveal correspondences that are then used to interpret the particular symbolism of certain classes of artefacts. In this way we have been able to learn about the meaning of items such as sceptres, nose-plugs, breastplates, sawfishes, etc. (see fig. 4.11). Unfortunately, very few codices survived the Spanish conquest and most of those that did survive are still in the process of being fully deciphered.

4.4. THE STATE OF THE ART IN OFFERING ANALYSIS

So far, the most comprehensive analysis of Mexica offerings is the one conducted by archaeologist López Luján (1994). He purposely seeks to

identify symbolic patterns by considering the distribution of offerings over the Sacred Precinct and by recognising variations and correspondences in the contents of the assemblages. In order to achieve this objective, López Luján proposes to formally assess similarity/dissimilarity in a universe of 108 caches by applying the method of Numerical Taxonomy.

Numerical taxonomy is a procedure originally proposed to solve problems of classification in biological systematics (Sneath and Sokal 1973; Sokal and Sneath 1963). In the late sixties, however, it became standard also in archaeology and continues to be used at the present, although with mixed results (Hodson *et al.* 1966).

Numerical taxonomy allows classifying a set of entities (i.e. offerings) upon the basis of how many characteristics they have in common. Such properties can be physical attributes or any features considered relevant within the context of a particular application.

In the case of the Mexica offerings, the taxonomic attributes are 109 categories of artefacts (i.e. object types) identified in the caches. The complete list is provided by López Lujan (1994: 156-159).[1] These are complemented with letter codes that indicate the proximity of each offering to architectural features of the Sacred Precinct. Such information excludes specific spatial data, such as 3D coordinates.

1. The first step of the analysis is to check for the 'presence' or 'absence' of each taxonomic attribute in every cache.

2. The second step is to compare every possible pair of offerings in order to determine the number of matches, both in terms of presence

[1] As a result of new discoveries in the Sacred Precinct, some items have been added to the list of 109 object types. Besides, the list has suffered some modifications due to recent improvements in the knowledge of the collection.

and absence. Through this procedure, each pair of offerings obtains a numerical value (i.e. similarity coefficient) expressing the degree of similarity of that particular couple.

3. The similarity coefficients provide the input for the third step, in which a clustering technique discovered groups of offerings that are sufficiently analogous as to form polythetic classes. A polythetic class is defined as a group of entities (e.g. offerings) that internally showed minimal variations between its members and at the same time exhibit maximum dissimilarities in relation to other classes. The stronger the affinities observed across offerings, the stronger the assumption that they might belong to the same class.

The result of this classification is rendered in a dendrogram, which presents all the offerings organised hierarchically according to their different values of similarity. The analyst usually cuts the dendrogram at the level that he/she considers more realistic in terms of the application.

In the case of the Mexica offerings, this method has led to the identification of 20 classes of offerings. Some of these groups fit well into the definition of polythetic classes, mainly because: (a) the offerings are homogenous in content; and (b) the group forms a branch of the dendrogram clearly isolated from other classes.

For example, the first group identified by López Luján, which he calls *Complex A*, is formed by 11 caches, namely offerings 1, 6, 7, 11, 13, 17, 20, 23, 60, 61, 88. These offerings occupy similar locations in the Temple; that is, they were found either in the corners of the pyramid or in symmetrical positions along 3 main axes. More importantly, they show strong correspondences in their contents (see fig. 4.12 and fig. 4.13). These facts surely are meaningful traits.

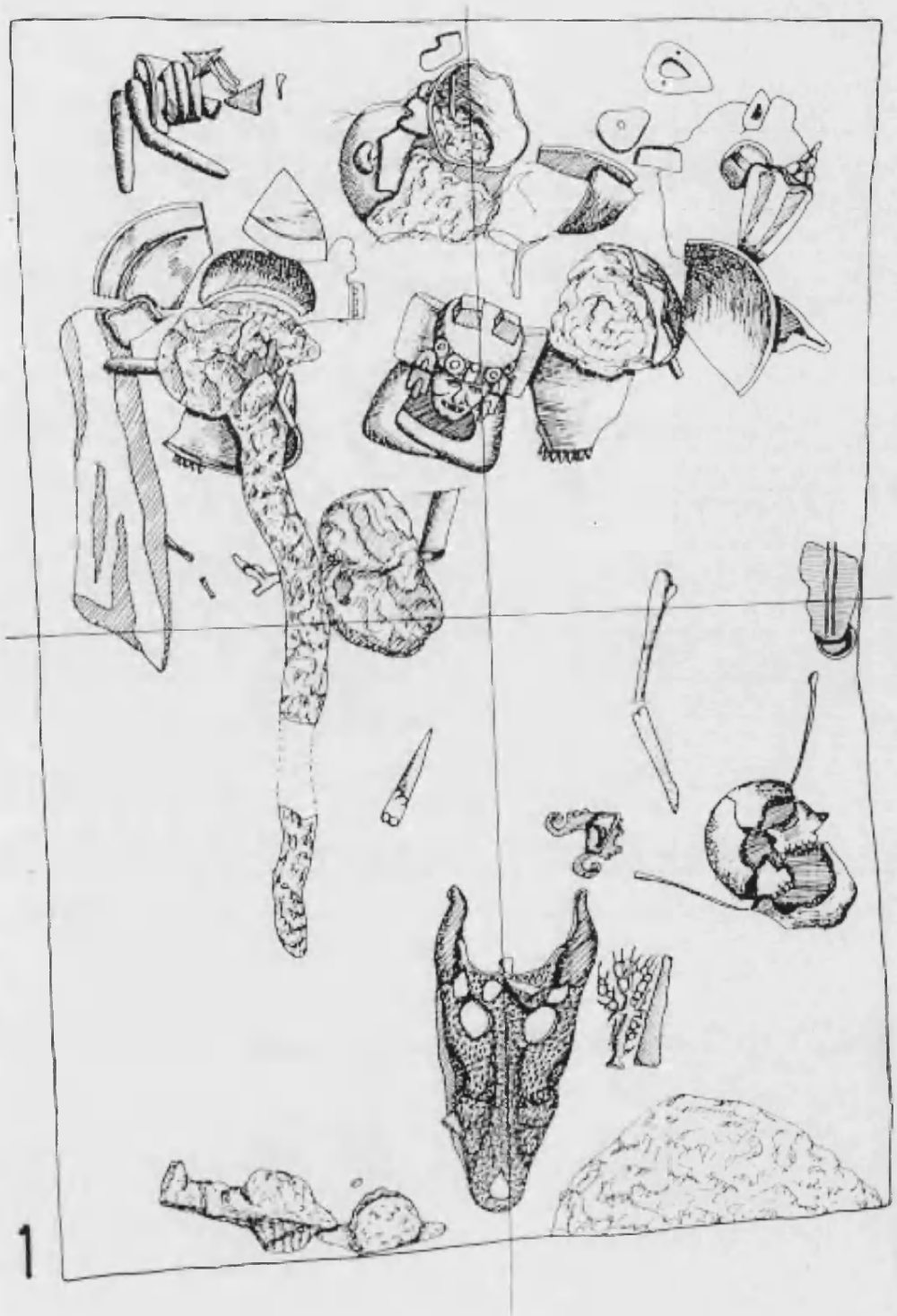

Figure 4.12. Offering 88 of the Great Temple of Tenochtitlan. This is one of the caches included in the group called 'Complex A' (López Luján 1994). Compare this with the very similar cache illustrated in fig. 4.13.

Figure 4.13. Offering 60 of the Great Temple of Tenochtitlan. This is another cache included in the group called 'Complex A' (López Luján 1994). Compare this with the very similar cache illustrated in fig. 4.12.

Another cohesive feature of *Complex A* is the placement of objects in layers. Although López Luján does not use any spatial records of the artefacts, his experience with these materials allows him to recognise a deposition of items in several levels.

In all eleven offerings, the deepest level was composed of small marine shells, sea-urchins, copper-bells and fish remains, followed by another layer of bigger shells and pieces of coral.

Covering the above items, the priests deposited skins and crania of some reptiles (crocodile), fish (especially sawfish) and some mammals, which gave this layer a corrugated texture (López Luján 1994: 254).

On top of that there was an interesting distribution of items described as divine paraphernalia, such as deer-head sceptres, serpentiform sceptres, chicahuaztli sceptres, sacred ornaments, cosmic symbols, etc., plus stone figures of two important gods in the Mexica pantheon: Tlaloc and Huitzilopochtli.

The offerings of Complex A were finally completed by placing cutting-piercing instruments, as well as skulls of decapitated persons, quails, and self-sacrifice instruments.

Such evidence led López Luján to propose the hypothesis that the layering reproduces three major divisions of the Mexica cosmos: underworld, earth surface, and heavens (see chapter 3).

The successful recognition of regularities in Complex A may give the impression that the type of analysis practised by López Luján is sufficiently adequate to provide all the answers about the nature of the offerings. We consider, however, that his approach presents two major limitations:

1. First of all, not all the offering complexes defined through numerical taxonomy are as homogenous and self-defining in symbolism as the one that we just described. In some cases neither the contents nor the general layout are consistent for all the offerings of the group.

2. On the other side, numerical taxonomy is able to detect a certain degree of similarity across offerings, but unfortunately it does not help to know what are those affinities nor provides procedures to explain them.

To illustrate these points let us consider Complex C; another group detected by López Luján´s taxonomy. This includes offerings 15, 22, 24, 58, 62, 70, and CA. These seven deposits appear together in the dendrogram forming a separate branch. However, in contrast to the offerings included in Complex A, which are remarkably similar, the members of Complex C show striking differences among them.

First of all, only 3 out of 55 object types appear in all the offerings of this complex. These are marine sand, coral, and small marine shells. Another 3 (i.e. bigger conch-shells, greenstone beads and skull masks) appear only in six offerings. Seven appear in five offerings (resine of copal, sawfish, sculpture of Xiuhtecuhtli, sea urchin, Tlaloc jar, turtle shell, knife for sacrifice). Four object-types (remains of fish, circle made of shell, wood remains, and sherds) seem more scarce and appear only in four caches.

The remaining 38 object types, that is 69% of the total number of artefacts in Complex C, appear only in 3 or less offerings.

The above observations illustrate a common problem of this kind of approach, namely that during the classification many offerings appear

"similar" (i.e. included in the same *complex*) not because they share a consistent number of object types, but because they lack 'many' of the remaining types of artefact.

Differences that are even more important appear if we examine together the seven offerings of Complex C. All of them are different, except perhaps for the pairs formed by offerings 15 and 60, as well as offerings 22 and 58. It is not likely that such differences are negligible and therefore this raises doubts about the inclusion of such offerings within the same polythetic group. In fact, in his book López Luján recognised that they might actually belong to different groups.

This highlights the need to complement numerical taxonomic results with some kind of spatial analysis, which target the differences in the internal spatial distribution of the artefacts. In this regard, it is relevant to ask whether the offerings are unarticulated assemblages, that is, whether they constitute random aggregations of items, which hold no significant relations between each other. Or on the contrary, whether they are the outcome of a symbolic system conceiving each object as element of an ordered context, within which each object acquires its meaning through its spatial relation with other objects.

It is fair to say that López Luján (1994) was the first scholar to answer that question in a positive way. He has repeatedly commented on the existence and importance of spatial patterns at the interior of the caches (López Luján, n.d.). Certainly, this has been one of his main contributions. As this author says:

> I believe that the first attempt at approximating the language of the offerings should begin with two kinds of analyses: an offering can be studied as a unit by itself or as part of a greater unit of analysis. In the first case, the offering is considered as a discursive unit in which three basic syntactical factors stand out: *the horizontal space*, which determines the association of the objects

> (imaginary axes and groups of similar elements); the *vertical* space, related to the placement of objects in certain patterns tied to the time of the ritual oblation; the pieces are distributed successively in levels of superposition; and the *three-dimensional space,* resulting from the accumulation and joining of horizontal levels during the course of the rite (López Luján 1994: 144-145).
>
> The most noteworthy pattern in the gifts is their organization about horizontal axes. The objects of each deposit are distributed along imaginary axes that run in a longitudinal and transverse direction, and often these paths serve to separate two symmetrical spaces. The same kind and number of objects are found on both sides of the axes. However, the organization of the materials was not limited to a simple bilateral symmetry. Objects that, according to Nahua cosmovision, had an opposed or complementary character were placed at the extreme ends of the principal axes. For example, flutes and horizontal drums, ash-containing braziers and Tlaloc jars, and images of Tlaloc (god of water and fertility) and Xiuhtecuhtli (god of fire) were found in opposite ends within the horizontal plane of the offering (López Luján 1994: 138).
>
> We found that objects with the same characteristics of shape and form tended to be grouped together, spatially associated in well defined groups. Groupings of shells, conch shells, fish, quail, representations of musical instruments, sacrificial knives, projectile points, anthropomorphic sculptures, thorns for self-sacrifice, and such were very common. Moreover, these clusters generally had a number of significantly repetitive components. For example, there were groups of 2, 3, 4, 5, 8, 9, 13, 18, 40, and 120 elements. We know some of these numbers -2, 3, 4, 5, 6, and 13- were of great importance in the Mexica model of the universe (see López Austin for the significance) (López Luján 1994: 139).

Thus, he recognised that the orderly placement of objects was significant for the Mexica and in fact based his interpretation of Complex A upon the spatial premise that offerings were organised in layers and in symmetrical axes. His conclusions, however, were presented without proposing formal procedures of spatial exploration, leaving the development of such procedures to future researchers.

In this thesis we have taken the challenge to produce such procedures. Hence, in the next section we define the objectives, that in our judgement, should have a new method of spatial analysis for the offerings.

4.5. OBJECTIVES FOR A NEW ANALYSIS APPROACH

It is our conviction that the Mexica offerings exhibit spatial regularities and that further patterns would emerge by applying appropriate procedures of spatial analysis. To be useful, however, any analysis method must avoid some of the mistakes made in the past while analysing the offerings. Three of them are of special concern and deserve a brief explanation:

1. The first one consists of assuming that every cache is unique both in composition and meaning. Although this may be true sometimes, it is not always the case. The uniqueness assumption has led specialists to analyse single units separately without comparing to each other, which in turn has prevented the recognition of similarity patterns among caches. Fortunately, as more and more offerings have been discovered, affinities among deposits are becoming evident to archaeologists. The analysis of López Luján, described in the previous section, contributes in great measure to overcoming such a mistake. But as we mentioned, his analyses still lacks an appropriate procedure that consider the spatial component of the offerings.

2. A second misconception consists in believing that the symbolism of a few selected objects could provide the clue for deciphering the meaning of the whole assemblage. For many years, archaeologists made a mistake in analysing only the most "remarkable" objects. Items of that kind normally included stone sculptures or elaborated pieces of pottery. By analysing these types of evidence, they expected to explain the motives behind the oblation and to deduce which deity was the recipient of the offering. Remaining articles -judged by their small size or rough appearance- were ignored or treated as secondary materials.

Figure 4.14. Marine shells found at the bottom of several Mexica offerings.

We know today that such a decision might cause unfortunate interpretation errors. Indeed, it is not always appropriate to appraise the symbolic importance of the objects simply by considering the "attractiveness" of a distinct property such as material, form, size or type of decoration. Rather than focusing on one or two characteristics, we should considered all those properties together, plus the quantity and combinations in which the objects appear.

Moreover, items appearing insignificant to modern eyes may have had extreme relevance during Aztec times. For instance, sets of seven small marine shells (*oliva sp.*), which appear constantly in caches, seem to have been used to represent important concepts related to fertility (Velázquez Castro 2000: 152-166). Similar cases are copper-bells that might have been associated with the underworld. Further examples are greenstone beads and tiny marine shells that the Aztecs used as metaphors of rain, water drops, and fertility (see fig. 4.14).

3. Finally, the biggest mistake of all is to overlook the internal spatial structure of the caches. Many studies still fail to study the neighbouring relations of artefacts in a formal way. In the past, this was attributable to the unavailability of coordinate records for the offering elements, which became accessible for the first time by the middle of the 1960's. Today, however, there is no reason for ignoring the spatial patterning of the artefacts.

Therefore, the new method of spatial analysis should concentrate on three specific objectives:

1. To provide means for comparing multiple offerings, not only in terms of their general contents but also in terms of their spatial structures.

2. To assess the relative importance of offering artefacts with criteria based on quantitative values of spatial *integration* and *control*, rather than on subjective speculations about their status.

3. To identify recurrent combinations of artefacts in a formal way, such that some symbolic themes could emerge from the analysis. This includes the recognition of spatial arrangements formed by specific categories of objects, whose degree of association can be asserted not only with a dissimilarity index but also through a technique based on interactive visualisation.

In the following chapter we concentrate on selecting appropriate geometric concepts to achieve those objectives.

5 GEOMETRIC FOUNDATIONS OF THE RN-METHOD

The previous discussion about the nature of Mexica offerings demonstrated the need to develop analytical procedures based primarily upon the relative position of the constitutive objects.

We can start by representing each artefact as a point in three-dimensional Euclidean space. In this way, it would be possible to model relationships among offering items in the form of 'links' joining adjacent points. If some patterns of association are discovered among specific categories of artefacts, then it would be appropriate to investigate whether the regularities express some significant concept. This situates the analysis within the realms of topology and graph theory. In this chapter, we elaborate on this issue and present some geometric constructs that would help to achieve our analytic goal.

5.1. STATING THE PROBLEM

Recognising spatial relationships among offering elements could be a straightforward procedure if the cache under study contains just a few objects. In such a case, a visual

examination of excavation records might be enough to discover regularity in the association of objects, which in turn may suffice to attempt an interpretation.

For those offerings including hundreds of objects, however, the task becomes more complex. In the latter situation, it is absolutely essential to consider multiple possible scenarios in which a particular item could be associated to the rest of the assemblage. Therefore, the main questions arising in relation to these offerings are:

- How to recognise those relationships that really matter?.
- How to retrieve a description of their structure both in quantitative and graphical ways?

The relevance of a quantitative level of analysis is obvious. It is needed to compare spatial regularities across offerings in a formal way. As for the graphic element, this may not seem very relevant at first, but it is extremely important. If we were able to retrieve and see some underlying structure in the adjacency and connection of specific categories of artefacts, then it would be easier to formulate hypothesis about the purpose and meaning of those object arrangements. Indeed, visual perception constitutes a strong mechanism for advancing knowledge based on human intuition, which is precisely the kind needed for the interpretation of offerings.

The only data available to achieve quantitative and graphic descriptions of patterns are the position vector for each object (i.e. 3D coordinates) and labels indicating object classes. Using this information, we must discover links that reveal an underlying coherent structure. The challenge is to find some mathematical concepts that formally identify associated objects and isolate them from those which are irrelevant.

Finding the appropriate notions for the Mexica offerings, however, is challenging. First, because we do not possess a complete 'key' to crack the exact symbolism of certain classes of artefacts when they appear in the context of others. All we have is some fragmentary knowledge given by historic sources, myths and iconography, of the type presented in chapters 3, and 4. And secondly, because we cannot discriminate automatically among different feasible relations.

To face such limitations, we propose to develop procedures that rely primarily on space itself. These must be independent of any *a priori* assumption about the symbolism of the artefacts. In this sense, they must have the so-called 'descriptive autonomy' that Hillier and Hanson (1984:5) see as a requirement for any study of 'space logic':

> First, [the analysis procedures] must establish for space a descriptive autonomy, in the sense that spatial patterns must be described and analysed in their own terms prior to any assumption of a determinative subservience to other variables. We cannot know before we begin what will determine one spatial pattern or another, and we must therefore take care not to reduce space to being only a by-product of external causative agencies. Second, it must account for wide and fundamental variations in morphological type, from very closed to very open patterns, from hierarchical to non-hierarchical, from dispersed to compressed, and so on. Third, it must account for basic differences in the ways in which space fits into the rest of the social system. In some cases there is a lot of order, in other rather little. This means that we need a theory that within its descriptive basis is able to describe not only systems with fundamental morphological divergences, but also systems which vary from non-order to order, and from non-meaning to meaning.

The procedures must also allow identifying different degrees of spatial association among objects, so archaeologists can heuristically determine which ones are more likely to be significant. Consequently, the analysis has to be exploratory; that is, it must rely on gradual, interactive, inductive steps for recognising patterns. We proposed a combination of topological and graph-theoretical concepts as foundations for our method.

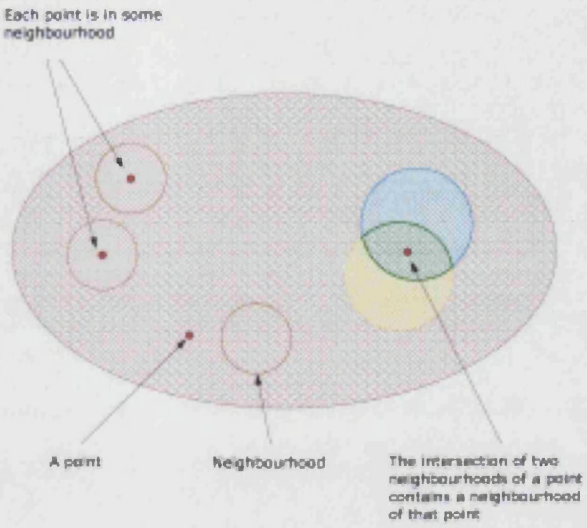

Figure 5.1. The concepts of topological space and neighbourhood (redrawn from Worboys 1995: 113, fig. 3.14).

Topology investigates the relative position of objects with regard to each other. This branch of mathematics is underpinned by the notion of *neighbourhood.* Worboys (1995:113) formalises this concept as follows:

> Let S be a given set of points. A topological space is a collection of subsets of S, called neighbourhoods, that satisfy the following two conditions:
>
> - Every point in S is in some neighbourhood.
> - The intersection of any two neighbourhoods of any point x in S contains a neighbourhood of x.

The above refers to a region of space associated to a point, which is well defined in terms of its boundary (see fig. 5.1).

The analysis of topological neighbourhoods allows identifying geometric relations that do not change under the motions of rotation, translation, and reflection, as well as those unaffected for size changes. This excludes Euclidean distance, for example, because this is dependent on scale. In contrast, proximity, connectedness, and adjacency are topological relations. Within the context of point set topology, proximity refers to the state of being nearby or relatively close; connectedness to the state of

being associated or linked, and implies the existence of a continuous path between two points. Finally, adjacency arises when the respective neighbourhoods of two points share a common boundary.

Adjacency relations are also studied in graph theory. In this field, lines are used to represent the spatial association of neighbouring points. It is worth noticing that given two points p_i and p_j, the adjacency relation satisfies two conditions:

(a) It is irreflexive, which means that neither point is considered a neighbour of itself.

(b) It is symmetric, which means that p_i is a neighbour of p_j if and only if p_j is neighbour of p_i

In section 5.5, we will introduce a principle known as relative neighbourhood, which satisfies the irreflexible and symmetric conditions, and therefore provides a good mechanism to reveal adjacency relations between points. Such a concept contrasts with other notions, such as nearest neighbour. The latter one is not symmetric, which is not surprising because it is based on absolute distance, a non-topological property.

Topological properties are particularly useful to model spatial relationships among offering items, because there is certain logic in the idea of two objects being meaningfully related if (a) they are relatively close to each other; (b) their respective neighbourhoods share some boundary; and (c) can be topologically connected. We will return to this topic later.

Delimiting certain classes of neighbourhoods for discrete elements of a point set can uncover their underlying topological structure. There are several mathematical constructs designed for this purpose and in the following sections we present a sample of these.

We start with the Convex Hull of the point set. Then, we describe the Voronoi Diagram and its dual the Delaunay Triangulation. Finally, we focus on the relative neighbourhood concept and its derivative graphs: the Relative Neighbourhood Graph, the Gabriel Graph, the Beta-skeleton, and the Limited Neighbourhood Graph. As we will explain, the Convex Hull is useful to define the contour or external shape of the point set, while the remaining structures reveal features related to its internal structure. Most of the discussion focuses on point sets in the plane. However, the reader should keep in mind that these constructs extend to three and higher spatial dimensions.

5.2. CONVEX HULL

One of the first challenges in analysing spatial structure is to define the boundary for a set of points. This is very helpful because once the contour of the points has been delimited it is easy to deal with more complicated problems, like partitioning the space into regions or mapping the adjacency, proximity and connectivity between the points. One way to draw such a contour is computing a structure called the Convex Hull (CH). We present the Convex Hull appealing to a practical example:

Imagine that we have a set of points $P = (p_1, p_2, \ldots, p_n)$ defined by their coordinates. Suppose also that we set a nail in each point. If we take an elastic rubber-band and let it go in order to enclose the nails, then the elastic band will form a polygonal figure whose vertices are the points of P with extreme coordinates (fig. 5.2).

No dents will appear in this polygon and consequently its edges define a convex boundary for the whole set P. The polygon embraces all points in P, it is unique with respect to P and is called its Convex Hull **CH(P)**.

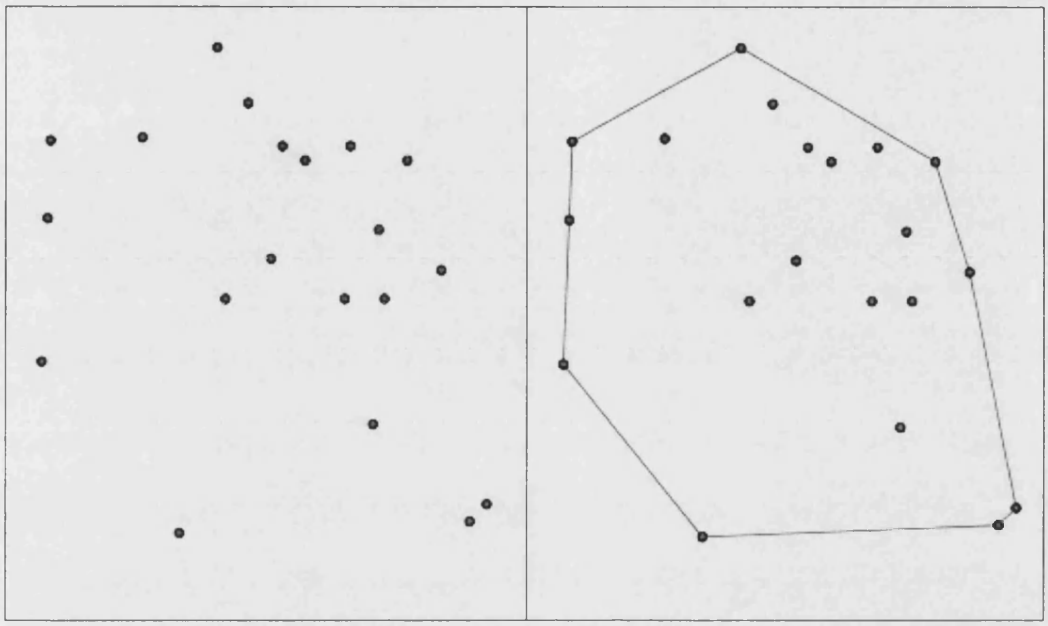

Figure 5.2. A point set and its corresponding Convex Hull

If the points are embedded in *d*-dimensional space, for example in 3D, the Convex Hull is a polyhedron wrapping the points (Berg et al. 1997: 3).

Algorithms to compute Convex Hulls are discussed in Barber et al. (1996), Dwyer (1988), Graham (1972), Jarvis (1973), Maus (1984), Preparata and Hong (1977).

5.2.1. PROPERTIES OF THE CONVEX HULL

Obviously the more significant characteristic of this construct is its convexity. However it has additional important properties:

1. The Convex Hull of a set of points P is the smallest convex polygon that encloses P in the plane; or the smallest convex polyhedron that encloses P in three dimensions. So, it bounds the minimum area embedding P (2D), or the minimum volume embedding P (3D).

2. The Convex Hull of a set of points P is the convex polygon with minimum perimeter (2D), or the convex polyhedron with minimum surface (3D).

In the context of this thesis the most relevant application for the Convex Hull is the identification of external boundaries for point sets representing Mexica offerings.

5.3. VORONOI DIAGRAM

Besides getting an external boundary with the Convex Hull, analysts often need to retrieve details of internal structure. A relevant approach is drawing the Voronoi Diagram (VD). In section 2.2 we mentioned this construct in the context of Central Place Theory and other territorial studies. Here, we expand the definition and describe its geometric properties.

Given a set of points, the Voronoi Diagram is a subdivision of space into cells, such that there is exactly one cell for each point. Each cell delimits the space *closer to one particular point than to any other point of the set.* Every region can be seen as the natural topological neighbourhood around its corresponding point. According to the application, its boundaries can represent the maximum possible *region of influence, field of action, domain,* etc. available for each point (Berg et al. 1997; Okabe *et al.* 1992: 1, 2000; O'Rourke 1994: 170).

Figure 5.3 shows a point set and its corresponding Voronoi Diagram. Notice that the Voronoi regions associated with the extreme points are not closed. This situation is corrected by computing the Convex Hull.

There are many efficient algorithms to compute the Voronoi Diagram in Euclidean space. Some of them are discussed by Aurenhammer (1991), Barber et al. (1996), Dwyer (1988), Fortune (1987), Shamos and Hoey (1975), Okabe et al. (1992, 2000). There are also algorithms for computing Voronoi Diagrams in the l_1 and l_∞ metrics (Lee 1980). Voronoi Diagrams

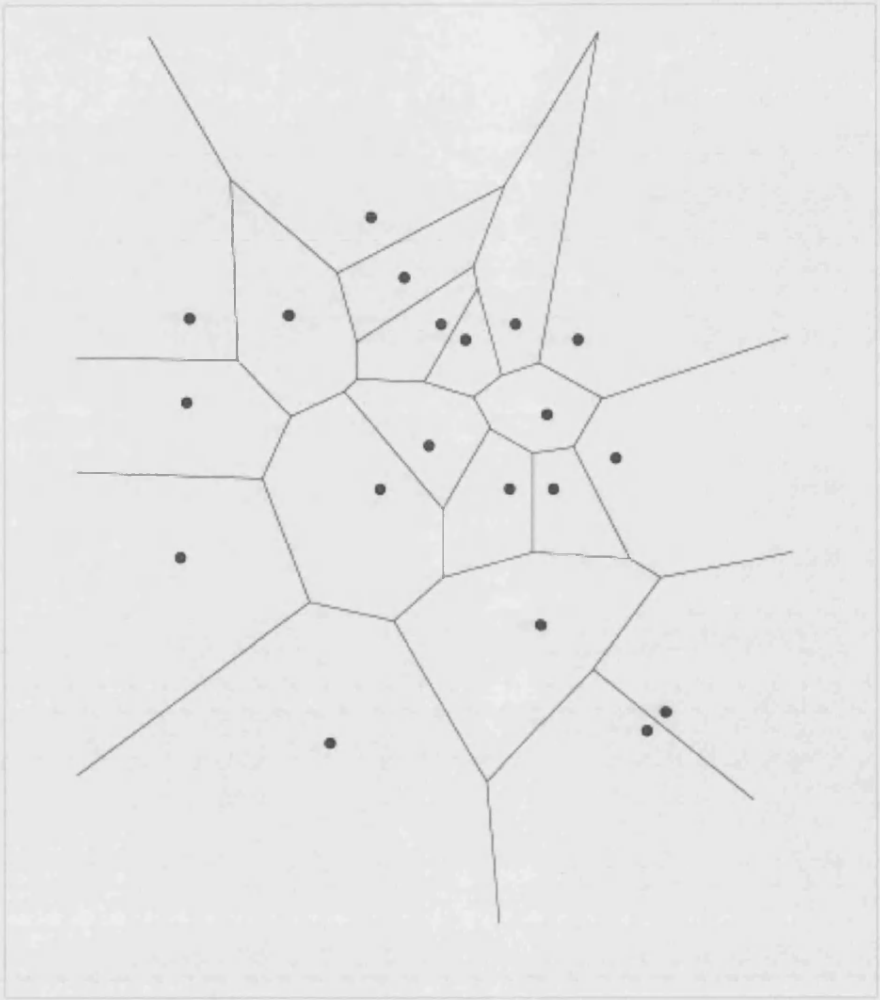

Figure 5.3. Voronoi Diagram of the point set shown in Figure 5.2a.

can also be computed to decompose simple polygons (Aggarwal et al. 1987). Additionally, some implementations are freely available on the Internet (Amenta 1997). One repository can be found in the website of the Geometry Center (University of Minnesota). Although the actual institution has been closed, its former researchers still maintain a directory of computational geometry software, which includes Voronoi computation programs.

The definition of Voronoi neighbourhood can be re-stated mathematically as follows:

Let $P = (p_1, p_2, \ldots p_n)$ be a set of two or more but finite number of points in the Euclidean plane, which are in general position. Hereafter, these will be called the 'generator' points of the Voronoi Diagram. A set of points is in general position in R^d if no $(d+1)$ of them belong to a common $(d-1)$ facet and no $(d+2)$ of them are cocircular or coespherical with respect to a given metric (Jaromczyk and Toussaint 1992). A violation of these conditions would lead to a 'degenerate' Voronoi Diagram. For an explanation about this topic see Okabe *et al.* (1992, 2000).

Also, let $d(x - p_i)$ be the Euclidean distance between any location x, not a member of P, and the position vector for the generator point p_i. Then, the cell, or 'Voronoi region', associated to the generator point p_i is defined by the expression:

$$v(p_i) = \{x \mid d(x - p_i) \leq d(x - p_j) \text{ for } j \neq i, \quad j = 1, 2, 3, \ldots, n\}$$

Where p_i and p_j are the position vectors (i.e. spatial coordinates) for the generator points p_i and p_j, respectively; and $v(p_i)$ is the set of all points that are nearer to p_i than they are to any other generator point. In other words $v(p_i)$ delimits the *Voronoi cell* –also known as Voronoi region- for the generator point p_i.

The last formula guarantees the condition that every location in the plane is associated to its nearest generator point. Therefore, the Voronoi Diagram of P can be expressed as a collection of Voronoi regions, one for each member of P, as follows:

$$VD(P) = \{v(p_1), v(p_2), v(p_3), \ldots v(p_n)\}$$

Where n = number of generator points.

The most important fact regarding this construct is that it "...records everything one would ever want to know about the geometric structure of a set of points (or more general objects)" (O'Rourke 1994: 168). This powerful role is due to some interesting geometric properties:

5.3.1. PROPERTIES OF THE VORONOI DIAGRAM

Assuming that the point set is in general position (see p. 105), the Voronoi Diagram has the following properties:

1 A Voronoi Diagram of a set of generator points $P = \{p_i, p_j, \ldots, p_n\}$ is a unique subdivision of P. Therefore **VD(P)** describes the topological structure of P.[1]

2 Each Voronoi cell inside the convex hull of P is convex.

3 Every location of the space defined by P is assigned to one generator point, except its boundaries (i.e. the Voronoi edges). In other words the Voronoi cells are mutually exclusive except for their boundaries.

4 One corollary of property 3 is that the Voronoi diagram is an exhaustive tessellation.

5 If p_j is the nearest generator point to p_i, then the line halfway between p_i and p_j is an edge shared by $v(p_i)$ and $v(p_j)$. The points along the line of a Voronoi edge are shared by two Voronoi cells.

6 A Voronoi polygon in the plane can have as many as *n*-1 edges and the average number of edges does not exceed six.

7 The nearest generator point to p_i is one of the generator points whose Voronoi cells share the edges of $v(p_i)$.

8 The nearest generator point to any location **x**, not member of P, is p_i, if and only if **x** lies inside $v(p_i)$ (the Voronoi cell of p_i).

---

[1] Mathematical proof for this and the following properties can be found in Okabe *et al.* (1992). See also O' Rourke (1994); and Berg *et al.* (1997).

9 Every Voronoi vertex v_i is the centre for a circle C_i, which passes through three generator points. That circle is empty.

10 Three edges intersect in very Voronoi vertex v_i if there are no degenerate points.

The above properties are useful to answer geometric questions related to proximity and adjacency of points. The most common examples are:

- When the location of the generator points for a Voronoi Diagram are unknown, it would be easy to use the properties 1, 2, 3, and 4 to find the original set of points P. In Cartography, for example, this would allow the discovery of the "centre of gravity" of convex polygons on a map.

- Property 7 is useful for identifying nearest-neighbours, because given a set of distinct generator points $P = \{p_i, p_j, \ldots, p_n\}$ it allows: (a) finding the nearest neighbour for every point p_i element of P, such that the nearest neighbour is also a member of P; and (b) determining which pair of points $p_{i\text{-}j}=\{p_i, p_j\}$, elements of P, have the minimum distance, among all possible distances between every pair of elements of P (Shamos and Hoey 1975). Both kinds of queries are particularly relevant for the single-link technique of cluster identification.

- On the other hand, property 8 offers an automatic solution to the so-called nearest-search problem: Given a set of distinct generator points $P = \{p_1, p_2, \ldots, p_n\}$, find the nearest neighbour point among P from a given location x; where x is not necessarily a point in P. The search is reduced here to a simple "point inside polygon" type of query.

In the context of this thesis, it is more convenient to emphasise the function of the Voronoi Diagram as a graphical picture of the topological arrangement of points, especially of the adjacency relations among point neighbourhoods. This is important because as Aurenhammer (1991: 346) points out: "...Human intuition is often guided by visual perception. If one sees an underlying structure, the whole situation may be understood at a higher level."

The view provided appears in the form of areas surrounding points. However, for the purposes of this thesis it would be even better to see relations in the form of lines joining adjacent points. This is precisely the function of another construct that we describe next.

5.4. DELAUNAY TRIANGULATION

As an alternative to the Voronoi Diagram, we can draw an edge joining every pair of points in P, whose Voronoi regions are adjacent (i.e share an edge). The latter produces an equivalent representation of topology called Delaunay Triangulation (DT). This new description records exactly the same information as the Voronoi Diagram. The only difference is that information regarding proximity and point adjacency is provided in graph form. Here, the original points become nodes and adjacency relations among Voronoi regions are represented by edges. This explains why the Delaunay Triangulation is considered the 'dual' of the Voronoi Diagram. The relationship between both constructs is illustrated in figure 5.4.

The Delaunay construct decomposes space into non-overlapping polyhedra called simplexes. If the points are embedded in d dimensional Euclidean space the construct will produce (d)-dimensional simplexes composed by (d-1)-dimensional facets. For example, in two dimensions the simplexes

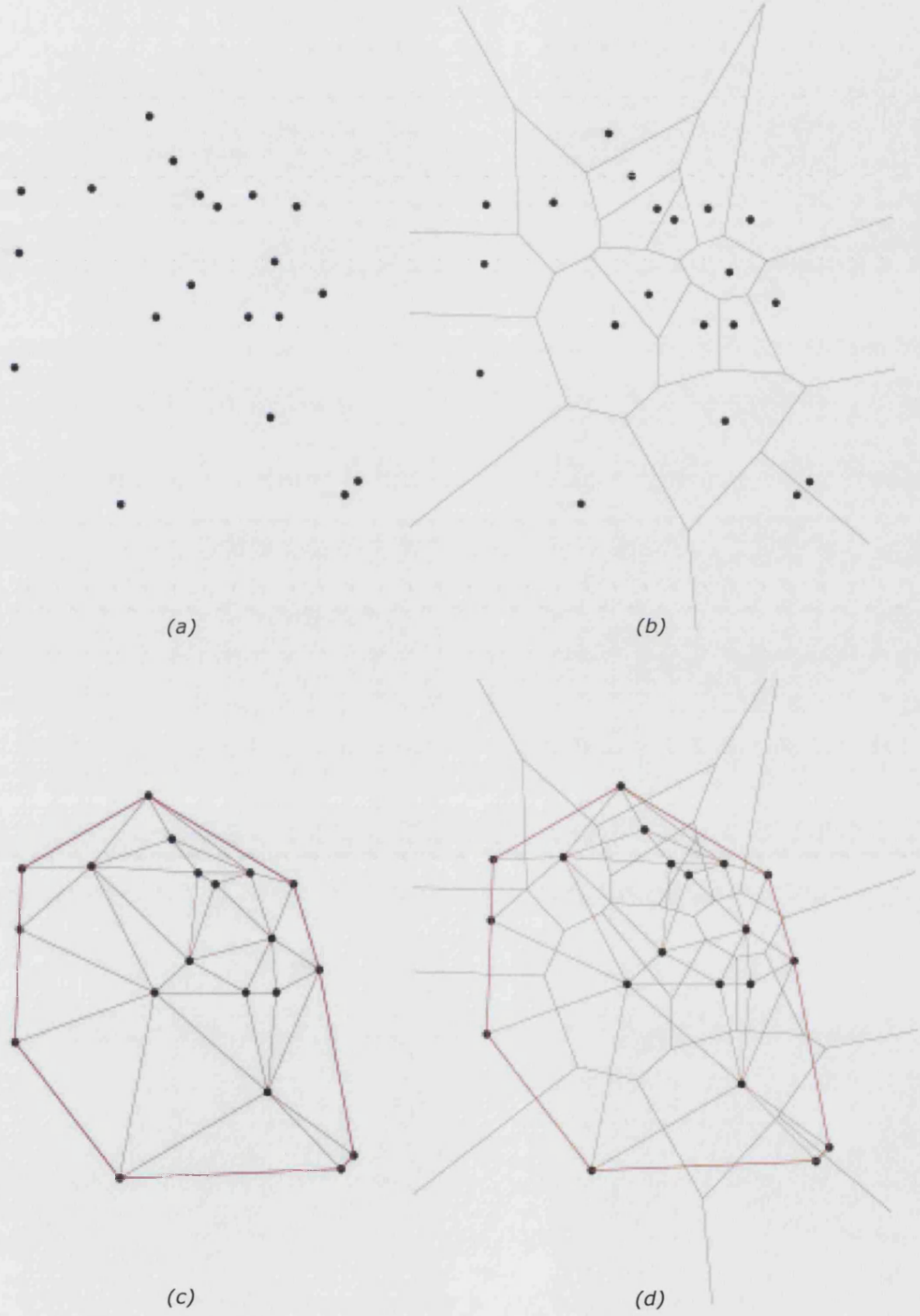

Figure 5.4. The relationship between Voronoi Diagram and Delaunay Triangulation: (a) A point set; (b) Voronoi Diagram; (c) Delaunay Triangulation; (d) Overlay of both constructs.

are triangles and the 'facets' are edges. In the more complex three-dimensional case (d)-simplexes are tetrahedra and the (d-1)-facets are triangles. All simplexes have the same number of facets (4 triangles in the case of a tetrahedron), but the size and angular properties of each simplex could vary from one another. For example, in a Delaunay Triangulation the simplexes can be big or small, right-angled, isosceles, or equilateral, depending on the topology of the original point set.

As in the case of Voronoi diagrams, there are algorithms especially developed to compute the Delaunay Triangulation for points in 2, 3 and higher dimensions (see Barber et al. 1996, Edelsbruneer et al. 1990; Fang and Piegl 1995; Maus 1984).

5.4.1 PROPERTIES OF THE DELAUNAY TRIANGULATION

We now mention the properties of Delaunay triangulations in the plane, some of which can be extended to three and higher dimensions. As in the case of Voronoi properties, we assume that the point set is in general position (see p. 105):

1 A Delaunay Triangulation of **P** is exhaustive because it includes all points of **P**. It is also a unique graph spanning **P** and therefore it describes the structure of **P**.

2 Each node of the Delaunay Triangulation corresponds to a region of the corresponding Voronoi Diagram **VD(P)**. In other words, the set of vertices for **DT(P)** is exactly the set of generator points **P**.

3 Each edge of **DT(P)** corresponds to an edge of **VD(P)**.

4 Each facet of **DT(P)** corresponds to a vertex of **VD(P)**. In *d* dimensional space, there are as many (*d*-1)-facets in D(P) as

vertices in V(P). If the Voronoi Diagram is non-degenerate (i.e. the generator points are in general position), then all the Voronoi vertices have degree three, and consequently all bounded facets of the Delaunay Triangulation **DT(P)** are triangles.

5 The external Delaunay edges constitute the convex hull of **P**.

6 Three points p_i, p_j, p_k elements of **P** are vertices of the same triangle of the Delaunay graph of **P** if and only if the circle through p_i, p_j, and p_k contains no other element of **P** in its interior.

7 A corollary of 6 is that all circumcircles of Delaunay triangles are empty circles.

8 Two points p_i, p_j elements of **P** form an edge of the Delaunay graph of **P** if and only if there is a close disc **C** that contains p_i and p_j on its boundary and does not contain any other point of **P**.

The fact that the Delaunay Triangulation is not just a tessellation, like the Voronoi Diagram, but also a graph, gives the possibility to investigate connectivity related questions such as finding shortest paths between points.

Additionally, the Delaunay Triangulation shares some applications with the Voronoi Diagram. In fact, both constructs are often used to investigate the geometric structure of many natural and social phenomena (Edwards 1993; Okabe et al. 1992, 2000; Stoyan et al. 1995). Among the many fields of application it is worth mentioning: statistical analysis of point distributions (Boots 1973, 1974, 1986; Vincent *et al.* 1976, 1977, 1983; Hutchings and Discombe 1986; Kendall 1981, 1990; Mardia 1989); locational optimisation; chemistry and cristallography (Frank and Casper 1958; Wigner and Seitz 1933); astronomy (Icke and van de Weygaert 1987; Páztor

1994), medicine (Pernus 1988; Singh *et. al.* 1996); biochemistry (Tropsha *et al.* 1995); social sciences (Edwards 1993; Singh and Singh 1975; Singh 1976); GIS (Gold 1994a, 1994b; Lattuada and Raper 1995); pattern recognition (Boissonnat and Kofakis 1985, 1986; Toussaint *et al.* 1984), etc.

5.4.2. STRENGTH AND WEAKNESS OF THE DELAUNAY TRIANGULATION

Given the graph format of the Delaunay Triangulation, as well as its geometric properties, we may think that such a construct is the best candidate to investigate relations among offering artefacts. Two properties make it especially attractive:

1. It offers a *complete* description of relative proximity, adjacency and connectivity between points.

2. More importantly, it shares with the Voronoi Diagram the property of being *unique*. Uniqueness means that there is a one to one correspondence between a point set and its Delaunay Triangulation. In other words, it is not possible that a point set yields two or more different Delaunay Triangulations.

Using both properties one would be able to compare two point sets and to quantify how similar/different they are.

Starting the analysis with a complete picture of the topological relationships, however, is not as good as it may appear at first. Mainly, because the Delaunay Triangulation often includes redundant edges. We could say that the Delaunay Triangulation offers excessive detail of topological structure (figure 5.5).

A second problem is that the Delaunay Triangulation constrains the detection of connectivity patterns to triangular forms and its derivatives.

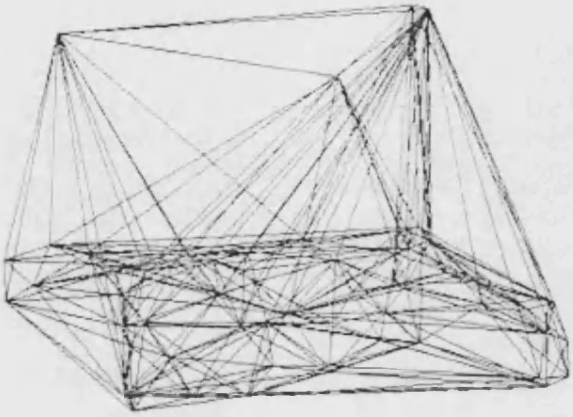

Figure 5.5. Delaunay Triangulation of a set of 66 points in three-dimensional Euclidean space. Notice the large quantity of edges and the difficulties involved in detecting patterns.

Unfortunately, there is a strong possibility that not all adjacency relationships recorded in the triangulation express something meaningful in terms of Mexica spatial symbolism. Therefore, we should account for patterns arising in variable shapes.

The previous observations leave us with the challenge of finding a better definition of neighbourhood, which preserves the strengths of the Delaunay triangulation without maintaining its weaknesses. Such a definition must satisfy the following conditions:

1. Retrieve a topological description of the point set which preserves the property of being unique.

2. Describe not too few but not too many relationships, so the most significant patterns would be easily detected, both quantitatively and in a visual way.

3. Extract morphological patterns without constraining them to pre-fixed shapes.

Exactly the same challenge exists in many applications of computer vision and pattern recognition. In both fields, analysts are given a set of points and it is expected that they find a geometric algorithm that discovers some significant shape (Edelsbrunner et al. 1983; Fairfield 1979, 1983; Kennedy and Ware 1978; Marr 1976; Medek 1981; Rosenberg and Langridge 1973; Toussaint 1980c, 1988; Zahn 1971). As we mention in section 2.4, this problem is similar to the children game of finding hidden figures. On this issue, Toussaint (1980a: 261) comments that:

> In many problems in pattern recognition, such as clustering and computational approaches to perception, one is given a set of points on the plane and it is desired to find some structure among the points in the form of edges connecting a subset of the pairs of points... In computational perception we would like an *algorithm to join pairs of points such that the final graph obtained is perceptually meaningful* in some sense (emphasis added).

What exactly does it mean perceptually meaningful? This is a difficult question, because, basically, the answer depends on the objectives of every application. In the case of the Mexica offerings, archaeologists need to perceive morphological arrangements of objects and to assess whether specific classes of artefacts are recurrently associated to certain other classes.

By considering procedures of visual cognition, some scholars agree that the basic principle to distinguish figures (i.e. morphological traits) in dot patterns is associating two points if they are closer to each other than to other points (Toussaint 1980a, 1980c).

Some authors have developed an interesting model that follows such principle and satisfies all the analysis requirements mentioned before. It is based on the notion of relative neighbourhood. In the following section we present this concept and justify its application in the analysis of spatial symbolic contexts such as the Mexica offerings.

5.5. THE RELATIVE NEIGHBOURHOOD CONCEPT

As its name suggests, the concept of relative neighbourhood captures the idea of points being 'relatively close,' which contrasts with notions based on absolute distances, such as 'nearest' neighbours, shared neighbours, k-neighbours, and 'farthest away' relations. This has applications in situations where we need to establish contextual relationships of one point, say x, with several adjacent points; that is, to determine whether x has other significant spatial associations besides its nearest neighbour.

In figure 5.6, for example, the closest distance criterion would suggest that point p_1 is more significant than point p_3 as a neighbour of point p_x, whereas relative neighbourhood would make both relationships viable (Kirkpatrick and Radke 1985: 228-229).

Figure 5.6. A point px and its possible significant neighbours.

Similar to the Voronoi model, the notion of relative neighbourhood is based on a region of influence, with the difference that this is not delimited around *individual* points but in the periphery of *pairs* of points. It is worth noticing that the extension of such a region varies according to the separation of any pair of points, which also explains why this is called *relative* neighbourhood (fig. 5.7).

One way to delimit relative neighbourhoods is intersecting two circles centred at opposite points. Another is to draw only one circle, providing that its circumference passes exactly through the pair of testing points. Both alternatives, discussed in sections 5.6 and 5.7 respectively, are appropriate for spatial analysis in two dimensions. Also, by replacing circles with spheres they can be extended to three and higher dimensions.

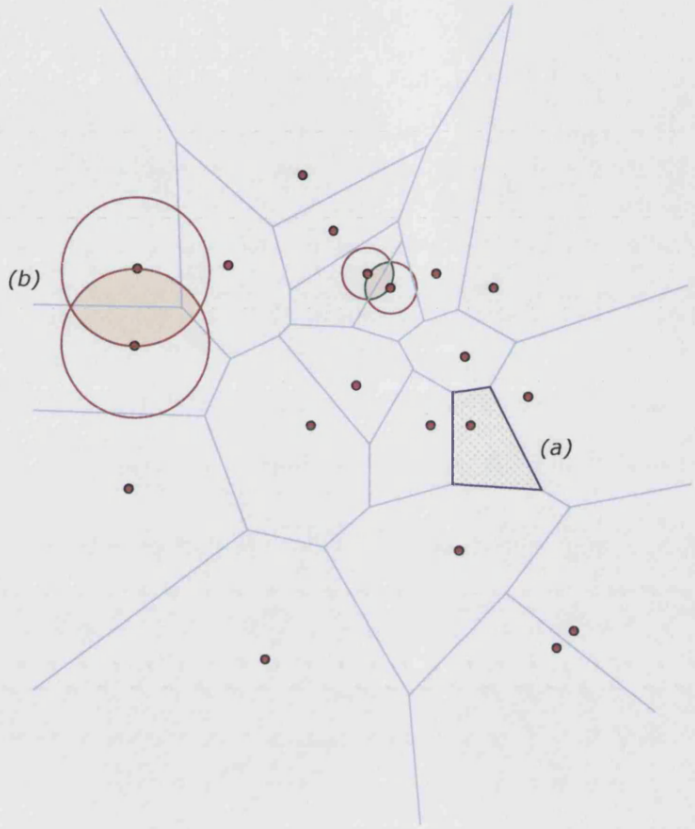

Figure 5.7. Neighbourhoods defined as regions of influence: (a) the Voronoi cell corresponds to a single point; (b) the relative neighbourhood involves an area between two points. Notice that the extension of relative neighbourhood varies according to the relative separation of each pair of points.

The analysis of 'relatively close' points dates back to 1969 when Lankford (1969) defined the concept mathematically and discussed its advantages for clustering. The same year, a similar notion, called the 'least square adjacency criterion,' or 'Gabriel neighbourhood', appeared in a publication dealing with geographic variation analysis (Gabriel and Sokal 1969). In the early 1980's, Toussaint (1980a) further developed the idea, promoting the construction of a diagram which joins relative neighbours in a particular point set with lines. The result became known as Relative Neighbourhood Graph (RNG). He also discussed the relevance of RNG for pattern recognition, visual perception and computer vision.

Since then, other scholars have contributed to the field suggesting variations of the original concept. Amongst the most important are the Gabriel Graph (Matula and Sokal 1980), Beta-skeleton (Kirkpatrick and Radke 1985; Radke 1982, 1988), Limited Neighbourhood Graph (Urquhart 1982), Sphere-of-influence Graph (Avis and Horton 1985; Toussaint 1988), Alpha-shapes (Edelsbrunner 1986; Edelsbrunner and Mücke 1994; Edelsbrunner *et al.* 1983; Saito *et al.* 1991), etc. Current publications refer collectively to all these constructs as proximity graphs (Dearholt and Harary 1991; Hurtado et al. 2001, 2003; Jaromczyk and Toussaint 1992; Toussaint 1991). As we argue in the remaining parts of this chapter, a sample of these proximity graphs has a role to play as geometric foundation for the RN-Method.

5.6. THE RELATIVE NEIGHBOURHOOD GRAPH

Constructing the Relative Neighbourhood Graph for a given point set $P = \{p_1, p_2, \ldots, p_n\}$ consists in testing any pair of points, say p_i and p_j, with the condition of region-emptiness:

First, we take distance $d(p_i, p_j)$ as the radius for drawing two circles C_i and C_j, centred at p_i and p_j, respectively. Their intersection delimits a region R, which represents the relative neighbourhood for the pair p_i, p_j. Secondly, we check if no other point, member of P, lies within such region. If the region is empty, it means that both points are at least as close to each other than they are to the rest of the points. Then we say that the pair is 'relatively close' in comparison with the remaining elements of the set. Thus we draw an edge between p_i and p_j and declare them relative neighbours (see fig. 5.8a). Applying the same procedure to any possible point-pair yields the Relative Neighbourhood Graph (RNG) (see fig. 5.8b).

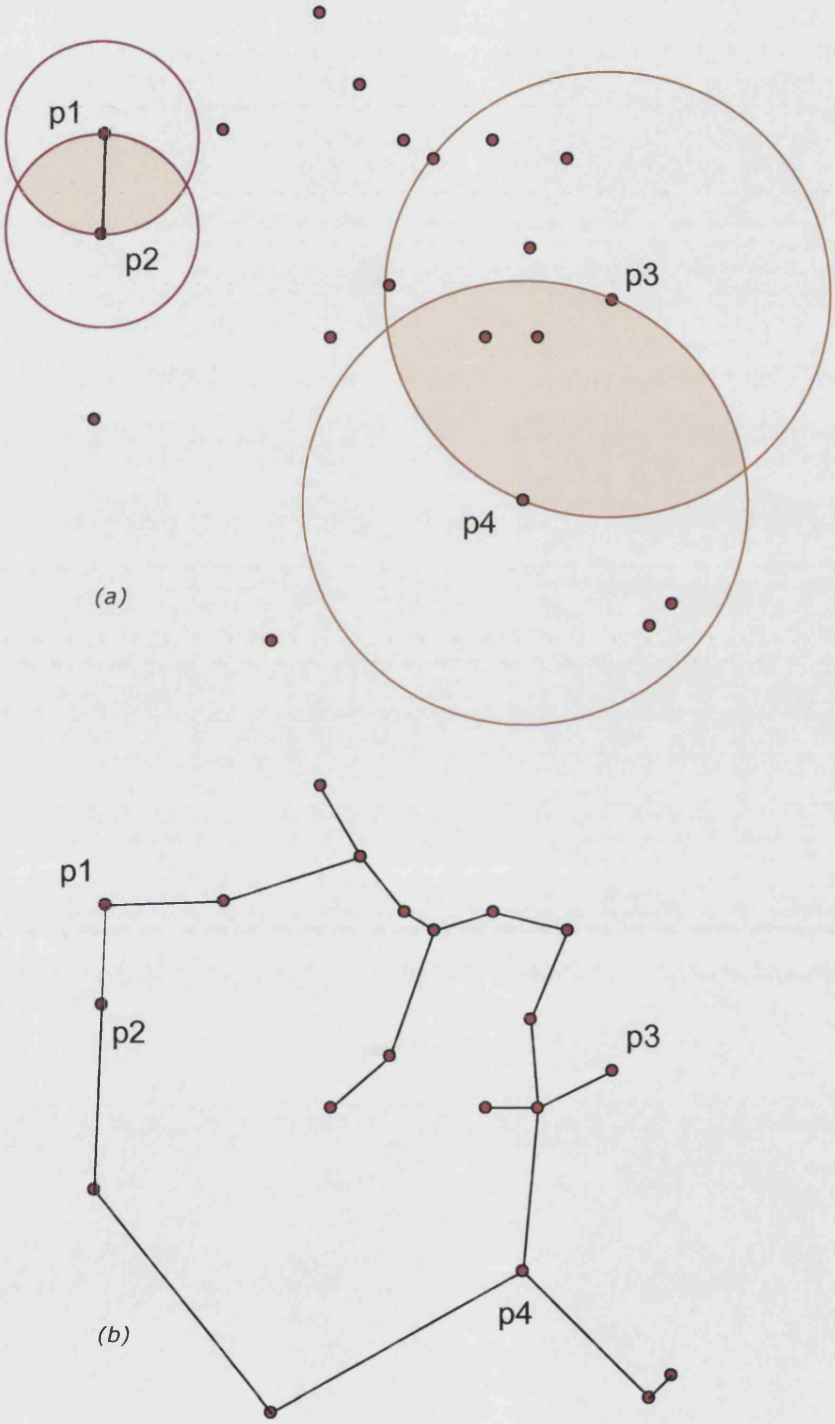

Figure 5.8. (a) Test of 'region emptiness' to define relative neighbours. In this example, the lune region among p_1 and p_2 is empty, therefore they are relative neighbours. In contrast, the area corresponding to p_3 and p_4 is not empty (i.e. no edge is drawn between such points). (b) The resulting Relative Neighbourhood Graph.

Notice that R always looks like a "lune" (i.e. the so-called Vesica Piscis). In two dimensions such a region is an area, but if we apply the concept in three or higher dimensional space it obviously become a volume produced by the intersection of two spheres. In mathematical notation, the lune-region and the resulting RNG are defined as:

$$Lune(p_i, p_j) = C_i(p_i, d(p_i, p_j)) \cap C_j(p_j, d(p_i, p_j))$$

$$RNG = (p_i, p_j) \in E \text{ iff } Lune(p_i, p_j) \cap P = 0$$

Where C_i and C_j are two circles centred at p_i and p_j respectively, both with the same radius (i.e. the distance between p_i and p_j), and **E** the set of RNG edges.

The same concept can be expressed in terms of relative distances. Given a set of points **P** = $\{p_1, p_2, \ldots, p_n\}$, any two points p_i and p_j, elements of **P**, are relative neighbours iff:

$$d(p_i, p_j) \leq \min\left[\max\left\{d(p_i, p_k), d(p_j, p_k)\right\}\right] \text{ for } k = 1,\ldots,n, k \neq i, j, \text{ and } p_k \in P$$

Where $d(p_i, p_j)$ is the distance between p_i and p_j; $d(p_i, p_k)$ is the distance between p_i and p_k; $d(p_j, p_k)$ is the distance between p_j and p_k, and *n* is the number of points in **P**.

The RNG holds interesting hierarchical relations with other geometric constructs. In particular, the RNG is a supergraph of the Minimum Spanning Tree (MST). The Minimum Spanning Tree is a graph connecting all the points in the set, such that the total edge-length is the shortest possible for that particular point set. It is well known that in some cases the same shortest edge-length can be achieved by linking points in different ways. Therefore, a point set can have more than one MST.

Such lack of uniqueness makes it difficult to identify the most appropriate MST for applications such as single-linkage clustering. Fortunately, if the point set has more than one MST, the RNG includes them all. As we will

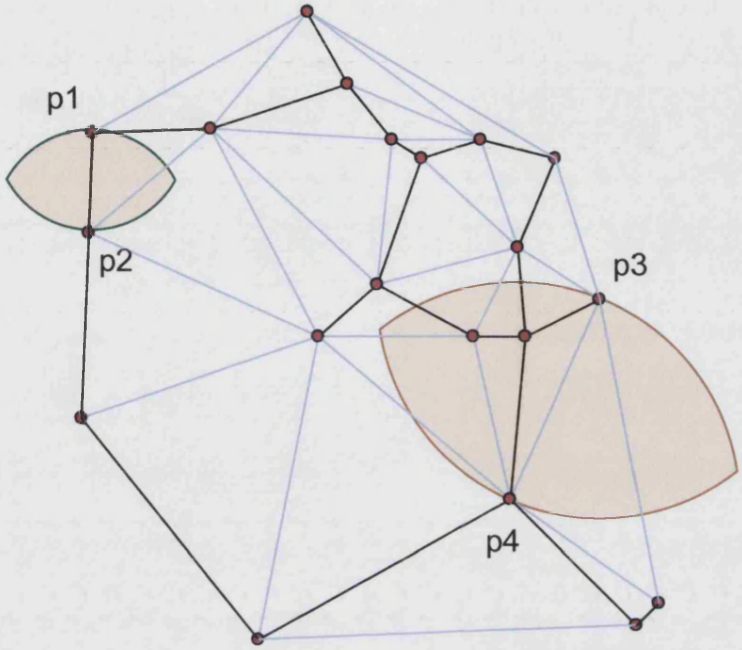

Figure 5.9. Relationship between Delaunay Triangulation (soft lines) and Relative Neighbourhood Graph (bold lines). Notice that no edge exists between p_3 and p_4, as their region of influence contains other points. In contrast, RNG has an edge joining p_1 and p_2, whose region is empty.

argue later, this makes the RNG a better descriptor of point set structure than the MST.

More importantly, the RNG is a subgraph of the Delaunay Triangulation, which situates the RNG at the middle of an interesting hierarchy of graphs (fig. 5.9):

$$MST(P) \subseteq RNG(P) \subseteq DT(P)$$

Providing that the point set is in general position, such relationships give rise to the following properties.

5.6.1. PROPERTIES OF RELATIVE NEIGHBOURHOOD GRAPHS

1. *Uniqueness.* The RNG preserves the DT property of being unique. That is, a point set has one and only one Relative Neighbourhood Graph. Using RNG uniqueness, one can compare the respective RNG of several point sets in order to assess how similar they are in terms of their internal structure.

2. *Connectedness.* The Delaunay Triangulation of a point set is always connected. As RNG is a subgraph of DT it follows that RNG is always connected. The property extends with some minor adjustments to arbitrary dimensions and other metrics (e.g. l *and* l_1) (see O´Rourke 1982).

3. *Planarity.* Any subgraph of a planar graph is also planar. In two-dimensional space, DT always constitutes a planar graph. As RNG is a subgraph of DT, it follows that RNG is always planar.

Together, planarity and connectedness allow calculating upper and lower bounds for the size (i.e. number of edges) of RNG. According to Euler's equation for planar graphs, the following bounds hold for the RNG of n points in two-dimensional space (Jaromczyk and Toussaint 1992): $(n-1) <= |RNG(P)| <= (3n-6)$ edges. As we explain in chapter 6, these bounds are useful for measuring network complexity in applications where the quantity of edges observed in an empirical RNG has to be compared with minimum and maximal values observed in ideal planar graphs (e.g. trees, lattices, random graphs, etc.).

Unfortunately, planarity does not hold for three or higher dimensions. Therefore, the assessment of graph complexity in those cases is not a straightforward task. Nevertheless, some studies provide useful approximate results. Jaromczyk and Kowaluk (1991), for example, determined

that the maximum number of edges of the RNG of n points in $d >= 3$ dimensions is $O(n^{3/2+e})$ for $e > 0$, where e is an arbitrary small real number. A more recent calculation, due to Agarwal and Matousek (1992), gives $O(n^{4/3})$ for RNG in three dimensions.

In synthesis, the RNG supersedes some properties of MST and inherits others from DT. Its middle position as a graph with not too few and not too many edges makes RNG a better descriptor of internal point set structure. By internal structure, we understand the 'skeleton' of the points, which is formed by those links that are 'essential' for producing a recognisable, meaningful shape in the point set. The following reasons justify such assertion:

In contrast to the MST, which by definition imposes a tree-like structure over the point set yielding one of the sparsest graphs of the hierarchy, the RNG includes more edges and responds very well not only to one but to many types of connectivity patterns, including trees and different types of cycles. This gives the RNG some advantages for describing the internal structure of point sets, especially of those lacking useful tree-like descriptions such as regular grids.

One the other side, the Delaunay Triangulation is the graph with the higher number of edges in the hierarchy. High edge-density has an adverse effect on the visualisation of patterns. Another disadvantage is that the only type of patterns retrievable from DT are 3-cycles (i.e. triangles) and its derivatives. Sometimes this triangulated picture gives a false sense of structure. In contrast, the RNG does not impose any specific type of pattern. Furthermore, RNG includes a smaller number of edges than the DT, an advantage in terms of visualisation because this produces a clearer picture of point topological relationships (Toussaint 1980a).

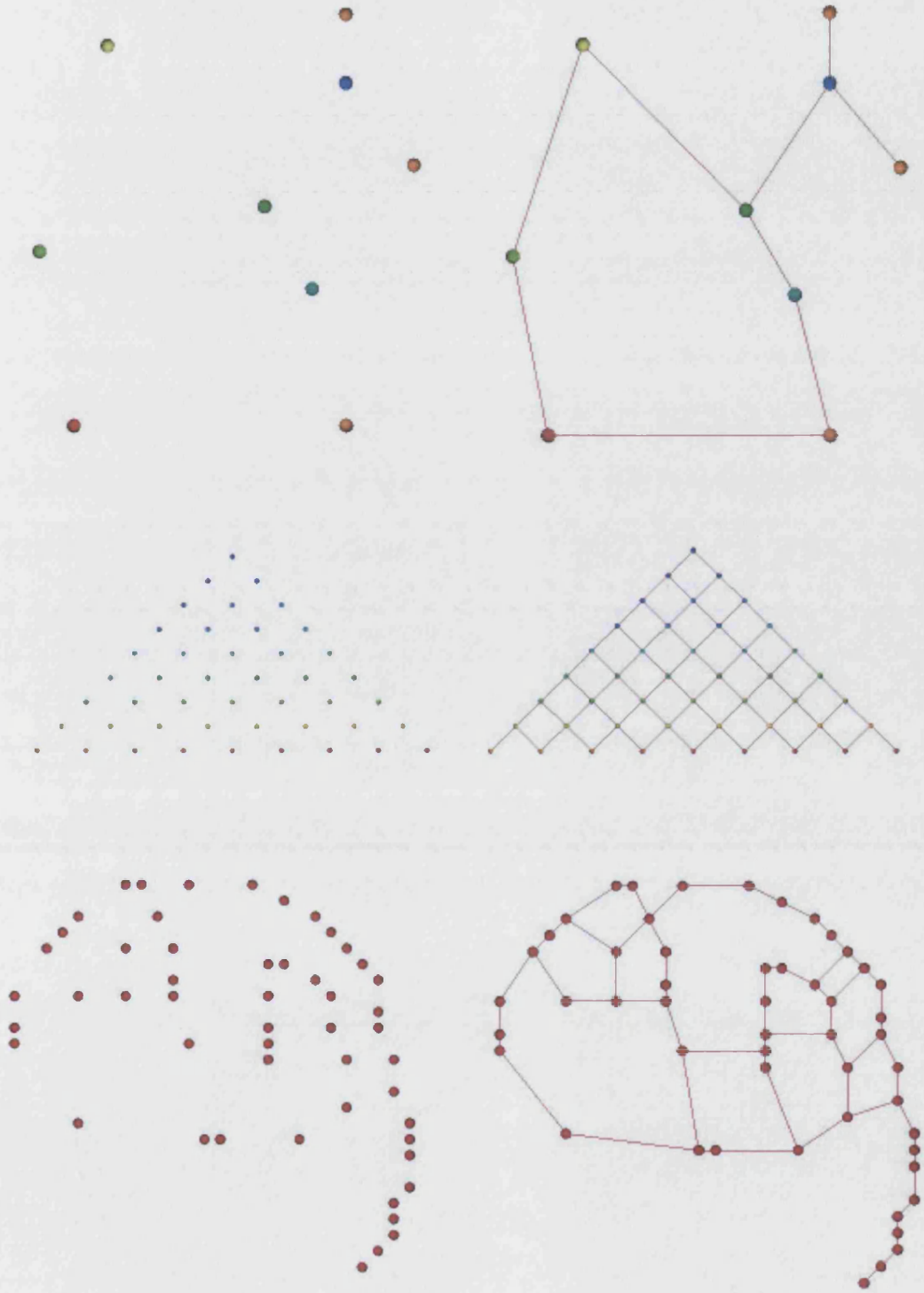

Figure 5.10. Three point sets with the corresponding Relative Neighbourhood Graph.

Figure 5.11. More examples of point sets and their corresponding Relative Neighbourhood Graphs.

As illustration of the above arguments we present figures 5.10 and 5.11, where several point sets are shown with their corresponding RNG. Notice that, in most cases, the RNG coincides with the human perception of the dot patterns.

5.7. THE GABRIEL GRAPH

A slightly different way to determine relative neighbourhood was proposed by Gabriel and Sokal (1969). This consists of drawing one circle of diameter $d(p_i,p_j)$, whose circumference passes through p_i and p_j. The test for 'region emptiness' is then performed on such a circle (G-Circle), rather than on the lune-like region. Any two points are said to be Gabriel neighbours if and only if all other points are outside their circle of influence. The procedure yields the so-called Gabriel Graph (GG) (Figure 5.12).

The inclusion of edges in a GG is a matter of checking which point pairs comply with the 'least square adjacency criterion,' expressed as follows:

Given a set of points $P = \{p_1, p_2, \ldots, p_n\}$, any two points p_i and p_j, elements of P, are Gabriel neighbours iff:

$$d(p_i,p_j) \leq min\left\{\sqrt{d^2(p_i,p_j)+d^2(p_k,p_j)}\right\} \forall\, k=1,\ldots,n; k \neq i,j, \text{and } p_k \in P$$

Where $d(p_i, p_j)$ is the distance between p_i and p_j; $d(p_i, p_k)$ is the distance between p_i and p_k; $d(p_j, p_k)$ is the distance between p_j and p_k, and n is the number of points in P.

Another equivalent definition, this in terms of angles, states that p_i and p_j are Gabriel neighbours unless there exists some other locality p_k member of P, such that in the triangle $D(p_i, p_j, p_k)$ the angle subtended at p_k is of 90° or more (Gabriel and Sokal 1969).

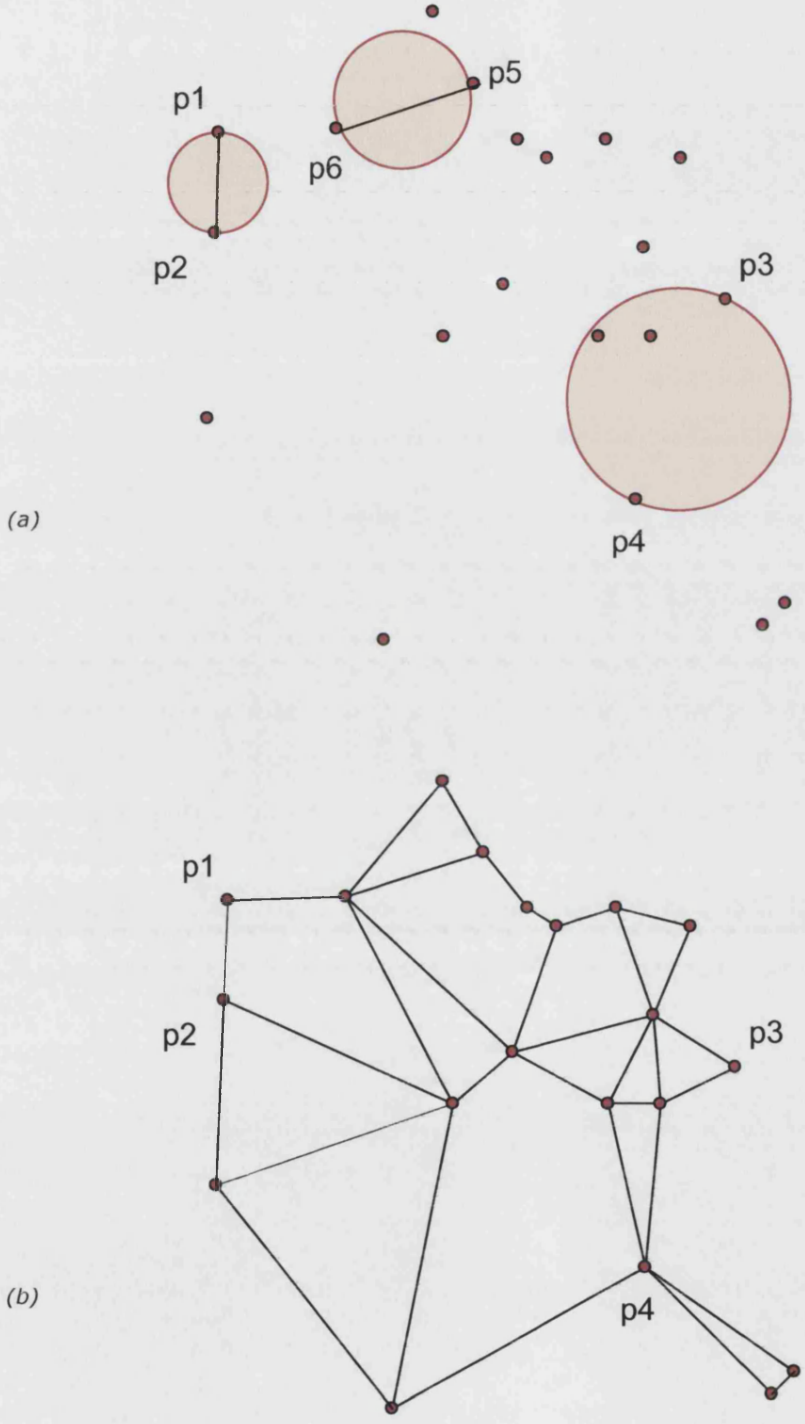

Figure 5.12. (a) Test of emptiness based on a circular region (i.e. Gabriel neighbourhood). Notice the empty regions corresponding to the point pairs (p1,p2) and (p5, p6). (b) The corresponding Gabriel Graph.

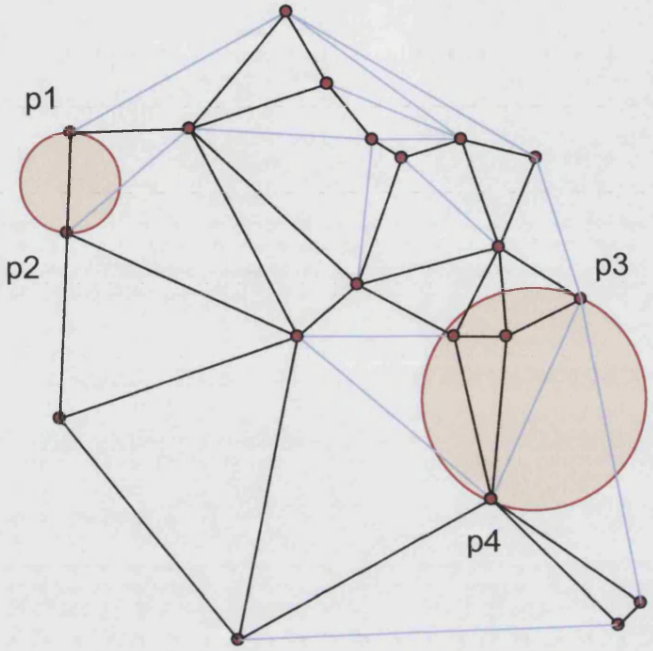

Figure 5.13. Relationships between Delaunay Triangulation (soft lines) and Gabriel Graph (bold lines).

5.7.1. PROPERTIES OF GABRIEL GRAPHS

Matula and Sokal (1980) have discussed GG geometric properties. In particular, they proved that the Gabriel Graph is a supergraph of both the Minimum Spanning Tree and the Relative Neighbourhood Graph, and a subgraph of the Delaunay Triangulation. This extends the hierarchy of proximity graphs as follows (fig. 5.13):

$$MST \subseteq RNG \subseteq GG \subseteq DT$$

Therefore, the properties of connectedness, planarity (only in 2D space), and uniqueness existing in DT and RNG also hold for GG. Simultaneously, the spatial analysis benefits of these properties, already discussed with respect to RNG, also extend to GG.

Moreover, Matula and Sokal (1980) provide more sophisticated ways to quantify graph complexity than those available for RNG. Specifically, they

suggest means to measure edge density, average size of face boundary, and planar face density. Additionally, they calculate the expected vertex degree for a set of random points in a unit square.

Calculation of those figures is based on the fact that the Gabriel Graph must have enough edges to contain a spanning tree, but can have no greater edge density than a maximal planar graph. From this, they conclude that a GG of *n* points in the plane cannot have less than *n*-1 edges (i.e. the value for MST). On the other side, a GG in the plane cannot have more than (3*n* - 8) or (3*n* - 9) edges for *n* >= 5. That means two or three edges less than the common bound for a maximal planar graph, which represents a better approximation than the figure available for RNG.

Regarding edge density, they suggest to obtain the edge-to-vertex ratio, and observe that "...any Gabriel Graph on *n* vertices must have an edge-to-vertex ratio of no less than 1-(1/*n*) and no greater than 3." (Matula and Sokal (1980: 216).

Furthermore, they use Euler's equation for planar graphs to prove that the edge-to-vertex ratio is directly related to the average size of face boundaries in a Gabriel graph and provide the following formula:

$$\mathbf{b} = \frac{2(e \div v)}{(e \div v) - 1 + (2 \div v)}$$

Where **b** = the average size of face boundaries of GG; ***e*** is the number of edges; and ***v*** is the number of vertices (generator points).

From the above formula, they conclude that:

> ...when the edge-to-vertex ratio is near the lower limit of 1-(1/number of vertices), the face boundary size is large as in the case of a single large cycle. If the edge-to-vertex ratio is near two, the average face boundary size is near four, and if the edge-to-vertex ratio is near the upper limit of three, the average face boundary is near three, so the graph is nearly triangulated (Matula and Sokal 1980: 216).

Those figures have relevance when comparing an empirical point set with some ideal regular distributions, such as trees, square grids and triangular lattices.

Additionally, Matula and Sokal (*ibid.*) adapt a common measure of graph complexity to the purposes of GG. This measure, called *planar network structure*, was originally developed by Kansky (1963), and then used by Haggett and Chorley (1969: 32):

$$\alpha(G)=\frac{e-v+1}{2(v)-5}$$

Where a is a measure of *planar network structure*; *e* is the number of edges; and *v* is the number of vertices.

The adaptation of Matula and Sokal is called *planar face density* and is given by:

$$\alpha(G)=\frac{\textbf{Number of interior faces in a GG diagram on } n \textbf{ vertices}}{\textit{Maximum} \textbf{ number of interior faces in any planar graph on } n \textbf{ vertices}}$$

Finally, there are calculations for the average expected degree of a vertex *v* in GG. For any GG constituted of *n* >=3 points randomly and homogeneously distributed on the unit square:

$$\lim_{n\to\infty} E(deg(v))=4$$

Similarly, Devroye (1988) calculated the expected degree of *v* for a GG in *d* dimensions:

$$\lim_{n\to\infty} E(deg(v))\geq 2^{d-1}$$

The above discussion proves that the Relative Neighbourhood Graph and the Gabriel Graph are better than the Delaunay Triangulation for revealing patterns closer to human visual perception. In figs. 5.14, and 5.15 we illustrate this fact comparing point sets with their GG's and RNG's.

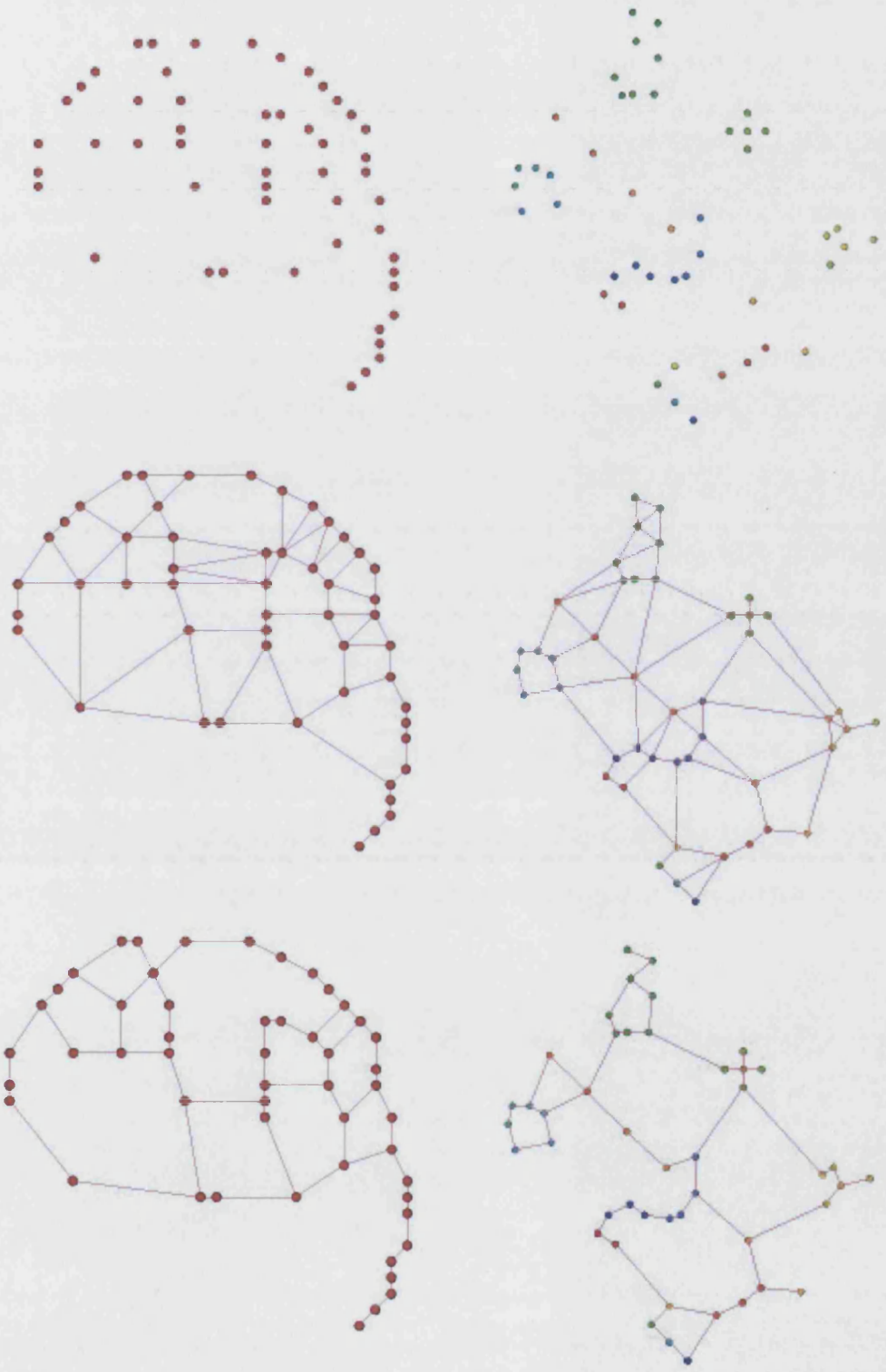

Figure 5.14. Two point sets with their respective Gabriel Graph and Relative Neighbourhood Graph. Notice the efficiency of these two constructs to reveal internal structure that matches human visual perception. This applies to any type of point distribution.

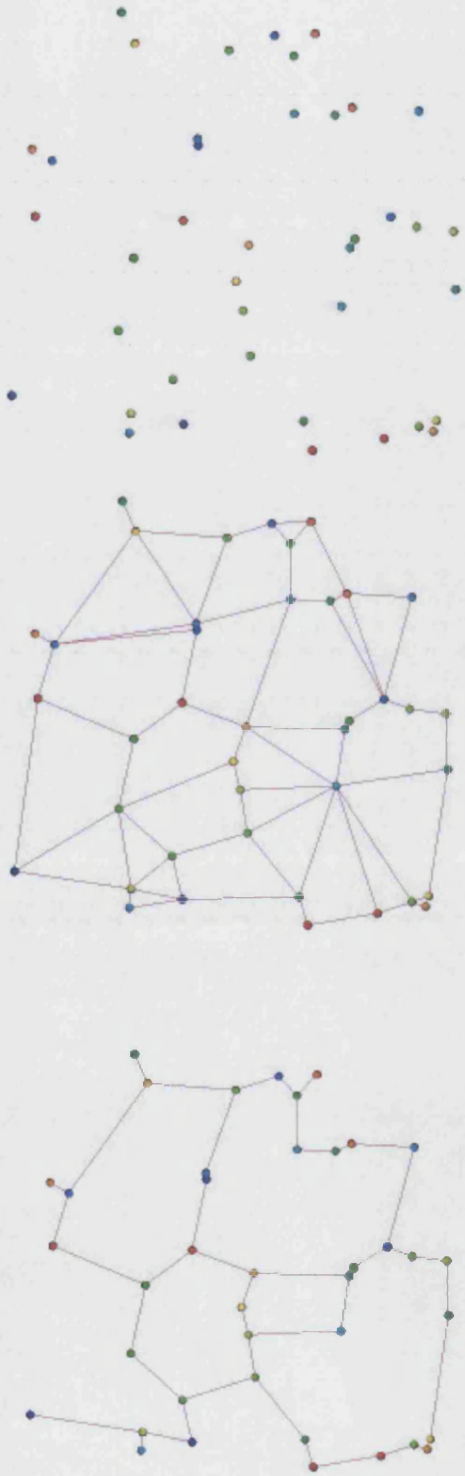

Figure 5.15. A set of random points with their respective Gabriel Graph and Relative Neighbourhood Graph. Notice the efficiency of these constructs to reveal internal structure that matches human visual perception.

Therefore they meet the two requirements established at the beginning of this chapter:

1. To quantify the structure of point sets

2. To recognise morphological traits in a visual way.

However, despite all their advantages, RNG and GG only produced a static view of the structure of the points. That is a restriction for the purposes of this thesis, because in the analysis of spatial symbolic contexts, and particularly in the study of Mexica offerings, it is required to explore different link-scenarios among the artefacts.

With the static view of point set morphology provided by RNG and GG, there is no way to determine if those graphs reflect the most significant associations in the offerings. In other words, it is impossible to know if the RNG or GG of a point set constitutes the 'necessary and sufficient' picture of significant patterns.

Besides, the offerings might include not only one, but a series of "nested" meaningful structures, which will remain invisible unless we were able to expose different levels of spatial association.

Fortunately, two variations of the relative neighbourhood concept provide an appropriate solution to this problem.

The first is based on the introduction of the parameter Beta, which modifies the size of the region of influence and produces a continuous spectrum of graphs describing internal structure (Kirkpatrick and Radke 1985: 219). The second one introduces a different parameter, sigma, which modifies the shape of the relative neighbourhood and isolates the most significant clusters within the point set (Urquhart 1982). We describe both proposals next.

5.8. BETA-SKELETONS

The first parameterised definition of relative neighbourhood is due to Radke (1982), who suggest the introduction of a value 'beta' to control the extension of the region of influence. This variant is called 'Beta-neighbourhood' (β-N).

As Kirkpatrick and Radke (1985) explain, Beta must be a positive real number (i.e. $b >= 0$). The objective is to enlarge or to reduce the neighbourhood of two points simply by changing the value of Beta.

Given a set of points $P = \{p_1, p_2, \ldots, p_n\}$, we say that p_i, and p_j are Beta-neighbours (i.e. neighbours according to the current value of the parameter Beta) if $\beta\text{-}N(p_i, p_j, b)$ contains no other point of P in its interior (see also Radke 1988).

Each value of Beta produces a graph with distinct edge density. We get a sparse graph if the value of Beta is big, and a dense graph if Beta is small. Generically, such graphs are called Beta-skeletons. A Beta-skeleton is a set of edges joining Beta neighbours for a particular value of Beta. A 3-Skeleton, for example, is a set of edges joining beta-neighbours when Beta equals 3.

According to Kirkpatrick and Radke (1985):

There is a range of Beta values, such that when $\beta = 0$, the function Beta-neighbourhood, denoted as $\beta\text{-}N(p_i, p_j, \beta = 0)$, defines the minimum region whose emptiness is a *necessary* condition to consider p_i, and p_j as Beta-neighbours.

Similarly, when $\beta \sim$ infinite, $\beta\text{-}N(p_i, p_j, b \sim \infty)$ is a large region whose emptiness defines a *sufficient* condition for p_i, and p_j to be considered as Beta-neighbours.

On the contrary, if the region is not empty, then it defines a necessary condition for the pair to be not neighbours. There are two ways to test for such relation:

5.8.1. LUNE-BASED BETA-SKELETONS

If the idea is adapted to the "lune-like" regions explained in the RNG section (5.6), the Beta neighbourhood is delimited by the intersection of two circles of diameter $\beta \cdot d(p_i, p_j)$ centred at the points $(1-\beta/2) \cdot p_i + (\beta/2) \cdot p_j$ and $(\beta/2) \cdot p_i + (1-\beta/2) \cdot p_j$, respectively. Where $d(p_i, p_j)$ is the distance between the points p_i and p_j.

Beta produces variations in the extension of neighbourhoods, as shown in figure 5.16a.

It is worth noticing that the application of Beta-skeletons does not exclude at all the possibility of retrieving the RNG or the GG of a point set. This is so because:

When $\beta = 1$ the skeleton corresponds exactly to the Gabriel Graph

When $\beta = 2$ the skeleton corresponds exactly to the RNG.

When $\beta \sim \infty$ the final graph corresponds to the MST (except in those cases where the points are not in general position).

When $\beta \sim 0$, the graph includes all pairs of points; that is, the skeleton is a complete graph.

5.8.2. CIRCLE-BASED BETA-SKELETONS

Another alternative is applying Beta to control the extension of circular regions, as explained below (also, see fig. 5.16b).

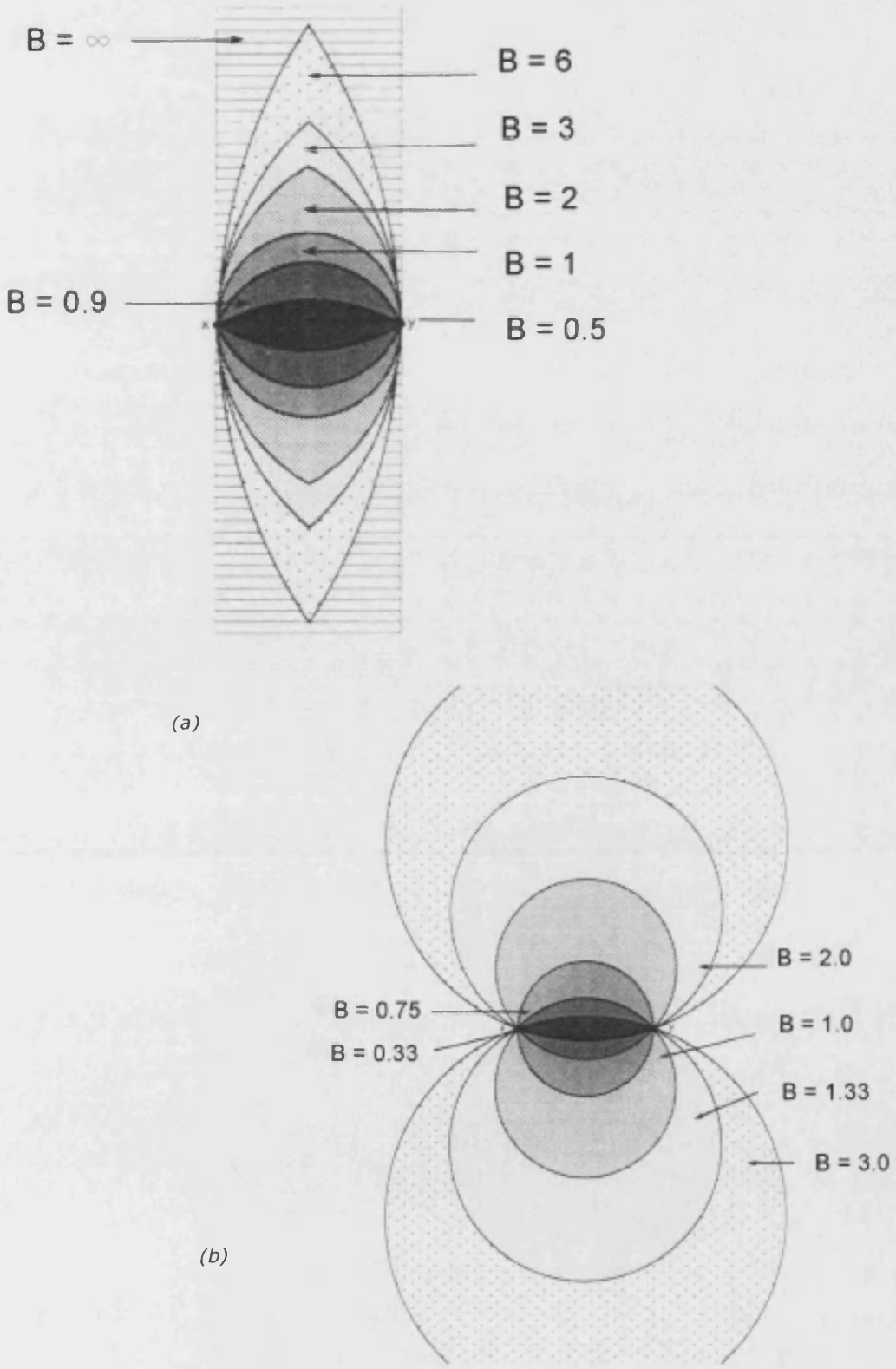

Figure 5.16. (a) Lune-based neighbourhoods for several Beta values. (b) Circle-based neighbourhoods for several Beta values. (Source: Kirkpatrick and Radke 1985: Figs. 4 and 5.

1. Within the range 0 <= **beta** < 1, the neighbourhood is the intersection of two circles of diameter $\beta \cdot d(p_i, p_j)/2$ that passes through both p_i and p_j. In that case:

When $\beta = 0$, the skeleton joins any possible pair of points.

When $\beta = 1$, the result corresponds exactly with the Gabriel Graph.

2. For any $\beta >= 1$, the neighbourhood is the union of two circles of diameter $\beta \cdot d(p_i, p_j)/2$ that pass through both p_i and p_j. Then:

When $\beta = 1$, the result corresponds with the Gabriel Graph.

When $\beta \sim \infty$ the graph is devoid of edges.

Extracting a family of Beta-skeletons for a particular point set gives us the possibility to see a "...spectrum of progressively more detailed descriptions of internal structure" (Kirkpatrick and Radke 1985). In other words:

> It allow us to visualize a spectrum of internal shapes of various edge densities. The entirety of this spectrum, including, in particular, the transitions between adjacent structures, provides an added dimension for the representation of structure. The second advantage is that it serves as a kind of benchmark with the aid of which empirical networks can be analyzed and, to some extend, compared (Kirkpatrick and Radke 1985: 222).

An example of such spectrum of Beta-skeletons is shown in figure 5.17 and the application of these is explored in full detail in chapter 6.

Figure 5.17. A point set and a series of Beta-skeletons. From left to right and top to bottom: Beta = 1.0 (GG), 1.5, 2.0 (RNG), 3.0, 10.0.

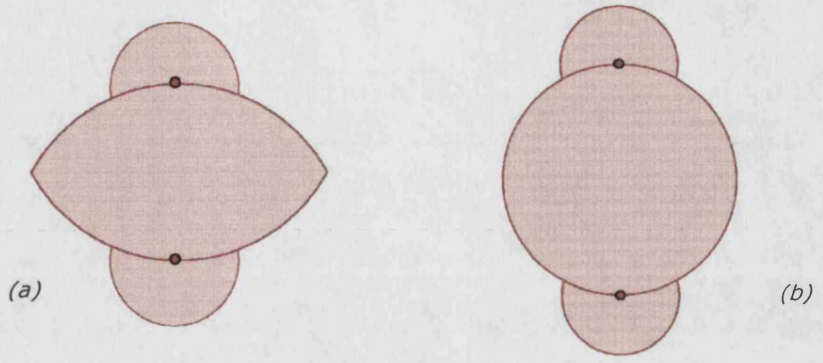

Figure 5.18. (a) Shape R_1, a limited neighbourhood derived from the RN-lune; (b) shape R_2, a limited neighbourhood derived from the Gabriel circle. Notice the addition of sigma in both cases.

5.9. THE LIMITED NEIGHBOURHOOD GRAPH

Urquhart (1982) proposes another variant of the relative neighbourhood concept adding the corresponding construct to the list of proximity graphs. This is called Limited Neighbourhood Graph (LNG). The new concept also defines regions of influence in relation to pairs of points and applies the parameter 'sigma' (σ) to them. However, instead of targeting only the extension of the regions, like the Beta-skeleton model, sigma has the additional role of defining two new shapes. These are composed by a combination of circles and lunes, as follows:

$$\mathbf{R}_2(\mathbf{p}_i, \mathbf{p}_j, \sigma) = \boldsymbol{G-Circle}(\mathbf{p}_i, \mathbf{p}_j) \cup \{\mathbf{x} : \sigma \min[\mathbf{d}(\mathbf{x}, \mathbf{p}_i), \mathbf{d}(\mathbf{x}, \mathbf{p}_j)] < \mathbf{d}(\mathbf{p}_i, \mathbf{p}_j) \forall \mathbf{i} \neq \mathbf{j}\}$$

$$\mathbf{R}_1(\mathbf{p}_i, \mathbf{p}_j, \sigma) = \boldsymbol{Lune}(\mathbf{p}_i, \mathbf{p}_j) \cup \{\mathbf{x} : \sigma \min[\mathbf{d}(\mathbf{x}, \mathbf{p}_i), \mathbf{d}(\mathbf{x}, \mathbf{p}_j)] < \mathbf{d}(\mathbf{p}_i, \mathbf{p}_j) \forall \mathbf{i} \neq \mathbf{j}\}$$

Where *Lune*(pi, pj) is a region defined on the relative neighbourhood principle; G-Circle(pi, pj) is a region defined on the least square adjacency criterion or Gabriel neighbourhood; and x is the variable representing those locations in space that defined the R shape.

R_1 corresponds to the shape illustrated in figure 5.18a, while R_2 corresponds to the region in Figure 5.18b.

The main effect of any of these two shapes is the fragmentation of the resulting graph into several components. These isolate the most obvious aggregations of points within the set. Therefore, LNG is a useful tool to analyse local patterns, complementing any knowledge given by the global ones retrieved by graphs that are always connected, such as RNG and GG.

As sigma controls local fragmentation of the graph, it is obvious that applying different values of sigma would produce a sequence of nested clusterings (Urquhart 1982: 177). Nested clusterings are the target of hierarchic methods, as opposed to the non-hierarchic. The latter ones seek a clustering that is optimal according to some criterion.

Urquhart presents evidence that his hierarchic strategy is useful as a visual clustering approach. As he characterises it: "A visual model of the clustering problem is one in which clusters are defined (...) in a way that relates to human visual perception" (Urquhart 1982: 173).

Visual clustering has a wider range of applications than other 'traditional' approaches, such as parametric methods, as well as those based on dissimilarity matrices (i.e. single-link and complete-link). Usually, the latter seek to analyse some ultra-metric property of point distributions which represent a sampled population, with the final goal of defining certain taxonomic order. The visual model, in contrast, has further applications, especially in pattern recognition. In this field, a point set is likely to represent a complete (as opposed to a sampled) population. Thus the purpose of clustering is to explore these data and to detect local morphological traits in some heuristic way. As we demonstrate in section 6.9, this latter application, rather than the taxonomic one, justify the use of LNG in the analysis of spatial symbolic contexts.

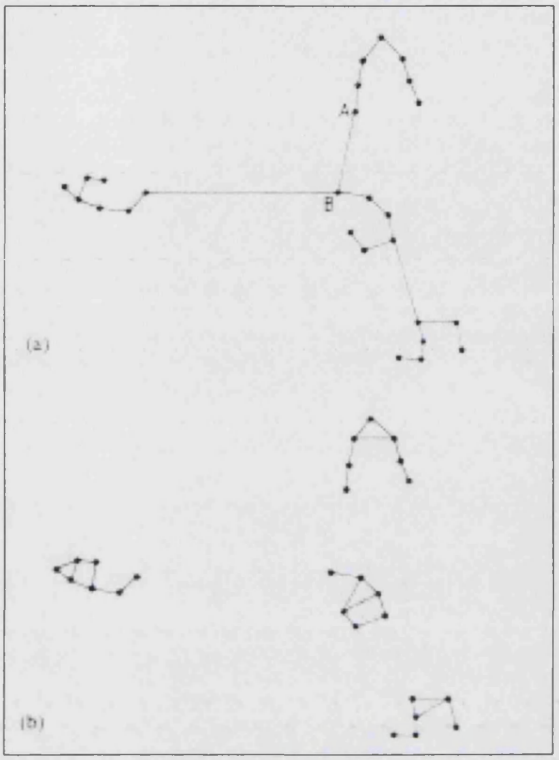

Figure 5.19. (a) A clustering with two 'inconsistent' edges (i.e. links that should not exist in the graph). (b) The LNG eliminates any inconsistent edge and at the same time includes all 'essential' edges. (Source: Urquhart 1982: fig. 2).

It is worth explaining how LNG compares with other methods of visual clustering. One of the most widely used was developed by Zahn (1971). This is based on nearest neighbour distances and Minimum Spanning Trees (see also Rohlb 1973). Zahn's approach, however, presents some major drawbacks. For example, certain clusters obtained through MST fail to break obviously inconsistent edges (Jarvis 1978; and Urquhart 1982). Inconsistent edges are those connecting two clusters that in reality should be separated (see fig. 5.19). Consistent edges, on the other side, are those that necessarily have to exist in order to define perceivable clusters, which explain why they are also referred to as 'essential' edges. Unfortunately, certain groupings detected through MST do not necessarily contain every consistent edge. Obviously, the absence of a single consistent edge may lead to an inappropriate clustering (Urquhart 1982).

Jarvis (1973) and Jarvis and Patrick (1973) tried to overcome the above problems by combining the MST approach with the concept of shared nearest neighbour. However, it is questionable whether this or other alternative solutions (e.g. k-nearest neighbours), could give the 'best' set of neighbours for representing data structure (Gowda and Krishna

1978; O'Callaghan 1975). Finally, another noticeable failure of these methods, equally related to their dependence on absolute distance concepts, is that they do not respond appropriately to variations in the density of the points. Indeed, they suffer of the so-called chaining effect, which is a tendency to artificially create clusters with "elongated" or "spherical" shapes (Bailey and Gatrell, 1995: 233).

In contrast, the limited neighbourhood concept solves many of the above problems. First, it does not assume any particular distribution of the data, nor impose a particular structure (e.g. tree or triangulation) in the clustering process. Furthermore, it allows retrieving a family of nested graphs, each one representing a specific point within a hierarchic clustering. Within this framework, sigma represents a factor of *relative edge consistency*, from which the index of dissimilarity for each clustering can be easily calculated: $d^*=1/\sigma$.

Graphs extracted with different values of sigma would immediately fulfil three important criteria of clustering (Urquhart 1982:175):

(a) Connectivity: all points within a cluster c_i E C(P) should be connected. This means that points belonging to the same cluster must be connected, while those belonging to different clusters must be separated.

(b) Consistency: for adding a new point *t* with a set of neighbours $N(p_i)$, if c_i is element of C(P) and $N(p_i) \subseteq c_i$ then there exists a cluster c'_i element of $C(P \cup p_i)$ such that c'_i is identical with $(c_i \cup p_i)$ for some partition of P. That is, if a point is recognised as member of a group of neighbours at some level, that membership should remain along the whole hierarchy containing the same group of neighbours.

(c) Local stability. Inserting a point p in cluster c_i should not affect cluster c_j, when $c_i \neq c_j$.

Consequently, the LNG is capable of detecting a much wider range of aggregation patterns than other visual approaches (Urquhart 1982: 174). In figures 5.20 and 5.21 we illustrate the range of cluster types detected by this particular method. These include not only well-separated groups, but also aggregations that exhibit local changes in point density, those with a 'bridge' connecting two subclusters, and points having a Gaussian distribution.

We conclude this chapter by highlighting the criteria that justify the adoption of proximity graphs in the analysis of spatial symbolic contexts:

1. The representation of artefact relations in the form of graphs facilitates the analysis, not only quantitatively but also in a visual way.

2. The Relative Neighbourhood Graph and its derivatives allows starting the identification of patterns without making any *a priori* assumption about the morphological features that would eventually emerge from the point set under study. Less appropriate graphs, like the Minimum Spanning Tree, forbid cycles. Others, such as the Delaunay Triangulation, only allow one type of pattern (i.e. 3-cycles). As Toussaint (1980a) points out: "...the RNG is more adaptive in the sense that it imposes less structure than either the MST or the DT" (Toussaint 1980a). That observation extends as well to Gabriel graphs, Beta-skeletons and Limited Neighbourhood Graphs.

3. Both RNG and GG satisfy the condition of being unique. That means that two or more different patterns can be compared in order to determine how similar they are with respect to each other. As

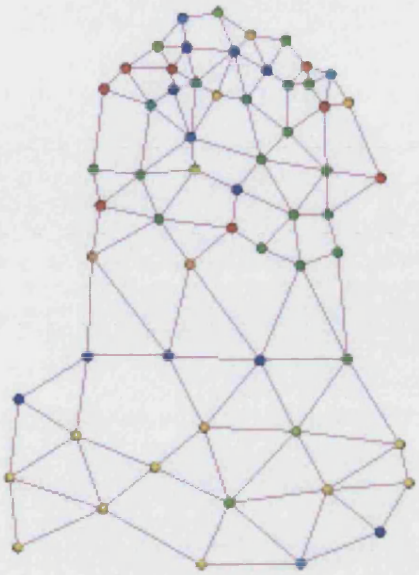

Gabriel graph of 60 points (i.e. Beta = 1)

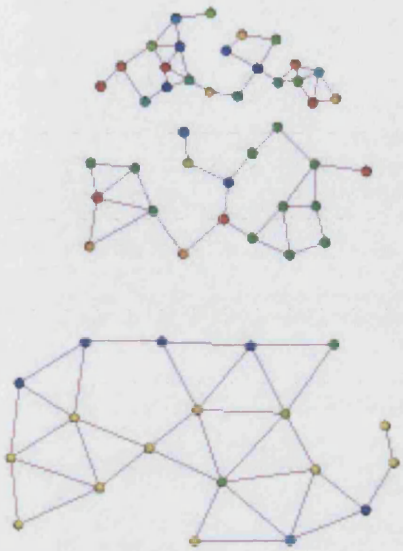

Limited neighbourhood graph Shape R1 (Beta = 1; Sigma 0.6)

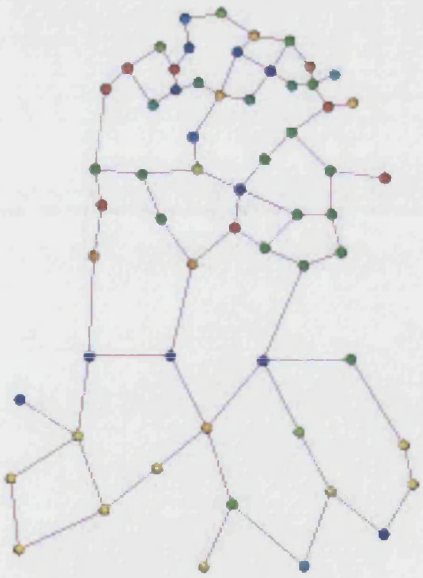

Relative neighbourhood graph of 60 points (i.e. Beta = 2)

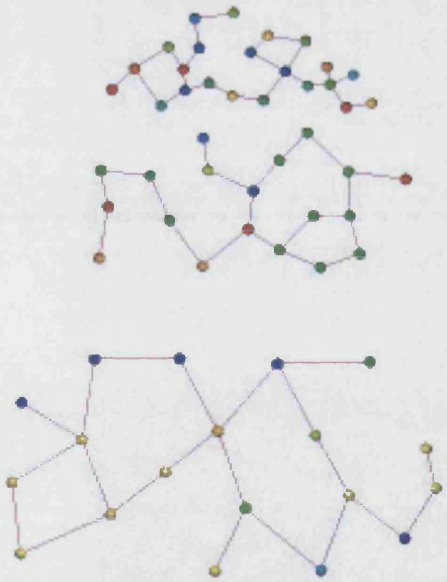

Limited neighbourhood graph Shape R2 (Beta = 2; Sigma 0.6)

Figure 5.20. Limited Neighbourhood Graphs (LNG) extracted using shapes R1 and R2, as defined by Urquhart (1982). On the left side, the GG and RNG from which the LNG's derive. Notice the effect of parameter Sigma, which despite the variable density of the pattern allows isolating clusters efficiently by the elimination of 'inconsistent' edges.

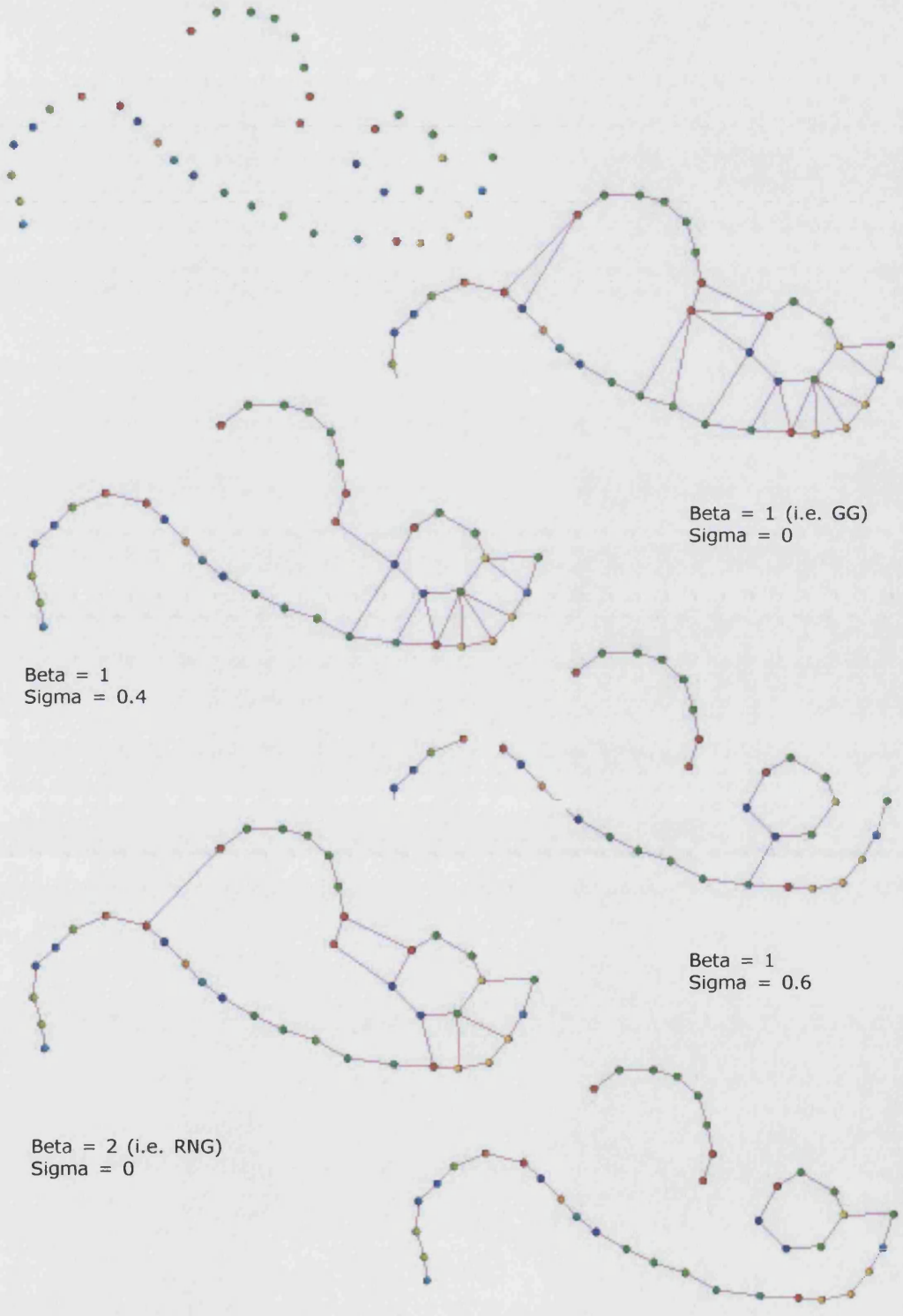

Figure 5.21. Limited Neighbourhood Graphs of a curved pattern. This illustrates the kind of exploration available with visual clustering. The form of the pattern emerges gradually, as different values of sigma and beta are applied. The graph at the bottom reveals a shape closer to human visual perception.

Kirkpatrick and Radke (1985: 218) say: "On one hand, we might like to know if two or more input sets () have the same or similar forms. Alternately, we might inquire whether the form of a single input set is regular or homogeneous, and if not, isolate the irregularities or homogeneous components."

4. The adoption of Beta-skeletons and Limited Neighbourhood Graphs brings additional benefits to the method:

   (a) Beta-skeletons allow identification of the most strong and consistent morphological features in the point set by highlighting those groups of nodes whose connections remain constant throughout changes in the region of influence.

   (b) Limited Neighbourhood Graphs on the other hand, reveal different possibilities of how the objects might be symbolically linked, attaching a dissimilarity measure to the point connections.

   (c) Together, Beta-skeletons and Limited Neighbourhood Graphs make the procedure suitable for exploratory spatial analysis.

   (d) Finally, they provide a formal way to compare systems across different levels of relative proximity.

6 THE RN-METHOD OF SPATIAL ANALYSIS

As shown in the previous chapter, a useful way to investigate the spatial structure of point sets is linking nodes that are related under the principle of relative neighbourhood. The concept involves the establishment of a region of influence for every combination of two points existing in the source data. Variations in the shape and extension of such region generate different sets of connections among the points, giving rise to several types of proximity graphs. Among the most important, we mentioned Relative Neighbourhood Graph, Gabriel Graph, Beta-skeleton, and Limited Neighbourhood Graph.

In this chapter, we apply those graphs as part of procedures to analyse spatially symbolic contexts. The approach is called the 'Relative Neighbourhood Method of Spatial Analysis', or RN-Method, for short.

6.1. PRESENTATION OF THE EXAMPLE

In order to demonstrate the usefulness of this approach, each procedure is explained using the example of three Mexica offerings.

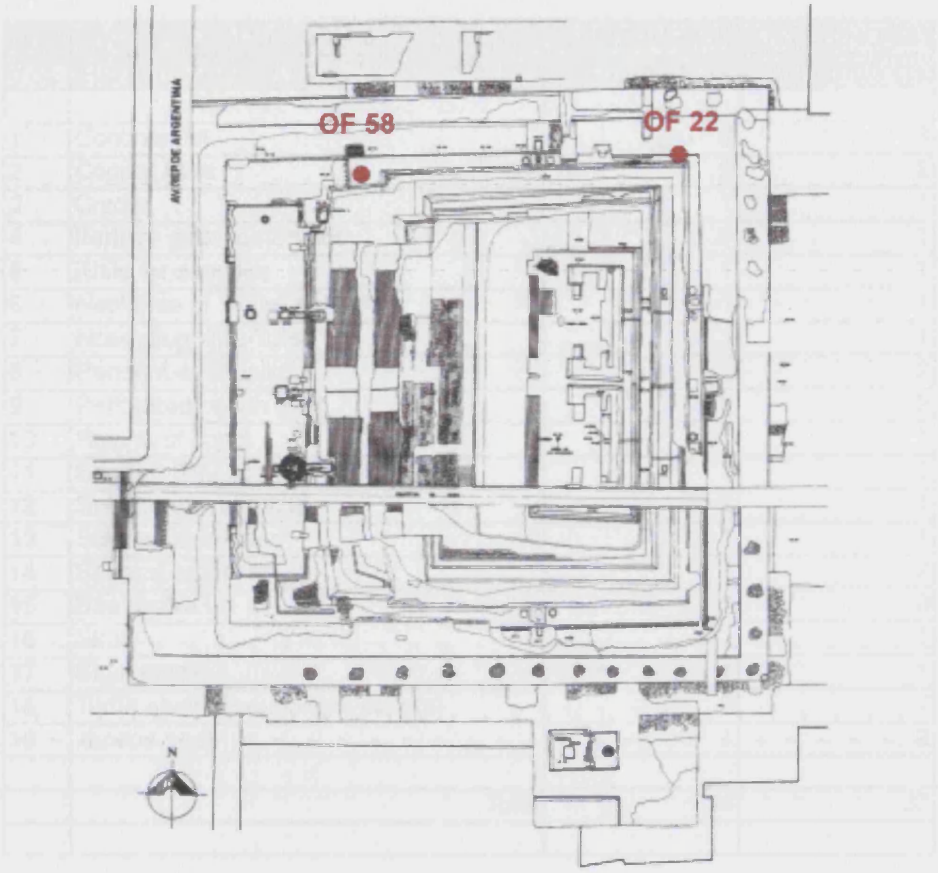

Figure 6.1. General plan of the Great Temple of Tenochtitlan, featuring the location of offering 22 and offering 58 (NE and NW corners, respectively).

6.1.1. OFFERING 22 AND OFFERING 58

The caches known as offerings 22 and 58 appeared respectively in 1979 and 1980 during the excavation of the Great Temple of Tenochtitlan. They were found on the north side of the pyramid, occupying opposite corners at the lowest platform of the building. Offering 22 measures 110 x 90 cm and was detected near the NE border, while offering 58 occupies 95 x 90 cm of space and was retrieved in the NW angle (see fig. 6.1). According to the most accepted chronology, the burial of both caches may have occurred sometime between A.D. 1469 and 1481. In archaeological terms, these contexts would belong to the fourth enlargement or 'constructive period' of the Great Temple.

	Object type	OFFERING 22	OFFERING 58
		Quantity	Quantity
1	Conch shell	6	9
2	Copper bells	2	2
3	Cradle	1	1
4	Fertility goddess on pot	1	1
5	Knife for sacrifice	1	1
6	Necklace of 7 olive shells	1	1
7	Nose-plug Xipe-Totec	1	1
8	Pendant oyohualli	2	2
9	Perforated conch shell	0	2
10	Resine of copal	1	1
11	Sawfish (Pristis pectinatus)	1	1
12	Sceptre chicahuaztli	1	1
13	Sceptre deer-head	1	1
14	Sceptre serpentiform	1	2
15	Sea urchin	5	0
16	Skull	1	1
17	Skull-mask	1	1
18	Turtle shell (Pseudemys scripta)	6	7
19	Xancus shell	1	2
	Total	34	37

Table 6.1. Object categories found in offerings 22 and 58.

Interestingly, these offerings contain similar object categories and approximately the same quantity of items: 34 and 37, respectively (see table 6.1). Among the most noteworthy objects are: human skulls, a sawfish, turtle shells, a pot portraying an unidentified deity, the model of a cradle, several sceptres, big marine shells (Xancus sp.), mother-of-pearl shells, etc.

Additionally, the offerings include certain quantities of tiny marine shells, greenstone beads and small fragments of broken artefacts. They were mixed with sand forming a homogeneous layer deposited at the bottom of each cache. This feature is common to many Mexica offerings and seems to be independent from the distribution of more meaningful items in the upper layer.

No coordinate records exist for elements found in the bottom layer, and therefore, they have been excluded from the spatial analysis. We are convinced, however, that such exclusion does not compromise the presentation of the RN-Method. In fact, the layer can be considered after analysing the topological structure of the remaining artefacts.

Some researchers have pointed out the possibility that offerings 22 and 58 contain interesting spatial features. The recognition of any pattern, however, is challenging for the following reasons:

1 *Bad graphic recordings.* Archaeologists documented offerings 22 and 58 with multiple drawings, five of which are reproduced in figures 6.2, 6.3, 6.4, and 6.5. Each drawing shows only a portion of the cache and is generally very sketchy. In consequence, acquiring a complete sense of these contexts would require overlaying three or more sketches, but even that operation would be difficult.

2 *Bad preservation.* Another obstacle for studying these offerings is that they have suffered severe damage due to deterioration processes. This is especially true in the case of offering 22, where most items appeared broken and poorly preserved.

Under such conditions it is extremely difficult to attempt an interpretation based exclusively upon direct observation. Thus, in both cases a formal method of analysis is not only desirable but necessary.

By applying the RN-Method, we will try to determine if content similarities actually match concordances in spatial layout. Hence, comparing their internal structure will be one of the main objectives throughout the several phases of the method.

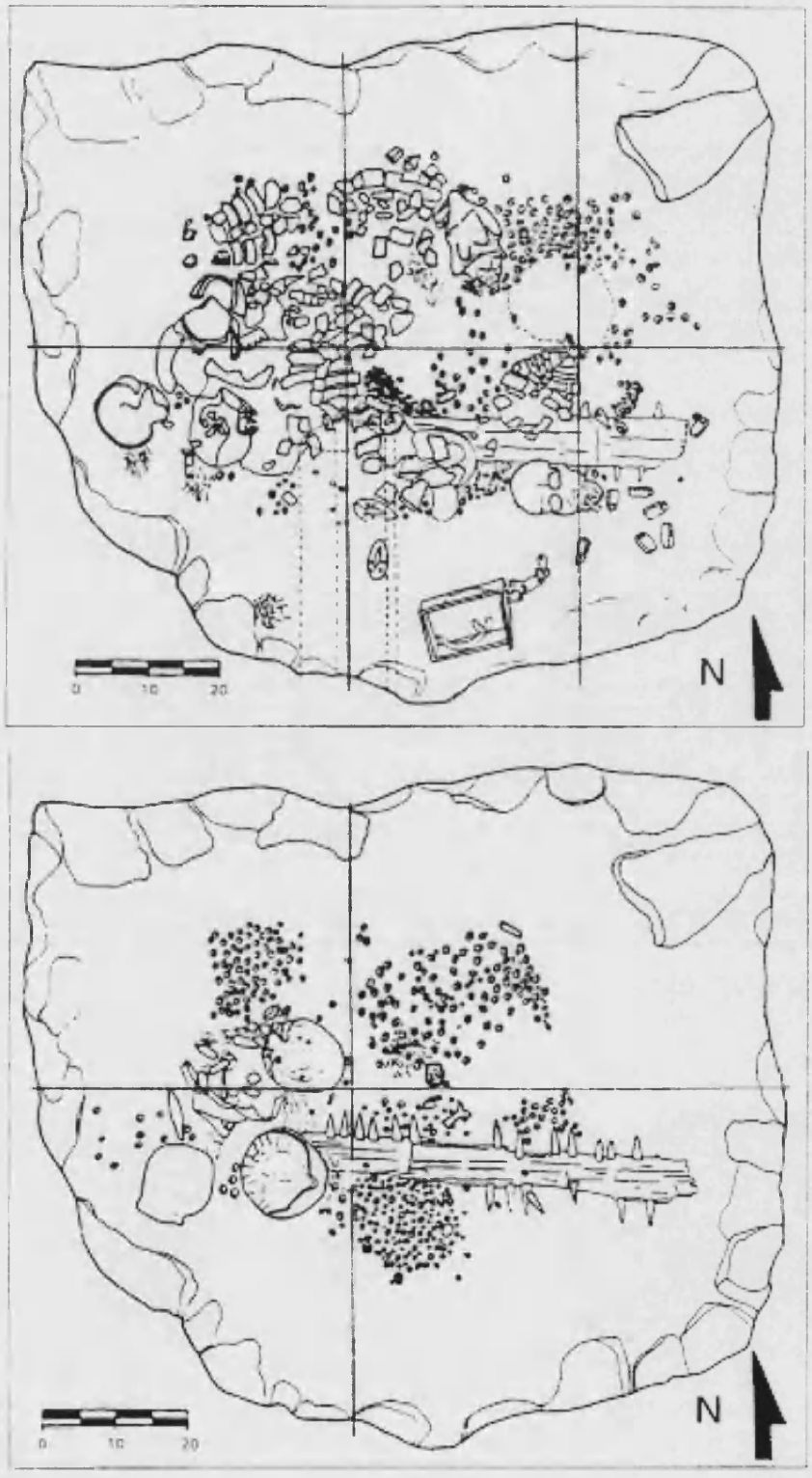

Figure 6.2. Excavation drawings of offering 22. Excavation levels 3 (i.e. shallowest) and 2.

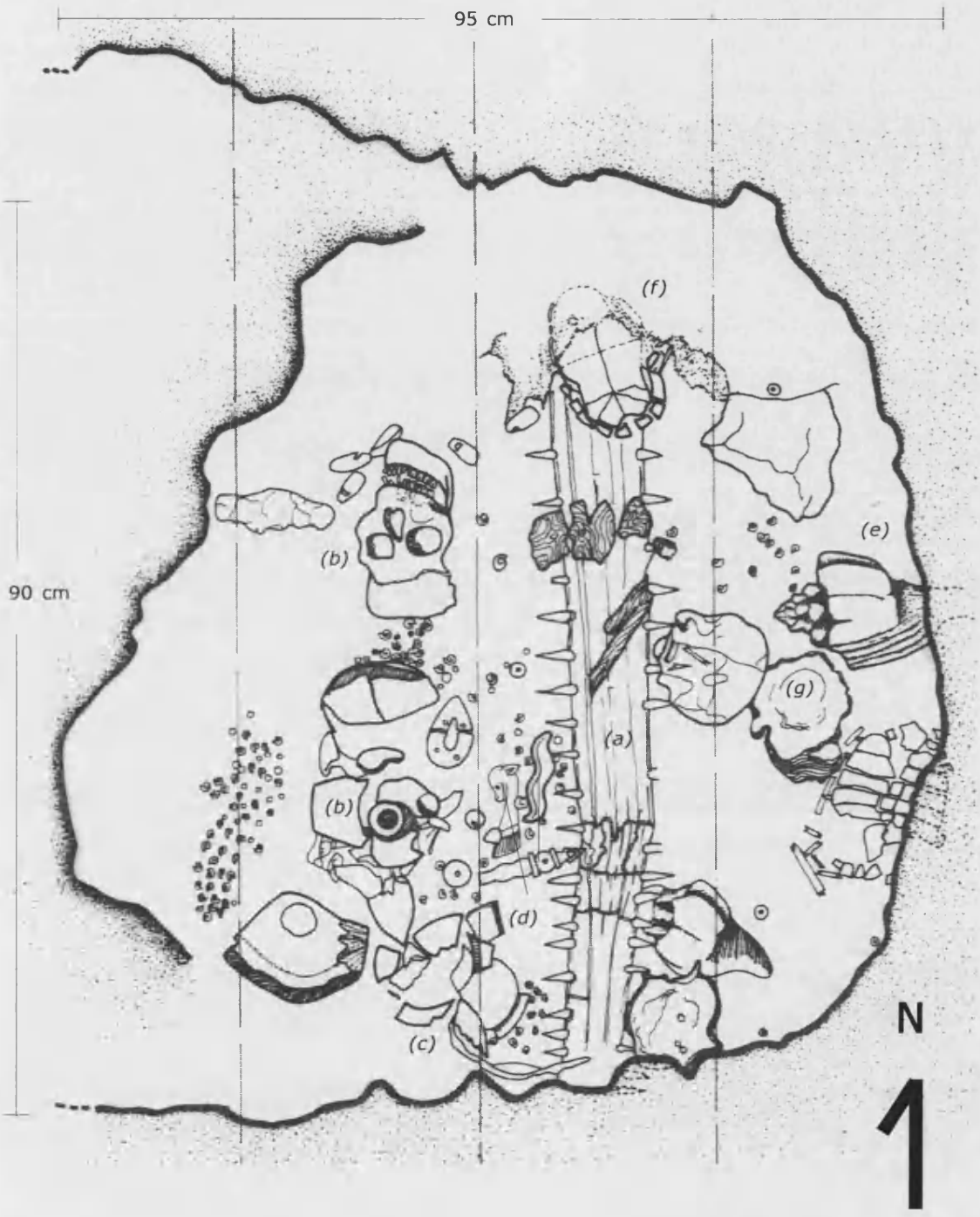

Figure 6.3. Excavation drawing of Offering 58: Excavation level 4 (i.e. shallowest). It features (a) sawfish; (b) two human skulls; (c) a broken pot with the effiigy of a fertility goddess; (d) three scepters (i.e. xicahuaztli, serpentiform, and deer-head); (e) Xancus shell; (f) turtle shells; and (g) mother-of-pearl shells.

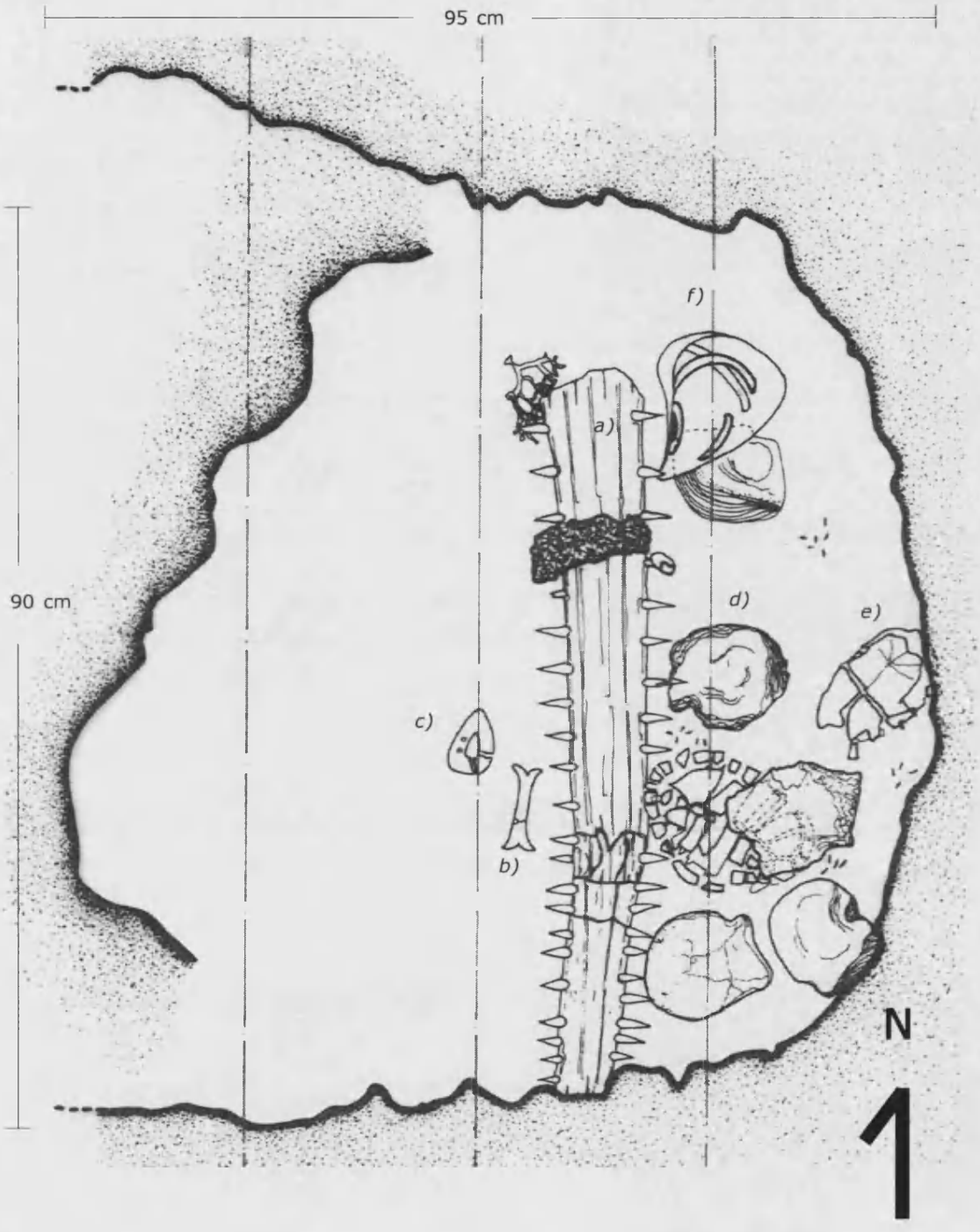

Figure 6.4. Excavation drawing of Offering 58: Excavation level 3. It features a) sawfish; b) obsidian nose-plug; c) pendant 'oyohually'; d) mother-of-pearl shells, e) turtle shells; f) model of a cradle in marine shell form.

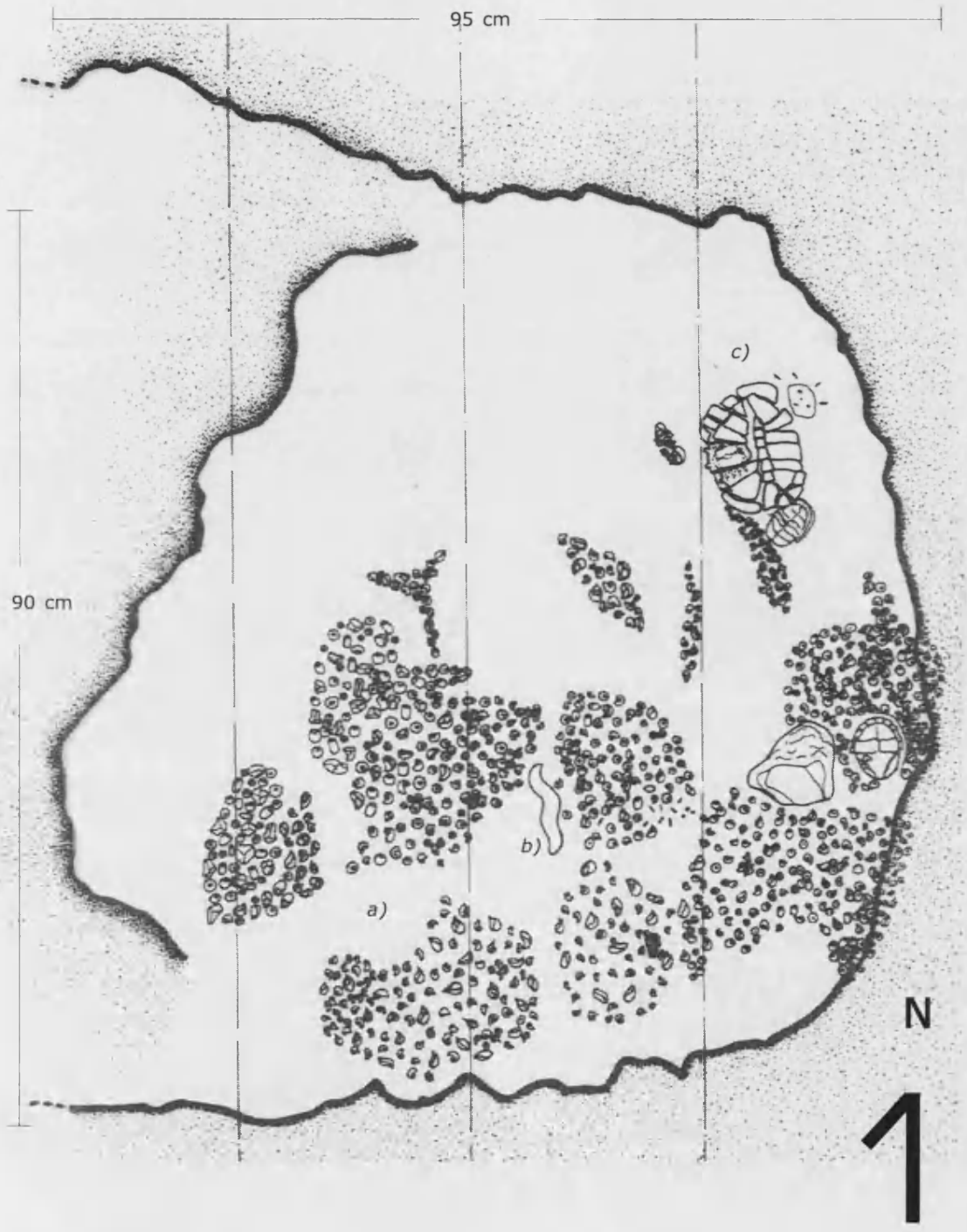

Figure 6.5. Excavation drawing of Offering 58: Excavation level 2. It features a) greenstone beads; b) sceptre 'serpentiform'; c) and turtle shells.

6.1.2. OFFERING U

Additionally, we include offering U in the example. This is a relatively simple, regular and well-known cache composed of 35 objects. The items were deposited inside a stone box, and in terms of spatial structure they appear arranged either around the corners of the container or along a vertical axis formed by a sawfish (see figs. 6.6 and 6.7).

Figure 6.6. Picture of offering U.

In a previous paper, Jiménez and Chapman (2002) demonstrated the potential of the RN-Method to expose significant patterns of this cache. Archaeologist López Luján (1998), on the other side, has discussed the evidence concerning the offering's meaning. He argues that the major spatial features observed in this offering are related to the main horizontal and vertical divisions of the Aztec model of the cosmos; the one we discussed in section 3.2.

We have chosen offering U as a 'contrasting case', because its layout and contents are substantially different from the other two. Indeed, only two features are shared by the three caches of the example:

a) The inclusion of a sawfish and Xancus shells among the contents

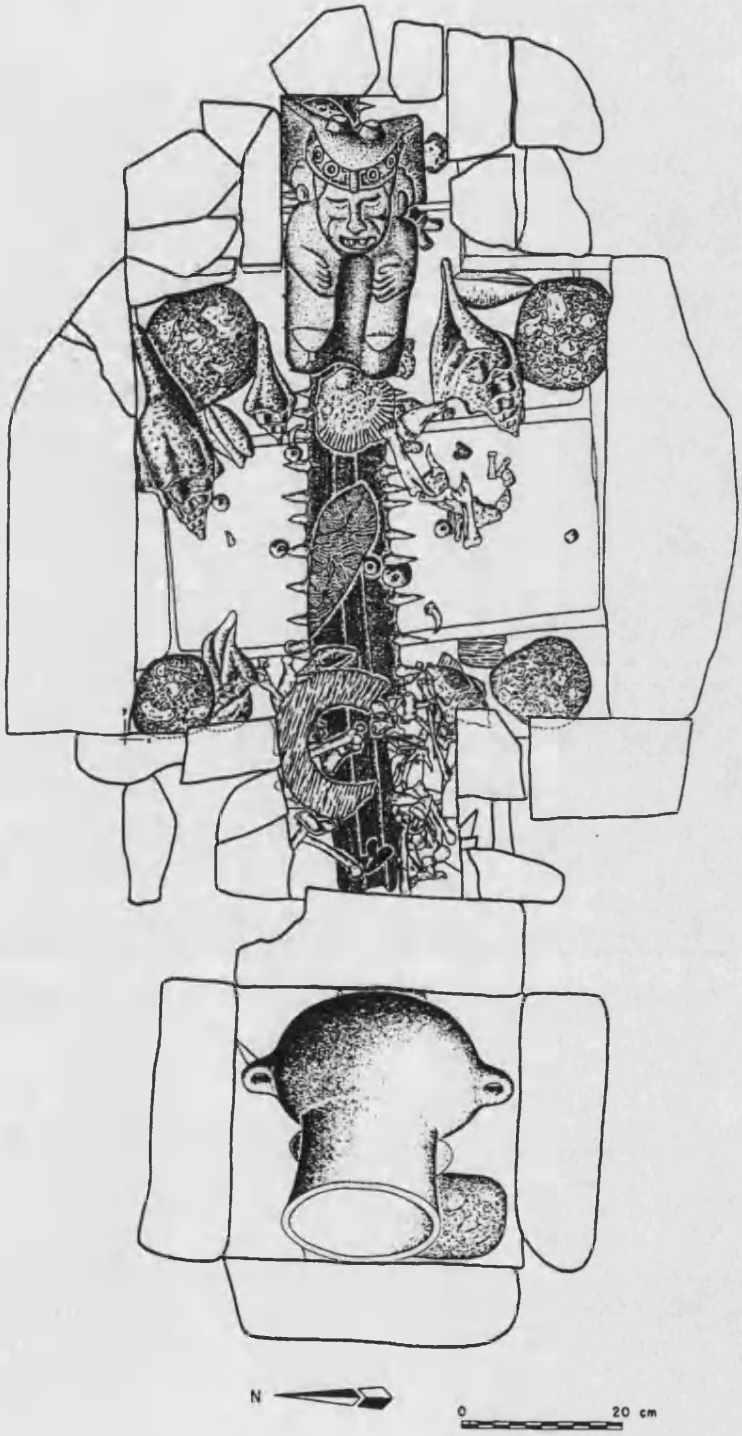

Figure 6.7. Excavation drawing of offering U. It features a sawfish, four copal balls, several marine shells, eagle and lynx remains, a pot with portray of Tlaloc, god of fertility, a sculpture of Xiuhtecuhtli, god of fire, a sacrifical knife, some greenstone beads, etc. (Drawing by Fernando Carrisoza, Museo del Templo Mayor, Mexico).

b) The existence of similar amount of objects

If the analysis method accomplishes its objectives, it must expose not only the potential similarities between offerings 22 and 58 but also their common differences with regard to offering U.

6.2. OVERVIEW OF THE RN-METHOD

The organisation of the RN-Method follows the logic of many applications of pattern recognition, computer vision and graph-theoretical spatial analysis. In these fields, analysts usually examine a problem through three different perspectives: a) morphological; b) perceptual; and c) cognitive (Toussaint 1978). Although such levels may exist independently from each other, it is appropriate to think of them as related in a sequence. This goes from the identification of purely geometric features through the perception of regularities in the connections of specific types of objects, and ends with the deciphering of meaningful spatial themes. The three levels coincide with the typical segmentation of a problem in methodological phases of description, analysis and interpretation.

The procedures of the RN-Method follow the same logic. They begin with some preliminary steps, followed by basic visualisation and the extraction of proximity graphs. The latter provide a topological description of the offerings.

Afterwards, the topological constructs are analysed, both with quantitative measurements and again through interactive visualisation. Such exploration focuses on the overall structure of the offerings (global analysis), but also on local characteristics (vertex analysis). The global procedures are appropriate for inter-offering comparisons, while the analysis at vertex

level highlights the relevance of some objects within the structure of the caches. An additional step is the application of a visual clustering technique, which allows the identification of combinatorial patterns; that is, groups of artefacts spatially adjacent, which could be significant.

The final stage consists in interpreting the spatial patterns recognised by the method using extra information provided by iconography and historic sources.

6.3. PRELIMINARY STEPS

6.3.1. COMPILING SPATIAL COORDINATES

Before the analysis procedure actually starts, it is necessary to compile coordinate records for each item of the offerings. These data, along with any other relevant information attached to the objects, should be stored in a database computer file. We suggest to use the Microsoft database format (*.mdb) since this is the most appropriate for working with the computer program supplied in this thesis. Such software is called RNG Explorer and provides most of the visualisation and analysis tools required here. The operation of the program forms the contents of Appendix B.

6.3.2. NORMALISING SPATIAL COORDINATES.

After compiling the coordinate records, it is convenient to verify that the corresponding points are in general position. As Jaromczyk and Toussaint (1992) explain, a set of points is in general position in R^d if no (d+1) of them belong to a common (d-1) facet and no (d+2) of them are cocircular or coespherical with respect to a given metric. Thus, especial attention must be given to avoid:

a) Cocircularity. In three-dimensional space, this refers to the existence of five points lying exactly on the surface of a sphere, while in 2D space it refers to four points on the perimeter of a circle. When this happens, it is advisable to correct the situation by slightly displacing one or two points, so that they no longer remain on the boundary of a perfect sphere (3D) or circle (2D). The *qhull* software, freely distributed by the University of Minnesota, includes a "joggling" routine, which can be used to normalise point coordinates.

b) Collinearity. This concerns the alignment of three (2D case), or four (3D case), equidistant points on a straight line. The above solution also applies for this case.

c) Point redundancy. Repetition of coordinates is another common problem of the data set available for Mexica offerings. In fact, in many occasions archaeologists decided to assign the same x,y,z values to 'groups' instead of individual artefacts. (A discussion of these and other recording irregularities is presented by Jiménez Badillo 1998). The solution is to disaggregate such objects getting new coordinates based upon information recovered directly from the corresponding excavation drawings.

Both cocircularity and collinearity cause the inclusion of extra edges in the Relative Neighbourhood Graph (RNG) and Gabriel Graph (GG). In contrast, when there is point redundancy RNG and GG become disconnected. Under those circumstances, some connectivity properties of the proximity-graphs are not longer guaranteed and many of the analytical procedures proposed below cannot be applied.Normalised coordinate records for offerings 22, 58, and U can be seen in the companion CD under the directory RNG_DATA.

6.4. BASIC VISUALISATION

6.4.1. DISPLAYING POINT DATA

The next step consists in plotting the normalised coordinates in order to get a first view of the point sets.

This can be done using the rendering facilities of RNG Explorer. Such a program operates in two and three-dimensional Euclidean space, providing a complete set of tools for spatial visualisation. These include options to rotate, translate and display objects in perspective or orthogonal projections.

Figure 6.8. A point view of offering U.

Figures 6.8, 6.9a, and 6.9b show frontal point views of offerings U, 22, and 58. It is worth saying that they have been rendered in three dimensions and all successive analysis will be performed in 3D space as well. As for the objects, they have been represented with points that are uniform in shape, size and colour. Each point corresponds to an individual object, except in the case of the sawfish existing in the three offerings. This element has been delineated with a series of seven points.

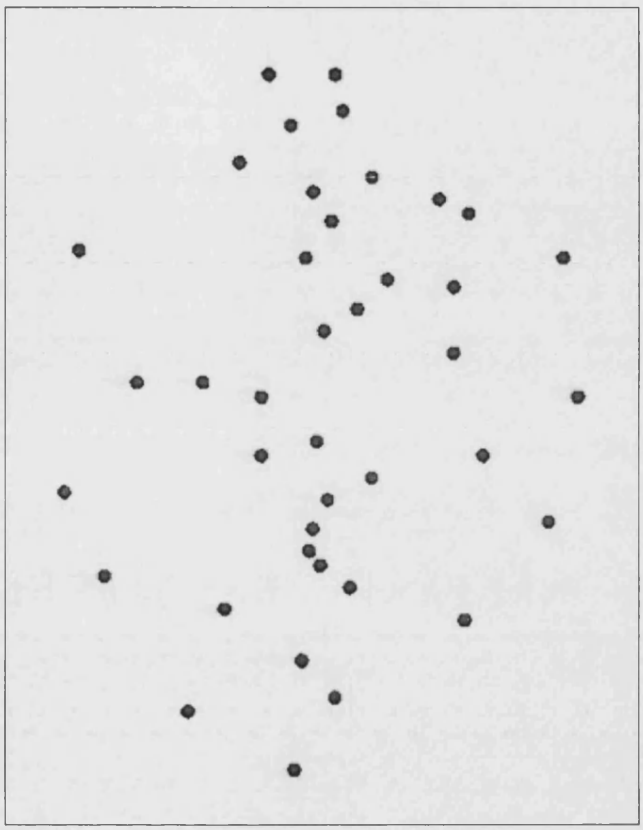

Figure 6.9a. A point view of offering 22.

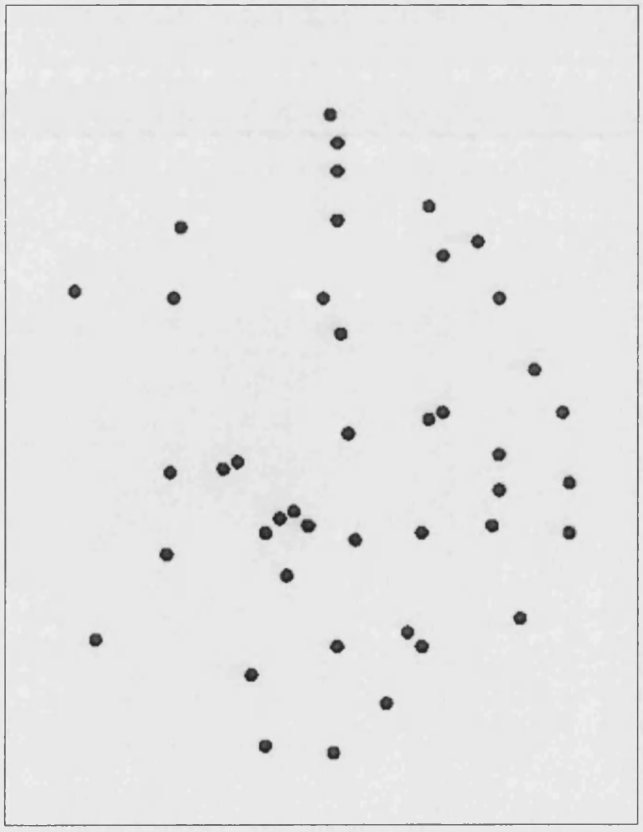

Figure 6.9b. A point view of offering 58.

Even a simple representation like this allows us observing some individual features of the caches. Offering U, for instance, shows a higher degree of linearity at the middle of the assemblage, as well as a certain concentration of items in its corners. In contrast, the other two caches seem to show only one aggregate in the lower portion, while the alignment is not as strong as in offering U. Whether or not those variations actually reflect different meanings of the caches is a question that the RN-Method would have to answer in a later step.

6.4.2. REPRESENTING OBJECT CATEGORIES WITH SYMBOLS

Further exploration is possible by producing a second view of the point sets. This time it is convenient to assign specific shapes, sizes and colours to different categories of objects. The outcome of this procedure is shown in figures 6.10, 6.11, and 6.12. It is necessary to mention that the shape and size chosen for each type of object is completely arbitrary and does not affect in any way the results of the spatial analysis procedures explained later.

These new representations of the offerings give us a better look of the location of specific categories of objects. Using the comparative display of figure 6.13, we can notice, for example, that offerings 22 and 58 have turtle shells in the right side and skulls on the left. Additionally, the aggregation detected earlier corresponds to four kinds of sceptres, elements that are absent in offering U.

On the other side, offering U shows a clear symmetric pattern formed by copal balls and Xancus shells in the corners, while different types of objects form an alignment along the vertical axis.

The above observations give the impression that offering U displays a more *regular structure* than offering 22 and offering 58, which by contrast

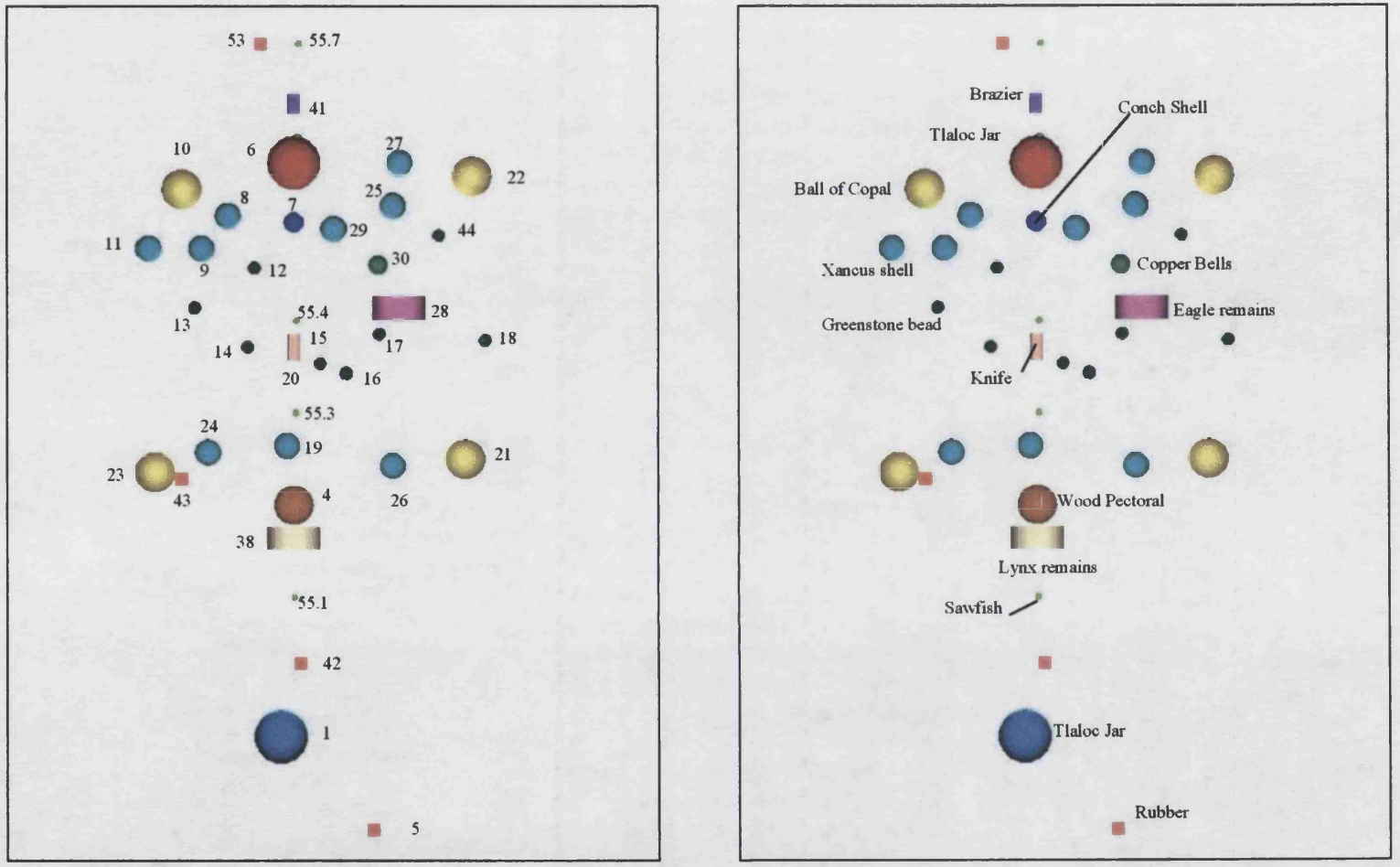

Figure 6.10. A view of offering U with distinctive symbols for different categories of objects. The numbers on the left-hand picture correspond to recording ID's, while the labels on the right-hand picture indicate object categories.

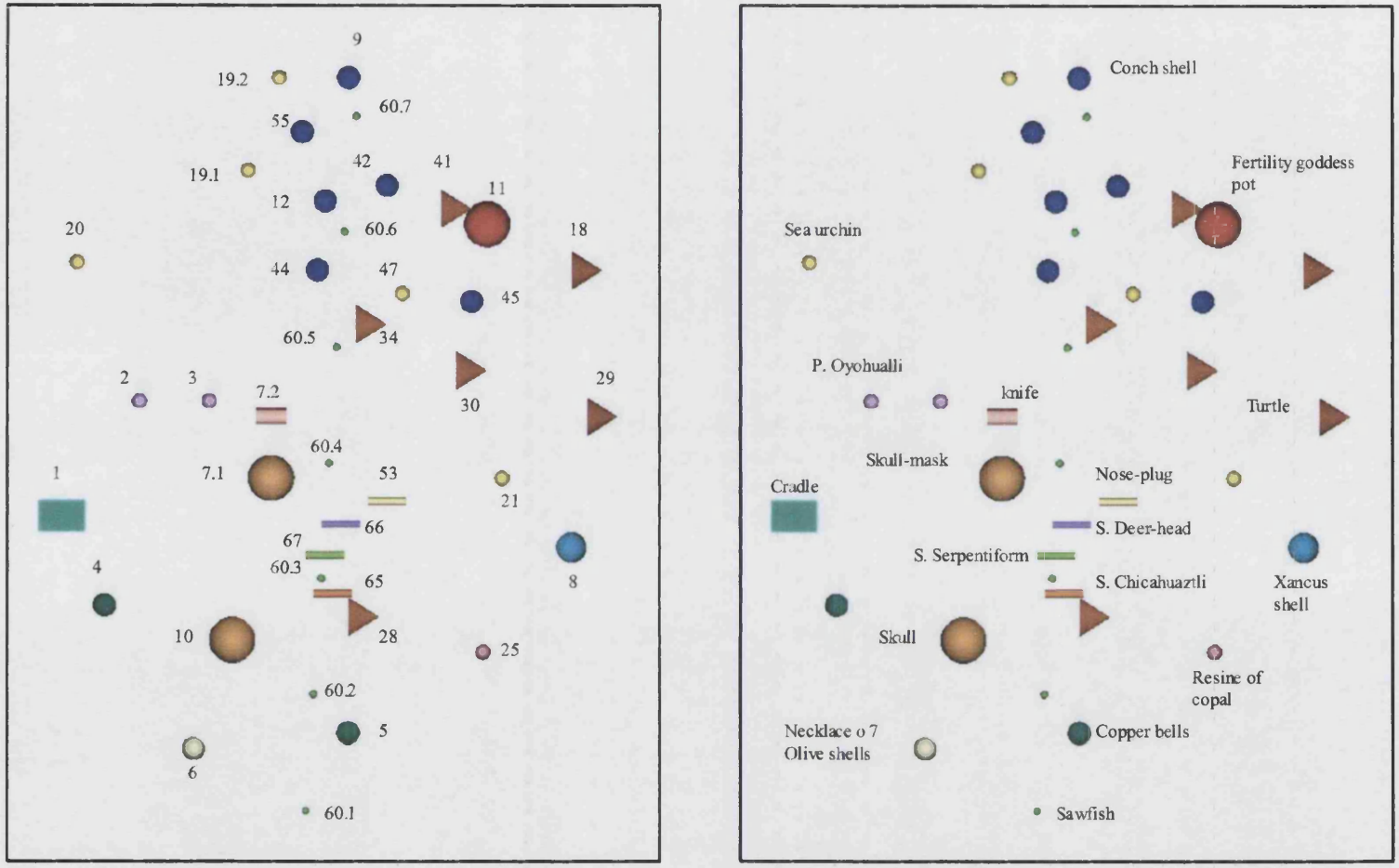

Figure 6. 11. A view of offering 22 with distinctive symbols for different categories of objects. The numbers on the left-hand picture correspond to recording ID's, while the labels on the right-hand picture indicate object categories.

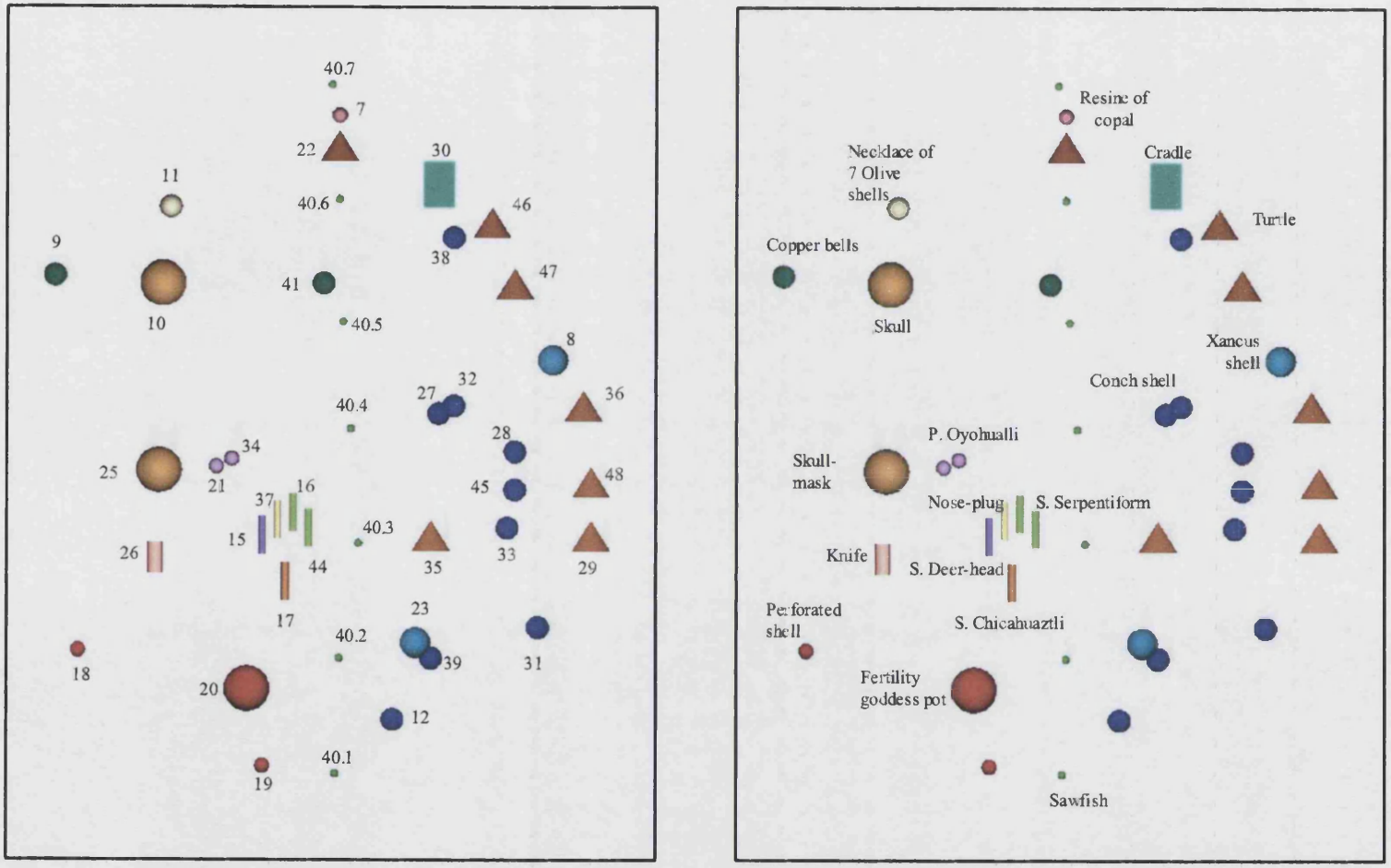

Figure 6. 12. A view of offering 58 with distinctive symbols for different categories of objects. The numbers on the left-hand picture correspond to recording ID's, while the labels on the right-hand picture indicate object categories.

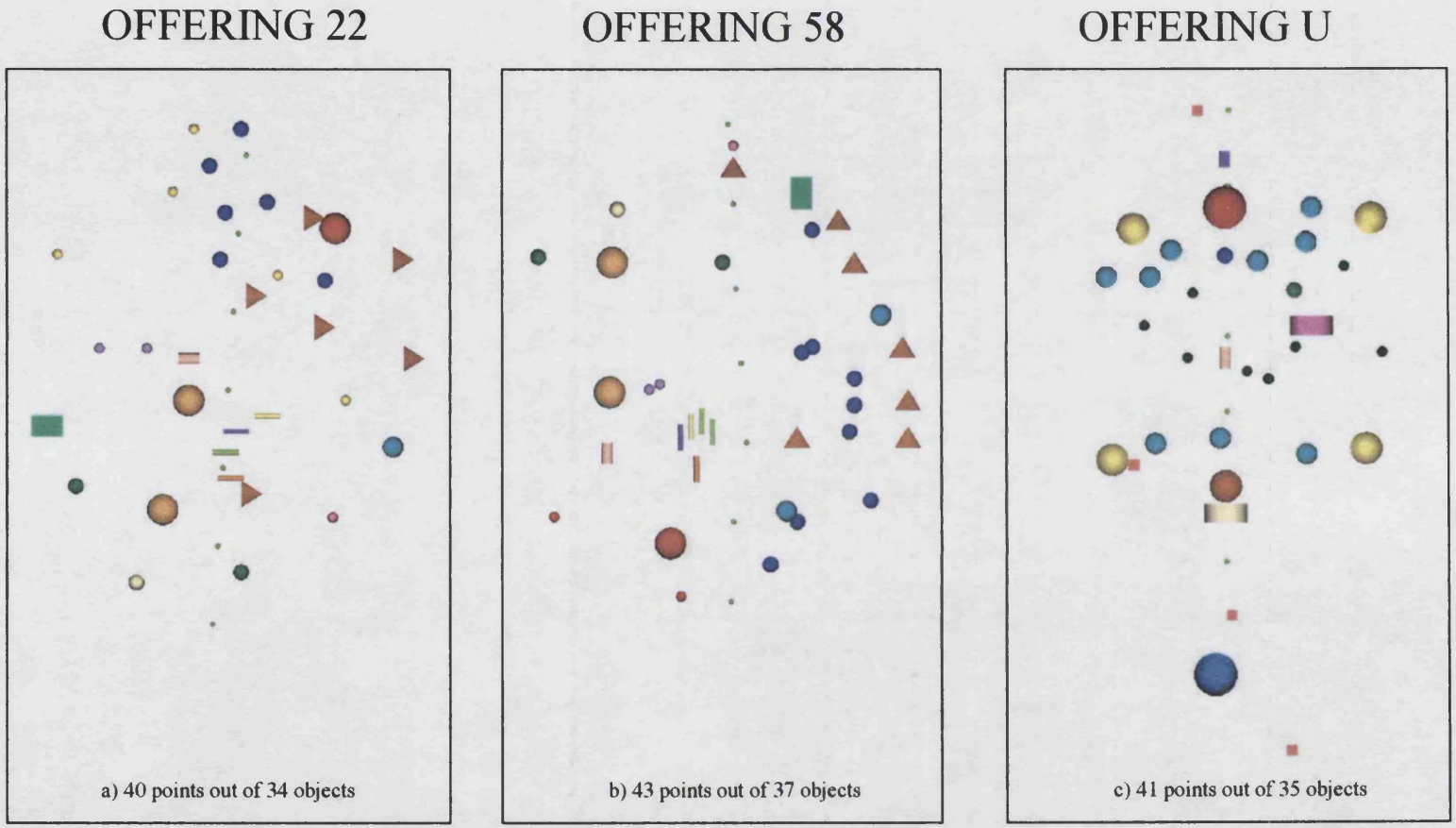

Figure 6.13. *Comparative view of offerings 22, 58, and U.* Notice the differences among the three examples despite their similar object counts: offering U shows certain degree of linearity as well as some concentration of items in the four corners. In contrast, none of those features are clear from offerings 22 and 58, except perhaps some linearity at the middle of both caches.

lead us to question whether offerings 22 and 58 have any structure at all. Such is the first question that we will try to answer in the following phase.

In order to do so, we will try to determine if they share some spatial features that relate them as closely as the similarities of their contents. If this hypothesis were true, then we need to find similar connectivity properties between offerings 22 and 58. Those concordances must exists both in global terms and at a local level. Additionally, it is necessary to find connectivity differences between each one of these deposits and offering U.

6.5. COMPUTING PROXIMITY GRAPHS

Once the preparation steps have been taken, the RNG method continues by producing a series of proximity graphs from the point sets under investigation, in the current example, offerings 22, 58 and U.

The first thing we need to decide is which type of adjacency graph is appropriate for the analysis. We are interested in graphs that expose a convenient amount of spatial relations, in other words, those containing not too many edges nor too few.

In chapter 5, we argued that using the Delaunay Triangulation would not be very useful because they normally contain too many redundant edges. This provides an excessive detail of spatial relations, complicating the observation of patterns. On the other hand, relying solely on the Minimum Spanning Tree, i.e., the sparsest connected graph of any point set, does not help much either, as this contains very few edges and provides too little information.

Therefore, instead of focusing exclusively on one type of graph we propose a broader approach, which examines graphs of variable edge-density. The best solution in our view is analysing a series of Beta-skeletons, which includes the Gabriel and Relative Neighbourhood Graphs of each offering. As explained in chapter 5, the defining function of this family of graphs uses a parameter, conventionally called Beta, which exposes neighbourhood relations among points progressively. In practice, this means that by making gradual changes to the value of Beta we get graphs revealing different levels of spatial integration within the point sets.

There are several algorithms for producing Beta-skeletons and any of them can work for such purpose. The simplest one is derived from Toussaint's RNG algorithm (1980a). We have described it in appendix A and has been implemented in RNG Explorer (appendix B). Other algorithms are more efficient, but also more difficult to implement, like the one proposed by Rao (1998).

The only rule that we impose during the current procedure is working with graphs that are connected. This means that for any two vertices of a Beta-Skeleton, say p_i and p_j, there must exist a path from p_i to p_j. The latter is no other but the normal definition of connectedness established in graph theory (Harary 1969; Hartsfield and Ringel 1994: 17). It is critical to follow this rule because the analysis performed below applies exclusively to connected graphs.

It is very important to establish beforehand the maximum and minimum values of Beta that are appropriate for extracting the Beta-skeletons. We refer to these values as *upper* and *lower* connectivity thresholds:

- Upper connectivity threshold is defined as the lowest Beta value that yields a connected Beta-skeleton with the largest number of edges in the sequence.

- Lower connectivity threshold is the highest Beta value producing a connected Beta-skeleton with the lowest number of edges in the sequence.

6.5.1. DETERMINING THE UPPER CONNECTIVITY THRESHOLD

As a convention we set the upper connectivity threshold as Beta = 1.0, which produces a proximity graph with high edge-density. We were inclined to choose such a limit because it corresponds to the Gabriel Graph. As we explained in chapter 5, this graph has been extensively studied and its properties are well known for different metrics and spatial dimensions, including of course 2D and 3D Euclidean space.

Four other reasons justify establishing the Gabriel Graph as an upper connectivity standard:

1. This function always yields a connected graph regardless of the configuration of the source points.

2. Additionally, the Gabriel Graph is "unique" in the sense that a particular set of points has one and only one Gabriel Graph. This means that a particular distribution of points cannot have two different Gabriel graphs, and therefore Gabriel graphs can be used as the "signature" of that particular point set. This is an advantage over other graphs, such as the minimum spanning tree, which are not unique and therefore cannot be used for comparison procedures.

3. A third important property of the Gabriel function is the guarantee of producing a planar graph, although this applies only when the point set is located in two-dimensional space.

4. Finally, the Gabriel graph fits the requirement of containing not too many but not too few edges.

6.5.2. DETERMINING THE LOWER CONNECTIVITY THRESHOLD

The lower connectivity threshold varies for each particular point set and therefore it must be determined on a case by case basis. The simplest way to do so is displaying the point set in RNG Explorer and trying different Beta values until finding the exact breaking point where the graph loses its condition of being connected. Be aware that such a limit is always greater than 2.0 because in all cases regions of influence within the range 1 <= Beta <= 2 guarantee the production of connected graphs (see chapter 5). Figures 6.14, 6.15, and 6.16 contain sequences of Beta-skeletons extracted from offerings 22, 58 and U, respectively.

Each series of Beta-skeletons was obtained through a trial and error process during which we applied a broad range of Beta values and then selected only those generating connected graphs.

For example, in the case of offering U we tried the following range of Beta values: {1, 1.1, 1.2, 1.3, 1.4, 1.5, 1.6, 1.7, 1.8, 1.9, 2.0, 2.1}.

From 2.0 to 2.1, the graph became disconnected, indicating that the lower connectivity limit was somewhere in between. We then refined the application of Beta values to {2.01, 2.02, ..., 2.09}. Finally, the minimum connectivity threshold of this offering was established at 2.08 because Beta = 2.09 yielded the first disconnected graph on the series. A similar procedure allowed us to determine the corresponding thresholds for offering 22 as Beta = 2.62 and for offering 58 as Beta = 2.74 (see table 6.2).

	Upper connectivity threshold	Lower connectivity threshold	Graph disconnected at:
Offering 22	1	2.62	2.63
Offering 58	1	2.74	2.75
Offering U	1	2.08	2.09

Table 6.2. Connectivity thresholds for offerings 22, 58, and U.

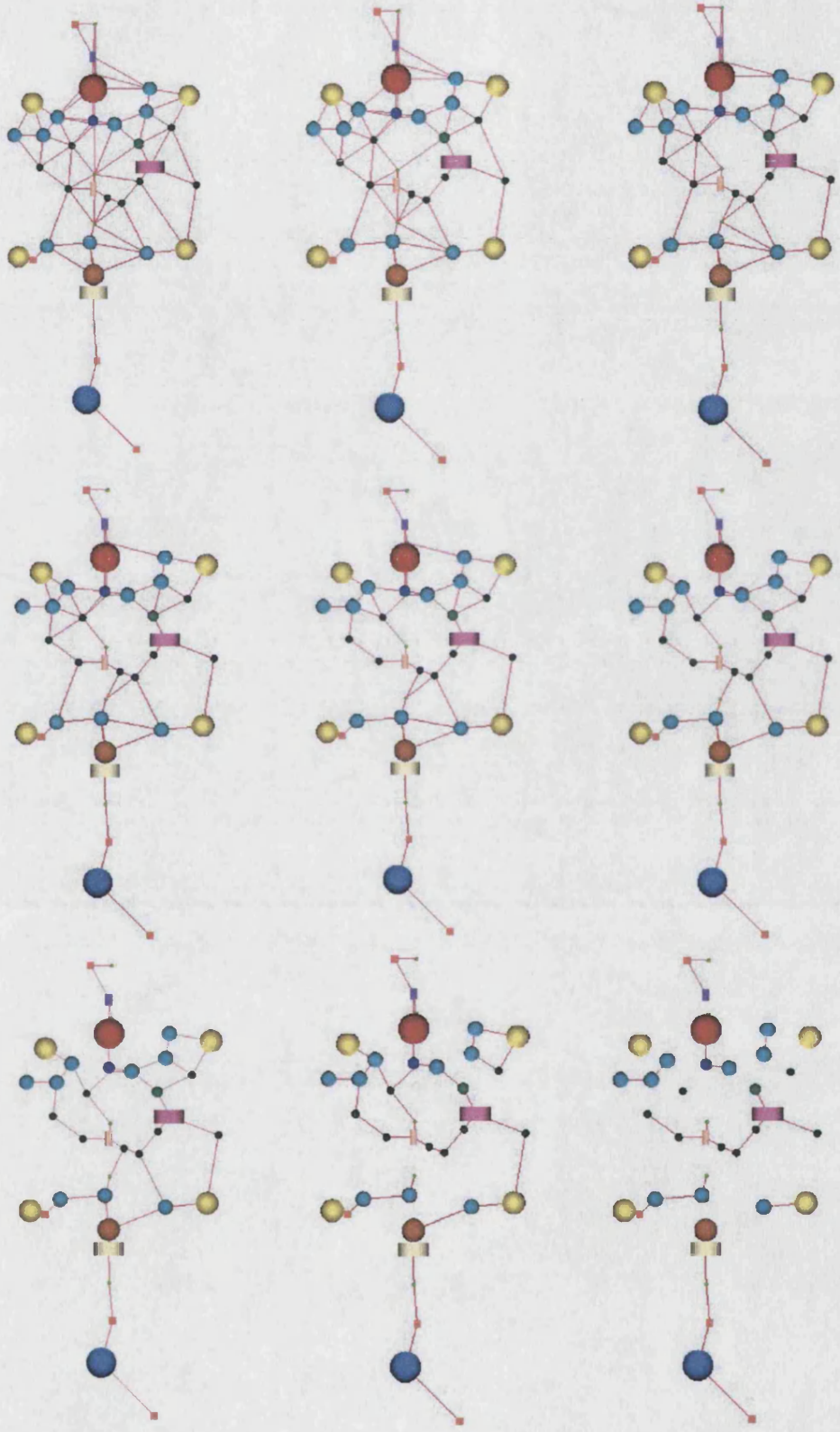

Figure 6.14. A family of Beta-skeletons extracted from offering U. From left to right and top to bottom: Beta = 1 (GG), 1.1, 1.3, 1.5, 1.7, 1.9, 2 (RNG), 2.2, and 3.4.

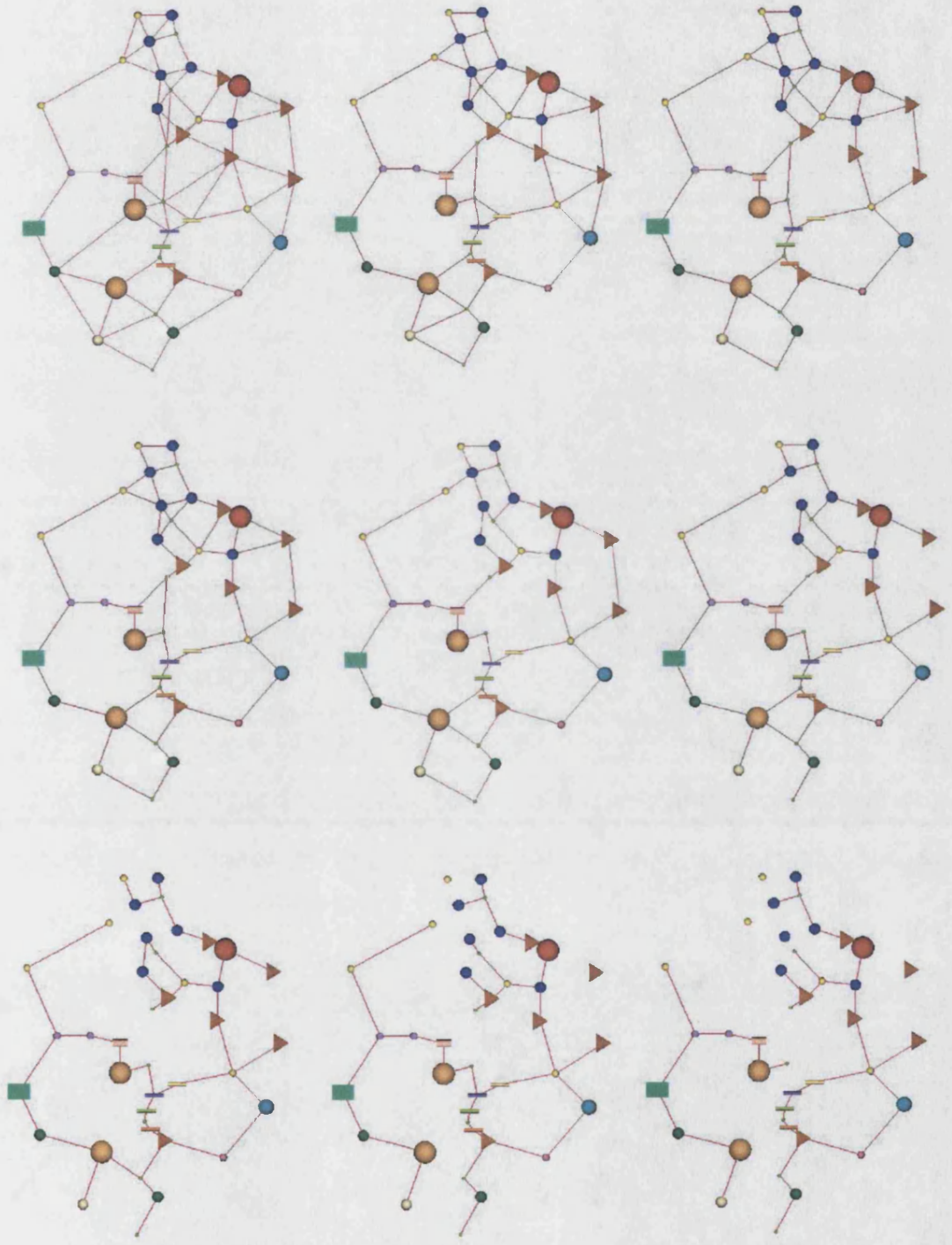

Figure 6.15. A family of Beta-skeletons extracted from offering 22. From left to right and top to bottom: Beta = 1 (GG), 1.3, 1.5, 1.8, 2 (RNG), 2.3, 2.62, 3.0, and 3.4.

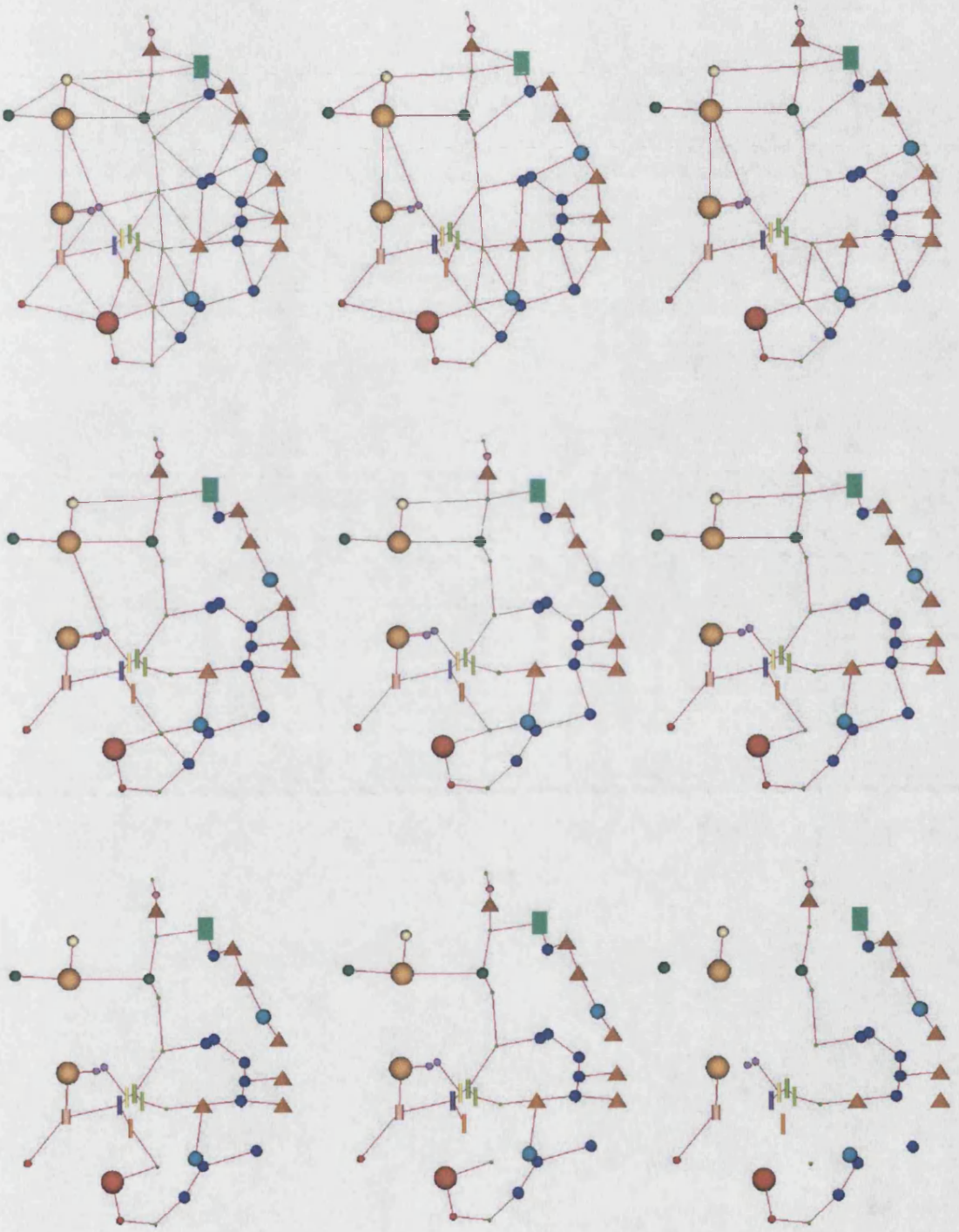

Figure 6.16. A family of Beta-skeletons extracted from offering 58. From left to right and top to bottom: Beta = 1 (GG), 1.3, 1.5, 1.8, 2 (RNG), 2.3, 2.5, 2.74, and 4.

6.6. ANALYSING GLOBAL STRUCTURE

During this step we focus on the Beta-Skeletons extracted previously in order to measure their global spatial properties. The most basic attributes are quantity of nodes and number of edges. Then we can observe other characteristics, such as the number of planar faces in 2D point sets or the number of induced cycles in 3D cases.

Additional properties include the so-called *edge to vertex ratio*. This is an edge-density measure indicating how many connections exist in relation to the number of vertices.

A similar type of measure is the *edge graph-structure:* a ratio indicating the proportion of edges actually existing within the graph in relation to an estimate of the maximum possible number of edges.

Similar measures, known as *face to vertex ratio* and *face graph-structure* can be obtained by replacing edge numbers with face or cycle counts.

This section contains brief explanations on how to measure these properties, while the next one, "Drawing connectivity profiles," presents an example of how to analyse them.

6.6.1. NUMBER OF VERTICES

Obviously, the number of vertices remains constant in every adjacency-graph of the sequence. Thus, getting this quantity requires no other operation except counting the points of the set once.

For instance, the three offerings that we are considering contain 33, 36 and 34 objects respectively, which can be denoted by single points. In addition, each offering contains one sawfish, which has to be represented as a linear arrangement of seven points. Adding up these quantities gives

a total sum of 40 vertices for offering 22, 43 vertices for offering 58, and 41 vertices for offering U (see table 6.3).

	Offering 22	Offering 58	Offering U
Vertices	40	43	41

Table 6.3. Vertex counts for offerings 22, 58, and U.

6.6.2. NUMBER OF EDGES

Similarly trivial is obtaining the quantity of edges in each Beta-skeleton (see table 6.4, p. 177). This operation, however, requires a computer program unless all the graphs are simple enough as to make the counting feasible through a human-driven process.

In order to facilitate the task we have included an edge-counting program within the tools of RNG Explorer. It is based on an algorithm known as *depth-first search*, which is a standard technique used in graph theory to visit every vertex and check every edge of the graph systematically. We refer the reader to Sedgewick (1992: 423-433), Hopcroft and Tarjan (1973) for technical descriptions of this algorithm.

6.6.3. EDGE TO VERTEX RATIO

We can perform more elaborate measurements of spatial structure using the edge counting results. One such measure involves the proportion of edges in relation to the number of nodes. It is called *edge to vertex ratio* or EVR and is given by a simple formula:

EVR = number of edges / number of vertices

The importance of this measure is that it provides a way to compare point sets of different sizes. For example, we can contrast the edge-density of a 50-vertices graph against the results of another graph, which could have 10, 120, 500 vertices or any other size.

In fact, we use this ratio to compare the spatial structure of the offerings under consideration. Remember that these are sets containing 40, 41 and 43 vertices. The variation among the first and last offerings represents a 7.5% difference. Therefore, during comparison procedures it is better to apply the EVR instead of a simple edge counting.

6.6.4. EDGE GRAPH STRUCTURE

Another interesting procedure is comparing the edge measures observed in an empirical point set with values retrieved or expected from 'ideal' point patterns. Such comparisons would be based on the following generic formulae, where EGS stands for Edge Graph Structure:

(2a) EGS = observed number of edges / minimum expected number of edges

(2b) EGS = observed number of edges / maximum expected number of edges

Both minimum and maximum expected-numbers of edges are deduced from the geometric properties of Beta Skeletons extracted from trees, square grids, triangular meshes, etc, and even from random distributions.

Regular grids do not change through Beta variations, so their connectivity profile always looks as a horizontal straight line. Therefore, it is possible to use such ideal graphs as benchmarks to assess how much an empirical graph departs from that kind of pattern.

Beta-skeletons of random point sets, on the other hand, could also be used, at least in theory, as benchmarks for testing the degree of randomness, regularity, or clustering of an empirical distribution. However, a complete statistical method has not been developed yet. One way to solve this problem would be to run a Monte Carlo simulation.

Anyone considering to develop such a method should notice the following available results:

Minimum expected number of edges. We know, for example, that a connected Beta-skeleton of *n* vertices cannot have less than *n*-1 edges. This bound corresponds to a spanning tree and stands as the minimum number of connections that we can expect in any connected Beta-skeleton. The reason is that, if we had fewer edges, then the graph would necessarily become disconnected.

Maximum expected number of edges. On the other hand, there is a maximum expected-number of edges, but such a bound has not been studied at large and therefore is not totally predictable. Devroye (1988) is one of the few scholars who has tried to solve this problem. His results indicate that the measure depends on space dimensionality rather than on the distribution itself. According to this, a set containing *n* points located in *d* dimensional space is expected to produce a Beta-skeleton containing no more than $2^{d-1}*|n|$ edges. In the case of offering 22 the expected figure would be $2^{3-1}*40 = 160$ edges and for offerings 58 and U the figures would be $2^{3-1}*43 = 172$ edges and $2^{3-1}*41 = 164$ edges respectively.

A more precise result applies exclusively to two-dimensional point sets. It was inferred by Matula and Sokal (1980:216) after observing that the Gabriel Graph (i.e. the skeleton for Beta = 1) of any 2D point set is necessarily planar. Planarity means that all the edges of a graph can be embedded into the plane without any crossings. A fundamental theorem of graph theory proves that a planar graph cannot have more than 3(*n*)-6 edges. When a planar graph reaches such a number of edges it is called *maximal*. Matula and Sokal discovered that Gabriel Graphs have normally two or three edges less than their maximal number and therefore they set the 2D Gabriel Graph's bound in 3(*n*)-8 or 3(*n*) -9 edges.

We propose to use the minimum and maximum expected figures as exploratory benchmarks to determine how close or far a graph stands from reaching both extremes.

The closest a Beta-skeleton can get to the *n-1 edges bound* is precisely when it reaches its lower connectivity limit. Some point distributions will get very close, or even reach exactly such bound, but others may stand far away.

Offerings 22, and U, for example, have 42 and 43 edges, respectively. Both figures include three more edges than the minimum possible of 39 and 40, respectively. Offering 58 is closer to its *n*-1 limit, as it has only one more edge than the minimum possible of 42 edges.

It is obvious that we will get closer to the upper bound when we reach the upper connectivity limit of the Beta-skeleton, that is when Beta = 1 (i.e. Gabriel Graph).

6.7. PRODUCING CONNECTIVITY PROFILES

In this section, we illustrate the application of the above calculations, using edge quantities of offerings U, 22 and 58, as recorded in table 6.4.

Offering	Beta value																	
	1	1.1	1.2	1.3	1.4	1.5	1.6	1.7	1.8	1.9	2	2.08	2.2	2.3	2.4	2.5	2.62	2.74
22	73	66	61	61	58	56	55	52	51	50	50	50	48	47	46	43	42	-
58	81	75	71	66	66	61	56	55	54	51	51	50	49	47	45	44	43	43
U	85	77	72	68	65	61	57	56	52	48	46	44	-	-	-	-	-	-

Table 6.4 Number of edges in each beta-skeleton of offerings 22, 58 and U.

As we can see, edge quantities vary in relation to the value of Beta used to produce each graph. Low values of Beta generate graphs with large

number of edges, whereas high Beta values yield graphs with less number of edges.

It is very important to explore deeper into this tendency in order to find out how specifically the connections change throughout Beta variations. In some cases, it may happen that tiny increases of Beta produce significant drops in the number of edges. In other situations, the numbers of connections may not change dramatically even with strong changes of Beta.

An easy way to observe those changes is drawing *connectivity profiles* of every point set under study. By "drawing profiles" we mean plotting onto a chart the observed values of certain graph property in order to reveal the form in which that characteristic behaves throughout the whole sequence of Beta-skeletons. This would allow comparing the global spatial structure of different offerings.

The group of 'profile' properties includes number of edges, number of faces, edge to vertex ratio, face to vertex ratio, edge graph structure, face graph structure, etc. Once these *connectivity profiles* are drawn, we can compare them and determine which caches have similar *connectivity behaviour*. We exemplify the procedure with edge-profiles in the following section.

6.7.1. EDGE PROFILES (E-P)

The simplest connectivity profiles are those containing edge counts. In figures 6.17 and 6.18, we use purple, green and red lines to represent the edge-connectivity profiles for offerings U, 22, and 58, respectively.

An interesting feature is the contrasting slope of the curves belonging to offerings U (purple line) and 22 (green line). Notice that despite carrying

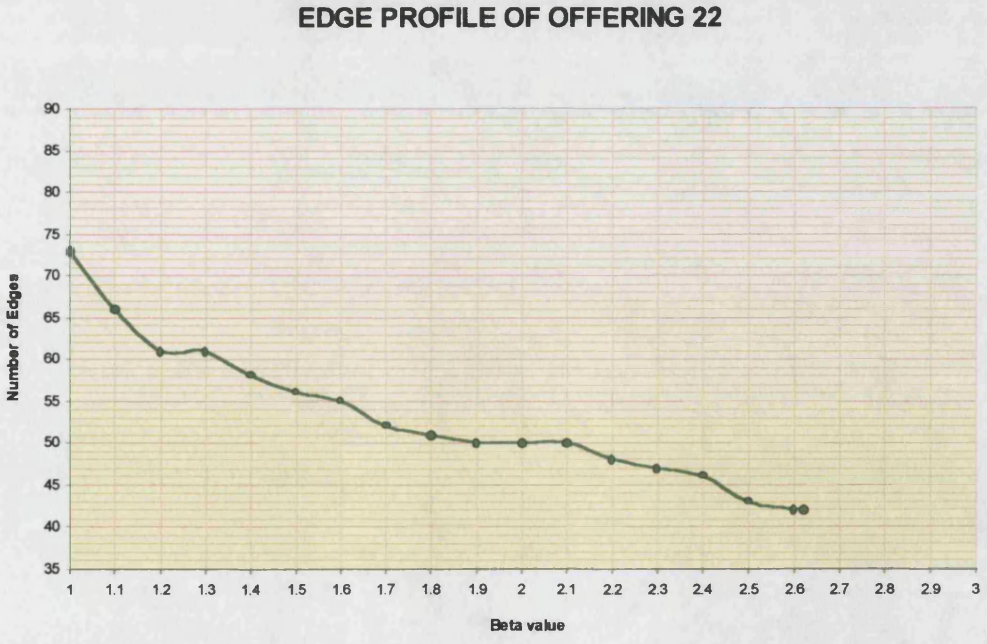

Figure 6.17. Edge connectivity profiles of offering U and 22. Notice the differences in the slope of the curves, the length, and the general shape.

Figure 6.18. Edge connectivity profile of offering 58. Notice the similarities in slope, length, and general shape with regard to offering 22 (see fig. 6.17).

almost the same quantity of vertices (41 and 40, respectively) these caches produced disparate numbers of edges. When Beta equals one, for example, offering U has 85 edges compared to 73 of offering 22. The latter figure represents 14% fewer edges than the number encountered in the former one. This figure is not suprising, because a higher quantity of edges is typical of offerings with more regular structure.

Besides, the purple line (offering U) is considerably shorter than the green and red ones, reaching its end at Beta 2.08, which is far from 2.62 (offering 22) and 2.74 (offering 58).

More importantly, the profile of offering U drops more abruptly than its counterparts, losing steadily, on average, five edges in each step of the sequence.

The only exception to this tendency occurs at Beta = 1.7 where the purple line almost remains the same.

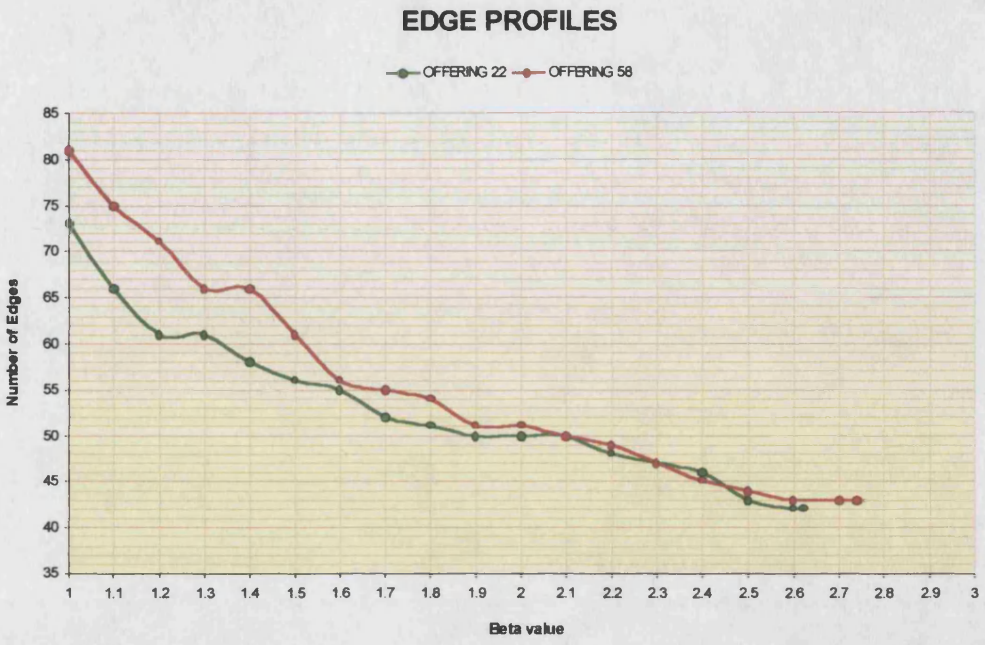

Figure 6.19. Comparison of edge profiles from offerings 22 and 58. Notice their great similarities in slope, length, and general shape.

In contrast, the curve of offering 22 (green line) drops abruptly only in the first two steps of the sequence. Then it suffers moderate losses from Beta = 1.3 to Beta = 1.6 and continues afterwards with small changes till the end.

Another interesting feature of the green profile is that it remains "stable" in several points of the sequence; that is for Beta = {1.3, 1.6, 1.9, 2, 2.1, and 2.6}.

The above observation is especially important because the same pattern is mirrored by the red profile. These comparisons are clearer in figure 6.19, where we display together the profiles of offerings 22 and 58. Interestingly, they run almost parallel. The only difference is that three "stability points" of offering 58 are displaced one step occurring at Beta = {1.4, 1.7, 1.8}, instead of Beta = {1.3, 1.6, 1.9}, as it is the case for

offering 22. The remaining stability points (i.e. Beta = {2.0, 2.1, 2.6 and 2.7}) and the general direction and length of the curves are much the same in both offerings.

6.7.2. EDGE TO VERTEX RATIO PROFILES (EVR-P)

The above tendencies become clearer if a second set of connectivity profiles is drawn using the edge to vertex ratios (see table 6.5).

EVR profiles are useful in comparing offering structures by plotting the results of two or more point sets onto the same chart. For example, figure 6.20 exhibits major differences between offering U and offering 22.

Offering	Beta value																	
	1	1.1	1.2	1.3	1.4	1.5	1.6	1.7	1.8	1.9	2	2.08	2.2	2.3	2.4	2.5	2.62	2.74
22	1.83	1.65	1.53	1.53	1.45	1.4	1.38	1.3	1.28	1.25	1.25	1.25	1.2	1.18	1.15	1.08	1.05	-
58	1.88	1.74	1.65	1.54	1.54	1.42	1.3	1.28	1.26	1.19	1.19	1.16	1.14	1.09	1.05	1.02	1	1
U	2.07	1.88	1.76	1.66	1.59	1.49	1.39	1.37	1.27	1.17	1.12	1.07	-	-	-	-	-	-

Table 6.5. Edge to vertex ratio from each beta-skeleton of offerings 22, 58 and U.

Both curves follow dissimilar paths and present a very clear intersection caused by a strong contrast of slope and differences in length.

In order to highlight such difference we overlaid tendency lines (the bold lines) using the standard polynomial formulae provided by MS-Excel. This simplifies the general shape of the curves facilitating comparison procedures. Notice, for example, that despite having almost the same number of items, offering U (purple line) starts with an EVR higher than 2.0, while its counterpart hardly reaches 1.7. On the other side, offering 22 (green line) is longer but finishes with almost as fewer edges than offering U.

The same pattern emerges when comparing offerings U and 58, though the differences among this pair are less dramatic (see fig. 6.21).

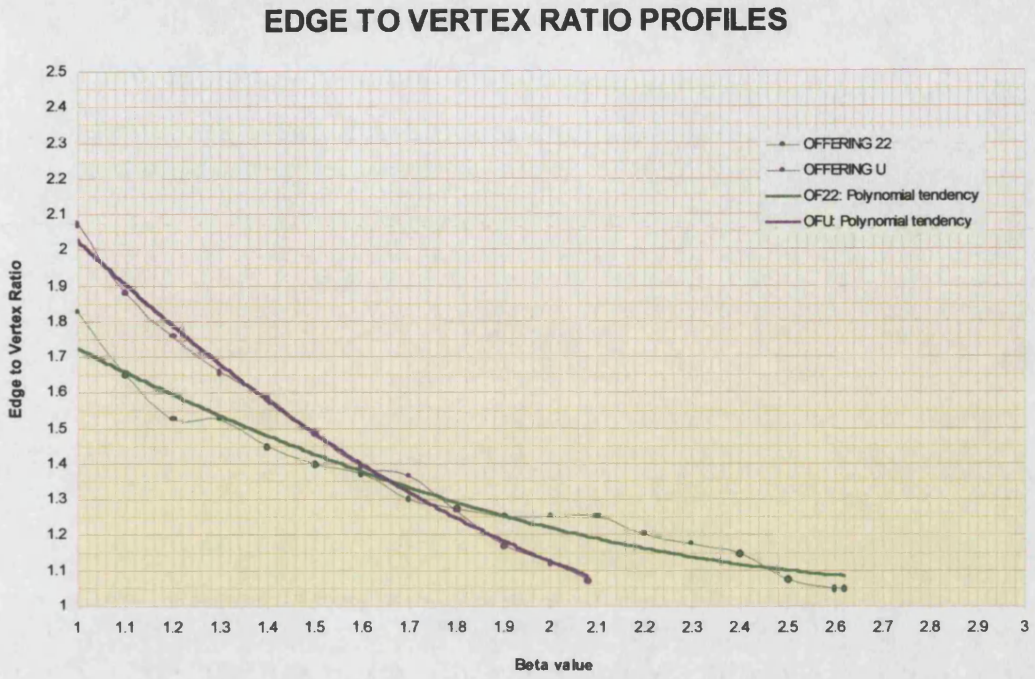

Figure 6.20. Comparison of edge-to-vertex ratio profiles from offerings 22 and U.

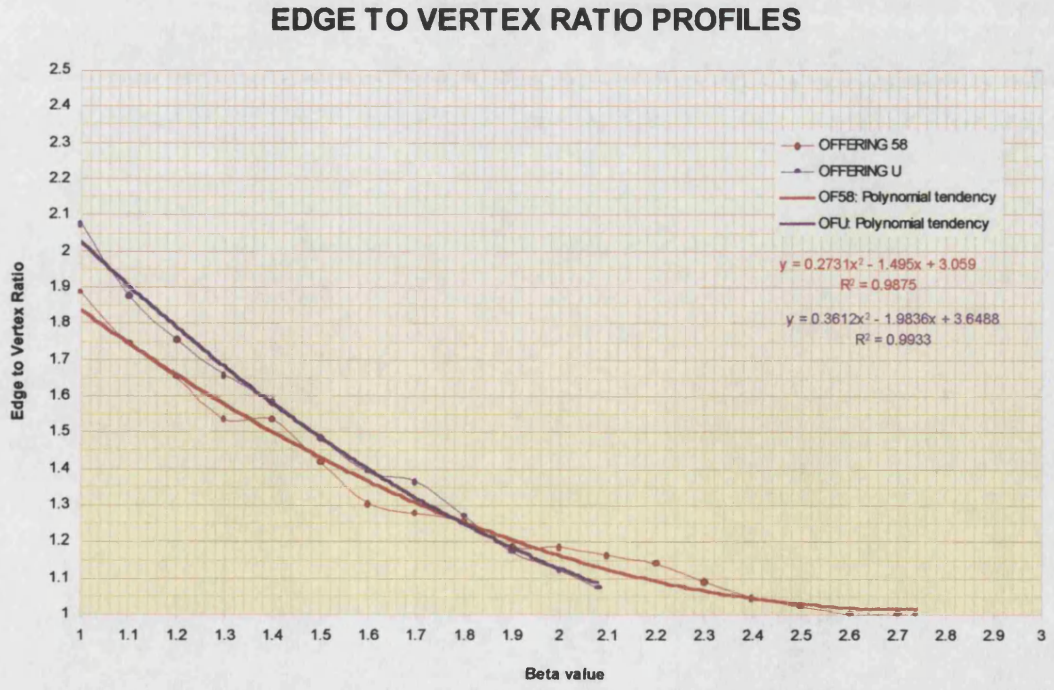

Figure 6.21. Comparison of edge-to-vertex ratio profiles from offerings 58 and U.

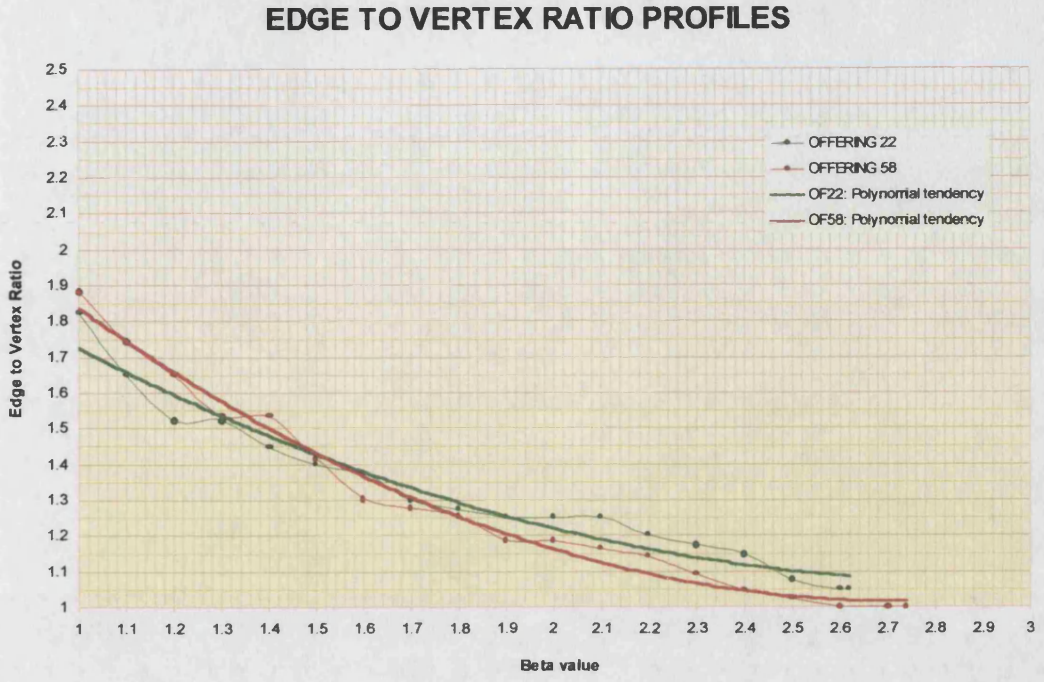

Figure 6.22. Comparison of edge-to-vertex ratio profiles from offerings 22 and 58.

In contrast, the comparison of offering 22 and 58 yield some important similarities (see fig. 6.22). The most remarkable is that they appear closer to each other in both shape and length. Both curves in fact follow mostly a parallel trajectory.

There is only a minor difference between the two. This is revealed by the intersection of both curves at Beta = 1.5, which is caused by the displacement of "stability points" referred before. However, if we displace one of the profiles to the right it is notorious that both curves coincide almost entirely.

What is the significance of these observations? Most of all, they provide a gross indication of global structural similarities and dissimilarities among

the three point sets under consideration. Concordances are stronger between offerings 22 and 58, whereas offering U represents a departure from both of them. This latter cache, for instance, shows a higher degree of linearity in the middle of the assemblage as well as certain concentration of items in its corners. In contrast, the other two caches seem to show only one aggregate in the lower portion, while the alignment is not as strong as in offering U.

This is not surprising given the fact that offerings 22 and 58 share almost the same type of objects.

Whether or not those variations actually reflect different meanings of the caches is a question that the RNG method would help to answer with additional measures oriented to discover patterns at a local level.

6.8. ANALYSING VERTEX CONNECTIVITY

The next step of the RN-Method focuses on measuring properties from the proximity graphs at a vertex level. This complements information obtained in the previous phase, when adjacency properties were explored for the graph as a whole. By measuring vertex properties we will try to assess the relative importance of artefacts situated in different locations. This responds to one of the objectives established in section 4.5.

Our vertex analysis relies on concepts originally developed by architects Hillier and Hanson in the book *The Social Logic of Space* (1984). This work is aimed at developing a new theory of how the built environment works, along with a set of interesting procedures to study it.

Despite the fact that most of the examples in that book come from the field of architecture, some ideas are applicable to other domains, especially

to those dealing with cultural phenomena that generate spatial patterns (i.e., kinship systems, rituals, etc.). We find interesting correspondences between the analysis of building complexes and the study of Mexica offerings. The major one is that in both cases the analyst faces the challenge of investigating morphological structure derived from the topology of sites.

The above justifies the adoption of certain number of Hillier and Hanson's ideas in this part of the thesis. They conceive architectural complexes as *systems of relations.* The most interesting feature of such systems is the dialectic intertwining of spatial and social relations. In order to make such a dialectic understandable, they explain how spatial organisation is in some sense a product of social structure and vice versa. On one side, settlements and buildings are human creations whose form is largely determined by social conventions. On the other side, once these complexes acquire certain layout, their physical structures influence cultural behaviour.

Within such systems, every unit of space acquires certain properties due to its adjacency and accessibility to other spaces. The latter applies both at the scales of settlement and building. Take for example a household complex. In this case, each room contributes to the structure of the premises by allowing or impeding access to neighbouring spaces. Within such a relational system, the specific role of each space depends among other factors on how accessible it is from other areas of the building. Another factor is how close or far are its neighbouring spaces and how much of the structure is controlled by each particular site. It is even more important to determine how the physical layout of the complex encodes other non-spatial meaningful relations.

Studying such questions requires an approach that provides certain degree of formality without being deterministic. For that reason, Hillier and Hanson

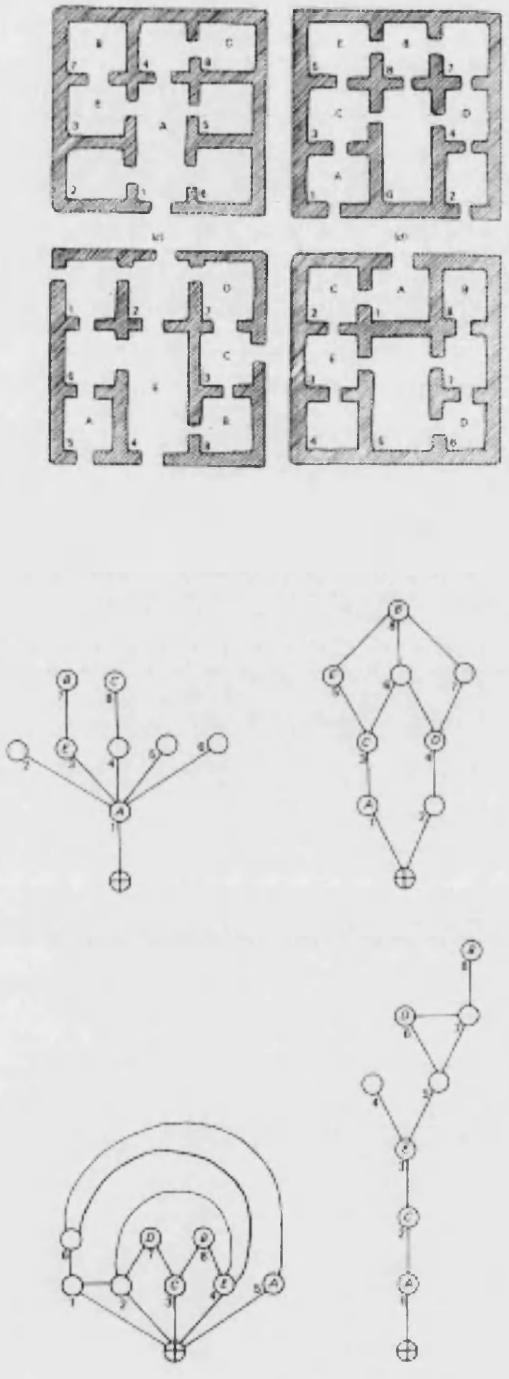

Figure 6.23. House buildings and graphs representing accessibility between rooms (Source: Hillier and Hanson 1984: 150-151,

(*ibid.*) choose a perspective that is morphological rather than statistical. They call it *space syntax*, because it involves the identification of *combinatorial spatial rules*. These are also known as *space generators,* because of their role in producing patterns of proximity, separation, spatial succession, enclosure and contiguity, all of which can exist among the elements of the systems under study. Two major steps of this approach are relevant for the RN-Method:

1. As a first step, Hillier and Hanson's method involves the extraction of an appropriate representation of the system. This is achieved using graph diagrams, which represent units of space as vertices and adjacency relations as edges (see fig. 6.23).

The solution of representing architectural systems as graphs coincides with our proposal of representing Mexica offerings as

proximity graphs. Nevertheless, it is convenient to say that the principles to generate such diagrams, that is, the definitions of neighbouring spaces, are different in each application. In the case of Mexica offerings, we use the relative neighbourhood concept, while Hillier and Hanson define relations simply by considering the actual accessibility from one place to another.

2. As a second step, they propose to analyse graphs by regarding their final form as the outcome of four types of relations: *symmetry*, *asymmetry*, *distributedness*, *nondistributedness*. These are precisely the *space generators*, whose combinations produce most of the patterns existing in empirical systems. We describe these relations before going into details of how they provide two useful measures called vertex-*integration* and vertex-*control*.

6.8.1. SYMMETRY

The relation of two vertices ***a*** and ***b*** is said to be symmetric with respect to each other if the relation of ***a*** to ***b*** is the same as the relation of ***b*** to ***a***. Figure 6.24 shows the simplest case of this situation. This occurs precisely when two vertices are directly adjacent. In Hillier and Hanson's book (*ibid.*), such relation may represent rooms sharing an entrance, but this may equally represent the direct proximity of two artefacts within the offerings studied in this thesis.

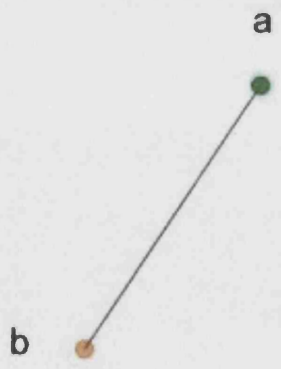

Figure 6.24. The simplest case of symmetry.

More complex examples of symmetry include arrangements of three and more vertices, as

in figure 6.25. Here, we represent vertices *a*, *b*, and *c* having equivalent relations with each other. Observe the relation of *a* to *b*, which is the same as *b* to *a*. Something similar occurs in the relation of *a* to *c* and *c* to *a*, as well as in *b* to *c* and *c* to *b*.

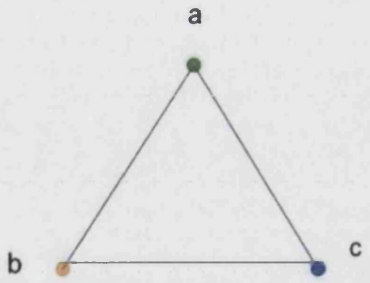

Figure 6.25. Another case of symmetry.

6.8.2. ASYMMETRY

The opposite case, namely the asymmetric relation, may appear too, both in architectural space and in the arrangement of artefacts. One example is illustrated in figure 6.26.

Compare the relation of *a* and *b* with respect to *c*. From *a* to *c*, one must necessarily pass through one intermediate vertex, in this example *b*, and therefore such connection includes two links. In contrast, the relation from *b* to *c* contains only one direct link.

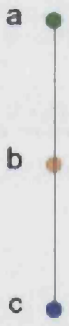

Figure 6.26. A simple case of asymmetry.

It is worth mentioning that asymmetric relations necessarily involve a sense of *depth*, that is, *topological distance*, from one starting vertex to one ending vertex. Such topological distance is measured by how many edges exist between these extreme vertices.

6.8.3. DISTRIBUTEDNESS

A third type of relation is distributedness. This is defined as the connection between two vertices ***a*** and ***c***, such that there is more than one non-intersecting path from ***a*** to ***c***. Figure 6.27 illustrates this situation. Going from ***a*** to ***c*** presents at least two possible alternatives: the first one is a direct link between ***a*** and ***c***; the second is a path passing through ***b***.

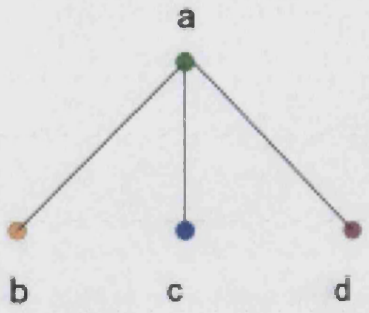

Figure 6.27. A simple case of distributedness.

6.8.4. NONDISTRIBUTEDNESS

The fourth type of relation, called nondistributedness, occurs when two vertices, say ***a*** and ***b***, are related in such a way that there is one, and only one, path connecting ***a*** to ***b***.

Figure 6.28 shows a group of vertices related in a nondistributed fashion. Notice that there is only one route to relate each pair of vertices and such path always passes through vertex ***a***.

This means that vertex ***a*** exercises some kind of *control* over the rest of the vertices. In fact, none of the vertices ***b***, ***c***, or ***d*** can communicate to each other unless they reach vertex ***a*** first.

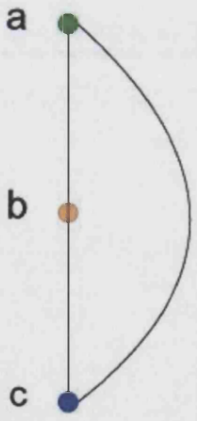

Figure 6.28. A simple case of nondistributedness

The above descriptions lead us to a useful distinction between distributed and nondistributed patterns:

1. Distributed patterns exist in systems where structure depends on a significant number of vertices.

2. In contrast, nondistributed patterns belong to systems where one or very few vertices tend 'to control' the structure.

A similar distinction can be made between symmetric and asymmetric patterns:

1. The first type arises in systems where vertices have relatively direct links to each other, causing high *integration* among the vertices of the structure.

2. Asymmetric patterns, on the other side, arise in systems where most vertices are only indirectly connected to others, involving one or more intermediary vertices in their paths. Because of such asymmetry, some vertices become *segregated* with respect to others (Hillier and Hanson, 1984:14).

Therefore, symmetry versus asymmetry equals *integration* versus *segregation*, while distributedness versus nondistributedness equals *control* versus *dependence.*

These relations may not only describe spatial arrangements, but interestingly they may duplicate symbolic relations as well.

Symmetric relations, for example, would reflect arrangements of elements holding certain amount of cohesion, unity, solidarity, etc. Alternately, asymmetric relations would identify those elements estranged by isolation, separation, confinement, exclusion, etc.

Likewise, distributedness would reflect cases of lower hierarchy, subordination, dependence, etc., while nondistributedness would reveal elements of higher hierarchy, control, power, authority, domination, etc.

Obviously, empirical systems such as architectural complexes or Mexica offerings do not contain exclusively one type of relational pattern. On the contrary, they embody a finite number of combinations of symmetry, asymmetry, distributedness and nondistributedness. Hence, the task of the analyst is to assess which of these patterns exist in every empirical case. This can be accomplished by measuring how much of the four relations (i.e. symmetry, asymmetry, distributedness, nondistributedness) are incorporated into each vertex of the system.

The measures of integration and control provide a way to explore such relations.

6.8.5. MEASURING VERTEX INTEGRATION

As it was said before, asymmetric relations involve the notion of depth or topological distance between vertices.

A vertex has an asymmetric relation with regard to other vertices if it lies two or more steps away from them. In general, proximity graphs where most vertices are a few steps away from each other are said to be *shallow*, while those graphs whose vertices lie many steps away are said to be *deep* (fig. 6.29).

The maximum shallowness exists when all vertices are connected directly to a single vertex. In this case, symmetric adjacency relations predominate among the vertices.

The maximum depth is registered in those systems where all spaces are arranged in a unilinear sequence away from one vertex.

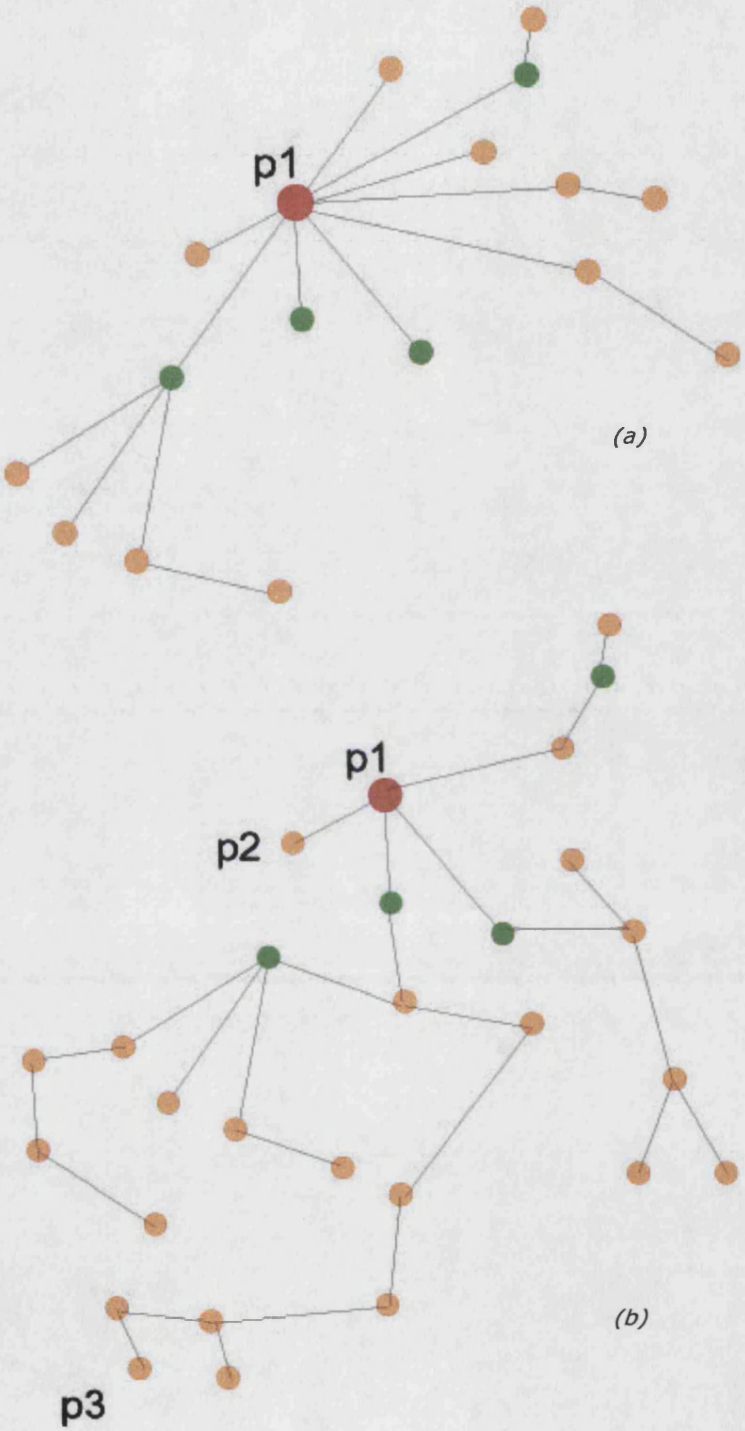

Figure 6.29. Shallowness and depth resulting from two different graph structures: (a) is a shallow graph for vertex p1, because almost all the remaining vertices are only one edge away. In contrast, (b) is deep for p1, because most vertices are many steps away. Indeed, only p2 is one edge away, while the distance between p1 and p3 is 8 edges.

The value of integration for one particular vertex depends precisely on its shallowness or deepness with regard to all the remaining vertices of the graph. In other words, integration measures the '*relative asymmetry*' from one particular vertex to all the remaining vertices of the graph. The following procedure allow us to extract the value of relative asymmetry:

1. Given a proximity graph **G**, take one vertex at a time, say p_i, calculate depth values from that vertex to all the remaining vertices. Depth is just another name for the topological distance $td(p_i, p_j)$, obtained by counting how many edges are included in each path from p_i to p_j, for all $p_j \in P$ and $p_j \neq p_i$.

2. Calculate the mean depth of p_i, denoted by md_i, by summing all the topological distances extracted previously and dividing the result by the total number of vertices less one.

3. Then, calculate the relative asymmetry RA_i of p_i as follows:

$$RA_i = \frac{2(md_i - 1)}{n - 2}$$

Where md_i is the mean depth of the *ith* vertex, and *n* is the total number of vertices in the system.

4. Repeat operations 1 through 3 for every vertex of the proximity graph.

The above procedure will give a value between 0 (maximum symmetry) and 1 (maximum asymmetry) for each vertex of the system.

A value closer to zero indicates that the system is shallow from that particular vertex. In other words, symmetric relations predominate between that particular vertex and the rest of the system. For this reason, the vertex tends to integrate the system.

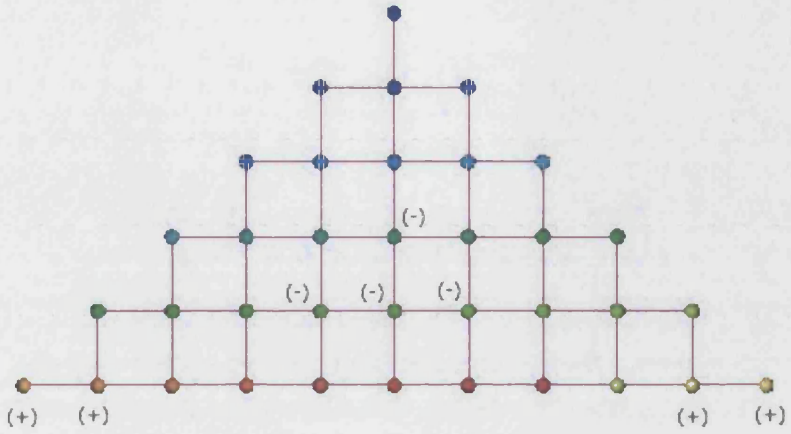

Figure 6.30. Extreme values of vertex integration in a regular lattice.
(-) = Lower relative asymmetry (i.e. integrated vertices);
(+) = Higher relative asymmetry (i.e. segregated vertices).

In contrast, a value closer to one indicates that the system is deep from that vertex, asymmetric relations predominate, and the vertex is segregated from the rest of the system (Hillier and Hanson, 1984: 109).

Figure 6.30 illustrates the Relative Neighbourhood Graph of a regular lattice, distinguishing vertices with lower (-) and higher (+) values of relative asymmetry. It is obvious that those vertices with lower relative asymmetry are most integrated, while those with high relative asymmetry are segregated. This applies to any type of point distribution (see fig. 6.31).

It is possible to obtain a measure of relative asymmetry not only for each vertex but also for the whole graph. Simply calculate the average from the relative asymmetry values of all the vertices.

Those calculations need to be done by computer, especially if the structure of the proximity graph under investigation is very complex. It is worth mentioning that RNG Explorer includes a routine to calculate the relative asymmetry for every vertex, as well as the mean relative asymmetry for the whole proximity graph.

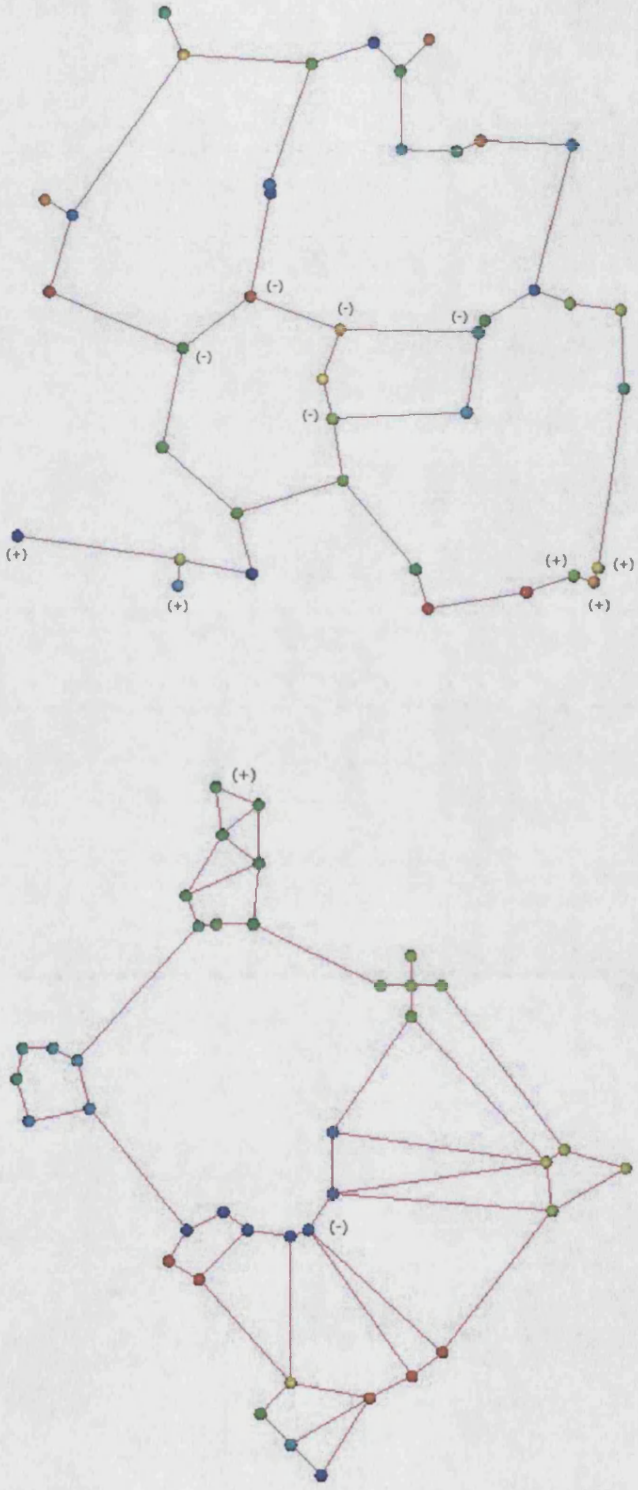

Figure 6.31. Extreme values of vertex integration in two graphs:
(-) Lower relative asymmetry (i.e. integrated vertices)
(+) Higher relative asymmetry (i.e. segregated vertices)

Extracting integration values is useful to evaluate the relative importance of certain artefacts within the Mexica offerings. There are two alternative ways to achieve this:

1. *Measuring relative asymmetry in a single Beta-skeleton.* The most significant choices for this task are (a) the 1-Skeleton (Gabriel Graph); (b) the 2-skeleton (RNG); or (c) the Beta-skeleton extracted with the lower connectivity threshold (see section 6.5.2).

   The above option gives an exact sense of how integrated is each vertex for a particular value of Beta. It is important to keep in mind, however, that certain vertices change from an integrated position to a segregated one when relative asymmetry is measured throughout several Beta-skeletons. The observation and analysis of those changes may become of utter importance for certain applications. For example, if the analysis focused on empirical networks instead of offerings, analysts would be interested to know the effects of different Beta values on the integration/ segregation of specific nodes. The question of how much integration is gained or lost by a vertex, given some changes in the Beta-skeleton, could be answered by producing a chart, which shows the corresponding relative asymmetry for different Beta values. Figure 6.31.shows one of those charts. Each line corresponds to a vertex, the shortest lines correspond to vertices with little variation in relative asymmetry, while the longer ones reflect strong changes in the integration status of the vertices.

2. *Measuring relative asymmetry in every Beta-skeleton and then extracting an average value for every vertex.* This second alternative is most appropriate for the Mexica offerings because it exposes overall integration/segregation tendencies.

Figure 6.32. Integration profile of offering 58

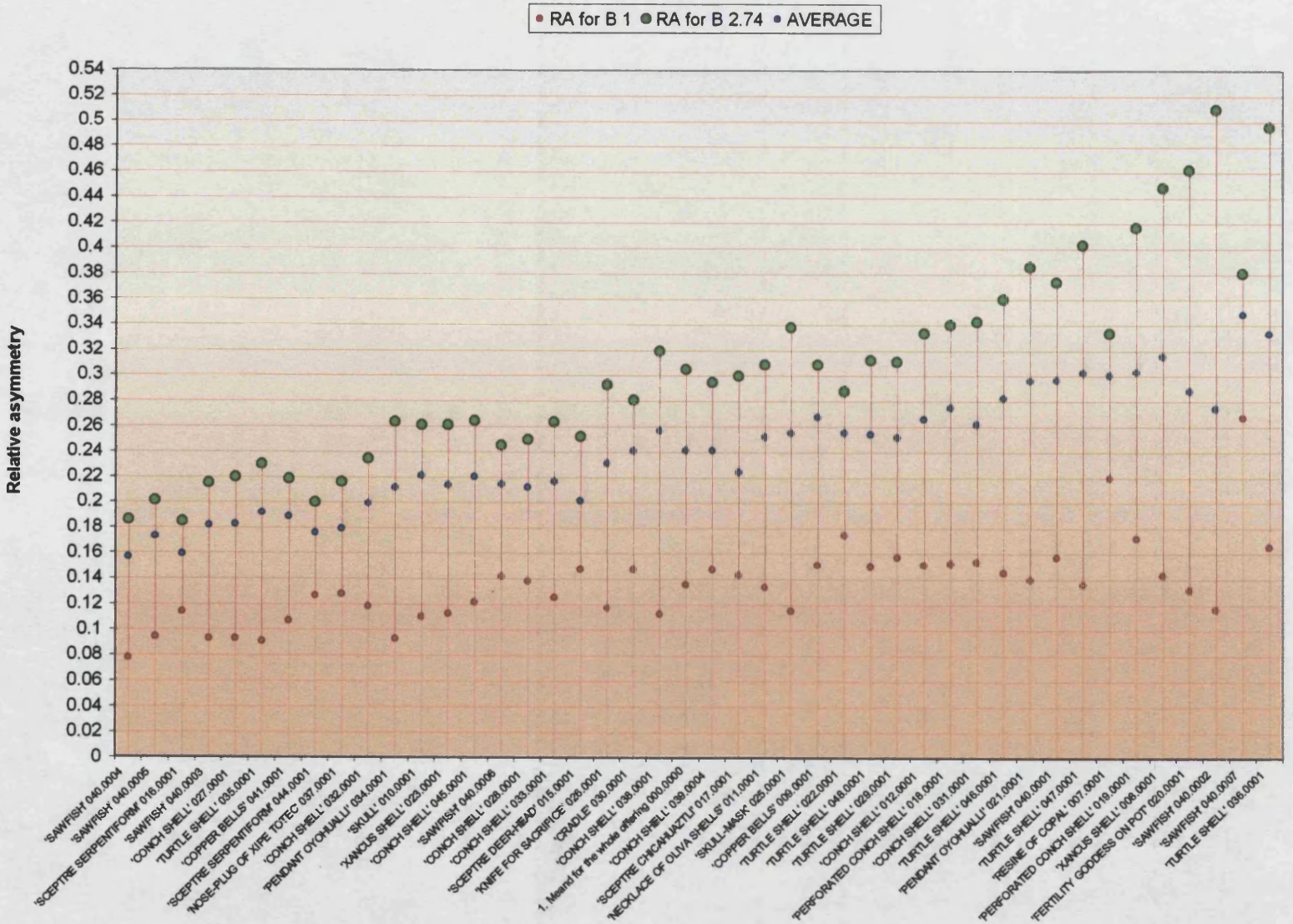

To illustrate the second alternative we produce integration views of each offering, distinguishing five categories of objects according to their integration/segregation status:

1. Big red balls: the most integrated vertices (i.e. low RA)

2. Big green balls: vertices with medium high integration

3. Dark blue balls: The most segregated vertices (i.e. high RA).

4. Light blue balls: vertices with medium high segregation

5. Yellow balls: average relative asymmetry

In offering U, for example, integration is stronger at the centre, diminishing in concentric zones towards the corners of the deposit. Considering the categories of artefacts situated in those different integration zones, the procedure helps to identify the following patterns (see figs. 6.33, 6.34, and table 6.6):

1. A trapezoidal arrangement made of four greenstone beads in highly integrated places (there is a possibility that such a figure may in fact have been a square distorted by post-depositional displacements).

2. One sacrificial knife, plus an additional greenstone bead, at the centre of the trapezoid. The latter is precisely the point with the highest integration of the whole offering.

3. The presence of eagle remains and copper bells also in highly integrated places.

4. A square arrangement formed by segregated objects, which marks the place of Xancus shells and balls of copal.

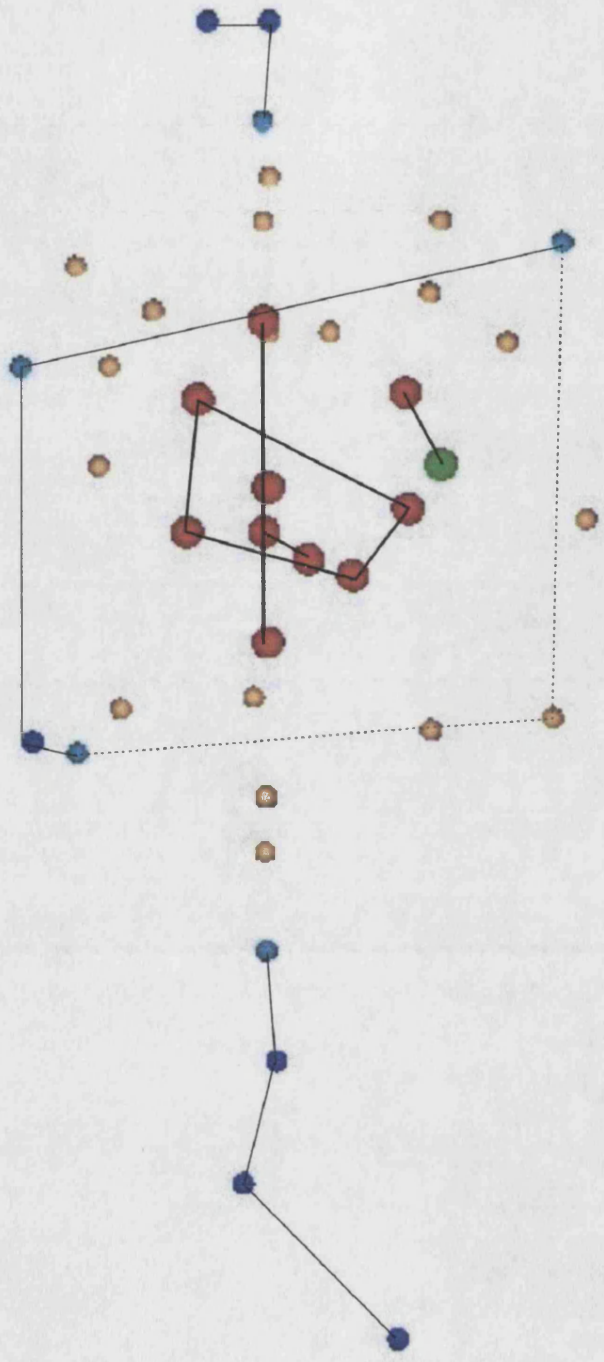

Figure 6.33. Integration view of offering U. The internal 'square' represents the area of highest integration (red balls). This includes four greenstone bead in the corners, plus another greenstone bead, the knife, and the central point of the sawfish. In contrast, the segregated vertices (blue balls) lie in the outer boundary. Finally, the vertex of medium high integration (green ball) corresponds to the eagle remains.
A list of the specific values of relative asymmetry for each vertex is provided in table 6.6, on page 198.
202

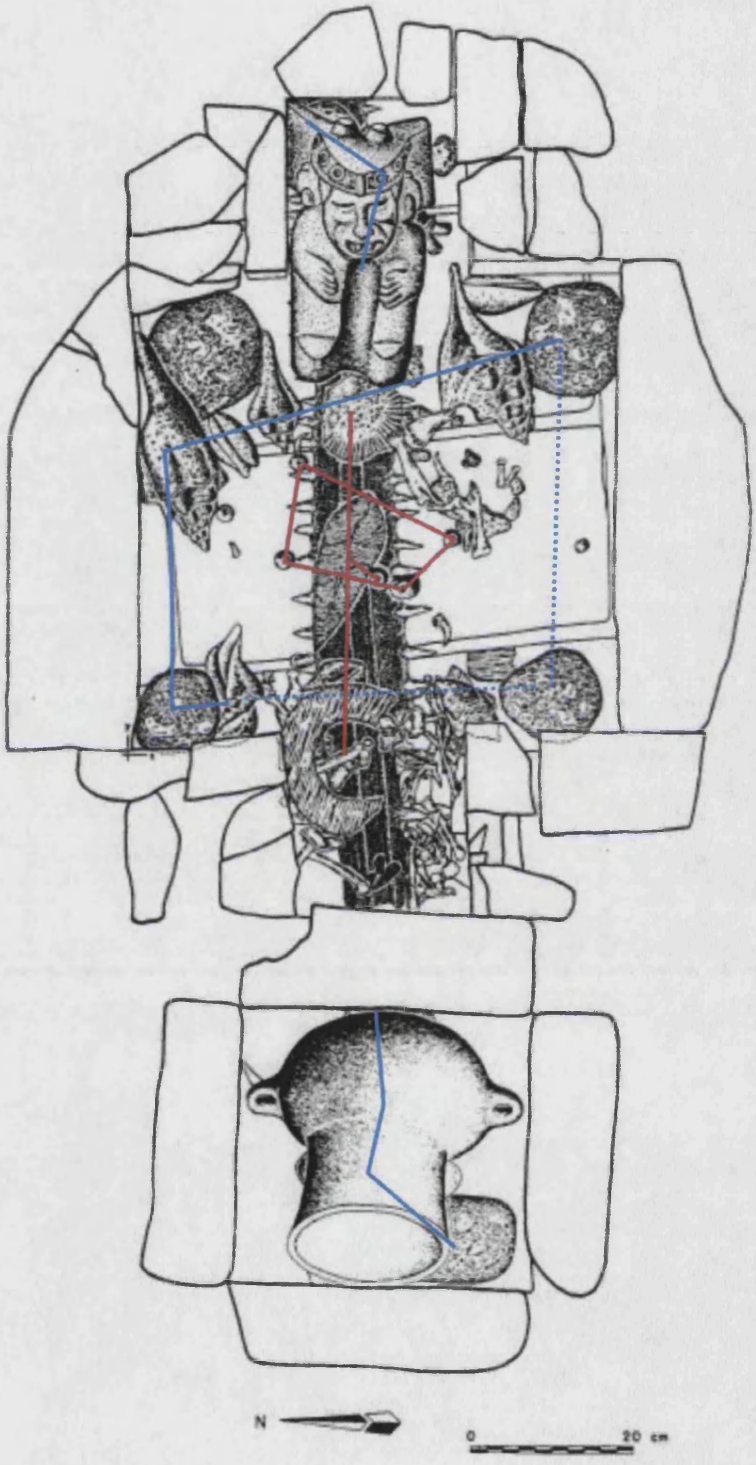

Figure 6.34. Drawing of offering U with boundaries of high and low integration. The red square' represents the area of highest integration. This includes four greenstone bead in the corners, plus another greenstone bead, the knife, and the central part of the sawfish. In contrast, the segregated boundary is represented by blue lines.
A list of the specific values of relative asymmetry for each artefact is provided in table 6.6, on the next page.

Object ID	DESCRIPTION	RA VALUE
016	GREENSTONE BEAD	**0.15555533**
012	GREENSTONE BEAD	**0.156624**
055.4	SAWFISH	**0.15779917**
055.3	SAWFISH	**0.16036342**
015	GREENSTONE BEAD	0.161111
020	KNIFE FOR SACRIFICE	**0.1615385**
026	XANCUS SHELL	0.164423
007	CONCH SHELL SPONDYLUS	**0.16506392**
030.11	COPPER BELLS	0.16549142
017	GREENSTONE BEAD	0.16634617
014	GREENSTONE BEAD	**0.16677333**
028	EAGLE REMAINS	**0.16858983**
029	XANCUS SHELL	0.17019225
019	XANCUS SHELL	0.17318383
021	BALL OF COPAL	0.18002125
018	GREENSTONE BEAD	0.18461525
055.5	SAWFISH	0.18525633
008	XANCUS SHELL	0.18589758
013	GREENSTONE BEAD	0.1864315
055.2	SAWFISH	0.18803417
024	XANCUS SHELL	0.19252117
025	XANCUS SHELL	0.19284183
009	XANCUS SHELL	0.19946567
006	XIUHTECUTLI	0.2004275
004	WOOD PECTORAL	0.20502142
044	GREENSTONE BEAD	0.209936
038	LYNX REMAINS	0.22382492
027	XANCUS SHELL	0.22713658
010	BALL OF COPAL	0.2320515
055.6	SAWFISH	0.23344033
043	RUBBER	**0.23995717**
041	BRAZIER	**0.24230758**
011	XANCUS SHELL	**0.24262808**
022	BALL OF COPAL	**0.245513**
055.1	SAWFISH	**0.26613242**
023	BALL OF COPAL	**0.28995717**
053	RUBBER	**0.29017092**
055.7	SAWFISH	**0.30747858**
042	RUBBER	**0.31100417**
001	TLALOC JAR	**0.35844008**
005	RUBBER	**0.40844008**
	Mean deviation =	0.04524411
	Mean =	0.21273189
	Variance =	0.00335167
	Standard deviation =	0.05789361
	Integration threshold =	0.16677333
	Segregation threshold =	0.23995717
	Coefficient of kurtosis =	2.33440604
	Coefficient of skewness =	1.53369239

Table 6.6. Values of relative asymmetry for the artefacts of offering U. At the top, the most integrated objects (lower RA); at the bottom, segregated objects (higher RA).*

A similar procedure allows the identification of integration cores for offerings 22 and 58. Remarkably, the categories of artefacts located in different zones of relative asymmetry coincide in both offerings (see figs. 6.35, 6.36, 6.37, 6.38, and tables 6.7, and 6.8):

1. The central portion of the sawfish (represented by three points) corresponds to the area of highest integration.

2. A less obvious -and therefore more interesting integration core- is formed by the group of sceptres. The best example of this pattern is found in offering 58, which includes four red balls representing two serpentiform sceptres, plus the deer-head sceptre and the nose-plug (fig. 6.35). Offering 22, on the other hand, includes the deer-head sceptre, the nose-plug and the sawfish in high integration places, plus the serpentiform sceptre in a location of medium-high integration (fig. 6.36). As we will explain in section 6.10, this cluster is highly relevant to decipher the overall meaning of the caches. Hence, the fact that the RN-method has been able to discover their relative importance is in itself indicative of the usefulness of the approach.

3. Additional artefacts show high levels of integration. These include conch-shells, turtles and sea urchin. However, they do not seem to form a consistent pattern in both offerings.

We believe that the most significant arrangement is the integration core formed by the four sceptres. As we will explain in section 6.10, the spatial combination of these artefacts transmits one the most important concepts of Aztec symbolism, and therefore it is relevant to decipher the overall meaning of the caches.

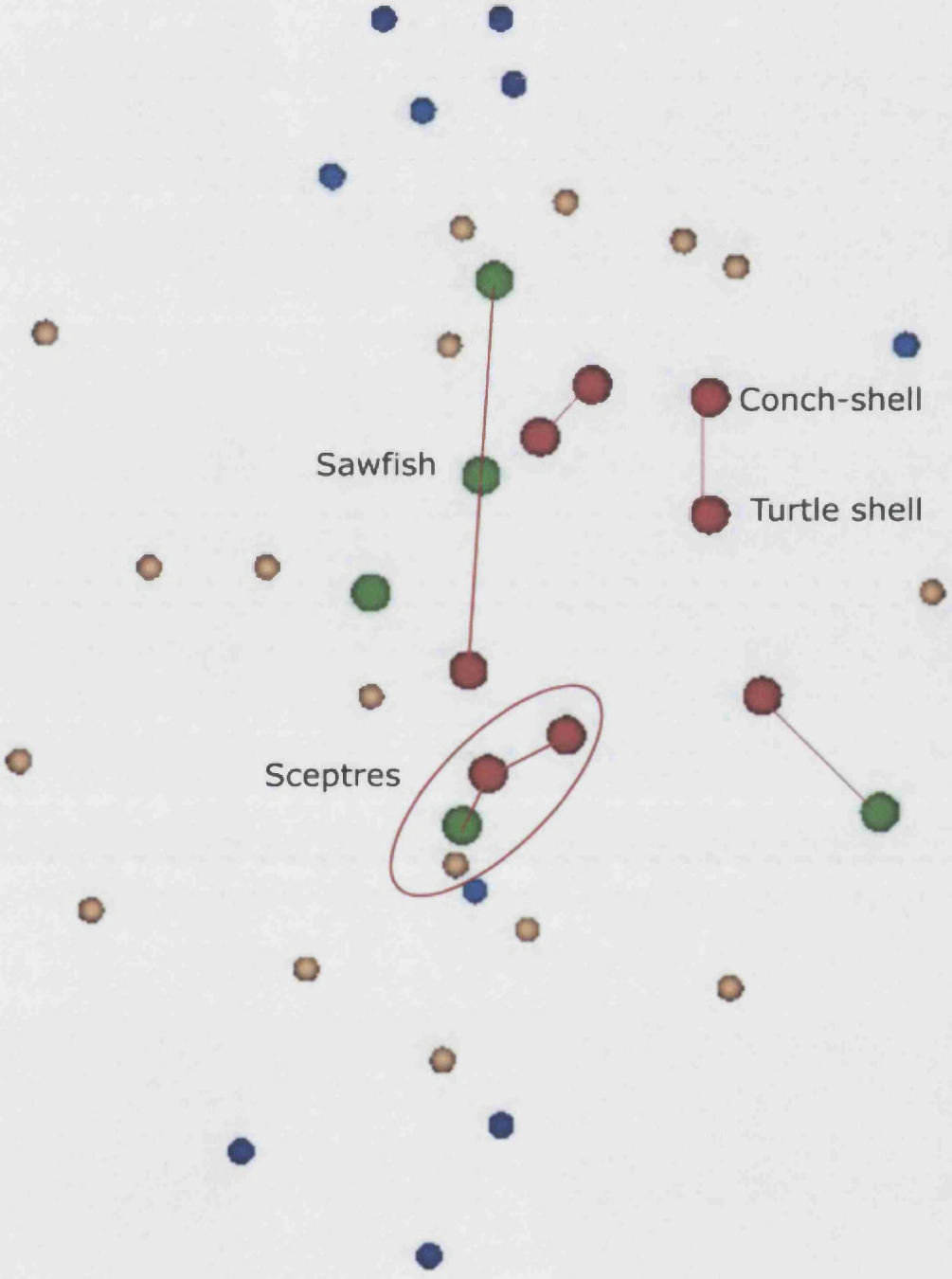

Figure 6.35. Integration view of offering 22. The area of highest integration corresponds to the group pf sceptres and the sawfish. Additional vertices of high integration are conch-shells and turtle shells. The pattern observed here is very similar to the one detected in offering 58 (see fig. 6.36 on the following page).

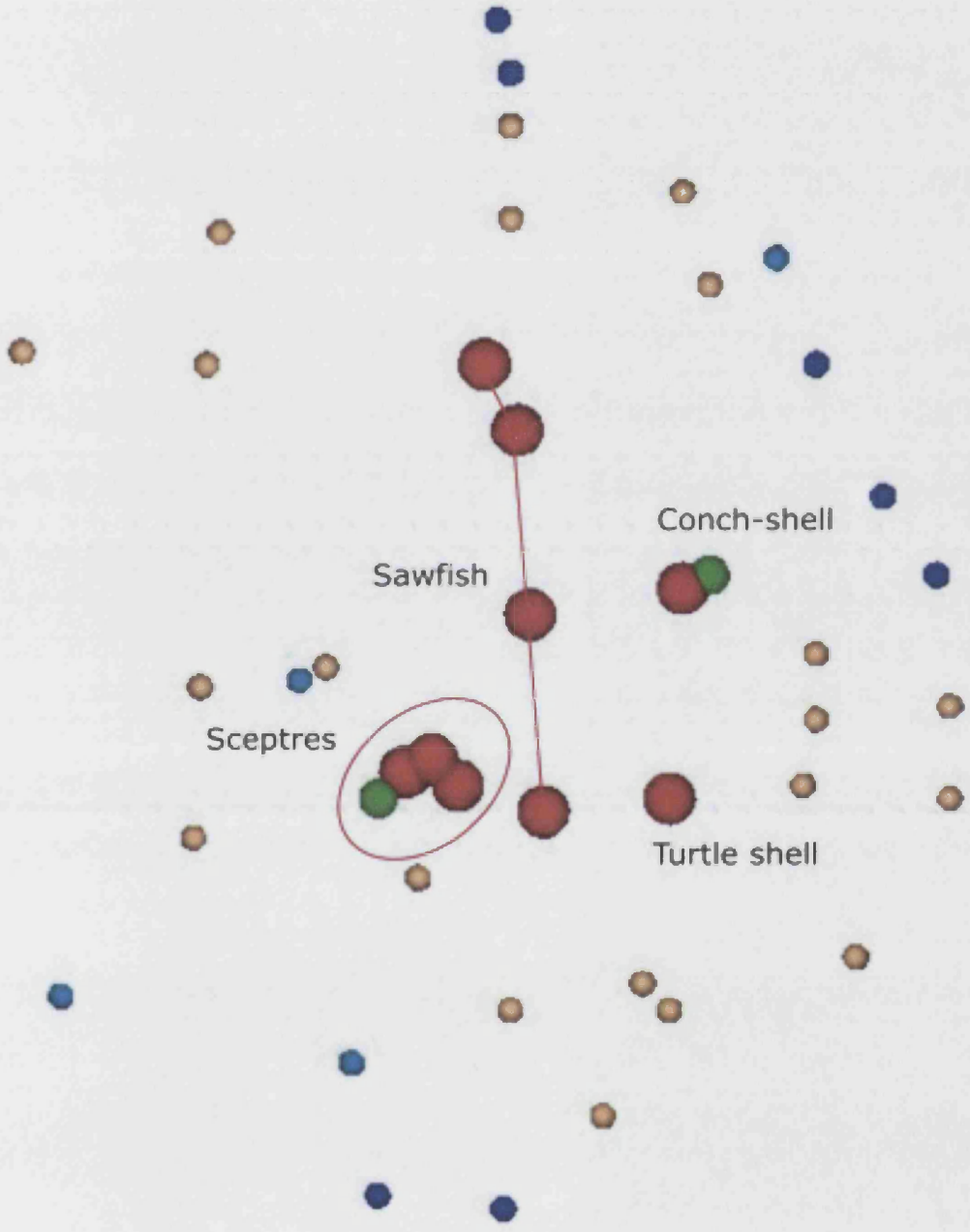

Figure 6.36. Integration view of offering 58. As in the case of offering 22 (see fig. 6.35 on the previous page), the area of highest integration corresponds to the group of sceptres and the sawfish. Additional vertices of high integration are conch-shells and turtle shells.

ID	Type	AVERAGE
021.0001	'SEA URCHIN'	**0.16829418**
030.0001	'TURTLE SHELL'	**0.16916718**
045.0001	'CONCH SHELL'	**0.17321594**
047.0001	'SEA URCHIN'	**0.17424771**
066.0001	'SCEPTRE DEER-HEAD'	**0.17472412**
060.0004	'SAWFISH'	**0.17845529**
053.0001	'NOSE-PLUG OF XIPE TOTEC'	**0.17861394**
034.0001	'TURTLE SHELL'	**0.17893147**
060.0005	'SAWFISH'	**0.185044**
008.0001	'XANCUS SHELL'	**0.18774312**
007.0002	'KNIFE FOR SACRIFICE'	**0.18877506**
060.0006	'SAWFISH'	**0.19155365**
067.0001	'SCEPTRE SERPENTIFORM'	**0.194729**
002.0001	'PENDANT OYOHUALLI'	0.19528447
029.0001	'TURTLE SHELL'	0.19607841
007.0001	'SKULL-MASK'	0.19631647
003.0001	'PENDANT OYOHUALLI'	0.19877729
011.0001	'FERTILITY GODDESS ON POT'	0.19996818
012.0001	'CONCH SHELL'	0.20131765
010.0001	'SKULL'	0.20227041
060.0003	'SAWFISH'	0.20274676
025.0001	'RESINE OF COPAL'	0.20377847
044.0001	'CONCH SHELL'	0.20608082
004.0001	'COPPER BELLS'	0.20687465
001.0001	'CRADLE'	0.20735106
041.0001	'TURTLE SHELL'	0.20981194
020.0001	'SEA URCHIN'	0.21100259
028.0001	'TURTLE SHELL'	0.21132
042.0001	'CONCH SHELL'	0.21306659
060.0002	'SAWFISH'	0.21314588
018.0001	'TURTLE SHELL'	**0.21393982**
019.0001	'SEA URCHIN'	**0.21735318**
055.0001	'CONCH SHELL'	**0.22124329**
065.0001	'SCEPTRE CHICAHUAZTLI'	**0.22680012**
060.0007	'SAWFISH'	**0.23354759**
006.0001	'NECKLACE OF OLIVA SHELLS'	**0.24482024**
005.0001	'COPPER BELLS'	**0.25641018**
019.0002	'SEA URCHIN'	**0.26934994**
009.0001	'CONCH SHELL'	**0.28006653**
060.0001	'SAWFISH'	**0.28308329**
		0.02032171
	Mean =	0.20663251
	Variance =	0.00077983
	Standard deviation =	0.02792542
	Integration threshold =	0.18851707
	Segregation threshold =	0.21334437
	Coefficient of kurtosis =	1.32001179
	Coefficient of skewness =	1.18246522

Table 6.7. Values of relative asymmetry for the artefacts of offering 22. At the top, the most integrated objects (lower RA); at the bottom, segregated objects (higher RA).

ID	Type	AVERAGE
040.0004	'SAWFISH'	**0.14356689**
016.0001	'SCEPTRE SERPENTIFORM'	**0.15053561**
040.0005	'SAWFISH'	**0.15995606**
040.0003	'SAWFISH'	**0.16537617**
044.0001	'SCEPTRE SERPENTIFORM'	**0.1661505**
027.0001	'CONCH SHELL'	**0.16686017**
037.0001	'NOSE-PLUG OF XIPE TOTEC'	**0.16711833**
041.0001	'COPPER BELLS'	**0.174216**
035.0001	'TURTLE SHELL'	**0.17576444**
032.0001	'CONCH SHELL'	**0.18531417**
015.0001	'SCEPTRE DEER-HEAD'	**0.18608867**
034.0001	'PENDANT OYOHUALLI'	**0.18802433**
023.0001	'XANCUS SHELL'	0.19299256
010.0001	'SKULL'	0.19841267
028.0001	'CONCH SHELL'	0.19970317
033.0001	'CONCH SHELL'	0.20002578
040.0006	'SAWFISH'	0.20086478
017.0001	'SCEPTRE CHICAHUAZTLI'	0.20202594
026.0001	'KNIFE FOR SACRIFICE'	0.2080915
045.0001	'CONCH SHELL'	0.20847839
039.0004	'CONCH SHELL'	0.21964122
030.0001	'CRADLE'	0.22331911
025.0001	'SKULL-MASK'	0.22389989
040.0002	'SAWFISH'	0.225771
011.0001	'NECKLACE OF OLIVA SHELLS'	0.22648078
038.0001	'CONCH SHELL'	0.22990061
029.0001	'TURTLE SHELL'	0.23196544
012.0001	'CONCH SHELL'	0.23583694
048.0001	'TURTLE SHELL'	0.23628839
031.0001	'CONCH SHELL'	0.23680494
022.0001	'TURTLE SHELL'	0.24093433
009.0001	'COPPER BELLS'	0.24409589
020.0001	'FERTILITY GODDESS ON POT'	**0.24712856**
018.0001	'PERFORATED CONCH SHELL'	**0.24861283**
046.0001	'TURTLE SHELL'	**0.25312933**
021.0001	'PENDANT OYOHUALLI'	**0.25893656**
040.0001	'SAWFISH'	**0.26726017**
047.0001	'TURTLE SHELL'	**0.26887339**
019.0001	'PERFORATED CONCH SHELL'	**0.27158339**
008.0001	'XANCUS SHELL'	**0.27216411**
036.0001	'TURTLE SHELL'	**0.28448839**
007.0001	'RESINE OF COPAL'	**0.28623044**
040.0007	'SAWFISH'	**0.33384944**
	Mean deviation =	0.03421729
	Mean =	0.21876189
	Variance =	0.00052301
	Standard Deviation =	0.0414697
	Integration threshold	0.1870565
	Segregation Threshold =	0.24561222
	Coefficient of Kurtosis =	-0.06827588
	Coefficient of skewness =	0.34324768

Table 6.8. Values of relative asymmetry for the artefacts of offering 58. At the top, the most integrated objects (lower RA); at the bottom, segregated objects (higher RA).

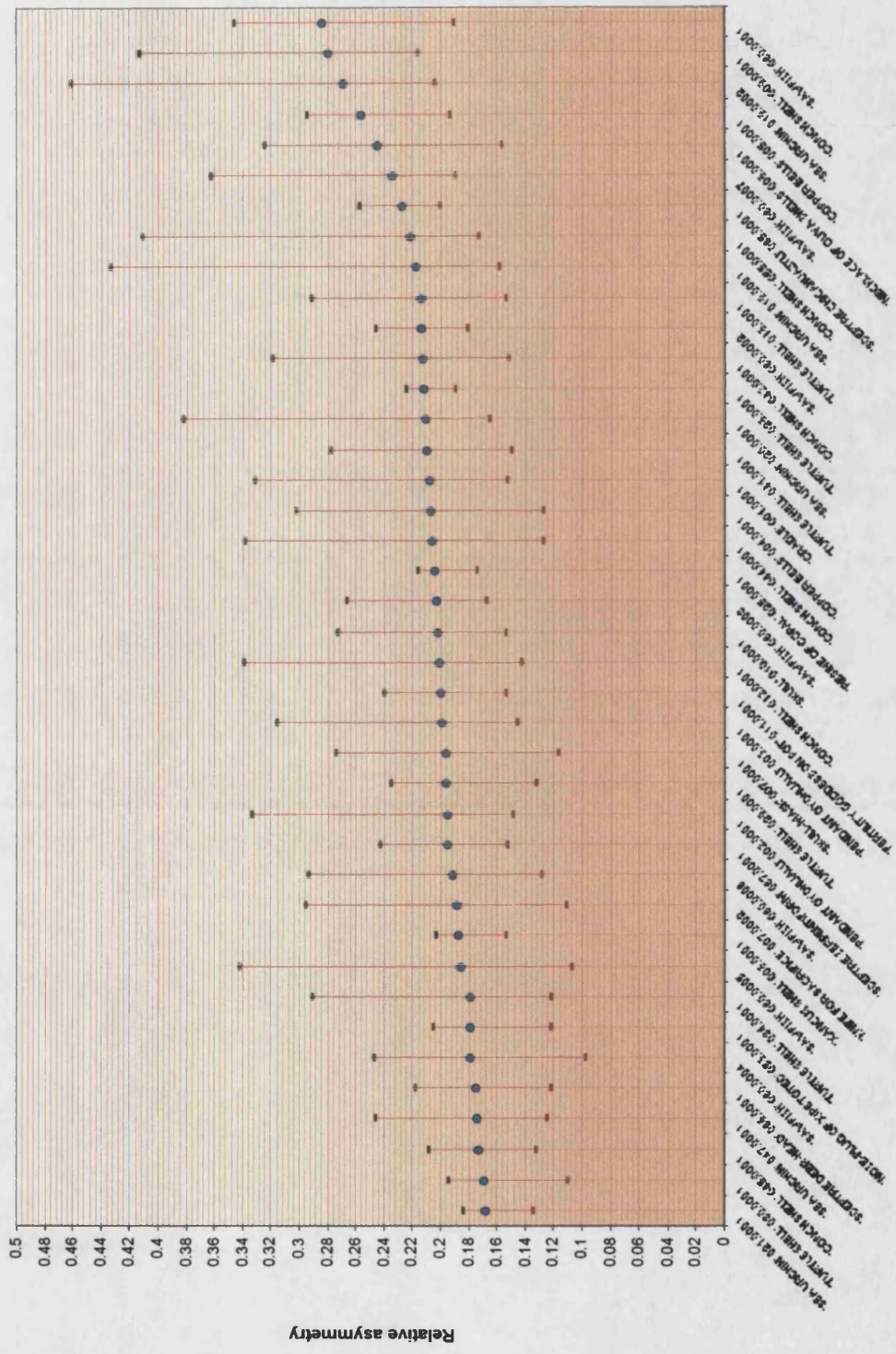

Figure 6.37. Integration chart of offering 22

Figure 6.38. Integration chart of offering 58

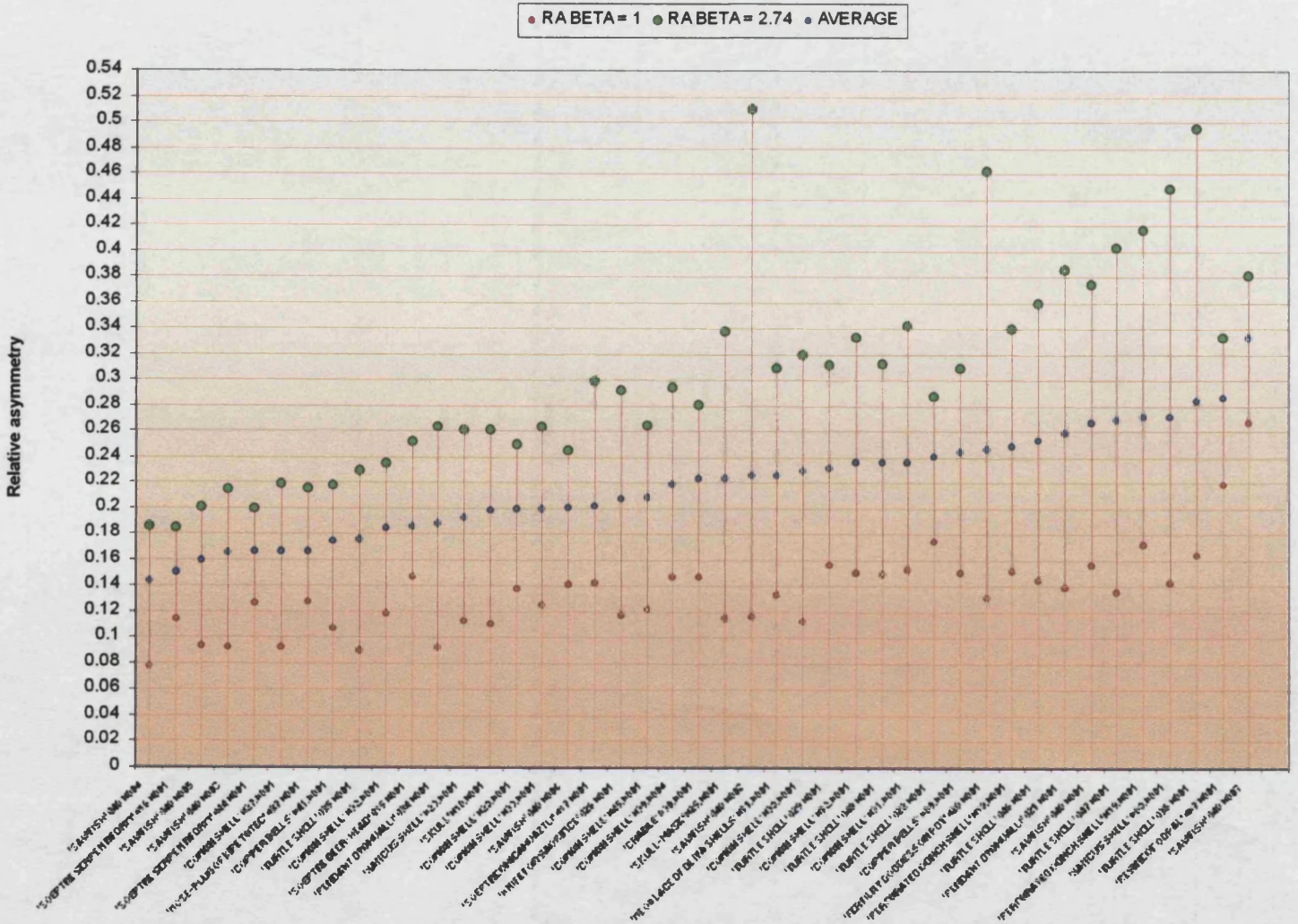

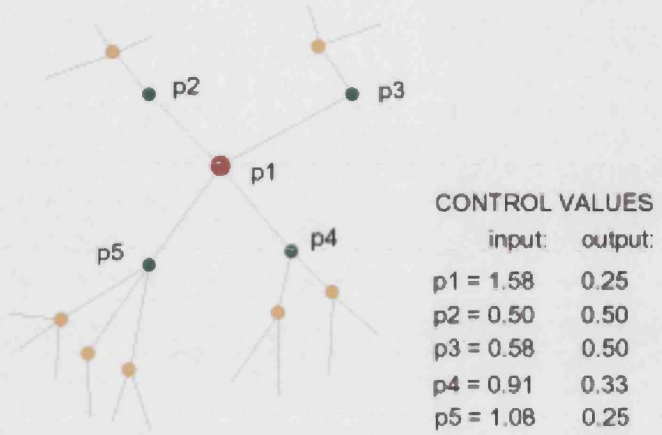

Figure 6.39. An example of vertex control. In this graph, p1 gives 0.25 of control to each of its four neighbours, while receiving 0.5 from p2, 0.5 from p3, 0.33 from p4, and 0.25 from p5. At the end, p1 acquires more control over the graph structure than its immediate neighbourhs.

6.8.6. MEASURING VERTEX CONTROL

The second measure we have adopted from Hillier and Hanson (1984) is called *vertex control*. This gives us a way to assess the relative importance of artefacts based on their local relationships.

Imagine that certain vertex, say v_1, *gives to* each of its immediate neighbours ***1/n*** of control (where *n* is the number of neighbours of v_1). At the same time, v_1 *receives* certain amount of control *from* its neighbours. This means that "...each space is partitioning one unit of value among its neighbours and getting back a certain amount from its neighbours (Hillier and Hanson 1984: 109).

Vertices with values considerably greater than one exercise more control over the graph structure than those vertices whose control value approaches zero. In the case illustrated in figure 6.39, for example, vertex p_1 partitions its unit of control among four direct neighbours (i.e. it gives 0.25 of control to each adjacent vertex), while receiving 0.50 from p_2, 0.5 from p_3, 0.33 from p_4, and 0.25 from p_5. The procedure exposes p_1 as

the vertex of highest hierarchy with a total control of 1.58. In contrast, p_2 has the lowest control. It receives only 0.25 from each of its two neighbours, which gives a total control of 0.5.

The extraction of control measures in offerings 22 and 58 highlights the local importance of some types of artefacts. In figures 6.40 and 6.41 we illustrate objects with high control linked to their corresponding neighbours (see also tables 6.9, and 6.10). This defines seven arrangements in each cache, four of which match in both:

1. In both offerings the sceptres are located within an area of high control. Interestingly, the zone corresponds precisely to the core of high integration. This fact reinforces the perception of the group of sceptres as a meaningful central theme in the offerings.

2. Another arrangement is formed by a skull (high control), a necklace of seven shells (*Oliva sp.*), and a set of copper bells at each side of the skull. This pattern is consistent in both offerings, and seems to reflect another important concept as explained in section 6.10.

3. A second skull, a knife, and two *oyohualli* pendants appear as an independent group in offering 58. The same objects appear together in offering 22, though in the latter case the arrangement also includes a cradle.

4. Finally, in both offerings a pot portraying an unidentified fertility deity appears surrounded by conch-shells, and in the case of offering 22, this also includes turtles.

To conclude this section, it is worth mentioning that the measures of integration and control provide formal criteria to assess the relative importance of specific artefacts based primarily on their spatial position.

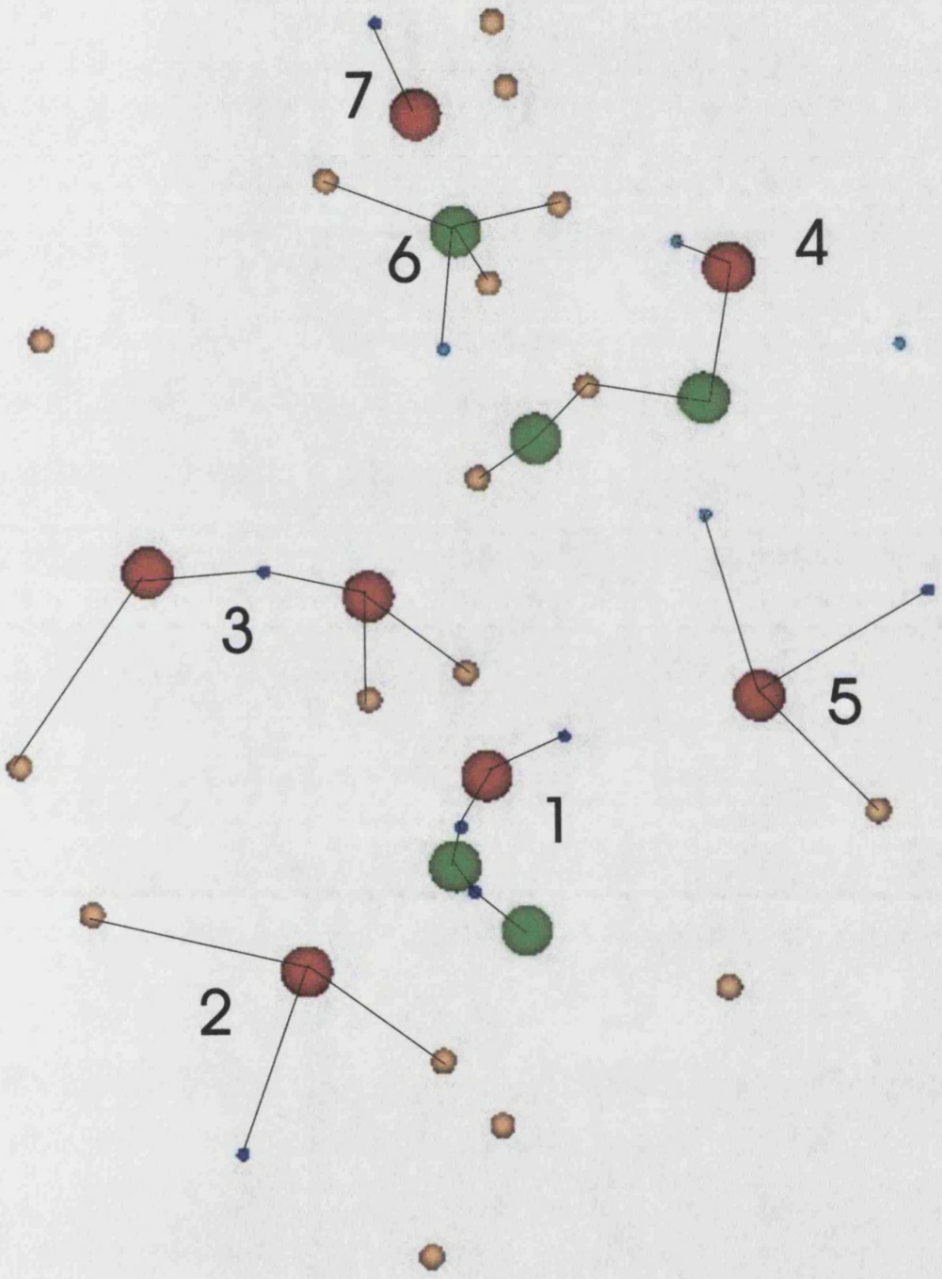

Figure 6.40. Patterns of control detected in offering 22. The numbers indicate the following arrangements: (1) sceptres; (2) Human skull, seven shells (Oliva sp.), and two sets of copper bells; (3) Another human skull, a knife, and two oyohualli pendants; (4) pot portraying an unidentified deity surrounded by conch-shells and turtles; (5), (6), and (7) represent different arrangements of conch-shells, turtle shells and se-urchin. Interestingly, the first four arrangements match with the patterns found in offering 58 (see next figure).

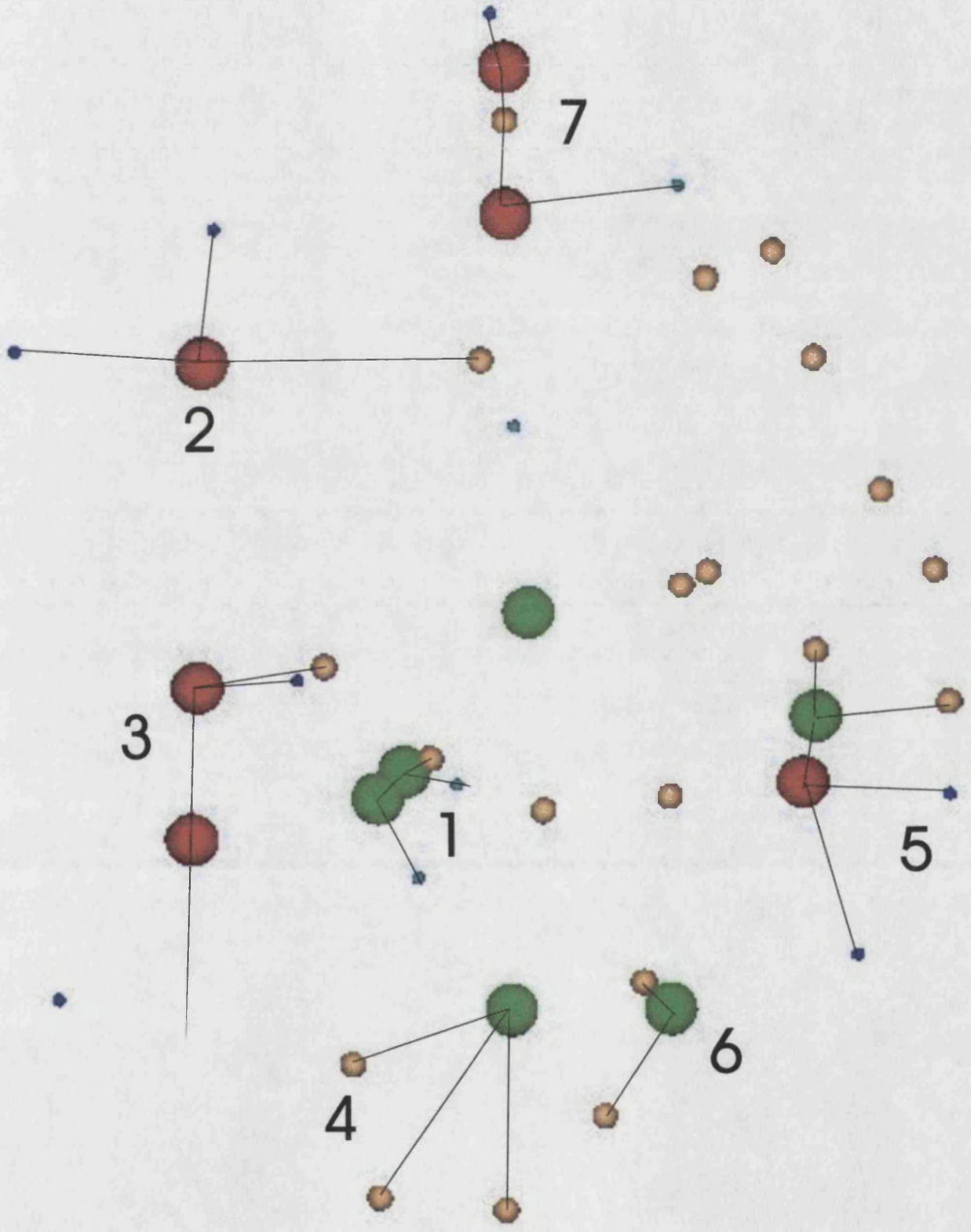

Figure 6.41. Patterns of control detected in offering 58. The numbers indicate the following arrangements: (1) sceptres; (2) Human skull, seven shells (Oliva sp.), and two sets of copper bells; (3) Another human skull, a knife, and two oyohualli pendants; (4) pot portraying an unidentified deity next to the sawfish and close to conch-shells; (5), (6), represent different arrangements of conch-shells, and turtle shells; while (7) associates the sawfish with a cradle and remains of copal. Interestingly, the first four arrangements match with the patterns found in offering 58 (see previous figure)

ID	LABEL	Average
053.0001	'NOSE-PLUG OF XIPE TOTEC'	**0.64901929**
029.0001	'TURTLE SHELL'	**0.66372547**
067.0001	'SCEPTRE SERPENTIFORM'	**0.67647076**
003.0001	'PENDANT OYOHUALLI'	**0.68137276**
065.0001	'SCEPTRE CHICAHUAZTLI'	**0.68627476**
019.0002	'SEA URCHIN'	**0.690196**
006.0001	'NECKLACE OF OLIVA SHELLS'	**0.70098035**
030.0001	'TURTLE SHELL'	**0.702941**
044.0001	'CONCH SHELL'	**0.71372541**
018.0001	'TURTLE SHELL'	**0.73039182**
041.0001	'TURTLE SHELL'	**0.74215688**
009.0001	'CONCH SHELL'	0.75882324
060.0005	'SAWFISH'	0.77745106
060.0001	'SAWFISH'	0.77941171
007.0001	'SKULL-MASK'	0.78137241
008.0001	'XANCUS SHELL'	0.78921565
004.0001	'COPPER BELLS'	0.78921565
020.0001	'SEA URCHIN'	0.79901959
001.0001	'CRADLE'	0.81862712
025.0001	'RESINE OF COPAL'	0.83333312
019.0001	'SEA URCHIN'	0.85588229
005.0001	'COPPER BELLS'	0.99509776
060.0006	'SAWFISH'	1.02058824
047.0001	'SEA URCHIN'	1.06764706
060.0004	'SAWFISH'	1.07058812
042.0001	'CONCH SHELL'	1.12549047
060.0007	'SAWFISH'	1.16078418
060.0002	'SAWFISH'	1.16666659
045.0001	'CONCH SHELL'	**1.20000029**
012.0001	'CONCH SHELL'	**1.20392159**
060.0003	'SAWFISH'	**1.22058824**
034.0001	'TURTLE SHELL'	**1.24901947**
028.0001	'TURTLE SHELL'	**1.28921541**
011.0001	'FERTILITY GODDESS ON POT'	**1.30882347**
007.0002	'KNIFE FOR SACRIFICE'	**1.33333318**
066.0001	'SCEPTRE DEER-HEAD'	**1.36960776**
055.0001	'CONCH SHELL'	**1.48921582**
002.0001	'PENDANT OYOHUALLI'	**1.5**
010.0001	'SKULL'	**1.68137276**
021.0001	'SEA URCHIN'	**1.92843141**
	Arithmetic mean =	0.99999995
	Variance =	0.10165274
	Standard deviation =	0.31883027
	Low control threshold =	0.73921562
	High control threshold =	1.21225491
	Kurtosis =	0.38822821
	Asymmetry coefficient =	0.95443114

Table 6.9. Control values of offerings 22. At the top, the artefacts with lower control, and at the bottom those with higher control.

ID	DESCRIPTION	AVERAGE
9.0001	'COPPER BELLS'	0.3537035
18.0001	'PERFORATED CONCH SHELL'	0.38425906
21.0001	'PENDANT OYOHUALLI'	0.46481472
40.0007	'SAWFISH'	0.5
11.0001	'NECKLACE OF OLIVA SHELLS'	0.65555539
29.0001	'TURTLE SHELL'	0.67592583
31.0001	'CONCH SHELL'	0.67592589
17.0001	'SCEPTRE CHICAHUAZTLI'	0.72777767
40.0005	'SAWFISH'	0.73333361
44.0001	'SCEPTRE SERPENTIFORM'	0.80555533
30.0001	'CRADLE'	0.82129628
27.0001	'CONCH SHELL'	0.83240711
36.0001	'TURTLE SHELL'	0.862963
23.0001	'XANCUS SHELL'	0.86574089
22.0001	'TURTLE SHELL'	0.87037022
19.0001	'PERFORATED CONCH SHELL'	0.91296289
12.0001	'CONCH SHELL'	0.91666633
46.0001	'TURTLE SHELL'	0.92777772
48.0001	'TURTLE SHELL'	0.92777772
40.0001	'SAWFISH'	0.93518506
32.0001	'CONCH SHELL'	0.95092583
47.0001	'TURTLE SHELL'	0.95555544
34.0001	'PENDANT OYOHUALLI'	0.95833328
40.0003	'SAWFISH'	0.97592561
28.0001	'CONCH SHELL'	1.01388883
41.0001	'COPPER BELLS'	1.0546295
38.0001	'CONCH SHELL'	1.07962967
16.0001	'SCEPTRE SERPENTIFORM'	1.08703733
20.0001	'FERTILITY GODDESS ON POT'	1.09629628
35.0001	'TURTLE SHELL'	1.12962944
8.0001	'XANCUS SHELL'	1.14074072
15.0001	'SCEPTRE DEER-HEAD'	1.14259278
45.0001	'CONCH SHELL'	1.14537044
37.0001	'NOSE-PLUG OF XIPE TOTEC'	1.16851878
40.0002	'SAWFISH'	1.30185183
40.0004	'SAWFISH'	1.30740722
39.0004	'CONCH SHELL'	1.31481489
25.0001	'SKULL-MASK'	1.35462939
7.0001	'RESINE OF COPAL'	1.44444433
33.0001	'CONCH SHELL'	1.48611122
40.0006	'SAWFISH'	1.55185161
26.0001	'KNIFE FOR SACRIFICE'	1.59814811
10.0001	'SKULL'	1.8916665
	Arithmetic mean =	0.99999994
	Variance =	0.10300022
	Standard deviation =	0.32093647
	Low control threshold =	0.67906347
	High control threshold =	1.3209364
	Kurtosis =	0.49554839
	Asymmetry coefficient =	0.35490457
	Quartil 1	0.82685169
	Quartil 3	1.14467603

Table 6.10. Control values of offerings 58. At the top, the artefacts with lower control, and at the bottom those with higher control.

Therefore, calculating control and integration represents an improvement over the customary selection of artefacts upon the basis of their appearance or 'attractiveness' and in this way we hope to have improved the assessment of the relative importance of the offering elements (see section 4.5).

6.9. VISUAL CLUSTERING

The next procedure of the RN-Method consists in exploring relationships among different categories of artefacts by applying the notion of limited neighbourhood. As explained in section 5.9, this is part of a visual clustering technique oriented to recognise groups of vertices strongly related. The identification of arrangements works regardless of the original distribution of the data.

Our purpose is to investigate whether the offerings contain any kind of clusters, and whether the same types of arrangements are found across different caches. If repetitive combinations of artefacts were found, then it would be reasonable to assume that such regularities were intentional. Therefore, they could be regarded as a 'symbolic theme'. The significance of those patterns could finally be interpreted with evidence provided by other sources of Aztec symbolism such as iconography, as well as historic and ethnographic information.

Suppose, for example, that we identify a cluster formed by four greenstone beads located at the corners of an imaginary square, plus one more at the centre complemented by a sacrificial knife. We assume this to be significant and therefore investigate whether other offerings contain arrangements with the same combination of artefacts. If the search is positive, we refer to the pattern as a symbolic theme.

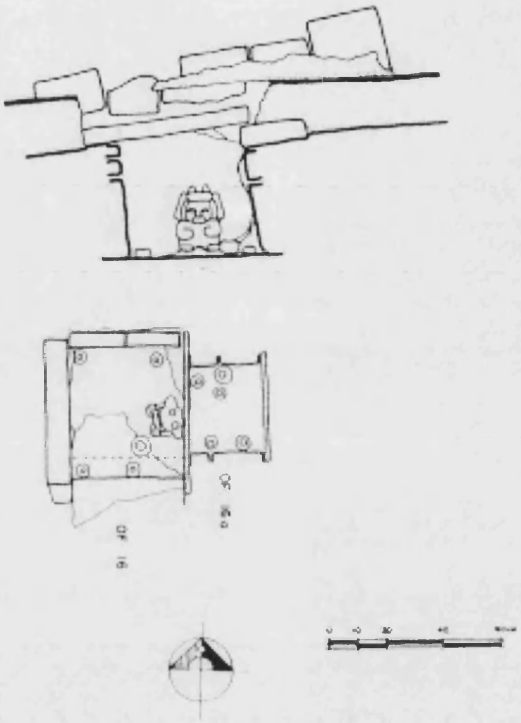

Figure 6.42. Offerings 16 and 16a from the Great Temple of Tenochtitlan. Notice the arrangements of greenstone beads in connection with Xiuhteuchtli, god of Fire. The arrangement is a simplification of the pattern found in offering U (see fig. 6.34).

Such a pattern actually exists. It has been found in the integration core of offering U and it is repeated in offerings 16 and 16a (see. Fig. 6.42). Some experts -based on iconographic analysis of codices, sculptures, ceramics, and documentary evidence-, interpret the pattern as *quincunx*, the most schematic reference to the five major points of the Aztec universe, which includes the four cardinal points plus the centre. Furthermore, López Luján (1994: 172-192) has found recurrent evidence for the association of this arrangement with the god Xiuhtecuhtli. It is worth mentioning that sculptures of this deity have been found in several caches, including offering U itself (compare fig. 6.42 with figs. 6.33, and 6.34).

The procedure is perhaps the most simple to follow and it is also one of the more useful of the RN-Method.

As explained in section 5.9, Limited Neighbourhood Graphs can be retrieved with RNG Explorer simply by combining several values of parameters Beta and Sigma. To start, we may choose a Beta value of 2. This, in addition to some Sigma value, would yield clusters based on the R_1 shape defined by Urquhart (1982) (see fig. 5.18a).

Alternatively, we may start with Beta = 1 and any value of Sigma, so the clusters would be based on the R_2 shape (see fig. 5.18b).

A third option, which we found particularly useful in offering analysis, is to begin with a Beta value that matches the lower connectivity threshold. In the case of offering U, this corresponds to Beta = 2.08, while in offering 22 Beta = 2.62, and in offering 58 Beta = 2.74. Such a threshold is then combined with any Sigma value.

As for the Sigma parameter, we recommend to apply a whole series of values within the range 0 < Sigma <= 1. For example: Sigma = {0.1, 0.2, 0.3, 0.4, 0.5, 0.6, 0.7, 0.8, 0.9, 1.0}.

Whatever the final combination of Beta and Sigma values, the purpose is to produce a family of nested graphs, each one representing a specific level within the hierarchic clustering process. Within this framework, an index of dissimilarity can be easily measured for each edge, by taking into account how long it remains connected to a cluster. This is calculated as follows:

$d^* = 1/s$.

An edge that disappears from the graph at Sigma = 0.1, for example, would have a very high dissimilarity value ($d^* = 10$); whereas an edge that remains present until Sigma reaches a value 0.9 would have low dissimilarity ($d^* = 1.11$).

In fact, sigma represents a factor of *relative edge consistency.* The level of consistency refers to how essential are certain edges for the structure of the pattern. Inconsistent edges are those that appear joining two clusters that should be separated. 'Inconsistency' also applied to redundant connections, which generally are not very meaningful.

It is worth mentioning that lower Sigma values tend to yield more 'inconsistent' edges than higher sigma values. This means that very few clusters appear in the graph, making it difficult to visualise any significant arrangement of artefacts.

In contrast, high Sigma values yield only the most 'consistent' edges. These represent the strongest, more meaningful connections, but would perhaps eliminate some other essential edges. Therefore, very high Sigma values might be insufficient to reveal interesting patterns.

Therefore, we suggest exploring each offering with different Beta/Sigma values until some pattern emerges. More attention should be given to arrangements perceived with Sigma values of 0.4, 0.5 or 0.6.

For the analysis of offerings 22 and 58 we choose the lower connectivity threshold as the value of Beta and keep it constant. Then, we try different values of Sigma. Part of this procedure is illustrated in figures 6.43 and 6.44. At the end, the combination Sigma = 0.6 and Beta = 2.63 for offering 22; and Sigma = 0.6 and Beta = 2.74, for offering 58 yielded the following patterns (see fig. 6.45):

Pattern one:

a) Sceptre deer-head

b) sceptre serpentiform

c) sceptre *chicahuaztli*

d) obsidian nose-plug.

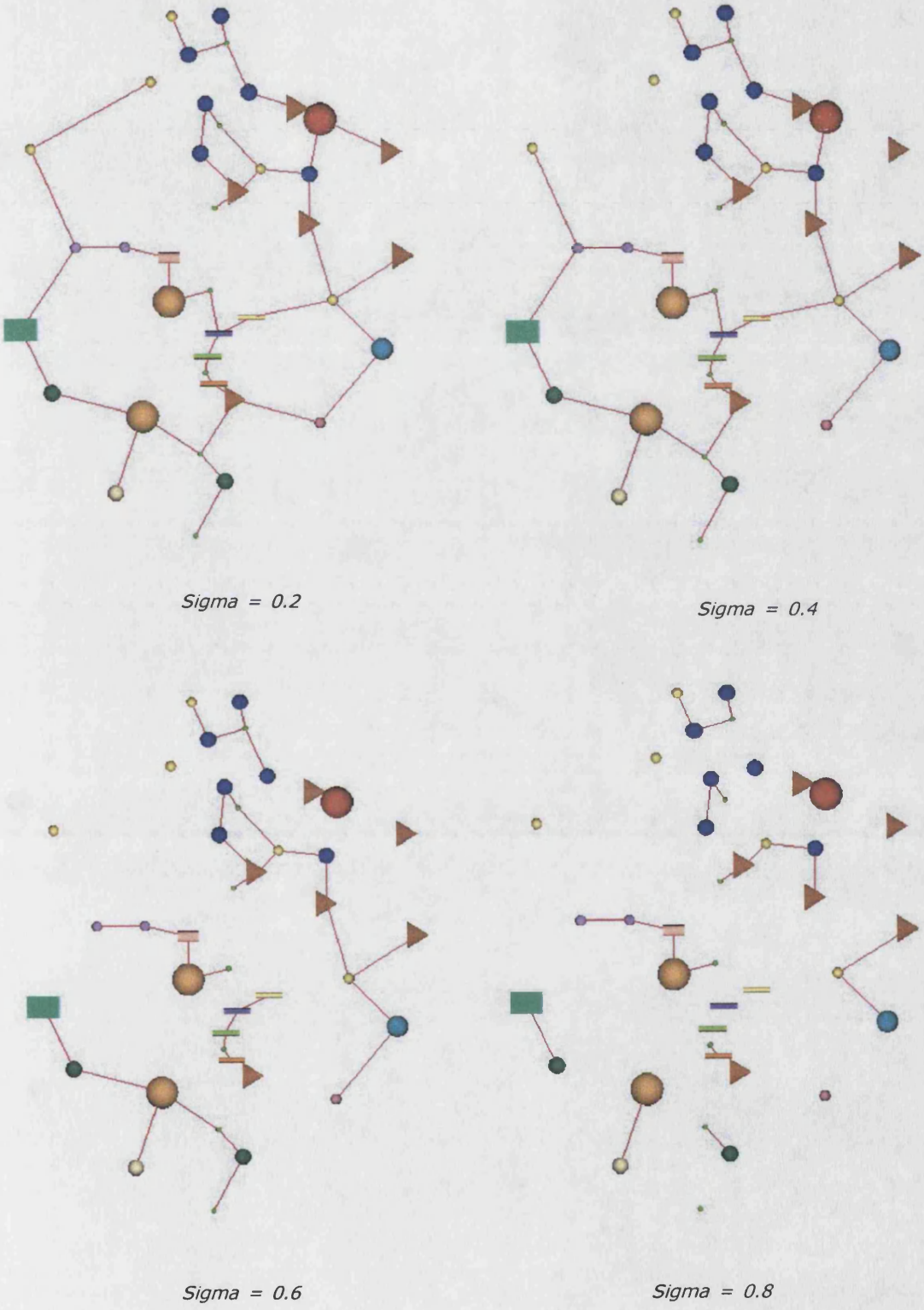

Figure 6.43. Visual clustering applied to offering 22. The value of Beta remains constant at 2.63 (i.e. the lower connectivity threshold for this offering), while Sigma varies to reveal clusters in a hierarchical way.

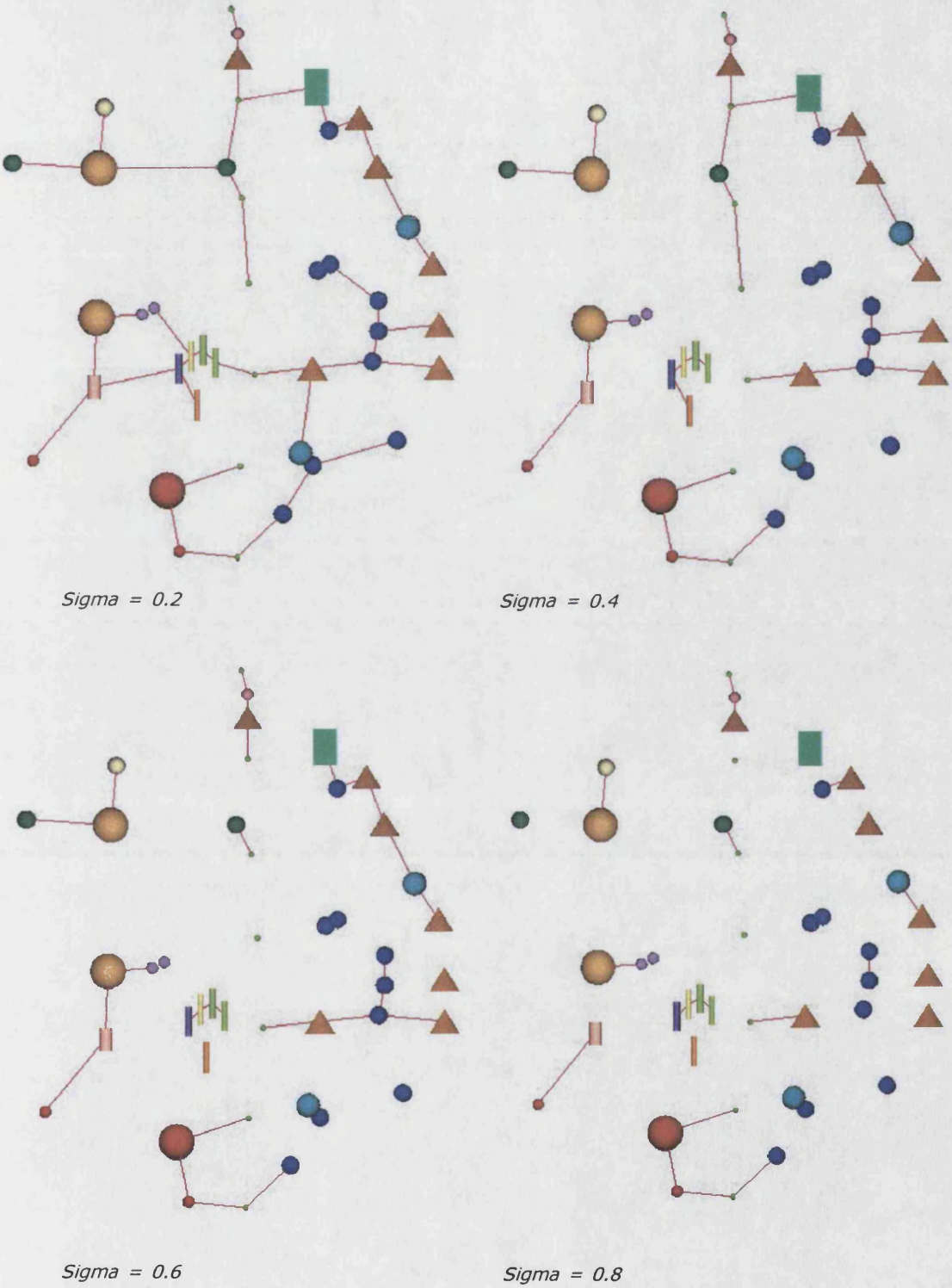

Figure 6.44. Visual clustering applied to offering 58. The value of Beta remains constant at 2.74 (i.e. the lower connectivity threshold for this offering), while Sigma varies to reveal clusters in a hierarchical way.

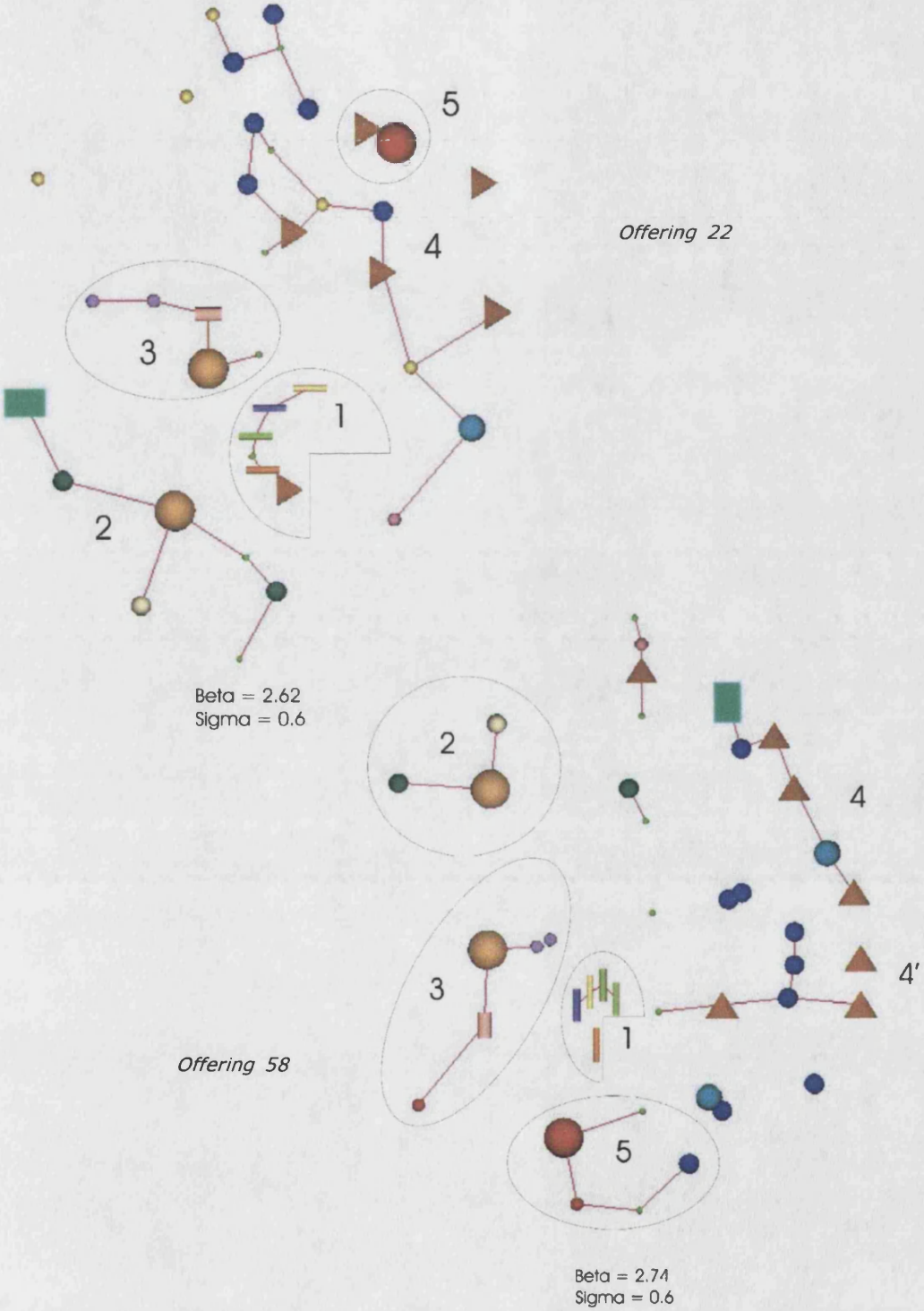

Figure 6.45. Comparison of clusters found in offerings 22 and 58. The numbers identified each pattern. (1) Deer-head sceptre, serpentiform sceptre, chicahuaztli sceptre, and nose-plug; (2) human skull, necklace of seven shells (Oliva sp), and copper bells; (3) Another human skull, sacrificial knife, and two oyohualli pendants; (4) Xancus shells, conch-shells, turtle shells and sea urchins; (5) pot portraying an unidentified deity and turtle (offering 22), or conch-shell (offering 58). The cradle appears linked to pattern 1 in offering 22, while in offering 58 it is associated to shells.

Pattern two

a) Human skull

b) Necklace of 7 *Oliva* shells

c) Copper bells

d) Cradle (only in offering 22)

Pattern three

a) Human skull

b) Sacrificial knife

c) Two *oyohualli* pendants

Pattern four

a) Several turtles

b) Several mother-of-pearl shells

c) *Xancus* shells

d) Sea urchins (only in offering 22)

Pattern five

a) Pot with human effigy

b) Either turtle shell or mother-of-pearl shell

6.10. INTERPRETATION

The evidence gathered through the previous steps of the RN-Method suggests the existence of five major significant patterns in offerings 22 and 58. In this section we formulate hypotheses about the meaning of each pattern and offer a general interpretation of the caches.

Before turning to such issues, it is worth emphasising the relative importance of the sawfish. This occupies three of the most integrated locations and has strong control on the overall structure of both caches. In fact, it

participates in the five patterns recognised in offerings 22 and 58 and therefore its connotation is critical for the global understanding of both deposits.

As mentioned in chapter 4, the symbolism of the sawfish derives from mythological beliefs that relate the appearance of this animal with that of Cipactli, the amphibian monster whose body was split in primeval times in order to produce the earth. Therefore, the presence of a sawfish in offerings 22 and 58 can be interpreted precisely as a metaphor of the earth monster.

6.10.1. PATTERN ONE

One of the most notable patterns of offerings 22 and 58 is the arrangement of four types of objects, three of them identified as small-scale models of 'ritual sceptres', plus another described as "an obsidian plaque with its two ends split like a bifid tongue or a swallow's tail" (López Luján 1994: 260). The latter might represent a nose-plug, but there are still some discussions about its real function. As for the shape of the sceptres, the first one resembles a serpent due to its undulated form; the second features a deer-head; and the third one represents the so-called *chicahuaztli,* a kind of rattle-staff used in fertilisation rituals (fig. 6.46).

Like the sawfish, these artefacts occupy nodes of very high integration within offerings 22 and 58 (see figs. 6.35 and 6.36); locations that also represent positions of great local control (fig. 6.40, and 6.41). If the RN-Method has been successful in recognising their relative importance, then it would be reasonable to expect a major role of these artefacts in the overall meaning of the caches. The following discussion proves that such assumption is correct.

For the interpretation of this pattern we rely on information provided by

Figure 6.46. Artefacts belonging to 'Pattern one'. From left to right and top to bottom: Chicahuaztli sceptre, deer-head sceptre, obsidian nose-plug, and serpentiform sceptre.

López Luján (1994: 255-266, 1998), who has analysed the objects in question using written and pictorial references from historic sources.

This author points out that in Aztec taxonomy deer were classified among the beings that possessed a high proportion of 'hot' energy. He proves his argument with different kinds of evidence, which identify this animal as symbol of fire, sun, and drought.

In Codex Borgia (Anders et al. 1993: pl. 33, see also Seler 1988), for example, a deer appears carrying the Sun. The same document contains a white deer and deer-heads as flames, which Seler (1988, v.1: 223; pl. 22) interprets as metaphors for 'abundance of food'. Likewise, Codex Telleriano-Remensis portrays the supreme god of fire, Xiuhtecuhtli, holding a deer-head sceptre similar to the ones found in offerings 22 and 58 (López Luján 1994: 258, fig. 113, 1998). The same artefact appears in the hands of Xochiquetzal, goddess of fertility (Codex Tonalámatl Aubin, pl. 20). More interestingly, written sources refer to the use of deer bones as weapons by igneous deities, symbolising, perhaps, their power to spread heat or cause drought over the earth (Historia de los Mexicanos, 1965: 37).

In contrast, serpents possessed 'cold' energies and were frequently used to represent currents of water and 'fertilising lightning bolts'. This is "one reason why [the serpent] is among the most characteristic attributes of the gods of rain" (López Luján 1994: 259, see also Gutiérrez Solana 1987: 36). For instance, the serpent sceptre appears in Codex Magliabecchi as part of the offerings to Chalchiuhtlicue, goddess of water currents (i.e. those running on earth), whose transfigurations include many fertility deities, like Xilonen (goddess of tender maize), Chicomecoatl (goddess of mature maize), etc.

Figure 6.47. Some Mexica gods holding chicahuaztli and serpentiform sceptres.

Given the above evidence, López Luján (1994) concludes that deer-head and serpentiform sceptres integrate a symbolic pair of opposite and complementary forces. If this were truth, then we would have a binary representation of heat, fire, and sun energies complementing cold, water, and earth forces.

The union of objects representing these specific cosmic energies is extremely important, because Aztecs believed that they were essential in many acts of hierogamic creation. Indeed, this was a primary theme in Mexica thought. López Austin (1994: 41-43) finds clear references to this concept in several myths of origin. In one story, solar rays dry and illuminate the dark, humid, and cold environment of primeval times at the precise moment when the world entities, including mankind, are created.

On the other side, the spatial adjacency of the 'nose-plug' and the *chicahuaztli* sceptre allow us to be more specific about the meaning of this pattern. Most scholars agree that *chicahuaztli* was a symbol of solar rays that penetrate the earth in order to fertilise it (Garibay 1958: 144-145; Soustelle 1969: 142-144). Indeed, there are written and pictorial references of the use of this artefact during sowing rites, which involve piercing the earth to deposit seeds.

Moreover, both *chicahuaztli* and nose-plug were insignia of Xipe Totec, a god of dual nature, who personified the fight of contrary cosmic forces in relation to fertility and the birth of maize:

> Xipe Totec was a deity in whom opposite forces (the complementary forces of sky and earth) joined and fought. In other words, there is a very close tie between the Xipe Totec cult and war, an activity the Mexica equated metaphorically with the atl-tlachinolli [i.e. binary opposition, the spiral intertwining of cosmic forces], and hierogamy. *It is clear that this deity was associated with fertility and the birth of maize, both phenomena resulting from the sexual union of sky and earth* (López Luján 1994: 294, emphasis added).

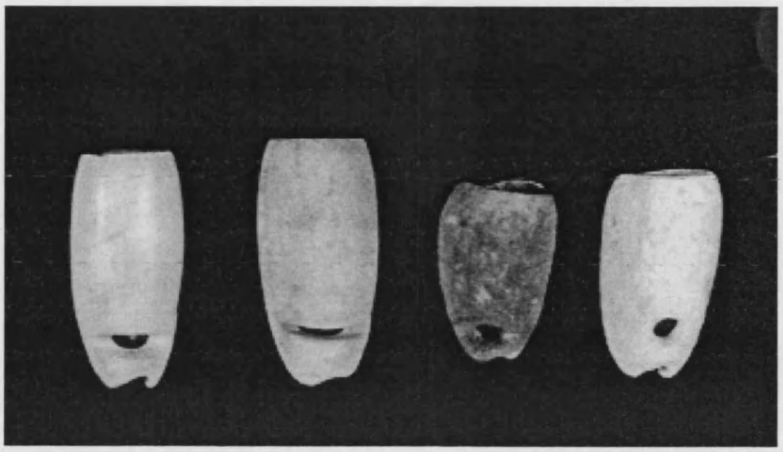

Figure 6.48. Four of the seven shells (Oliva sp.) belonging to the so-called 'pattern two' found in offerings 22 and 58. Our interpretation suggests that they may have symbolised maize seeds.

Another deity associated with *chicahuaztlis* was Cihuacoatl Quilaztli. In one prayer, she is described planting seeds with that instrument (Garibay 1969: 300-301; Mateos Higuera 1998, v.I: 146-147). This important deity personified the mother-earth goddess in her roles of facilitating birth and vegetation renewal. Like Xipe Totec, she also presents a dual aspect: appearing in some contexts as an elderly woman (Cihuacoatl Ilamatecuhtli) and in others as a young maiden (Cihuacoatl Quilaztli).

Therefore, given the above evidence we can interpret the adjacency of the three types of sceptres and the 'nose-plug' with split ends as a metaphor of the contrasting and complementary energies needed in the most imporant creative act: the fertilisation of earth, represented here with the sawfish.

6.10.2. PATTERN TWO

The skull of a sacrificed human being, a group of seven marine shells (*Oliva* sp.), two groups of copper bells, and the sawfish constitute the second pattern recognised in offerings 22 and 58 (fig. 6.48).

The first key to decipher the spatial association of these objects comes from the characteristics of the human remains themselves. In both offerings, the skull belongs to a young child, probably 3-4 years old, whose gender cannot be determined due to the bad preservation of the remains.

At such a tender age, children were particularly appreciated as offerings for being free of the contamination produced by sexual intercourse. As López Austin (1994: 173, 1989, v.1: 324, 326) points out, within Aztec cultural taxonomy sex was classified among the deadly energies that eroded human vitality and it was related with other negative earth influences. The word for sex *tlalticpacayotl* translates indeed as 'the earthy'. Within such logic, the act of offering an infant must be interpreted as the intention to communicate with gods through a messenger who has not yet been contaminated with 'sex/death' and therefore has his/her vital potential intact.

Especially eager to receive children sacrifices was the group of deities which scholars refer collectively as the *water-earth complex* (Nicholson 1971; López Austin 1994). The group includes male and female divinities with varied functions, including rain control and fertility (Tlaloc), earth regeneration (Cihuacoatl Quilaztli), motherhood (Cihuacoatl), and maize growth (Xilonen and Chicomecoatl).

Tlaloc, for example, received sacrificial oblations in the middle of lakes and other aquatic environments. The purpose of infant killings was to regulate the rain cycle and consequently to obtain good harvests (Graulich 1999: 265-278).

In Tlaloc ceremonies, however, it was common to offer the full body of children (see Roman Berrelleza 1987), while in offerings 22 and 58 only

Figure 6.49. The earth goddess Cihuacoatl beheading a human being, possibly a child. The image on the left is from Codex Borgia, and the figure on the right proceeds from Codex Laud (source Mateos Higuera 1998, v.1: 146, figs. 16.11 and 16.13).

the head was deposited. The remains under study contain in fact traces of a deliberate act of beheading, which should be taken into account for deciphering this pattern.

One goddess in particular is portrayed in codices in the act of decapitating a child. This is Cihuacoatl, who as indicated above was an earth-mother deity. One aspect of her powers represents sterile earth (Cihuacoatl Ilamatecuhtli), while another was linked to vegetation renewal (Cihuacoatl Quilaztli) (fig. 6.49).

Indeed, beheading was very common in sowing and harvesting rites, which emulated different stages of maize growth. Those known as Ochpaniztli, Tititl, and Huey Tecuilhuitl lasted twenty days each, were performed every year to mark different phases of the agricultural cycle, and included the decapitation of teenage girls that personified earth, water, and maize deities (Graulich 1999: 233-252, 379-401). Huey Teculhuitl, for example, coincided with the arrival of corn in cultivated fields. At that time, a

teenage girl (approximately 12 years old) was dressed with the attire of the goddess Xilonen, which included a necklace of gold pendants with corncob shape. Xilonen personified a 'tender corncob' and by dressing like the goddess the girl was supposed to acquire her germination powers. At a certain point of the rite, the girl's heart was extracted and her throat cut with the snout of a sawfish. Only after the girl was killed, the common people were allowed to harvest and consume the earth's new fruits (Durán 1984: v. I, ch. XIV: 135-141; Sahagún 1956, v. 1, b. 2, ch. XXVI: 173). The same happens to a girl dressed as Chicomeacoatl ('mature maize') in Ochpaniztli; and a similar rite was performed in Tititl, just before the starting of the sowing season.

The ceremony obeyed the deities' request of devolving the germination powers to earth in order to renew the agricultural cycle. This request is established in the myth of Cipactli, in which the monster explicitly demanded sacrifices and blood offerings from mankind as restitution for the life that she would provide on Earth. Interestingly, the snout of the sawfish was called *acipactli*, which translates as 'tool for sacrifice'.

Furthermore, one transfiguration of that original monster, this one with human form, was equally eager of human sacrifices. The deity in question was Cihuacoatl, who as we mentioned before belongs to the complex of mother-earth deities (Durán 1984, v.1, ch. XIII: 130).

The concept of sacrifice with the purpose to obtain new life was so embedded in Aztec mentality, that the whole existence was conceived as a cyclic process of life and death (i.e. as opposed to a linear one). In this mind set, the idea of devolving vital forces to earth was accepted as a natural act of preservation of the entire cosmos. In this regard, López Austin (1994: 204) points out that this cyclic philosophy was underpinned by the notion of 'restitution'. This consisted of returning supernatural

forces to their original source by dressing a human being with the attire of a certain deity and killing him/her afterwards. The idea of restitution and the metaphorical connection between human growth and maize development explains why so many young individuals were victims of sacrifice. Examples of the metaphor exist in many documents. For instance, the word used to describe the human body *tonacayo (i.e. 'our aggregation of flesh')* was also given to the maize plant. Additionally, children were referred sometimes as 'seeds', and a generic term for teenage girls was *jilotl (*i.e. *'tender corncob').*

It is precisely in this symbolic context that we can interpret the spatial association of the skull with seven marine shells of the *Oliva* gender. We agree with other researchers that these molluscs were metaphors for maize seeds (Del Olmo Frese 1999, Velázquez Castro 2000: 152-166). Evidence of such association still exists among the Tzotziles (Vogt 1983) and Totonacas (Ichon 1973), two contemporary ethnic groups that preserve most of their pre-Hispanic cultural background. These peoples see a resemblance between maize seeds and small shells by assuming that they possess the same germination energies. In consequence, Tzotziles avoid eating molluscs while there is still corn growing in the fields. A violation of this norm, they believe, would hinder maize development.

The number of shells is also very important because 'seven' was an esoteric number related to maize deities. It appears, for example, in Chicomecoatl ('Seven Serpents'), the name given to the goddess of mature maize; that is, the one responsible for facilitating maize growth at the final stage. Regarding this deity, López Austin (1994: 198) points out:

> It must be remembered that maidens associated with her cult carried groups of seven ears from which the seeds of the next crop would be extracted. The seven serpents can be interpreted, then, as the *germination powers of the goddess* (López Austin 1994: 198, emphasis added; translated from Spanish).

Furthermore, an Aztec prayer that specifically calls upon the generative powers of this goddess refers to her as 'seven ears' instead of 'seven serpents' (Garibay 1969: 304), and one of the names given to another earth-mother goddess was 'Cozcamiauh', which means 'necklace of ears' (López Austin and García Quintana 2000: 1261, Sahagún 2000, b.II, ch. XVI: 165).

Under such logic, it is reasonable to state that in the context of offerings 22 and 58, the seven *Oliva* shells represent the seeds (or corncobs) embedded with the germination powers of maize deities.

Finally, it is necessary to interpret the copper bells found at each side of the infant skull. Some scholars suggest that in general metal objects were classified as materials of cold and humid nature. Therefore, metals were appropriate to symbolise the Tlalocan, the mythical region imagined as repository of vital energies and home of water-earth deities (López Austin 1990: 372, López Luján 1994).

The copper bells fit well into this frame. They are seen in some codices as part of the attire of earth-water deities, appearing in ankles, headdresses, or as part of musical instruments (i.e. rattles). Moreover, one expert highlights their use in rituals celebrating human and agricultural fertility (Hosler 2000: 233):

> Bell sound replicate the sounds of thunder, rain, and the rattle of the rattlesnake, and we probably can add to that the roar of the jaguar, since Hunt (1977) links thunder to it (Hosler 1994: 233, 235).

Given the individual meaning of all the objects discussed above, it is reasonable to interpret 'pattern two' as a reference to germination forces, specifically of those that guarantee maize growth. If this were true, the burial of a child head attired with seed symbols would constitute an act

of 'sowing'. In a broader connotation this would also mean the return of germination forces to Earth in order to facilitate the beginning of the next agricultural cycle.

This conclusion coincides with the meaning of a Maya myth, in which the young god of maize is decapitated and then buried. Historian Enrique Florescano (1993: 95, 1994: 206-208) sees in the beheading a metaphor of ripping ears during the harvest period, and the subsequent burial of the god's head as a sowing act performed to renew the agricultural cycle.

6.10.3. PATTERN THREE

A second skull was deposited in each offering in association with a knife and a pair of shell pendants with oval form. The latter are called *oyohualli* (Figure 6.50).

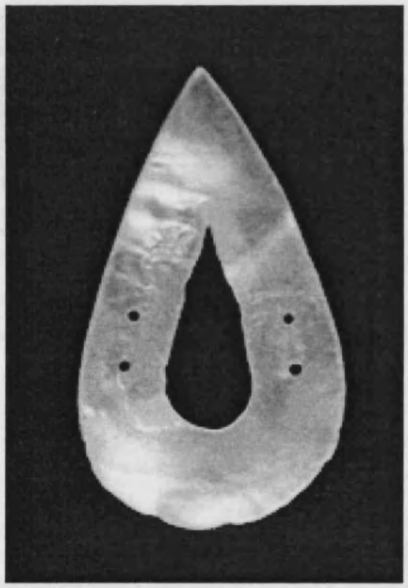

Figure 6.50. One of two oyohualli pendants that participate in the third pattern found in offerings 22 and 58.

The skull found in offering 22 (element 7) belongs to a young individual (18-20 years old approximately) who was subjected to severe deformation of the forehead, Such deformation constituted a common practice among Aztecs. It was usually performed immediately after birth, allegedly to mark high status or for religious reasons.

On the other side, the skull in offering 58 (element 25) was originally recorded as a child. In a recent examination, however, Physical Anthropologist Juan A. Roman Berrelleza (personal communication) calculated the age of this individual at approximately 18 years old.

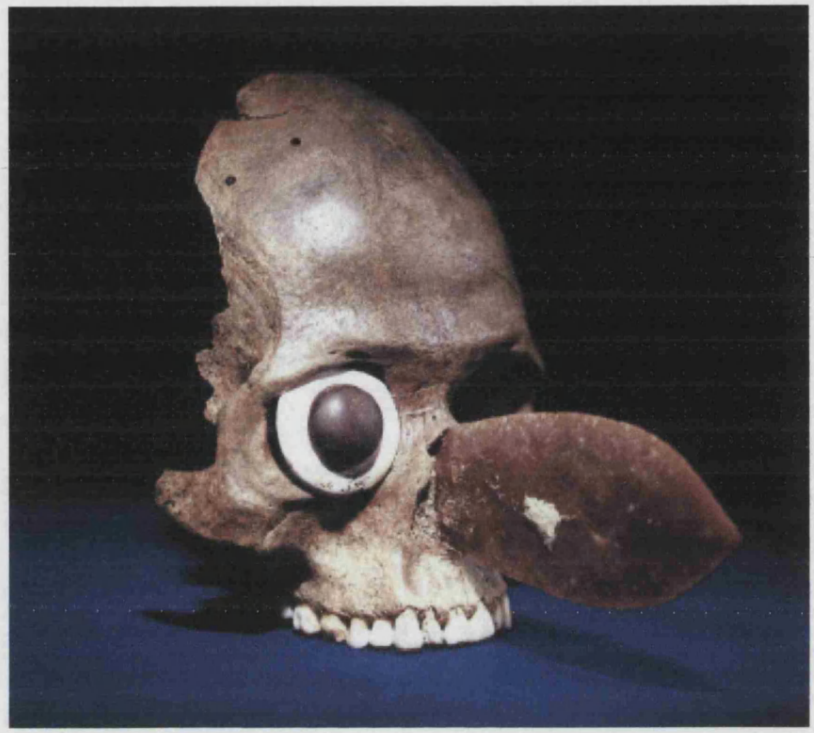

Figure 6.51. Skull-mask of the type found in offerings 22 and 58. This is an important element of the third pattern detected with the RN-Method (Photograph by Fernando Robles, source: Bonifaz Nuño 1981, fig. 49).

The latter conclusion is based on the existence of the third molar, dental piece that only appears after childhood. Unfortunately, it was impossible to achieve an accurate determination of gender for any of these skulls.

Age is not the only difference of these remains with the previous pattern: while the children heads discussed before were deposited with flesh, the crania of these young adults were placed without it. This reveals the intention of depositing osseous matter, suggesting a different meaning of the skull in relation to 'pattern two'.

A second difference is that in each offering the skull is very close to a flint knife. Such an object may in fact have been inserted either through the mouth or through the nasal cavity, forming what some scholars describe as a 'skull-mask', as opposed to a person's 'head' (see fig. 6.51).

It is likely that such masks were made from the remains of war prisoners or sacrificial victims long before placing them in the offerings. Also, they appear as glyphs of 'death' or 'sacrifice' in some codices.

To decipher the symbolism of this pattern we rely on interpretations made by Furst (1982), López Austin (1989, 1994) and Chávez Valderas (2002), who have discovered a relationship between skeleton parts and regeneration concepts.

According to López Austin (1989: 197-251), Aztecs believed in three 'souls' or 'animic entities' that maintained people alive. One in particular, called *tonalli* was conceived as a 'hot' radiation, which invigorated and fortified organisms propitiating growth. The possession of tonalli was not exclusive of humans. Other beings, especially plants and animals, also needed this energy to exist.

The amount of *tonalli* possessed by each individual varied through life. A very small quantity was first acquired in the womb, but as the person grew older this energy increased. It was important to keep it inside the body and to compensate any drastic fluctuations that may occur. Finally, when the person died, part of his/her *tonalli* remained in the bones. Interestingly, the major source of *tonalli* was the sun and its main repository in the human body was precisely the head (López Austin 1988: 223-251). This allows us to speculate that perhaps the deformation of the skull had the purpose of enlarging the container of *tonalli*.

In this context, it is worth noticing that Velázquez Castro (2000: 156) - expert in the analysis of Mexica shell ornaments- points out that 'heat' and 'renascence' are two ideas seemingly represented by the *oyohualli* pendants. He based his hypothesis upon pictorial evidence, which shows these objects as earplugs and pectorals of certain *solar-fertility* deities

(who complement the 'cold' divinities of the water-earth complex). They were in possession of a high proportion of *tonalli*. The group includes, among others, Tlahuizcalpantecuhtli (planet Venus), Macuilxochitl (god of pleasures, including feasting, gaming, etc.) and Huehuecoyotl (god of sexual instinct, music and dance).

According to Nicholson (1971: 417) this group expressed not only "generative power in the abstract –and sexual lust which promoted it..." but also "a lighter side of the sanguinary solar-war-sacrifice cult-" and more importantly, these gods had very close connections with Centeotl, the young god of maize.

Therefore, we can interpret these 'skull-masks' wearing *oyohuallis* as repositories of the *tonalli* radiation needed for the germination of maize. According to this hypothesis, the purpose of the skull-mask of 'pattern three' -representing *growing* energies- would be to liberate the *germination* powers symbolised by the child head and the *Oliva* shells (i.e. the seeds) of 'pattern two'.

The idea of recycling osseous matter in order to produce new life is a fundamental theme in Aztec mythology. In one story, Quetzalcoatl (a male deity) steals bones from Mictlan (home of the dead) and crushes them with the intention to create the first human being. However, the release of vital forces stored in the bones is only possible with the help of Cihuacoatl Quilaztli, who made her germination powers available during the process. It is worth repeating, once again, that among other important functions Cihuacoatl Quilaztli was responsible of controlling the renewal of vegetation and the generation of human beings. In fact, her name translates as 'the arrival of staple food" or 'the arrival of vegetables' (López Austin 1994: 205-209).

Figure 6.52. Pictorial representation of Cihuacoatl during the rite of Tititl. During that ritual a girl was beheaded and a priest wore a mask made with her remains. Here, the goddess appears showing her skull instead of her face (source: Mateos Higuera 1998, v.1: 144, fig. 16.7).

We should also remember that an opposite aspect of this goddess (Cihuacoatl Ilamatecuhtli, sterile earth) is directly involved with beheading during the agricultural rite known as Tititl. In such a ceremony, a priest wore a 'mask' made from the remains of a decapitated girl (Graulich 1999: 233-252). Furthermore, in some codices, the goddess appears showing her skull, instead of her face (see fig. 6.52).

6.10.4. PATTERN FOUR

The fourth pattern of offerings 22 and 58 has the following elements: *Xancus* shells, mother-of-pearl shells, sea urchins, and turtle shells, all distributed over the area opposite to the skulls. One mother-of-pearl shell and one turtle in each offering constitute the local centre of this pattern, which reinforces the idea of similarity between both caches.

There is general agreement among scholars about the meaning of marine objects in Aztec religion. Tiny molluscs, for example, were used to represent water and raindrops, especially to indicate the humidity existing in Tlalocan (sustenance place) and Mictlan (home of dead). These cosmic regions were imagined as cold, damp, and misty environments. We believe that this is precisely the meaning of the bottom layer of the offerings (i.e. the one excluded from the topological analysis), in which there is marine sand, a great amount of tiny shells and greenstone beads (see section 6.1.1). Some scholars believe that such a connotation extends to bigger species, like the mother-of-pearl shells and *Xancus* specimens found in offerings 22 and 58. Under such logic, the shells would simply mean the Tlalocan or the underworld.

We believe, however, that the spatial adjacency of shells in pattern four expresses a different, more complex concept, whose specific meaning depends on the precise combination of objects describe here. First, it is well known that some concave shapes were associated with the womb. This is particularly true with regard to mother-of-pearl, *Xancus*, and *Spondylus* species (the latter is not present in offerings 22 and 58), and probably applies as well to the sea urchin and the turtle shell. The metaphor may have been based on the protective quality of these structures, as well as on the softness of the animal living inside, which might have resembled a foetus.

Whatever the reason, Aztecs imagined that some vivifying energy existed inside these shells, because in many pictorial and sculptural representations they appear 'giving birth' to human beings. For instance, some reliefs from Chichen Itza, a Maya city which received strong Nahua influence during the XII century, portray gods emerging from marine shells (fig. 6.53a).

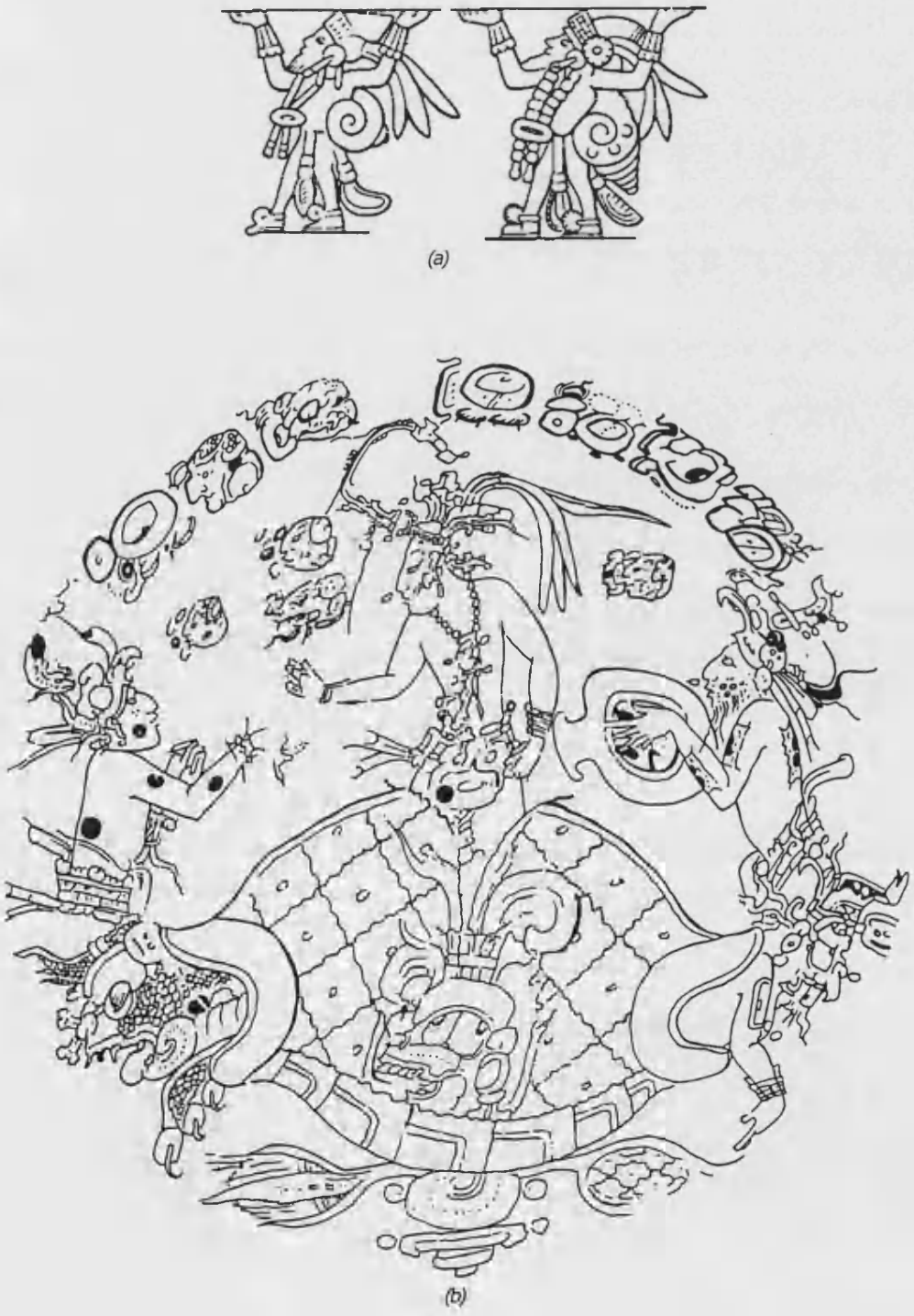

Figure 6.53. Maya gods emerging from marine shells (a); and from a turtle (b). The figure emerging from the turtle has been identified as the god of maize (sources: (a) is from Thompson 1984: 159, fig. 13, and (b) is from a Maya plate).

As we said, such symbolism might extend to other animals. Figure 6.53b also represents the young god of maize emerging from a turtle shell. Obviously, the image represents the blossoming of the maize plant, thus the turtle is chosen here as a symbol of earth. However, the precise phenomenon portrayed in the image is maize 'birth', which made the artist to select the turtle, allegedly a container of womb-like energies, as the most compelling metaphor for the gestation process.

Another example is an Aztec sculpture that portrays a solar deity –identified as Macuilxochitl- also emerging from a turtle. Interestingly, the god wears *oyohualli* pendants, which as we explained before are important elements of offerings 22 and 58 (see fig. 6.54).

Figure 6.54. The god Macuixochitl emerging from a turtle (from the collection of Museo Nacional de Antropología, Mexico).

In addition, some ceramic figures found recently in another offering of the Great Temple represent human beings (perhaps maize deities) emerging from turtle shells.

The relation of turtles with womb-like energies becomes even more compelling if we consider the name given to another mother-earth goddess, Ayopechcatl. This one was specifically related to gestation. According to Garibay (1969) the word *ayopechcatl* derives from *ayotl* (turtle), and translates as 'the one who is on the layer of turtles' or 'the inhabitant of the bed of turtles'. No much information has survived about this deity, but it is repeatedly mentioned in pregnancy rites as the first woman in

giving birth. One scholar summarises her role as follows (see also Garibay 1958: 128, 1969: 300; León Portilla 1958):

> Her influence fell over the womb of the pregnant woman. It seems that the maternal chamber was her habitat, at least from the beginning of gestation till childbirth Mateos Higuera (1998, v.1: 137, translated from the Spanish original).

The goddess Ayopechcatl was closely related to Cihuacoatl, and in fact may have been the same deity. Both were honoured by midwifes. One spell pronounced while women were in labour says:

> "In some place, in some place,
> In the home of Ayopechcatl...
> The mature wombs attain life.
> Get up, come,
> Be sent, get up, come,
> New child,
> Get up, come..."

Interestingly, midwifes used certain shells, called *ticicaxitl* ('bowl of female doctors' i.e. midwifes), to make predictions about children's health and destiny. The group of *ticicaxitl* included, among others, the mother-of-pearl shells. Apparently, Aztecs observed the iridescent layer of these molluscs in order to foresee children's future (Sahagún, 2000, b. XI, ch. III; López Austin and García Quintana 2000: 1323).

The above evidence indicates that the four kinds of shells of this pattern represent containers of fecundity forces; that is, incubation structures from which humans and maize could emerge. It would be even possible to suggest that the pattern contains incubation forces of earth (turtles), plus incubation forces of aquatic nature (marines shells), though much harder evidence needs to be gathered to support such argument.

Figure 6.55. An unidentified deity portrayed on a clay pot. It shows features related to water, earth, and fertility. Especially interesting are the flowers and trilobed forms modelled around the neck, as well as the spikes emerging from the crown, which might represent 'corncob shairs' (source:

6.10.5. PATTERN FIVE

The above discussion leads us to an explanation of the last pattern of offerings 22 and 58. This one is very simple. It contains a pot sitting over a turtle shell (offering 22), or over a perforated conch-shell (offering 58). Needless to say, the pot occupies an important position in the control and integration structures of the offerings and it is clearly isolated from all the other patterns of the caches.

The pot shows a human face modelled on the front, presenting "features which apparently are related to water, earth, and agriculture" (Heyden 1987: 113). It is most likely a deity, but unfortunately no one has been able to identify who exactly is portrayed (fig. 6.55).

Part of the problem derives from the lack of gender attributes (the pot shows only the face and the upper torso). Another cause of difficulties is that the features seen in this vessel are common to many deities from water-earth and maize complexes. These include a paper headdress in the form of a pleated fan; many spikes emerging from a crown (*amacalli*) which scholars interpret as corncob-hairs; a circular pectoral, etc. All or parts of these attributes are seen in Tlaloc, Chalchiuhtlicue, Xilonen, Ayopechcatl, Chicomecoatl, Centeotl, Xochiquetzal, Tonacacihuatl, Huixtocihuatl, etc.

Doris Heyden (1987) has attempted an interpretation of this type of vessel focusing on certain flowers and trilobed forms modelled around the neck, as well as two eccentric forms at either side of the vessel.

She believes the flower species corresponds with *Tagetes erecta*, known in English as marigold and in Nahuatl as *cempoaxuchitl*. These flowers were used in some of the annual rituals of vegetation, both in connection with water deities, as well as with solar ones. López Luján (personal communication) rightly notices, however, *that Tagetes lucida*, instead of *Tagetes erecta*, might be represented on the pot. The distinction is important, because the latter seem related with gods of fire, while the former received the name *yauhtli* and was clearly associated with aquatic and cold 'earth' divinities. Yauhtli was in fact a medicinal plant used to dull the pain of burns.

If *yauhtli* flowers were modelled on the vessel, then the trilob and eccentric forms would also make sense. The trilob form, also known as 'triple droplet' represents raindrops (von Winning 1987), while the eccentric shapes at either side of the vessel have been interpreted as clouds. Rain, clouds, and misty environments belong to the cold, earthy regions of cosmos, and refer to the inhabitants of Tlalocan (i.e. place of sustenance).

Therefore we would have a pot portraying one of the earth-water fertility deities, as opposed to a solar one.

The vessel in question would also form a complementary pair with another group of similar pots found in Tlatelolco, the twin city of Tenochtitlan. There are eight vessels from that site, which are almost identical to the one we are examining. The only differences are that, instead of flowers, they represent ears of maize, and instead of raindrops they show 'jewel' symbols (i.e. a metaphor of successful harvest). Furthermore, instead of containing copal (incense resin), they contain a human skull. As Heyden points out:

> The Tlatelolco vessels differ from those of the Templo Mayor in that they have ears of corn flanked by jewel symbols in place of the trilobed motif (Fig. 9). Furthermore, they contained human skulls instead of copal incense. I have found no reference to the sex of these skulls, but if they were female, the urns adorned with corn may have been used in rites of sustenance where Chicomecoatl's impersonator was decapitated as a ritual metaphor for the cutting of the ears of maize *at harvest time* (Durán 1967, I: 139). On the other hand, the Templo Mayor vessels or incense burners, with copal in their interiors, are perhaps connected with water rites. In Prayer to Tlaloc (Sullivan 1965: 43) this god is called not only the "Lord of the Sweet-scented Marigold" but also the "Lord of Copal" (Heyden 1987: 126, emphasis added).

We believe that the above hypothesis is correct with regard to the Tlatelolco vessels. Pots portraying a fertility deity with maize ears would be appropriate to symbolise *harvest* and the pots would be relevant for honouring Chicomeacoatl or Xilonen.

On the other side, Heyden's hypothesis could be refined with regard to the vessels in offerings 22 and 58. In our view, a vessel with symbols of Tlalocan would be more appropriate in rituals involving the idea of *sowing*, that is, of returning seeds to mother-earth. This would explain why the vegetation deity portrayed in the Templo Mayor pots does not show signs of mature maize. Instead, those vessels might have been appropriate to

call upon the powers of Cihuacoatl Quilaztli, rather than Tlaloc.

This is supported by the general context of offerings 22 and 58: a child head, as opposed to a young individual, who represents maize seeds, as opposed to a grown plant; 'hot' growing energies deposited in bones (pattern three); cold gestation forces represented by three types of shells and the cradle (pattern four); and the union of these forces at the centre of the deposits (pattern one); all placed to call upon the earth goddess (pattern five), in the womb-region Tlalocan (the latter symbolised here with the bottom layer of tiny shells and greenstone beads excluded from the topological analysis).

With such interpretation concludes our presentation of the RN-Method. We hope that the procedures explained here would provide appropriate tools to study the Mexica offerings in particular, as well as other spatial symbolic contexts in the future.

7 CONCLUSIONS

At the beginning of this thesis, we mentioned spatial symbolism as an important component of many cultures around the world. We pointed out that such phenomenon consists in the projection of metaphysical ideas through the ordering of artefacts and other entities over space.

We also mentioned that this gives rise to complex systems, usually underpinned by mythological and religious beliefs, whose main outcomes are the so-called 'spatially symbolic contexts'. In section 2.4, we defined these as "... object arrangements ordered in such a way that the literal significance of each item acquires a parallel, deeper meaning *thanks to its spatial associations with the rest of the group.*"

Spatial symbolic contexts appear frequently as a subject of study in archaeology. Unfortunately, until the starting of this project, there were not many appropriate methods to investigate them. One reason for such scarcity has been the great diversity of forms in which the contexts appear. This indeed has complicated the creation of generic procedures that specifically target the analysis of their spatial structure.

We undertook the challenge of improving such a state of affairs by developing analytical procedures suitable to the Mexica offerings. By focusing on this particular case of spatial symbolic contexts, we adopted a bottom up approach, which hopefully can be extrapolated to other applications in the future.

This explains the great attention given in this thesis to the Mexica offerings. Our project started with an investigation of Aztec religion and cosmology, two crucial aspects that motivated the deposition of these contexts (cf. Chapter 3).

Then, we gathered specific information about the offerings: first, by examining their role in Aztec culture; secondly, by identifying their most distinctive characteristics; and finally, by reviewing previous approaches for the study of these contexts.

With regard to their physical characteristics, we realised that the Mexica offerings were the outcome of combinatorial principles which prescribed where to place each kind of object and how to associate several of them in order to communicate a ritual message. Some of these principles were detected a long time ago by one of the scholars involved in offering interpretation (López Luján 1994: 138-145). These include, among others, the distribution of artefacts along 'imaginary axes' that run in longitudinal and transverse directions, the symmetric location of artefacts with contrary meanings, the aggregation of items which according to Nahua cosmovision represented similar concepts, the juxtaposition of those that had complementary character, the repetition of certain classes in specific numbers, and so on. The same scholar suggested that many of those features replicated the Mexica model of the cosmos.

Another important discovery was that, despite the recognition of space

as a fundamental dimension in the analysis of Mexica offerings, specialists had avoided the development of formal means to discover spatial patterning. Therefore, we assessed previous studies in order to learn from their strengths and weaknesses. This lead us to identify three major issues that hindered the analysis of offerings in the past (cf. section 4.5):

The first one consisted in examining offerings as isolated units, that is, without comparing the cache's structure with other deposits. Although some caches are genuinely unique, this is not always the case. In fact, some time ago one scholar suggested that there were groups of offerings remarkably similar (López Luján 1994). To prove that assertion, he applied the method of Numerical Taxonomy and compared the types of objects included in a sample of 108 caches. He finally recognised 20 groups of similar offerings. That study marked a breakthrough in offering interpretation, but unfortunately it was limited to comparing the caches' contents, as opposed to targeting the distribution of artefacts inside each deposit.

A second mistake of previous approaches was the tendency to analyse only the most 'remarkable' objects. This narrowed the possibilities of reaching correct interpretations because ignored the value of the most unattractive items, which might have been extraordinarily meaningful in Aztec times.

Finally, the major mistake of all was to overlook the internal structure of the caches. This has been especially regrettable because, as we hope to have proven in this thesis, recognising spatial ordering is critical to decipher the purpose and meaning of the offerings.

Therefore, during the course of this research we searched for new analysis

procedures that specifically targeted the correction of the above mistakes. This led us to outline the following objectives for the new method:

1. To provide means for comparing multiple offerings, not only in terms of their general contents but also in terms of their spatial structures.

2. To assess the relative importance of offering artefacts with criteria based on quantitative values of spatial *integration* and *control*, rather than on subjective speculations about their status.

3. To identify recurrent combinations of artefacts in a formal way, such that some symbolic themes could emerge from the analysis. This includes the recognition of spatial arrangements formed by specific categories of objects, whose degree of association can be asserted not only with a dissimilarity index but also through a technique based on interactive visualisation.

To achieve those objectives, we represented each offering as a set of points in three-dimensional Euclidean space and proposed to consider the relative position of the artefacts. That is in contrast with traditional methods of spatial analysis, which focus on the absolute location or points (e.g. nearest neighbour).

Following such proposal we developed the *RN-Method*. This includes topological concepts, graph theoretical measures, and pattern recognition techniques oriented to describe the offerings internal structure. The description focuses on the adjacency of points and relies on the so-called proximity graphs, which include Relative Neighbourhood Graph (RNG), Gabriel Graph (GG), Beta-skeleton (b-S), and Limited Neighbourhood Graph (LNG). These were developed in the field of pattern recognition by Lankford (1969), Toussaint (1980), Gabriel and Sokal (1969), Urquhart (1982), and

some other scholars. Such constructs expose the topological shape of point sets in the form of edges connecting a subset of the pairs of points.

The underpinning concept of proximity graphs is the notion of relative neighbourhood. This is based on the establishment of a *region of influence* for every combination of pairs of points existing in the source data. Two points are said to be relative neighbours, that is, topologically adjacent, if and only if no other point is located inside their respective region of influence. Variations in the shape and size of the region of influence generate different sets of connections among the points, which gives analysts the possibility to assess whether such connections represent a 'significant pattern'. This takes advantage from human capabilities to perceive patterns by visual means, and therefore, it is appropriate as a foundation for the RN-Method.

The incorporation of proximity graphs into the RN-Method offers the following advantages for the analysis of spatial symbolic contexts in general, and the Mexica offerings in particular:

1. The relative definition of neighbourhood is useful to assess whether one artefact has other significant spatial relationships besides its nearest neighbour. Therefore, the adoption of the concept represents an appropriate mechanism to explore contextual relationships in Mexica offerings.

2. The application of proximity graphs allows searching for patterns without considering prior assumptions about the morphological features that would eventually emerge from the point set under study. Less appropriate graphs like the Minimum Spanning Trees or Delaunay triangulations are less flexible and reveal only certain types of geometric arrangements like trees or triangular patterns.

3. Both RNG and GG have the property of being 'unique'. This means that a point set has one and only one RNG and GG. Using this property, two or more different patterns can be compared in order to determine how similar they are with respect to each other. In the case of the Mexica offerings, this allows identifying caches that have similar artefact distributions. The latter represents an improvement over previous approaches, which consider only similarities in the type of contents, and ignore the spatial dimension (see section 4.4).

4. The adoption of Beta-skeletons and limited neighbourhood graphs brings additional benefits:

   a) Beta skeletons represent a parameterised family of topological descriptions of the point set, which progressively exposes more details of point connections. By focusing on those groups of nodes whose connections remain constant throughout changes in the region of influence, it is possible to discover which are the strongest and more consistent morphological features of the point set, and therefore, of the offerings.

   b) Limited Neighbourhood Graphs, on the other side, reveal different alternatives of clusters, which might correspond to symbolic links among the artefacts. An advantage of these LNG's is that they expose those clusters not only through a dissimilarity measure, but also in a visual way.

   c) Together, Beta-skeletons and Limited Neighbourhood Graphs make the procedure suitable for exploratory spatial analysis.

5. Beyond the recognition of geometric features, proximity graphs also allow including categorical information into the analysis. During the last part of the method, vertices were labelled according to the class of artefact that each one represented. Eventually, this was the key to discover meaningful combinatorial themes in the offerings of the example.

As for the specific advantages of RN-Method, we can offer the following conclusions:

1. The RN-Method is useful to analyse the topological structure of the offerings based primarily on the adjacency of points.

2. The representation of artefact relations in the form of graphs facilitates the analysis, not only quantitatively but also in a visual way.

3. The RN-Method provides means to quantify both global and local spatial properties of the offerings. The different measures of graph structure, along with the production of connectivity profiles, represent a useful tool to explore global tendencies. This responds to the first analysis objective outlined in section 4.5.

4. As for the local level, the measures of integration and control, borrowed from the space syntax method of Hillier and Hanson (1984), represent a formal way to assess the relative importance of different types of artefacts within spatial symbolic contexts. This represents an improvement over the subjective analysis of artefacts based on their simple appearance. Therefore, with the adoption of such measures we have met the second objective outlined in section 4.5.

5. Finally, the RN-Method facilitates the identification of artefact combinations, which can lead to the proposal of hypothesis about the offering meaning. These hypotheses are still based on external information (i.e. iconography, historic sources, and ethnology) but at least they are formulated on the basis of formal measures of artefact spatial associations. We believe that the latter represents a major improvement with regard to other traditional approaches. In many previous works, spatial associations among artefacts have been established in subjective ways with the intention to support preconceived hypotheses; that is, patterns have been *imposed* rather than *discovered*. The approach presented in this thesis reversed such logic. We focused primarily on the spatial component of the offerings identifying morphological traits first, and formulating hypotheses only after some regularities had been discovered.

6. Furthermore, the RN-Method works independently of prior assumptions about the symbolism of individual items. In this sense, it complies with the descriptive autonomy that Hillier and Hanson (1984) identify as a requirement for any method dealing with space logic. In particular, patterns are described an analysed in their own terms; the method accounts for fundamental variations in morphological type; and it is equally useful for analysing highly organised structures, as well as those showing little order.

We expect that further developments would allow extending the range of applications for the RNG method to other kinds of problems. For example, if the connections integrate an empirical network (e.g. roads connecting towns) instead of a symbolic context, then the procedures described here may be also useful, for example, to establishing the degree of *accessibility* of certain locations in relation to others. They may also be

valuable to assess the relative *hierarchy* or *control* that each settlement exercises over its neighbours given its relative position in the network structure. Within the field of archaeology, an interesting application for such analysis may be found in the study of settlement patterns. At the present time we are working on a new research that pkans to orient the benefits of the RN-Method in that direction.

APPENDICES

A ALGORITHMS TO COMPUTE PROXIMITY GRAPHS

Among the many algorithms that have been proposed for computing proximity graphs, the most robust and easiest to implement is the one proposed by Toussaint (1980:266), which extracts only the relative neighbourhood graph.

A.1. ALGORITHM RNG-1

Step 1. Compute the distance between all pairs of points: $d(pi, pj) \quad i, j = 1, \ldots, n; \quad i \neq j$

Step 2. For each pair of points (pi, pj) compute:

$$d^k_{max} = max\{d(p_k, p_i), \quad d(p_k, p_j)\} \quad for \quad k = 1, \ldots, n; \quad k \neq i, k \neq j.$$

Step 3. For each pair of points (pi, pj) search for a value of d^k_{max} that is smaller than d(pi,pj). If such point is not found, draw an edge between pi and pj.

Toussaint RNG-1 algorithm allows computing relative neighbourhood graphs in any number of space dimensions. However, it performs (n^3) operations. Therefore is not very efficient in terms of timing and uses a very large segment of computer memory.

None of these inconviniences, however, pose serious problems for applications involving less than 2000 points. Thanks to the current speed of most PC´s the three steps implemented in a language such as C or C++ would take from a couple of seconds to a few minutes.

For larger data sets, it is advisable to use more efficient algorithms. Some of these are discussed in publications by ElGindy and Toussaint (1988), Huang (1990), Hurtado et al (2001), Ichino and Sklansy (1985), Jaromczyk and Kowaluk (1987, 1991), Katajainen (1988), Katajainen and Nevalainen (1986a, 1986b, 1987), Katajainen et al. (1987), Lee (1985), Olariu (1989), Rao (1998), Su and Chang (1990, 1991a, 1991b, 1991c), Supowit (1983), Toussaint (1980b, 1980d), Toussaint and Menard (1980), Urquhart (1980, 1983), etc.

Point set representations of Mexica offerings don't include more than 500 points. This would allow us to choose the above algorithm for computing the relative neighbourhood graph. However, we also need to extract other kinds of adjacency networks. For this reason we have decided to generalised Toussaint's algorithm in order to make it useful not only for extracting relative neighbourhood graphs but also Gabriel graphs and the series of Beta-Skeletons that are needed for this research.

The later is possible considering that the Gabriel graph always corresponds to the skeleton obtained with Beta = 1. Likewise, the relative neighbourhood graph corresponds to Beta = 2. Therefore, all we really need is to be able to extract skeletons with different values of Beta. This can be accomplished with algorithm described in the following pages.

A.2. BETA-SKELETON ALGORITHM

GIVEN A SET OF POINTS:

$$S\{p_1(x_1, y_1, z_1), p_2(x_2, y_2, z_2), \ldots, p_n(x_n, y_n, z_n)\} \qquad \text{for } n \geq 3;$$

STEP 1

Get the value of Beta.

STEP 2

Compute the distance between all pairs of points: $d(p_i, p_j)$ $\text{for } i, j = 1, \ldots, n;\ i \neq j$:

STEP 3

For each pair of points $p_i(x_i, y_i, z_i), p_j(x_j, y_j, z_j)$ perform the following operations:

a) Compute the radius of the regions of influence $r(p_i, p_j)$:

$$r(p_i, p_j) = \text{Beta} * d(p_i, p_j) \div 2 \quad \text{for } i = 1, \ldots, n;\ j = 1, \ldots, n;\ i \neq j;\ \text{Beta} \geq 1$$

b) Calculate coordinates for the centres of two circles C_i, C_j whose intersection delimits the relative neighbourhood of p_i, p_j:

$$\begin{aligned} x_{ci} &= ((1 - (Beta \div 2)) * x_i) + ((Beta \div 2) * x_j); \\ y_{ci} &= ((1 - (Beta \div 2)) * y_i) + ((Beta \div 2) * y_j); \\ z_{ci} &= ((1 - (Beta \div 2)) * z_i) + ((Beta \div 2) * z_j); \end{aligned}$$

$$\begin{aligned} x_{cj} &= ((Beta \div 2) * x_i) + ((1 - (Beta \div 2)) * x_j); \\ y_{cj} &= ((Beta \div 2) * y_i) + ((1 - (Beta \div 2)) * y_j); \\ z_{cj} &= ((Beta \div 2) * z_i) + ((1 - (Beta \div 2)) * z_j); \end{aligned}$$

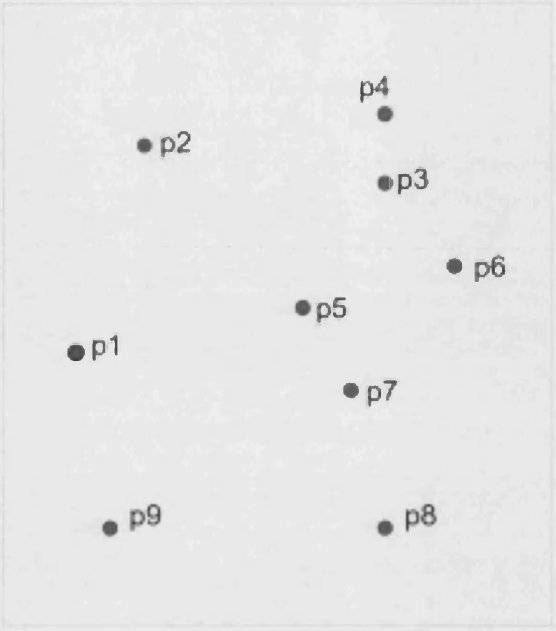

Figure A.1. A sample distribution of nine points.

STEP 4

For each point p_k different than p_i and p_j do the following:

a) Get the maximum distance:

$$d^k_{max} = max\{d(p_k, c_i), \quad d(p_k, c_j)\} \quad for \quad k = 1, \ldots, n; \quad k \neq i, k \neq j.$$

b) Search for a value of d^k_{max} that is smaller than $r(p_i,p_j)$.

c) If such value is not found, it means that no other point lies within the relative neighbourhood of p_i, p_j and therefore an edge must be drawn between p_i and p_j.

A.3. DESCRIPTION

In order to illustrate the logic of the above algorithm lets consider the group of nine points shown in figure A.1 and suppose that we wish to

extract the Gabriel graph, the relative neighbourhood graph and a series of Beta Skeletons.

Step 1 introduces the parameter Beta as a way to control the size of the region of influence and in that way determining which type of proximity graph will be obtained. As explained in chapter 5, for any point distribution Beta = 1 gives rise to the Gabriel graph; Beta = 2 produces the relative neighbourhood graph; and any other value of Beta, say x, yields the corresponding X-Skeleton.

Step 2 consists in computing distances between every combination of two points. The total number of operations required during this step is given by the well-known combinatorial formula $(n*n\text{-}1)\div c$, where *n* is the total number of points and *c* refers to the number of elements in each combination, in this case 2. $C_i \cap C_j$

The point set of figure A.1, for example, will require the calculation of 36 distances, as there are $(9*8)\div 2$ possible two-point combinations. Figures A.2a and A.2b show labels for two point pairs (p_1,p_2) and (p_3,p_4) as well as the lines representing their distances.

The algorithm proceeds in steps 3 and 4 with a series of operations focused on each particular pair of points:

Step 3 defines radius and centre coordinates for two circles C_i and C_j, whose intersection will delimit the *relative neighbourhood* of p_i and p_j. The radius is obtained multiplying the distance $d(p_i, p_j)$ by the parameter Beta and then dividing the result between 2. On the other side, centre coordinates for both circles are calculated using the formulae included in the above algorithm (step 3b), which were developed by Kirkpatrick and Radke (1985).

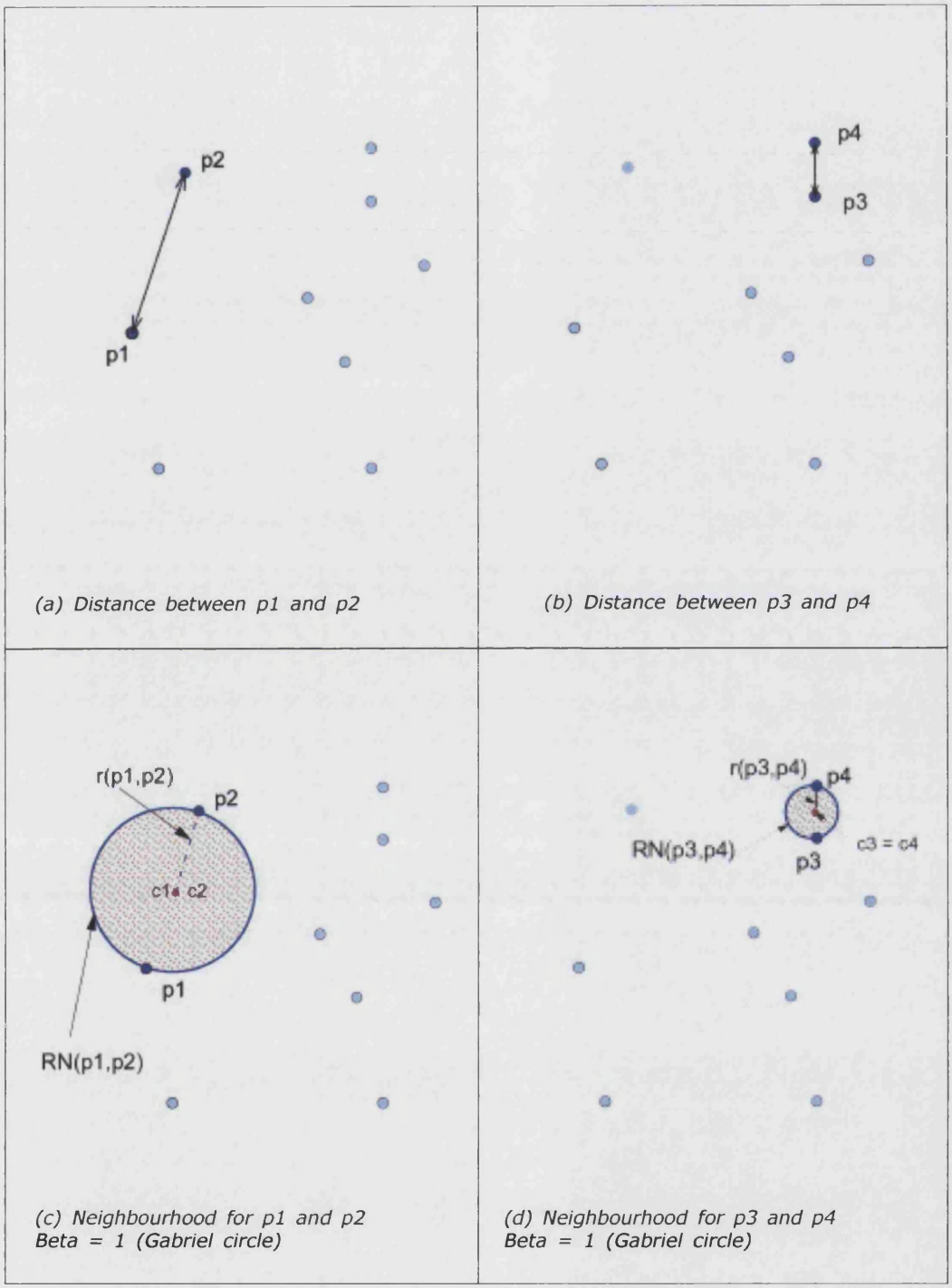

Figure A.2. Relative neighbourhood for the pairs (p_1,p_2) and (p_3,p_4) when Beta = 1. *On the right side, the relatively small distance between p_3 and p_4 produces a minor neighbourhood, while the opposite happens for p_1 and p_2 on the left side despite that in both cases Beta remains constant.*

Notice that the length of the radius, as well as the location of the circle centres, are proportional to the distance between each individual pair of points and to the value of Beta. Both factors will in fact determine the amount of space covered by the circles intersection and therefore such extension will be different for each point pair. This explains why we qualify such kind of neighbourhood as "relative."

In order to appreciate the effect of the distance factor compare figure A.2c with figure A.2.d. They illustrate the relative neighbourhoods for the pairs (p_1,p_2) and (p_3,p_4) respectively. In both cases, the value of Beta remains the same, but the distance between the points is different and so it is the size of the resulting neighbourhood.

Equally important is considering the effect of Beta changes. Figure 7.3 shows the relative neighbourhood belonging to points p_1 and p_2 for three different values of Beta. Observe the changes in the shape of region $RN(p_1,p_2)$ as Beta increases, as well as the different locations given to centres c_1 and c_2.

For example, when Beta = 1 both centres lie exactly at the middle of $d(p_1, p_2)$ and the relative neighbourhood $RN(p_1,p_2)$ present a circular form (see fig. 7.3b). Such case corresponds to the Gabriel graph.

As Beta increases the relative neighbourhood will acquire a "lune" shape. A clear example of this is when Beta = 2 (i.e. the relative neighbourhood graph). In that case the circles centres will coincide with the points p_1 and p_2 (see fig. A.3c).

Any other value of Beta will yield centres in other locations symmetrical to p_1 and p_2 (see fig. A.3d).

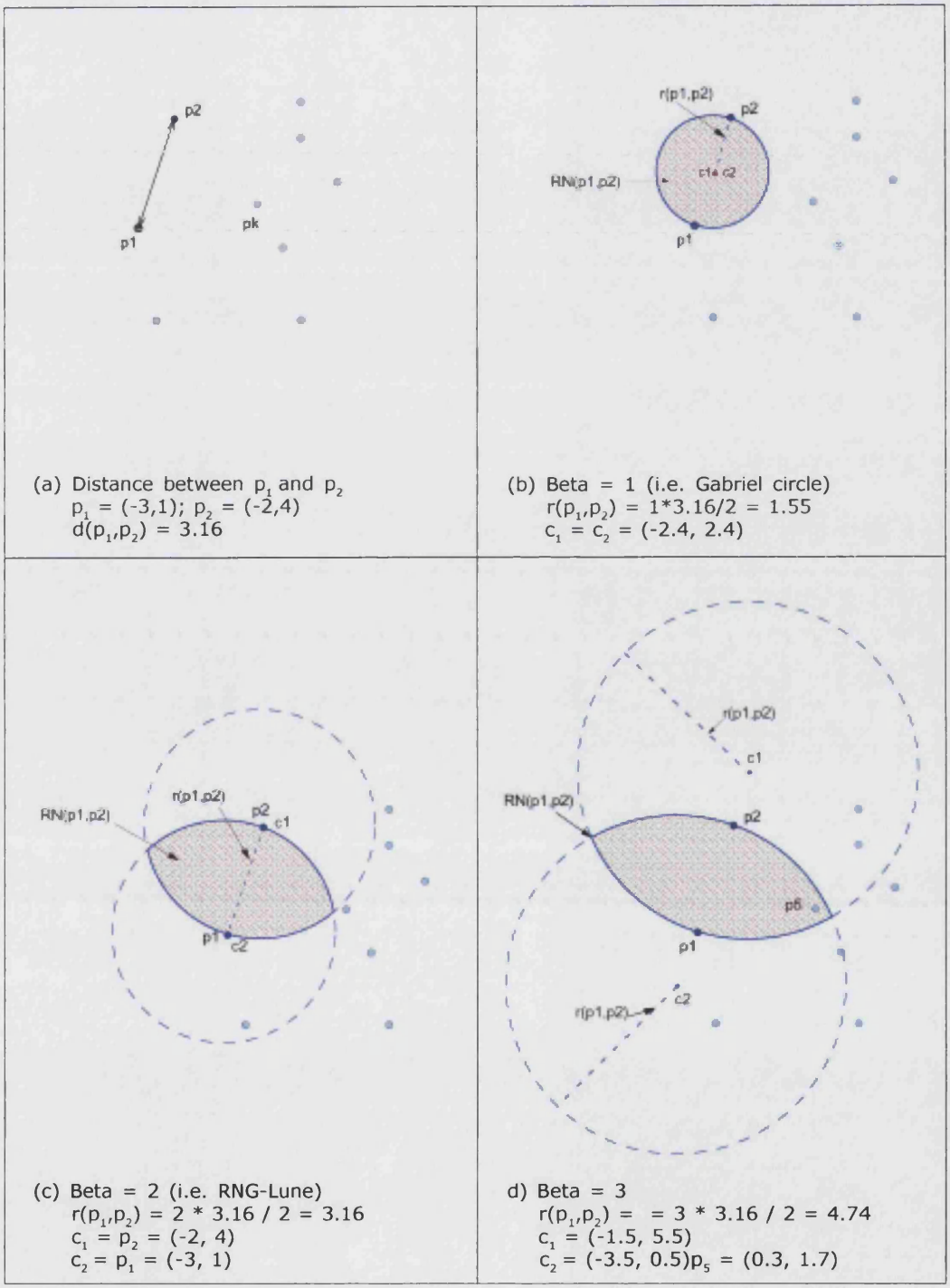

(a) Distance between p_1 and p_2
p_1 = (-3,1); p_2 = (-2,4)
$d(p_1,p_2)$ = 3.16

(b) Beta = 1 (i.e. Gabriel circle)
$r(p_1,p_2)$ = 1*3.16/2 = 1.55
$c_1 = c_2$ = (-2.4, 2.4)

(c) Beta = 2 (i.e. RNG-Lune)
$r(p_1,p_2)$ = 2 * 3.16 / 2 = 3.16
$c_1 = p_2$ = (-2, 4)
$c_2 = p_1$ = (-3, 1)

d) Beta = 3
$r(p_1,p_2)$ = = 3 * 3.16 / 2 = 4.74
c_1 = (-1.5, 5.5)
c_2 = (-3.5, 0.5)p_5 = (0.3, 1.7)

Figure A.3. Examples of neighbourhoods produced with three different values of Beta. The point set is the same in each figure and the only variation is the increase in the value of Beta. The radius of the neighbourhood is calculated as follows:
$r(p_1,p_2)$ = Beta$d(p_1, p_2)$/2*

Finally the last operations of the algorithm are oriented to test whether the region of influence previously defined is empty or not. Remember that if such region is empty, i.e. no other point lies within its boundaries, the two points under consideration are considered neighbours.

The test begins in step 4a with the calculation of distances from each centre c_i and c_j to any point (p_k) different to the pair which is being examined. In the case of the pair (p_1, p_2), the algorithm calculates distances from c_1 to p_3, p_4, p_5, p_6, p_7, p_8 and p_9, as well as distances from c_2 to p_3, p_4, p_5, p_6, p_7, p_8 and p_9. Then it compares $d(c_1, p_3)$ with $d(c_2, p_3)$ and stores the one with the maximum length. The same operation applies to $d(c_1, p_4)$ and $d(c_2, p_4)$, and successively to all the remaining distances.

The result of the previous step is a series of maximum distances, identified generically as d^k_{max}. During step 4b every one of such distances is compared to the radius $r(p_1, p_2)$, which was obtained in step 3a. If one of the distances d^k_{max} is smaller than $r(p_1, p_2)$ this indicates that a point lies within the relative neighbourhood $RN(p_1, p_2)$ and therefore they cannot be considered as neighbours. In contrast, if none of the distances d^k_{max} is smaller than $r(p_1, p_2)$ it means that all points (i.e. p_3, p_4, p_5, p_6, p_7, p_8 and p_9) are outside the relative neighbourhood $RN(p_1, p_2)$. In this later case a link must be drawn between p_1 and p_2 as they will be considered neighbours.

To illustrate both situations lets give a second look to Figure A.3. It is clear that when Beta = 1 (see fig. A.3b) the neighbourhood $RN(p_1, p_2)$ is empty and therefore an edge must be drawn in that particular case. The same happens with Beta = 2 (see fig. A.3c).

However, when Beta = 3 (see fig. A.3d) it is evident that the region $RN(p_1, p_2)$ includes the point p_5. The algorithm detects this when testing p_1, p_2 against p_5, which have the following values:

$p_1 = (-2, 4)$; $p_2 = (-3, 1)$;

$d(p_1, p_2) = 3.16$;

Beta = 3;

$r(p_1, p_2)$ = Beta * $d(p_1,p_2)/2 = 3 * 3.16 / 2 = 4.74$

$c_1 = (-1.5, 5.5)$; $c_2 = (-3.5, -0.5)$; $p_5 = (0.3, 1.7)$;

$d(c_1, p_5) = 4.20$; $d(c_2, p_5) = 4.39$;

Therefore, $d^5_{max} = d(c_2, p_5) = 4.39$.

It is obvious that $d^5_{max} = 4.39$ is smaller than $r(p_1, p_2) = 4.74$ and therefore p_1 and p_2 are not neighbours for Beta = 3.

Once the above operations have been completed for all possible combinations of two points the algorithm produces adjacency networks like the ones shown in the following page (fig. A.4).

It is important to notice that the number of edges in the graph diminishes as the value of Beta increases. Therefore, the network with the highest edge-density will always be the Gabriel graph. Also, notice that the range 1 >= Beta <= 2 will always produce a connected graph, whereas Beta > 2 might yield a disconnected graph. This is a logic consequence of the expansion of the relative neighbourhood as Beta gets higher values.

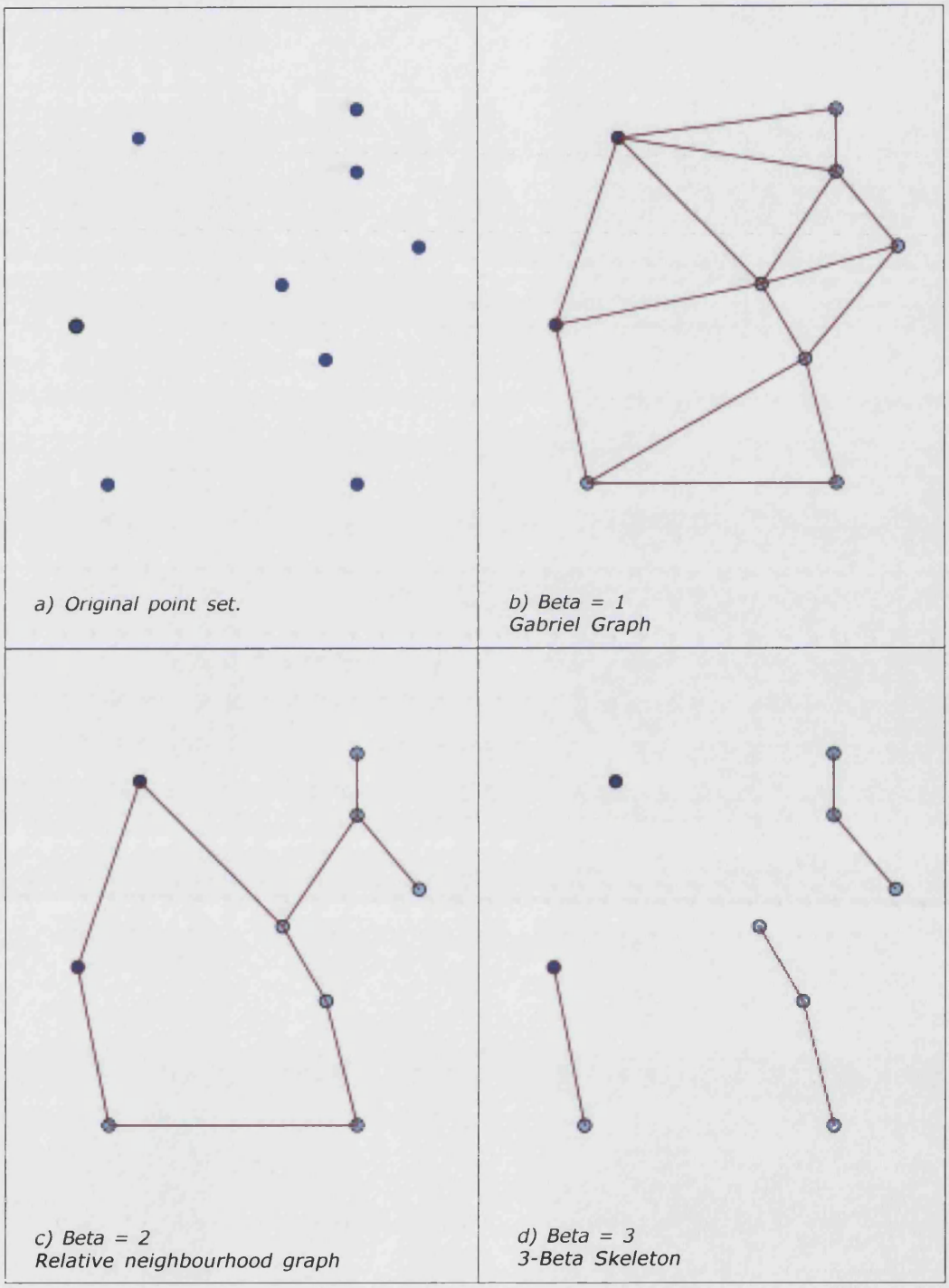

Figure A.4. Examples of proximity networks produced with three different values of Beta. Notice the smaller amount of edges as the value of Beta increases. The graph with more edge-density is always the Gabriel graph (Beta = 1). Also, remember that both Gabriel graph and relative neighbourhood graph are always connected, whereas higher values of Beta might yield disconnected graphs.

B RNG EXPLORER

This section introduces RNG Explorer; the computer program designed to implement the RN-Method. Its name stands for *Relative Neighbourhood Graph Explorer*. The program includes three main modules:

1. Rendering and visualisation facilities
2. Database functionality
3. Analysis procedures

This object-oriented software was written in Visual C++, using the MFC library of Microsoft Windows. The database functionality relies on the Data Access Object library (DAO), also from Microsoft. On the other side, the visualisation module was implemented with OpenGL and a library called Cosmo 3D, produced by Silicon Graphics.

The following sections explain how to operate the program, using some of the source data found in the companion CD under the directory RNG_DATA.

B.1. INSTALLATION

At the present, RNG Explorer does not include a set-up program. Therefore, a manual installation is required. The process, however, is simple. Just copy the file *RNG_Explorer.exe* to your hard disk. Then create a directory for your source data. This can have any name. Finally, you need to copy some libraries used by RNG Explorer to the directory C:\Windows\System of your computer. Such libraries are included in the companion CD under the same directory, that is, C:\Windows\System. If your system already contains some of the libraries, don't remove it, but work with your existing version. Any questions regarding the installation or operation of RNG Explorer can be addressed to Diego Jiménez at: rng_explorer@yahoo.com.

Additionally, you may want to create a directory to store images of artefacts or any other objects related to your proximity graphs. At the present, RNG Explorer requires that such images be stored exactly in the following directory: 'C:\RNG\Images'. We are working at the present to allow users defining their own directory path and names for storing images and data results.

B.2. DATA ISSUES.

To explore a point set you need at least a set of spatial coordinates, plus any attribute information associated with each point.

B.2.1. DATABASE FORMAT

These must be stored in a database file. We recommend to create such file using the 1997 version of MS-Access (i.e. *.mdb file format). The current release of RNG Explorer does not support databases of MS-Access 2000. Alternately, you may want to use ODBC files or ISAM databases.

B.2.2. TABLE FORMAT

To operate properly, RNG requires some fields, whose name and properties must be exactly as follows:

Fieldname	Type	Size
SELECTED	Numeric	Integer
OFRENDA	Text	4
NO_ELEMENT	Text	8
X	Numeric	Double
Y	Numeric	Double
Z	Numeric	Double
FUNCION	Text	32

The fieldnames *ofrenda*, *no_element*, and *funcion* follow existing conventions for the Mexica offering data. These stand for 'number of offering', 'number of element' (i.e. artefact id), and 'artefact function' (i.e. object category). You can adapt such format to other applications by using *ofrenda* for pointset ID's, *no_element* for point ID's, and *funcion* for labels describing each point category.

As for the coordinate fields (i.e. x, y, z), they must be filled completely. Thus, if you are working with a two-dimensional point set, it is necessary to fill in the z field anyway. We recommend using a constant value, such as 1 or -1 for all z's.

Another warning refers to fields *no_element*, *ofrenda* and *funcion*. None of these can be left empty. Thus, if you no value exists for some of these fields, you must fill in the corresponding space anyway, perhaps with the word "empty". Otherwise, the database file won't be opened.

In the following sections, we guide the reader through a typical working session with RNG Explorer.

B.3. STARTING THE PROGRAM

RNG Explorer runs as any other Windows application. You may start from the desktop by double clicking on the RNG Explorer's icon, or alternately by double clicking the filename "rng_explorer.exe."

B.4. LOADING DATA

This section explains how to load data into RNG Explorer. To open a database file, go to the *Database Menu*, select *Connect,* and then click on the type of database file you are using. Throughout this exercise, we will use an MS-Access file, so we select 'MDB' (see fig. B.1). Alternately, you may want to use ODBC files or ISAM databases.

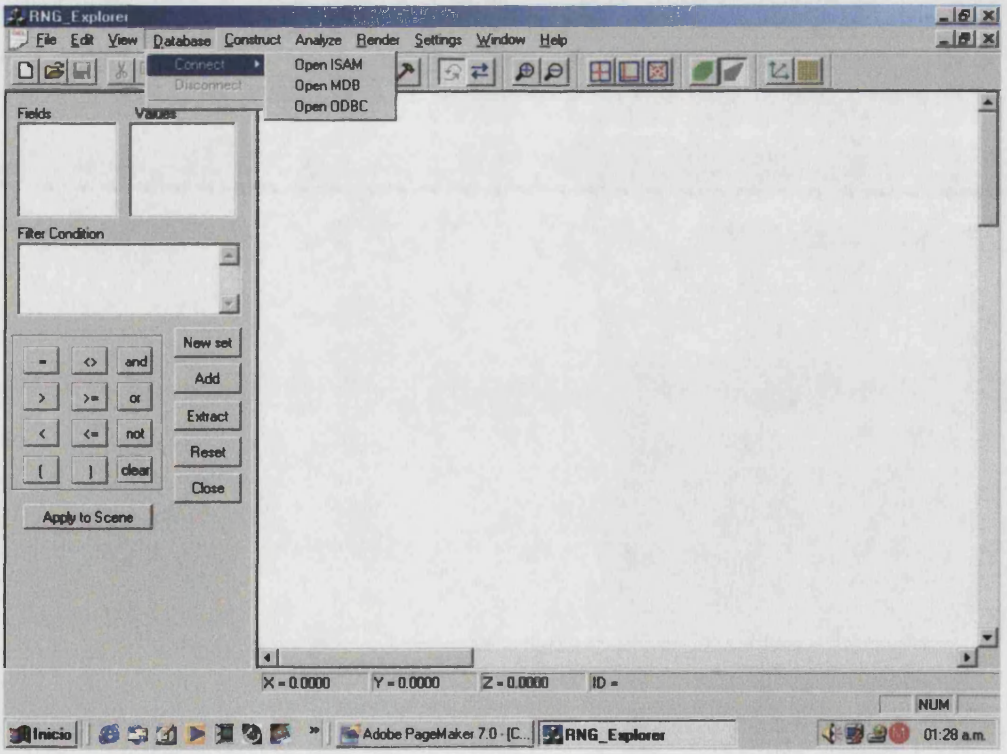

Figure B.1. The Database Menu of RNG Explorer.

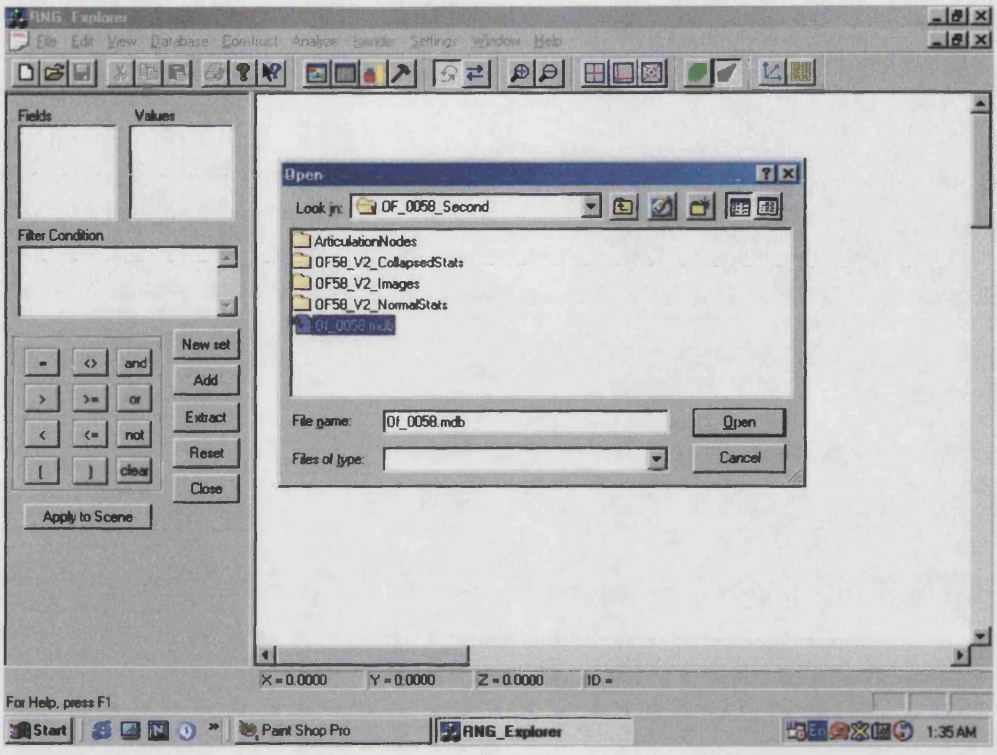

Figure B.2. Opening a database file.

This displays the *Open Dialog-box*, as seen in figure B.2. This allows you browsing your computer hard disk to search for the desired file. The chosen file in this example is 'OF_58.mdb'.

Once you select a database file, another dialog box appears (see fig. B.3). Here, you select the specific table containing coordinate and attribute data, for example 'OF_0058'. The procedure opens the table and renders the current data as points in 3D space.

The first view of the offering normally appears too small (fig. B.4). Therefore, it is necessary to enlarge the point set using some rendering facilities of RNG Explorer. Clicking on the Control Buttons located immediately above the rendering screen can do this. The purpose of each button is described as follows:

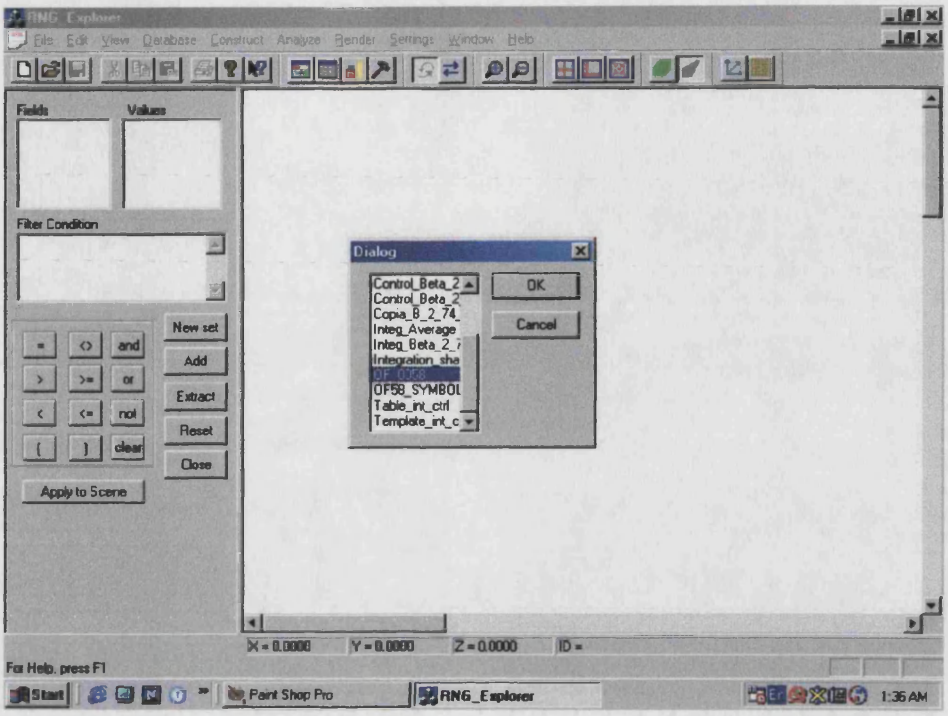

Figure B.3. Selecting the table with the source data.

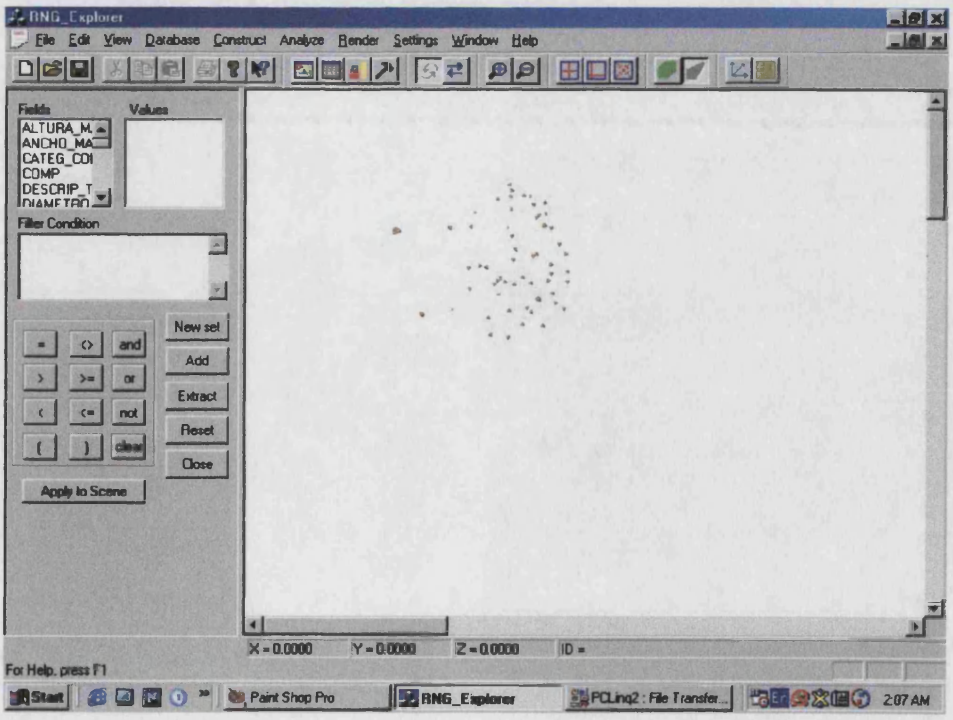

Figure B.4. First view of the point data.

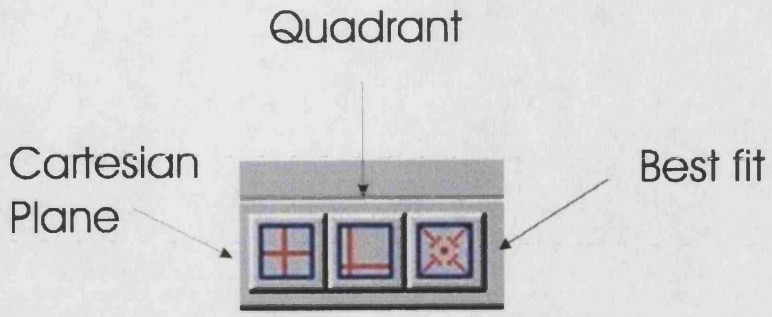

1. Best fit. This gets the rendering camera closer to the scene, so you obtain the larger possible view of the whole point set.

2. Cartesian plane. This focuses the camera on the centre of the Cartesian plane (or cube in 3D space). The rendering view covers the four portions of the Cartesian space. You may want to use this option to see how much of that space is covered by your point set.

3. Quadrant. This orientates the camera to cover only one quadrant of the Cartesian space. Such quadrant corresponds to the plane where most members of the point set are located.

The same effects can be obtained from the *Render Menu*: Click on *Camera Scope,* and then select any of the three options explained above.

In addition to a larger view, you may want to add coordinate axis to the scene, and/or a reference grid. Two control buttons exist for these purposes:

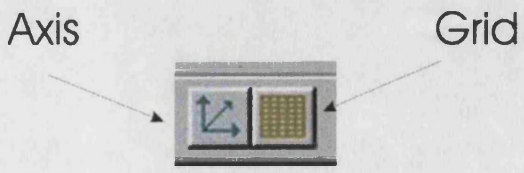

1. Show/Hide Axis

2. Show/Hide Grid

Needless to say, these too have their corresponding entries in the Render Menu.

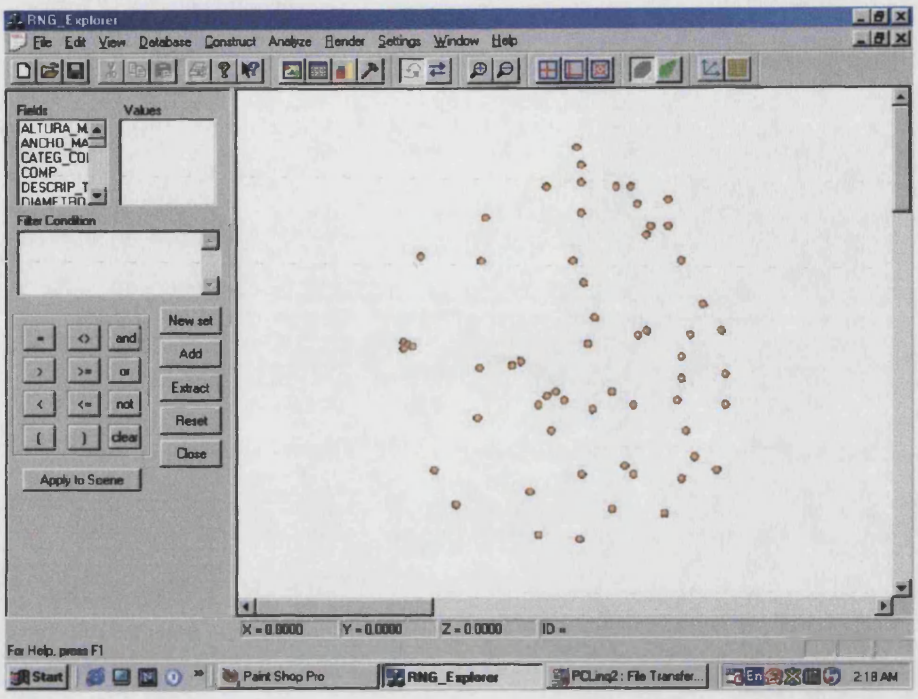

Figure B.5. View of the point data after clicking on the button 'Best Fit'.

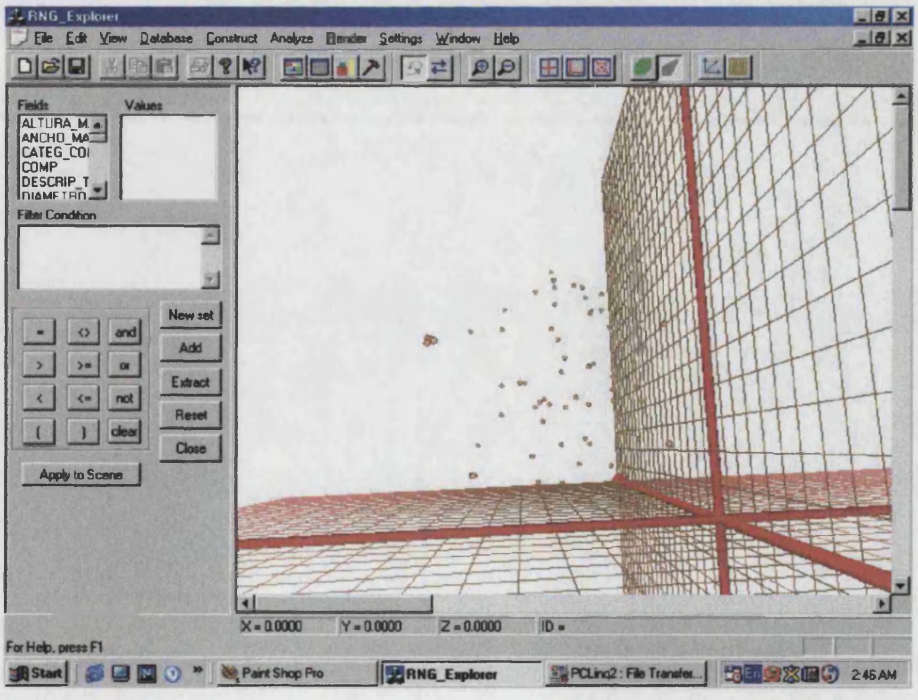

Figure B.6. View of the data with a reference grid and the Cartesian axis.

B.5. BASIC VISUALISATION

The next appropriate step is to attach symbols to each object category contained in the point set. In this way, some basic visualisation becomes possible.

Go to the *View Menu* and then click on *Switch to Shape Builder*. This changes the left side of the screen as illustrated in figure B.7. The new view allows users to assign different shapes to different object categories.

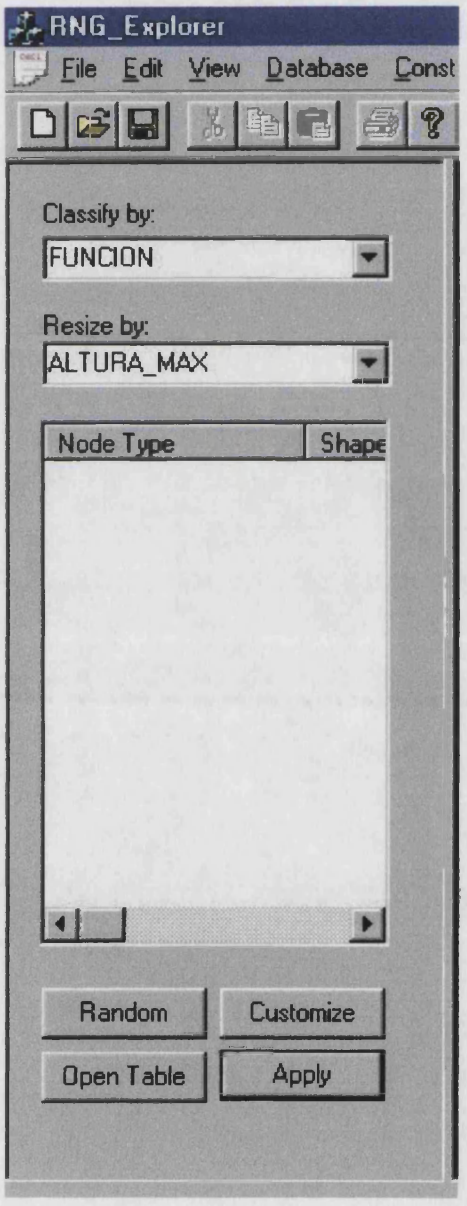

Figure B.7. Shape Builder.

For example, you may want to represent turtle shells with brown cones, as opposed to golden yellow spheres symbolising skulls. Complete definitions for these 'symbols' include the shape and material for each object category. This information can be stored in a separate table but must be included within the same database file of the coordinate data. The table used in this example is included in the companion CD.

To attach new shapes to the points, select one of the options that appear in the scroll window located under the heading 'Classify by'. This shows

all the field names of your source data. The most common choice is to select the field *funcion* to classify the objects into different shapes.

Once you click on *funcion*, all the values contained in your table would appear. At this point you have two alternatives:

1. Choosing a random assignment of shapes: click on *Random*, and then *Apply*. The result is a point view with one random colour for each object category.

2. The second option is to represent objects with the shapes that you have previously stored in a table. To do so, click on *Open Table* and wait for the *Open Dialog Box* to appear. This allows you to select the tablename, which contains your shape definitions (fig. B.8). In this example 'OF_22_Symbols'. Finally, click on *Apply.* The result is illustrated in figure B.9.

The *Shape Builder* also provides editing capabilities, so you can alter the shapes previously defined. First, click on the artefact name that you want to change. Then, press the button *Customise*. This opens the *Shape Editor*. You can define new shape and dimensions for the selected artefacts. Additionally, you may want to click on the button *Customise Material* and a new window would allow you to alter the colours defining the appearance of the objects. Among the characteristics that you can re-define is worth mentioning four types of colours given by Red Green and Blue codes (i.e. integers from 1 to 255). The four types of colours are ambient colour, diffuse colour (perhaps the most important), specular colour, and emissive colour. Additionally, you can redefine shininess and transparency of the material (fig. B.9).

Once you are done with all the changes you select OK. If you want to exit without applying the changes simply select Cancel.

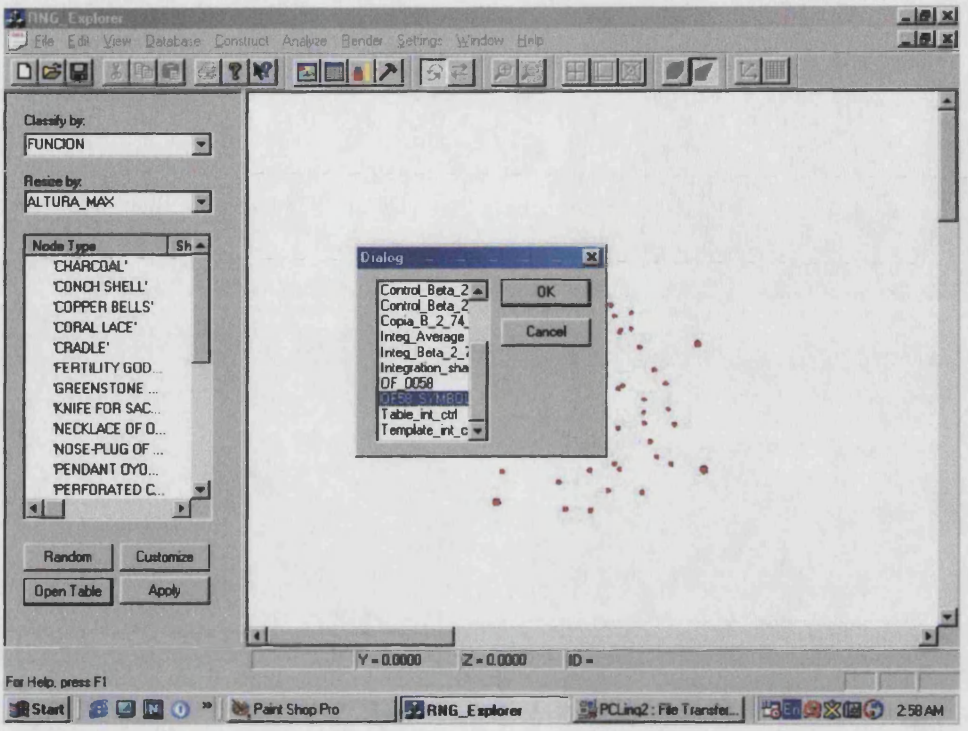

Figure B.8. Selecting a table to assign shapes to the point data.

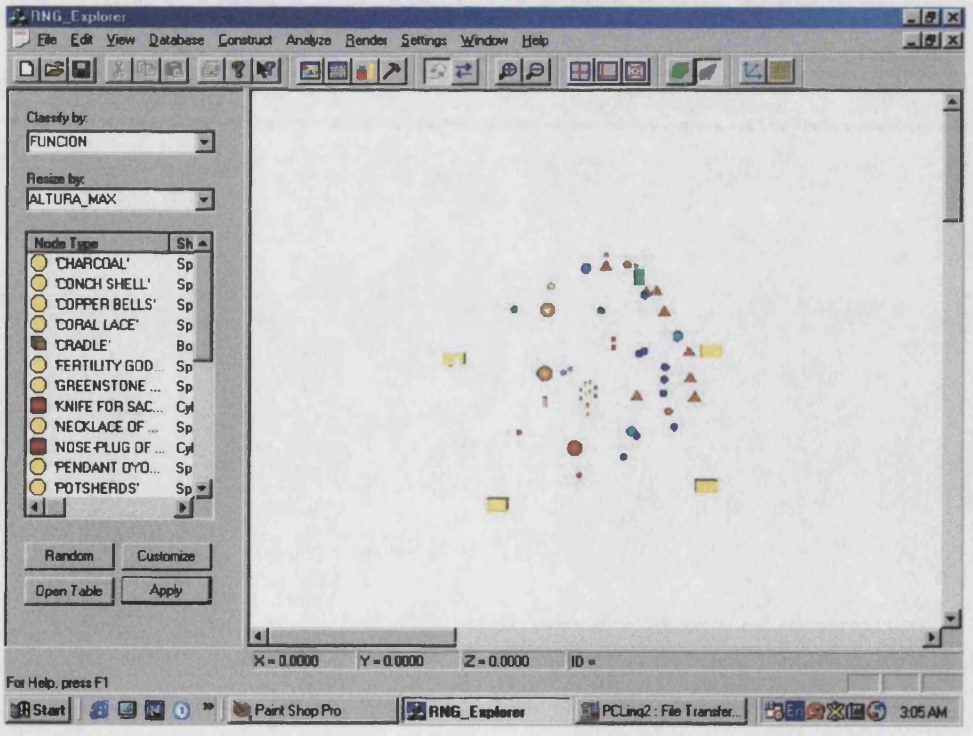

Figure B.9. The shapes obtained after the operation of the Shape Builder.

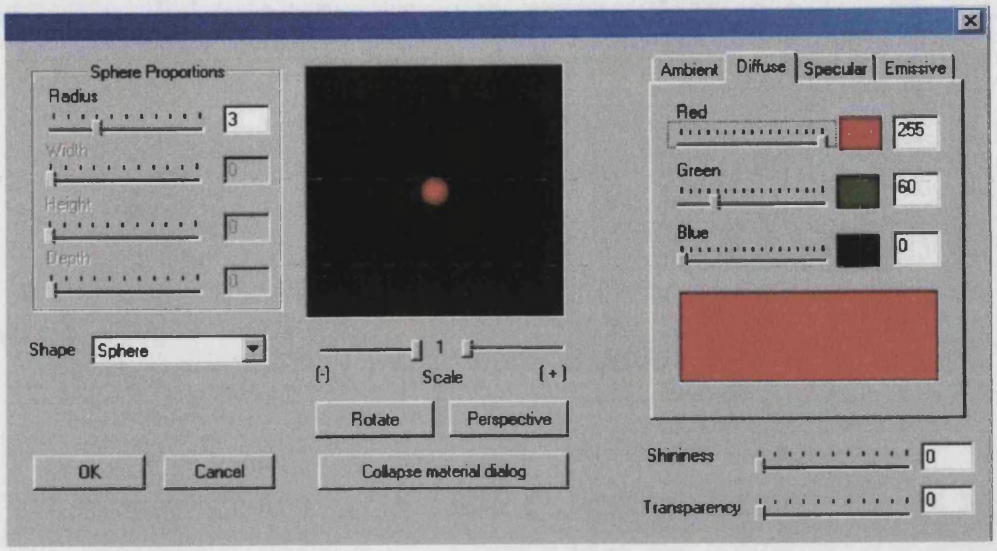

Figure B.10. The shape editor of RNG Explorer.

Finally, click on the button Apply to visualise the changes in the rendering screen.

B.6. DATA SELECTION FROM THE QUERY BUILDER

RNG Explorer contains some query functions, which allow you to perform selections from you data files. This is very useful in situations when some filtering is necessary, so that only the most relevant records are included in the analysis.

In order to select data from your files you must access an interface called Query Builder. This appears by default at the beginning of RNG Explorer on the left side of the screen (fig. B.11). Alternately, you can access the Query Builder by clicking the button picturing a hammer, or by selecting the View Menu and then clicking Switch to Query Builder.

The following is a typical selection procedure: Imagine that your file contains some unnecessary records concerning *quail remains*, which need

to be eliminated from subsequent analyses. First, you browse the scroll-window called Fields, and double-click the field name FUNCION. As a result, the word FUNCION appears in the box named Filter Condition. Now, you must select the appropriate query operator from any of the buttons marked as {=, <>, >, >=, <, <=, (,), and, or, not}. Alternately, you may want to restart or cancel your query selecting 'clear'. In this example, it is convenient to choose the operator '='. The next step is to scroll the window Values, which contain all the names recorded in the field FUNCION. Scroll the list until finding 'QUAIL REMAINS' and double-click on it. The result of the query condition must be 'FUNCION = QUERY REMAINS'. Then, you must decide what to do with such condition. The alternatives are:

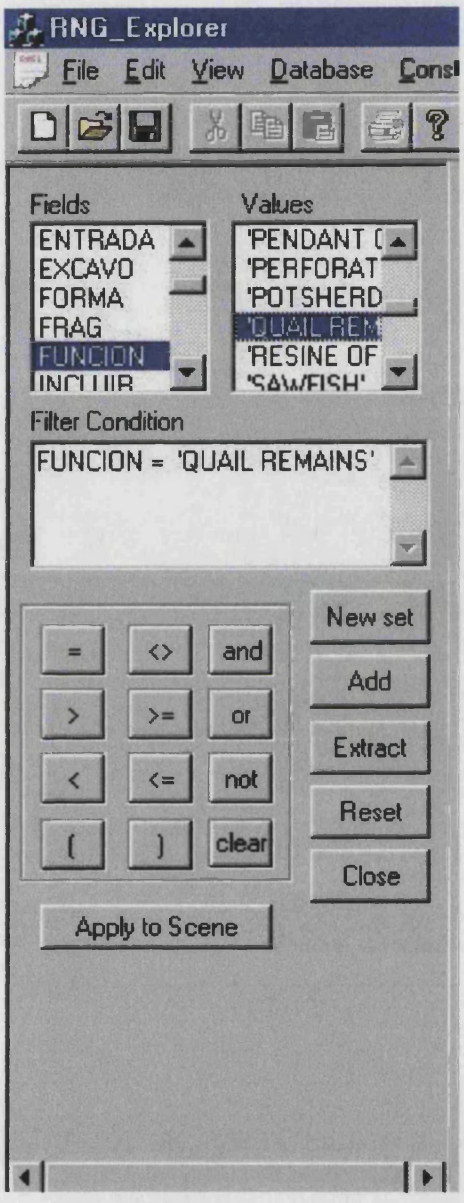

Figure B.11. Query Builder.

a) To create a new set. This will filter all records, except those belonging to QUAIL REMAINS.

b) Add records. This will add the records of QUAIL REMAINS in the analysis. For instance, if you have excluded such data in a previous operation, the add button will reintroduce them.

c) Extract records. This will exclude QUAIL REMAINS data from the subsequent analysis. The latter is precisely the operation that we want in this example.

d) Reset. This button will restore all records for subsequent analysis.

After selecting from the above options you must press the button 'Apply to the scene', so the changes can take place.

With the above procedure you can apply all kinds of logical operations to make selections. Additionally, you may want to browse your data directly from a table. The following section explains how to do that.

B. 7. DATA SELECTION FROM TABLE VIEW

RNG Explorer allows you visualising and selecting records in table format. First, you must access the appropriate interface by selecting the View Menu and then clicking on the option Switch to Table View (fig. B.12).

This will display all the records contained in your data file. Normally, the table will appear on the left side of the screen, but you can also open an independent window by selecting the option Table View, instead of Switch to Table View.

You can enlarge the Table View to fit your needs. Simply click on the split line that separates the Table and Render views and drag it to a new position.

Additionally, you can adjust the width of each column by clicking on the corresponding division line and dragging it to a new position. Then you can move through the table using the horizontal and vertical scrolling bars.

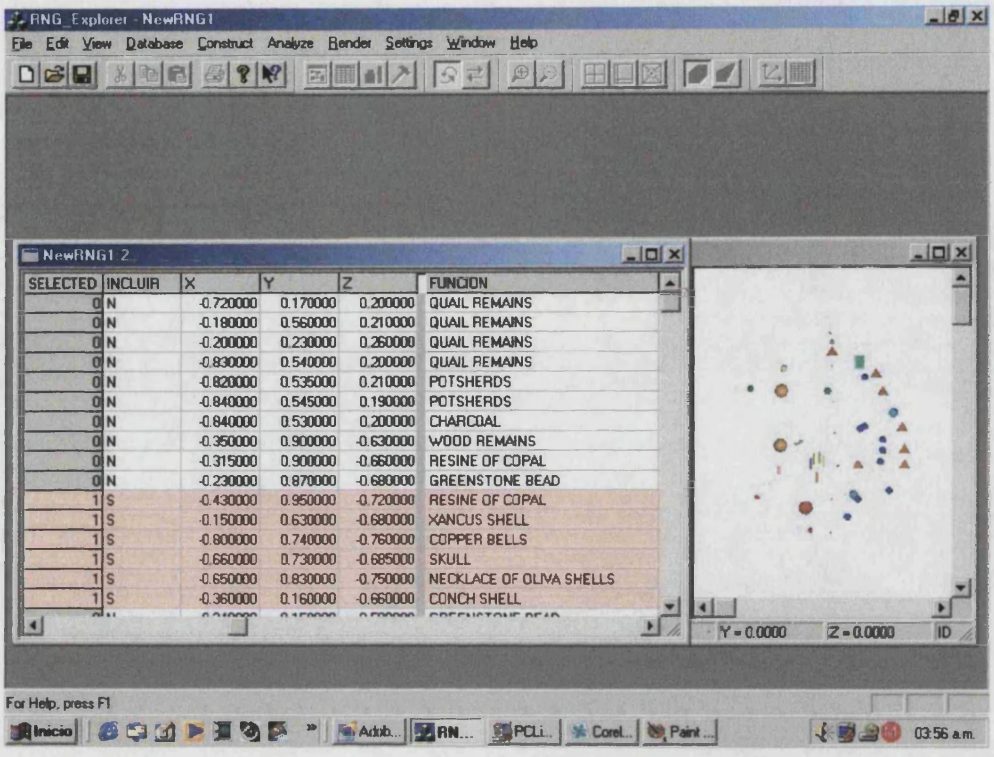

Figure B.12. The Table interface of RNG Explorer. Objects selected in this table appear highlighted in the render screen (right side). It is also possible to add and eliminate objects from the rendering screen by selecting on the table. The records over white background are those which are not included in the current set.

The records highlighted in colour are the ones currently selected for analysis, while those over a white background are excluded.

You can change the current status of the records at any time. To do so, locate the appropriate row and double-click the first column of that row. For instance, if you want to include a record, which is currently excluded, simply apply a double-click in the corresponding cell. The point will immediately appear on the rendering screen. On the contrary, if you want to exclude a record currently included in the analysis, double-click on the corresponding cell, so it disappears from the rendering screen.

Additionally, you may want to know which object in the rendering screen corresponds with the text record in the Table View. The procedure is

known as brushing. When you click (one time) on some row of the Table View, a red ball appears in the rendering screen indicating the spatial location of the point-record.

The Table View also allows you to sort data. To do so, choose one column and then click on the cell that contains the appropriate fieldname, for example FUNCION. If the field contains alphanumeric data, the procedure will sort data in alphabetic order. If the field is numeric, the rows will be sort from lower to higher numbers.

B.8. RETRIEVING PROXIMITY GRAPHS

Once you are sure that all the relevant data are included, it is possible to extract a series of proximity graphs. The Graph View of RNG Explorer makes this process extremely simple (Details of the algorithm implemented in RNG Explorer are given in Appendix A).

From the View Menu select Switch to Graph Builder. This will display the Graph Builder interface. Some buttons are self-explicatory. For instance, clicking on the RNG button will automatically produce the Relative Neighbourhood Graph. Likewise, clicking on the Gabriel Graph button will produce a Gabriel Graph of the current records (fig. B.13).

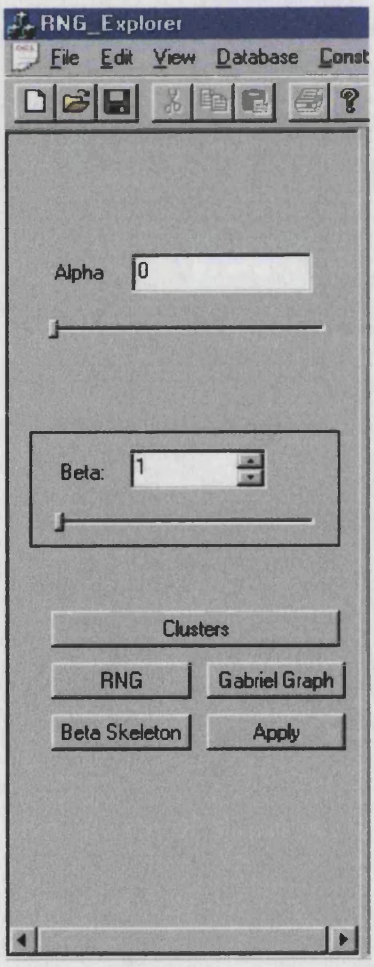

Figure B.13. Graph Builder

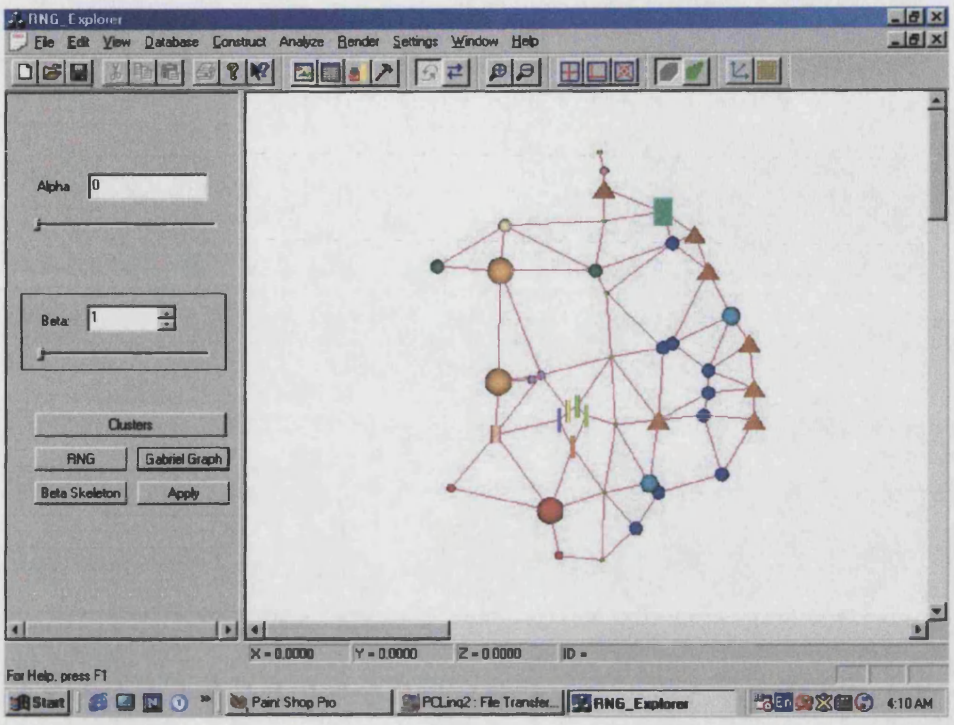

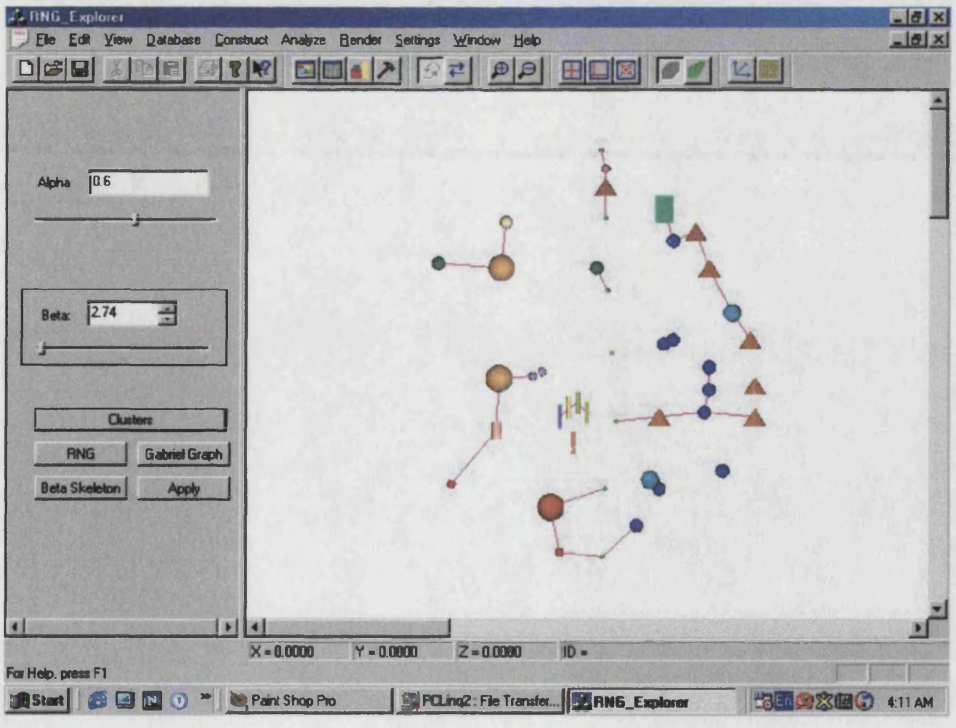

Figure B.14. Two proximity graphs produced with Graph Builder. At the top the Gabriel Graph, and at the bottom a Limited Neighbourhood Graph (Beta = 2.74; Sigma 0.6).

Additionally, you may want to produce a Beta-skeleton. To do so, simply input a value in the text-box labelled as 'Beta'. As explained in chapters 5 and 6, the value of Beta affects the number of edges retrieved in the proximity graph. High values of Beta yield low-density graph. In contrast, low Beta values, such as 1, produce higher edge density (fig. B.14).

The extraction of several Beta-skeletons is a fundamental step of the RN-Method (see section 6.5). Start with Beta = 1 (i.e. Gabriel graph) and then press the button Beta-skeleton. Then, increase the value gradually until getting the first disconnected graph of the series. In the case of offering 58 (i.e. our current example), we can retrieve Beta-skeletons with the following values: 1, 1.1, 1.2, 1.3, 1.4, 1.5, 1.6, 1.7, 1.8, 1.9, 2.0, 2.1, 2.2, 2.3, 2.4, 2.5, 2.6, 2.7, and 2.74.

Alternately, you may want to extract Limited Neighbourhood Graphs. The latter procedure requires entering two values, one for Beta, and the other for the parameter Sigma. After entering these two values, you must press the button Limited Neighbourhood Graph. The result will be a clustering based upon that particular combination of Beta and Sigma. This procedure is essential during the implementation of the visual clustering technique explained in section 6.9 of this thesis.

B.9. SPATIAL ANALYSIS FUNCTIONALITY

Count Vertices and Edges. A necessary step of the RN-Method is to get the quantity of nodes and edges in each proximity graph. From these two figures you can calculate other important spatial measures such as edge/ vertex ratio, edge graph structure, average size of face boundary, etc. (see sections 5.7.1, and 6.6).

To obtain these quantities open your graph; go to the Analyse Menu; and select the option Count Vertices and Edges. A box will appear with the result.

Once you obtain these quantities, it is convenient to export the data to a datasheet in order to produce the charts that we have called 'connectivity profiles' (see section 6.7). Examples of these datasheets and format for the connectivity profiles can be found in the directory DATA, in the companion CD of this thesis.

Additional options of the Analyse Menu are:

Calculate Control. This obtains control measures for each vertex of the current graph. As explained in section 6.8.6, these measures are useful to assess the relative importance of each vertex for the spatial structure of the proximity graphs.

When you click this option, RNG Explorer produces a text file called '*control.txt*'. This is sent to the current directory, which is where your source database file resides. The *control.txt* file includes the name of your source data table, the number of vertices and edges in the current graph, as well as the values of Sigma and Beta used for retrieving the proximity graph. More importantly, the *control.txt* file lists the control values for each vertex. Such report is given in three columns under the headings CONTROL, ID, and LABEL, which refer respectively to the control measure, the identification number of each vertex, and the description of each vertex. The following is an example of the contents of such file:

```
# Graph label = OF_0058
# 43 Vertices
# 81 Edges
# Sigma = 0.000000
# Beta  = 1.000000

# CONTROL  ID          LABEL
1.333333  007.0001  'RESINE OF COPAL'
1.033333  008.0001  'XANCUS SHELL'
0.450000  009.0001  'COPPER BELLS'
1.366667  010.0001  'SKULL'
1.150000  011.0001  'NECKLACE OF OLIVA SHELLS'
0.833333  012.0001  'CONCH SHELL'
0.783333  015.0001  'SCEPTRE DEER-HEAD'
0.833333  016.0001  'SCEPTRE SERPENTIFORM'
1.033333  017.0001  'SCEPTRE CHICAHUAZTLI'
0.400000  018.0001  'PERFORATED CONCH SHELL'
0.533333  019.0001  'PERFORATED CONCH SHELL'
1.616667  020.0001  'FERTILITY GODDESS ON POT'
0.416667  021.0001  'PENDANT OYOHUALLI'
1.000000  022.0001  'TURTLE SHELL'
0.866667  023.0001  'XANCUS SHELL'
1.066667  025.0001  'SKULL-MASK'
1.450000  026.0001  'KNIFE FOR SACRIFICE'
0.833333  027.0001  'CONCH SHELL'
1.333333  028.0001  'CONCH SHELL'
0.833333  029.0001  'TURTLE SHELL'
1.116667  030.0001  'CRADLE'
0.916667  031.0001  'CONCH SHELL'
```

0.950000 032.0001 'CONCH SHELL'

1.083333 033.0001 'CONCH SHELL'

1.650000 034.0001 'PENDANT OYOHUALLI'

1.366667 035.0001 'TURTLE SHELL'

0.700000 036.0001 'TURTLE SHELL'

0.833333 037.0001 'NOSE-PLUG OF XIPE TOTEC'

1.283333 038.0001 'CONCH SHELL'

0.916667 039.0004 'CONCH SHELL'

1.366667 040.0004 'SAWFISH'

1.566667 040.0002 'SAWFISH'

1.083333 040.0003 'SAWFISH'

0.816667 040.0005 'SAWFISH'

1.033333 040.0006 'SAWFISH'

0.500000 040.0007 'SAWFISH'

1.150000 041.0001 'COPPER BELLS'

0.783333 044.0001 'SCEPTRE SERPENTIFORM'

0.866667 045.0001 'CONCH SHELL'

0.700000 046.0001 'TURTLE SHELL'

1.033333 047.0001 'TURTLE SHELL'

1.116667 048.0001 'TURTLE SHELL'

1.000000 040.0001 'SAWFISH'

Control mean = (Sum of control values/Vertices) = 43.000001/43 = 1.000000

Once you obtain this file, it is easy to export it to a datasheet in order to sort the values and separate those vertices of high control from those with lower control. Using a program like MS-Excel you can also produce charts to analyse the control tendencies in each proximity graph, as well as to make the appropriate comparisons (see section 6.8.6). Some examples

of the datasheets and graphics used in the analysis of Mexica offerings can be found in the file OF_58_V2_Control_Series.xls, included in the companion CD under the following directory:

RNG_Data\OF_0058_Second\OF58_V2_NormalStats\OF58_V2_Control_Series\

Calculate Relative Asymmetry. Another analytical option is obtaining measures of relative asymmetry. As explained in section 6.8.5, these allow assessing how integrated is each vertex of a proximity graph. Low values of relative asymmetry indicate vertex integration, and vice versa, high values of relative asymmetry indicate vertex segregation. RNG Explorer calculates automatically these measures with a simple click. As in the case of control measures, the results of relative asymmetry are sent to an external file called *integration.txt*. The file contains three columns, with the relative asymmetry value (i.e. RA), the identification number, and the description of each vertex. Additionally, it includes the average relative asymmetry for the whole graph. The following is an example of *integration.txt* file:

RA Value ID Type
0.219512 007.0001 'RESINE OF COPAL'
0.142857 008.0001 'XANCUS SHELL'
0.150987 009.0001 'COPPER BELLS'
0.110337 010.0001 'SKULL'
0.133566 011.0001 'NECKLACE OF OLIVA SHELLS'
0.150987 012.0001 'CONCH SHELL'
0.147503 015.0001 'SCEPTRE DEER-HEAD'
0.113821 016.0001 'SCEPTRE SERPENTIFORM'
0.142857 017.0001 'SCEPTRE CHICAHUAZTLI'
0.152149 018.0001 'PERFORATED CONCH SHELL'

0.171893 019.0001 'PERFORATED CONCH SHELL'

0.131243 020.0001 'FERTILITY GODDESS ON POT'

0.139373 021.0001 'PENDANT OYOHUALLI'

0.174216 022.0001 'TURTLE SHELL'

0.112660 023.0001 'XANCUS SHELL'

0.114983 025.0001 'SKULL-MASK'

0.117305 026.0001 'KNIFE FOR SACRIFICE'

0.092915 027.0001 'CONCH SHELL'

0.138211 028.0001 'CONCH SHELL'

0.156794 029.0001 'TURTLE SHELL'

0.147503 030.0001 'CRADLE'

0.153310 031.0001 'CONCH SHELL'

0.118467 032.0001 'CONCH SHELL'

0.125436 033.0001 'CONCH SHELL'

0.092915 034.0001 'PENDANT OYOHUALLI'

0.090592 035.0001 'TURTLE SHELL'

0.164925 036.0001 'TURTLE SHELL'

0.127758 037.0001 'NOSE-PLUG OF XIPE TOTEC'

0.112660 038.0001 'CONCH SHELL'

0.147503 039.0004 'CONCH SHELL'

0.077816 040.0004 'SAWFISH'

0.116144 040.0002 'SAWFISH'

0.092915 040.0003 'SAWFISH'

0.094077 040.0005 'SAWFISH'

0.141696 040.0006 'SAWFISH'

0.267131 040.0007 'SAWFISH'

0.106852 041.0001 'COPPER BELLS'

0.126597 044.0001 'SCEPTRE SERPENTIFORM'

0.121951 045.0001 'CONCH SHELL'

0.145180 046.0001 'TURTLE SHELL'

0.135889 047.0001 'TURTLE SHELL'

0.149826 048.0001 'TURTLE SHELL'

0.156794 040.0001 'SAWFISH'

Mean RA for the whole graph = 0.135537

Once you get the relative asymmetry measures, it is convenient to export them to a datasheet in order to sort the values and identify which vertices are in integrated positions and which ones are segregated.

Using a program like MS-Excel you can also produce charts to analyse the integration tendencies in each proximity graph, as well as to make the appropriate comparisons (see section 6.8.5). Some examples of the datasheets and graphics used in the analysis of Mexica offerings can be found in the file OF_58_V2_Integration_Series.xls, included in the companion CD under the following directory:

RNG_Data\OF_0058_Second\OF58_V2_NormalStats\OF58_V2_Control_Series\

Calculate Node Degrees. Although the RN-Method does not use counts of node-degrees directly, we have included an option to extract such values because future applications might use such information. By clicking this option, the user can obtain a file called *degrees.txt*, which stores the degree for each vertex.

Find Graph Components. Clicking on this option produces a text file called 'Components.txt' in the current directory. Such file contains a list of every cluster or graph component appearing in the graph. This includes the name of the graph, the total number of vertices, the total number of edges, the value of Beta and Sigma used to produce the graph, and the ID and description of the nodes in each graph component.

Find Articulation Nodes. This option produces a text file called 'Articulation.txt', containing ID's and description of each node, whose location is essential to keep the graph connected. In other words, the removal of an articulation node would break the graph into two or more pieces. In terms of spatial structure, graphs with no articulation nodes represent more stability than those with great number of articulation nodes. Observing articulation patterns would complement the measures related to integration and control.

Graph Depth-Tree. This option produces a text file called 'G_Depth-Tree.txt', which describes the topological relations of every node with regard to the remaining nodes of the graph. This is useful to find out which are the neighbours of a particular object, and more importantly, to get information about how many steps they are away. For example, suppose that we want to know all the neighbours of the artefact 'skull'. We open the file 'G_Depth-Tree.txt', then look for the group that starts with the legend 'Depth 0 Node 001.0001 'SKULL. This means that such list corresponds to the node skull. The immediate neighbours are listed with the label 'Depth 1 Node...', the second relative neighbours are identified as 'Depth 2 Node...', and so on, until reaching the deepest level in the hierarchy of neighbours.

Some other functions of RNG Explorer can be intuitively found. Most options are self-explanatory and easy to use. We invite the reader to try the program and sen any comments or questions to:

Diego Jiménez
Museo del Templo Mayor
Seminario 8, Col. Centro
Mexico , DF, CP 06060
e-mail: rng_explorer@yahoo.com

BIBLIOGRAPHY

Agarwal, P. K., and J. Matousek. 1992. Relative neighbourhood graphs in three dimensions. In *Proceedings of the Third Annual ACM-SIAM Symposium on Dicrete Algorithms*, 58-67 (forthcoming in: *Computational Geometry: Theory and Applications*).

Agarwal, P. K., H. Edelsbrunner, O. Schwarzkopf, and E. Welzl. 1990. Euclidean minimun spanning trees and bichromatic closest pairs. In *Proceedings of the Sixth ACM Symposium on Computational Geometry*, 203-210.

Aggarwal, A., L. J. Guibas, J. Saxe, and P. W. Shor. 1987. A linear time algorithm for computing the Voronoi diagram of a convex polygon. In *Proceedings of the 19th Annual ACM Symposium on the Theory of Computing*, 39-45.

Ahuja, G. 1991. *El Tlalocan en el Templo Mayor de Tenochtitlan: Análisis de los materiales de la ofrenda Cámara II.* Thesis submitted in partial fulfilment of the requirements for the degree of Licenciado en Arqueología (i.e. Bachelor in Archaeology), Escuela Nacional de Antropología e Historia, Mexico.

Amenta, N. 1997. Computational geometry software. In *Handbook of Discrete and Computational Geometry*, ed. J. E. Goodman and J. O'Rourke, 951-960. Boca Raton, Florida: CRC Press LLC.

Anders, F., and M. Jansen. 1993. *Manual del adivino: Libro explicativo del llamado Códice Vaticano B.* Mexico: Sociedad Estatal Quinto Centenario, Akademische Druck-Und Verlagsanstalt, and Fondo de Cultura Económica.

Anders, F., M. Jansen, and L. Reyes García. 1993. *Los templos del cielo y de la oscuridad: Oráculos y liturgia. Libro explicativo del Códice Borgia.* Mexico: Sociedad Estatal Quinto Centenario, Akademische Druck-Und Verlagsanstalt, and Fondo de Cultura Económica.

Angel, E. 1997. *Interactive computer graphics. A top-down approach with OpenGL.* Reading, Massachussetts, Addison-Wesley.

Ash, P. F., and E. D. Bolker. 1985. Recognizing Dirichlet tessellations. *Geometria Dedicata* **19**: 175-206.

Aurenhammer, F. 1988. *Voronoi diagrams: A survey. Report 263 of the Institute for Information Processing*, Technical University of Graz.

Aurenhammer, F. 1991. Voronoi diagrams: A survey of a fundamental geometric data structure. *ACM Computer Surveys* **23 (3)**: 345-405.

Avis, D., and J. Horton. 1985. Remarks on the Sphere of Influence Graph. In *Discrete geometry and convexity*, ed. J. E. Goodman, E. Lutwak, J. Malkevitch, and R. Pollack, 323-327. New York: The New York Academy of Sciences.

Bailey, T. C. and A. C. Gatrell. 1995. *Interactive spatial data analysis.* Essex: Longman Scientific and Technical.

Barber, B. C., D. P. Dobkin, and H. Huhdanpaa. 1996. The Quickhull algorithm for convex hulls. *ACM Transactions on Mathematical Software* **22** (**4**): 469-483.

Baudez, C-F. 1999. Le sens caché des caches. *Bulletin du Societé Suisse des Americanistes* **63**: 11-23.

Bell, M. G. H. and Y. Lida. 1997. *Transportation network analysis.* Chichester: John Wiley & sons.

Berg, M. de, M. van Kreveld, M. Overmars, and O. Schwarzkopf. 1997. *Computational geometry: Algorithms and applications.* Berlin: Springer Verlag.

Blankholm, H. P. 1989. ARCOSPACE: A package for spatial analysis of archaeological data. *Archaeological Computing Newsletter* **19**: 3.

Blankholm, H. P. 1991. *Intrasite spatial analysis in theory and practice.* Denmark: Aarhus University Press.

Boissonnat, J-D. 1988. Geometric structures for three dimensional shape representation. ACM Transactions on Graphics **3** (**4**): 266-286.

Boissonnat, J-D. and M. Teillaud. 1986. A hierarchical representation of objects: The Delaunay tree. *Proceedings of the Second Annual ACM Symposium on Computational Geometry,* 260-268.

Boissonnat, J-D., and P. Kofakis. 1985. Use of the Delaunay triangulation for the Identification and the localization of objects. *IEEE Conference on Computer Vision and Pattern Recognition*, 398-401.

Boland, J. W., R. C. Brigham, and R. D. Dutton. 1987. The difference between a relative neighbourhood graph and a wheel. *Congressus Numerantium* 58: 151-156.

Bonifaz Nuño. 1981. *El arte en el Templo Mayor,* with photographs by Fernando Robles. Mexico: Instituto Nacional de Antropología e Historia/SEP.

Boots, B. N. 1973. Some models of the random subdivision of space. *Geografiska Annaler* **55B**: 34-48.

Boots, B. N. 1974. Delaunay triangles: An alternative approach to point pattern analysis. *Proceedings of the Association of American Cartographers* **6**: 26-29.

Boots, B. N. 1986. Using angular properties of Delaunay triangles to evaluate point patterns. *Geographical Analysis* **18** (**3**): 252-260.

Boots, B. N. and A. Getis. 1988. *Point Pattern Analysis.* Newbury Park, California: Sage Publications, Sage Scientific Geography Series Vol. 8.

Bourdieu, P. 1973. The Berber House. In *Rules and Meaning,* ed. M. Douglas, 98-110. Suffolk: Penguin Books.

Britton, J. 1999. *Symmetry and tessellations: Investigating patterns.* Englewood Cliffs, New Jersey: Prentice-Hall.

Broda, J., D. Carrasco, and E. Matos Moctezuma. 1987. *The Great Temple of Tenochtitlan. Center and periphery in the Aztec world.* Berkeley: University of California Press.

Broda, J. 1987. Templo Mayor as ritual space. In *The Great Temple of Tenochtitlan. Center and periphery in the Aztec world,* ed. J. Broda, D. Carrasco, and E. Matos Moctezuma, 61-123. Berkeley: University of California Press.

Brunet, P. 1992. 3-D structures for the encoding of geometry and internal properties. In *Three dimensional modelling with geoscientific information systems,* ed. A. K. Turner, 159-188. Dordrecht: Kluwer.

Buchanan, H. 1996. Computational techniques for determining three-dimensional topology. In *Innovations in GIS 3,* ed. D. Parker, 105-115. London: Taylor & Francis.

Buckley, J. J., and Y. Hayashi. 1993. Fuzzy genetic algorithms for optimization. *Proceedings of the International Joint Conference on Neural Networks (IJCNN'93),* 725—728. Nagoya.

Bunge, W. 1966. *Theoretical geography.* Lund: Lund Studies in Geography.

Burrough, P. A. 1990. Methods of spatial analysis in GIS. *International Journal of Geographical Information Systems* **4**, (**3**): 221-223.

Carr, C. 1985. Alternative models, alternative techniques: Variable approaches to intrasite spatial analysis. In *For Concordance in Archaeological Analysis, ed.* C. Carr, 302-473. Fayetteville, Arkansas: Westport Publishers.

Carr, C. 1991. Left in the dust. Contextual information in model-focused archaeology. In *The Interpretation of Archaeological Spatial Patterning,* E. M. Kroll, and T. D. Price, 221-256. New York and London: Plenum Press.

Carrasco, D. 1987. Myth, cosmic terror, and the Templo Mayor. In *The Great Temple of Tenochtitlan: Center and periphery in the Aztec world,* ed. J. Broda, D. Carrasco, and E. Matos Moctezuma, 124-162. Berkeley, University of California Press.

Chang, M., C. Tang, and R. Lee. 1991. Solving the Euclidean bottleneck matching problem by K-relative neighborhood graph. *Algorithmica.*

Chang, M., C. Tang, and R. Lee. (1992). Solving the Euclidean bottleneck biconnected edge subgraph problem by 2-relative neighborhood graph. *Discrete and Applied Mathematics* **39**: 1-12.

Chávez Balderas, X. 2002. *Rituales funerarios en el Templo Mayor de Tenochtitlan.* Thesis submitted in partial fulfilment of the requirements for the degree *of Licenciado en Arqueología* (i.e. Bachelor in Archaeology), Escuela Nacional de Antropología e Historia, Mexico.

Christaller, W. 1933. *Die zentralen orte in süddeutschland.* Jena: Gustav Fisher. (Translated by C. Baskin, *Central Places in Southern Germany.* Englewood Cliffs, New Jersey, 1966, Prentice Hall).

Clark, P. J., and F. C. Evans. 1954. Distances to nearest neighbour as a measure of spatial relationships in populations. *Ecology* **35**: 445-453.

Clarke, D. L. 1972. *Models in archaeology.* London: Methuen & Co.

Clarke, D. L. 1977. *Spatial archaeology.* London: Academic Press.

Clarke, D. L. 1979. Spatial information in archaeology. In *Analytical Archaeologist. Collected Papers by David L. Clarke,* 453-482. London: Academic Press.

Cliff, A. D., P. Haggett, and K. K. Ord. 1979. Graph theory and geography. In *Applications of Graph Theory,* ed. R. J. Wilson, and L. W. Beineke. London: Academic Press.

Codex Telleriano-Remensis. 1899. Facsimile. Introduction by Ernest Theodore Hamy. Paris.

Códice Telleriano-Remensis. 1964-1967. Facsimile. In *Lord Kingsborough, Antiguedades de México,* 4 vols., ed. E. Corona Nuñez, vol. 1, 151-337. Mexico: Secretaría de Hacienda y Crédito Público.

Tonalámatl de Aubin. 1981. Ed. Carmen Aguilera, Tlaxcala, Mexico: Estado de Tlaxcala [facsimile E. Seler, ed., 1900-1901].

Codex Magliabechi. 1970. Facsimile. Introduction by F. Anders. Graz: ADEVA.

Cox, K. R., and J. A. Agnew. 1976. The spatial correspondence of theoretical partitions. *Syracuse University, Department of Geography, Discussion Paper Series* 24.

Crang, M., and N. J. Thrift, eds. 2002. Thinking space (critical geographies). Routledge.

Cressie, N. A. C. 1991. *Statistics for spatial data.* Chichester: John Wiley & sons.

Cundy, H., and A. Rollet. 1989. *Mathematical models,* third edition. Stadbroke, England: Tarquin Publishers.

Cunningham, C. E. 1973. Order in the Atoni house. *In Right and left: Essays on dual symbolic classification*, ed. R. Needham, 204-238. Chicago: University of Chicago Press.

Dacey, M. F. 1964a. Two-dimensional random point patterns: A review and an interpretation. *Papers of the Regional Science Association* **13**: 41-55.

Dacey, M. F. 1964b. Modified Poisson probability law for point patterns more regular than random. *Annals of the Association of American Geographers* **54**: 559-565.

Dacey, M. F. 1965. The geometry of Central Place Theory. *Geografiska Annaler*, Series B **47**: 111-124.

Dearholt, D. W., and F. Harary, eds. 1991. *Proceedings of the First Workshop on Proximity Graphs.* New Mexico: New Mexico State University, Computer Research Laboratory, Memoranda in Computer and Cognitive Science MCCS-91-224.

Del Olmo Frese, L. 1999. *Análisis de la ofrenda 98 del Templo Mayor de Tenochtitlan.* Mexico: Instituto Nacional de Antropología e Historia (INAH), Colección Científica 384.

Densham, P., and G. Rushton. 1988. Decision support systems for locational planning. In *Behavioural Modelling in Geography and Planning*, ed. R. Golledge, and H. Timmermans, 56-81. London: Croom Helm.

Densham, P., and Rushton, G. 1991. *Designing and implementing strategies for solving large location-allocation problems with heuristic methods.* National Center for Geographic Information and Analysis, Report 91-10.

Devroye, L. 1988. The expected size of some graphs in computational geometry. *Computers and Mathematics with Applications* **15** (1): 53-64.

Diggle, P. J. 1983. *Statistical analysis of spatial point patterns*, first edition. New York and London: Academic Press.

Diggle, P. J. 2003. *Statistical analysis of spatial point patterns.* second edition, Oxford: Oxford University Press.

Dirichlet, G. L. 1850. Über die reduction der positiven quadratishen formen mit drei unbestimmten ganzen Zahlen. *Journal für die Reine und Angewandte Mathematik*, **40**: 209-227.

Douglas, M. 1972. Symbolic orders in the use of domestic space. In *Man, settlement and urbanism*, eds. P. J. Ucko, R. Thringham, and D. W. Dimbleby, 512-521. London: Duckworth.

Durán, fray Diego. 1984. *Historia de las indias de Nueva España e islas de tierra firme* (Introduction, notes and glossary by A. M. Garibay), 2 vols., Mexico: Editorial Porrua, Biblioteca Porrua 37.

Dwyer, R. 1988. *Average case analysis of algorithms for convex hulls and Voronoi diagrams.* Ph.D. Thesis, Carnegie-Mellon University.

Edelsbrunner, H. 1986. Edge-skeletons in arrangements with applications. *Algorithmica* 1: 93-109.

Edelsbrunner, H. 1987. *Algorithms in combinatorial geometry.* New York and Berlin: Springer-Verlag.

Edelsbrunner, H., and E. O. Mücke. 1994. Three-dimensional alpha shapes. *ACM Transactions on Graphics* 13, (1): 43-72.

Edelsbrunner, H., D. Kirkpatrick, and R. Seidel. 1983. On the shape of a set of points in the plane. *IEEE Transactions on Information Theory* 29, (4): 551-559.

Edelsbrunner, H., F. P. Preparata, and D. B. West. 1990. Tetrahedrizing point sets in three dimensions. *Journal of Symbolic Computation* 10: 335-347.

Edwards, G. 1993. The Voronoi model and cultural space: Applications to the social sciences and humanities. In *Spatial information theory. A theoretical basis for GIS, eds. A. U.* Frank, and I. Campari, 202-214. Berlin: Springer-Verlag.

Egber, S. L., and T. A. Slocum. 1992. EXPLOREMAP: An exploration system for choropleth maps. *Annals of the Association of American Geographers* **82**, (**2**): 275-288.

Egenhofer, M. 1991. Reasoning about binary topological relations. *In Proceedings of the Second Symposium SSD'91: Advances in Spatial Databases*, Zurich, Switzerland. *Lecture Notes in Computer Science* 525: 143-160. *Berlin:* Springer-Verlag.

Egenhofer, M. 1992. Reasoning about gradual changes of topological relationships. International Conference on GIS, Pisa, Italy. *Lecture Notes in Computer Science 639: 196-219. Berlin:* Springer Verlag.

Egenhofer, M., and R. Franzosa. 1991. Point-set topological spatial relationships. *International Journal of Geographical Information Systems* **5**, (**2**): 161-174.

Egenhofer, M. and Herrin. 1991. High-level spatial data structures for GIS. In *Three dimensional applications in geographical information systems*, vol. 1, ed. J. F. Raper, 227-237. London: Taylor & Francis.

Egenhofer, M. J., and K. K. Al-Taha. 1992. Reasoning about gradual changes of topological relationships. In *Proceedings of the International Conference of GIS: From space to territory: theories and methods of spatio-temporal reasoning*, Pisa, Italy. *Lectures Notes in Computer Science* 639: 196-219. *Berlin:* Springer-Verlag.

ElGindy, H. A., and G. T. Toussaint. 1988. Computing the relative neighbourhood decomposition of a simple polygon. In *Computational Morphology*, ed. G. T. Toussaint, 53-70. North Holland: Elsevier.

Endre, R. 1983. *Data structures and network algorithms.* Philadelphia: Society for Industrial and Applied Mathemathics.

Erlander, S., and N. F. Stewart. 1990. *The gravity model in transportation analysis. Theory and extensions.* Utrecht, The Netherlands: VSP.

Evans, I. E. 1967. The properties of patterns of points, measured by space filling and angular relationships. *Geographical Articles* **8**: 63-77, Cambridge.

Fairfield, J. 1979. Contoured shape generation: forms that people see in dot patterns. In *Proceedings of the IEEE Conference on Cybernetics and Society*, 60-64.

Fairfield, J. 1983. Segmenting dot patterns by Voronoi diagram concavity. *IEEE Transactions on Pattern Analysis and Machine Intelligence,* PAMI-5: 104-110.

Fang, T.-P., and L. A. Piegl. 1995. Delaunay triangulation in three dimensions. *IEEE Computer Graphics and Applications*, **15 (5)**: 62-69.

Fernández, J. (1959). Una aproximación a Xochipilli. *Estudios de Cultura Náhuatl,* **1**: 31-41.

Fik, T. J., R. G. Amey, and G. F. Mulligan. 1992. Labor migration amongst hierarchically competing and intervening origins and destinations. *Environment and Planning,* **29 (9)**: 1271-1291.

Fisher, M. M. 2000. Spatial interaction models and the role of geographical information systems. In *Spatial models and GIS. New potential and new models,* eds. S. Fotheringham, and M. Wegener, 33-43. London: Taylor & Francis.

Florescano. E. 1993. *El mito de Quetzalcóatl.* Mexico: Fondo de Cultura Económica.

Florescano, E. 1994. *Memoria Mexicana, second edition.* Mexico: Fondo de Cultura Económica.

Fortune, S. 1987. A sweepline algorithm for Voronoi diagrams. *Algorithmica*, **2**: 153-174.

Frank, F. C., and J. S. Casper. 1958. Complex alloy structures regarded as sphere packings: 1. Definitions and Basic Principles. *Acta Crystallographica*, **11**: 184-190.

Freidel, D., L. Schele, and J. Parker. 1999. *El cosmos maya. Tres mil años por la senda de los chamanes.* Mexico: Fondo de Cultura económica.

Furst, J. L. 1982. Skeletonization in Mixtec art: A re-evaluation. In *The art and iconography of Late Post-Classic Central Mexico,* comp. E. H. Boone, 207-225, Washington D. C., Dumbarton Oaks Research Library and Collections.

Gabriel, K. R., and R. R. Sokal. 1969. A new statistical approach to geographic variation analysis. *Systematic Zoology,* **18**: 259-278.

Gardner, M. 1988. Tilings with convex polygons. In *Time Travel and other mathematical bewilderments*, 162-176. New York: W. H. Freeman Publishers.

Garibay, A. M. 1958. *Veinte himnos sacros de los nahuas*. Mexico: Universidad Nacional Autónoma de México.

Garibay, A. M. 1969. Apéndice II. Los himnos de los dioses. In *Historia general de las cosas de la Nueva España,* B. Sahagún, vol. 4, 291-314. Mexico, Editorial Porrúa.

Gatrell, A. C. 1994. Density estimation of spatial point patterns. In *Visualisation and Geographical Information Systems*, eds. H. J. Hearnshaw, and D. J. Unwin. Chichester: John Wiley & sons.

Gatrell, A. C. and B. Rowlingson. 1994. Spatial point process modelling in a GIS Environment. In *Spatial Analysis and GIS*, eds. S. Fotheringham, and P. Rogerson, 147-163. London: Taylor & Francis.

Gatrell, A. C., T. C. Bailey, P. J. Diggle, and B. S. Rowlingson. 1996. Spatial point pattern analysis and its application in geographical epidemiology. *Transactions of the Institute of British Geographers,* **21**: 256-274.

Getis, A. 1964. Temporal land-use pattern analysis with the use of nearest neighbour and quadrat methods. *Annals of the Association of American Geographers*, **54**: 391-399.

Getis, A. and B. Boots. 1978. *Models of spatial processes. An approach to the study of point, line and area patterns.* Cambridge: Cambridge University Press.

Gold, C. M. 1994a. Three approaches to automated topology, and how computational geometry helps. In *Advances in GIS Research 1. Proceedings of the Sixth International Symposium on Spatial Data Handling*, eds. T. C. Waugh, and R. G. Healey, 145-158. London: Taylor & Francis.

Gold, C. M. 1994b. Advantages of the Voronoi spatial model. At *http://plato.gmt.ulaval.ca/homepages/gold/papers/eurocart.html*, 7 pp.

Gold, C. M. 1992. The meaning of 'neighbour'. *Lecture Notes in Computer Science* **639**: 220-235. *(Proceedings of the international conference on GIS. From space to territory: Theories and methods of spatio-temporal reasoning*, eds. A. U. Frank, I. Campari, and U. Formentini,. Berlin: Springer-Verlag).

Goodman, J. E., and J. O'Rourke. eds. 1997. *Handbook of discrete and computational geometry.* Boca Raton, Florida: CRC Press.

Gosh, A. and G. Rushton. 1987. *Spatial analysis and location-allocation models.* Reinhold, New York: Van Nostrand Publishers.

Gowda, K. C., and G. Krishna. 1978. Agglomerative clustering using the concept of mutual nearest neighborhood. *Pattern Recognition,* **10**: 105-112.

Gower, J.C., and G. J. S. Ross. 1969. Minimun spanning trees and single linkage cluster analysis. *Applied Statistics,* **18**: 54-64.

Graham, R. L. 1972. An efficient algorithm for determining the convex hull of a finite planar set. *Information Processing Letters,* **1**: 132-133.

Graulich, M. 1987. Les incertitudes du Grand Temple. In *Les Azteques: Tresors du Mexique ancien,* ed. A. Eggebrecht, 121-131. Hildescheim, Germany: Roemer-und Pelizaeus Museum.

Graulich, M. 1990. *Mitos y rituales del México antíguo.* Madrid: Ediciones Istmo.

Graulich, M. 1999. *Fiestas de los pueblos indígenas. Ritos Aztecas. Las fiestas de las veintenas.* Mexico: Instituto Nacional Indigenista.

Gregory, D., and J. Urry. eds. 1985. *Social relations and spatial structures.* London: Macmillan Publishers.

Greig-Smith, P. 1952. The use of random and contiguous quadrats in the study of the structure of plant communities. *Annals of Botany,* **16**: 293-316.

Greig-Smith, P. 1964. *Quantitative plant ecology.* London: Methuen & Co.

Gutierrez Solana, N. 1987. *Las serpientes en el arte Mexica.* Mexico: UNAM.

Gutiérrez Solana, N. 1989. Diez años de estudios sobre el Templo Mayor de Tenochtitlan (1978-1988). *Anales del Instituto de Investigaciones Estéticas de la UNAM,* **60**: 7-31.

Haggett, P. 1965. *Locational analysis in human geography.* London: Edward Arnold Publishers.

Haggett, P., and R. J. Chorley. 1969. *Network analysis in geography.* London: Edward Arnold Publishers.

Haggett, P., A. D. Cliff, and A. Frey. 1977. *Locational models. Locational analysis in human geography,* second edition, 2 vols. London: Edward Arnold Publishers.

Hammond. N. D. C. 1972. Locational models and the site of Lubaantun: A classic Maya centre. In *Models in Archaeology,* ed. D. L. Clarke, 757-800. London: Methuen & Co..

Hammond, N. D. C. 1974. The distribution of late classic Maya major ceremonial centres in the Central Area. In *Mesoamerican Archaeology: New Approaches*, N. D. C. Hammond, 313-334. Texas: University of Texas Press.

Harary, F. 1969. *Graph theory.* Reading, Massachussetts: Addison-Wesley.

Harstfield, N., and G. Ringel. 1994. *Pearls in graph theory: A comprehensive introduction.* London: Academic Press.

Harvey, D. W. 1966. Geographical processes and the analysis of point patterns. *Transactions of the Institute of British Geographers,* **40**: 234-242.

Haynes, K. A., and A. S. Fotheringham. 1984. *Gravity and spatial interaction models.* Beverly Hills, California: Sage Publications.

Heyden, D. 1987. Symbolism of ceramics from the Templo Mayor. In *The Aztec Templo Mayor*, ed. E. H. Boone, 109-127. Washington D. C.: Dumbarton Oaks Research Library and Collections.

Hietala, H. ed. 1984. *Intrasite spatial analysis in archaeology.* Cambridge: Cambridge University Press.

Hillier, B. and J. Hanson. 1984. *The social logic of space.* Cambridge: Cambridge University Press.

Hills, M., and F. Alexander. 1989. Statistical methods used in assessing the risk of disease near a source of possible environmental pollution: A review. *Journal of the Royal Statistical Society*, Series A, **152**: 353-363.

Historia de los mexicanos por sus pinturas. 1965. In *Teogonía e historia de los mexicanos, ed. A. M. Garibay, 21-90,* México: Editorial Porrúa [original 1523].

Hodder, I. 1972. Locational models and the study of Romano-British settlements. In *Models in Archaeology*, ed. D. L. Clarke, 887-909. London: Methuen & Co..

Hodder, I., and C. Orton. 1976. *Spatial analysis in archaeology.* Cambridge: Cambridge University Press.

Hopcroft, J., and R. Tarjan. 1973. Efficient algorithms for graph manipulation. *Communications of the ACM,* **16, (6)**: 372-378.

Hopcroft, J., and R. Tarjan. 1974. Efficient planarity testing. *Journal of the Association for Computing Machinery,* **21, (4)**: 549-568.

Hodson, F. R., P. H. A. Sneath, and J. E. Doran. 1966. Some experiments in the numerical analysis of archaeological data. *Biometrika*, **53 (3-4)**: 311-324.

Hosler, D. 1994. *The sounds and color of power. The sacred metallurgical technology of ancient West Mexico.* Cambridge, Massachussetts: The MIT Press.

Hotteling, H. 1929. Stability in competition. *Economic Journal*, **39**: 41-57.

Hsu, S., and C. E. Tiedemann. 1968. A rational method of delimiting study areas for unevenly distributed point phenomena. *Professional Geographer*, **20**: 376-381.

Huang, N.-F. 1990. A divide-and-conquer algorithm for constructing relative neighbourhood graph. *BIT*, **30**: 196-206.

Hudson, J., and P. Fowler. 1966. *The concept of pattern in geography.* Iowa: University of Iowa, Department of Geography.

Hurrion, R. D. 1986. Visual interactive modelling. *European Journal of Operational Research,* **23**: 281-287.

Hurtado, F., G. Liotta, and H. Meijer. 2001. Optimal, suboptimal, and robust algorithms for proximity graphs. *Lecture Notes in Computer Science*, **2115**: 2-13.

Hurtado, F., G. Liotta, and H. Meijer. 2003. Optimal and suboptimal robust algorithms for proximity graphs. *Computational Geometry: Theory and Applications*, **25:** 35-49.

Hutchings, M. J., and R. J. Discombe. 1986. The detection of spatial pattern in plant populations. *Journal of Biogeography*, **13**: 225-236.

Icke, V., and R van de Weygaert. 1987. Fragmenting the universe. 1. Statistics of two-dimensional Voronoi foams. *Astronomy and Astrophysics,* **184**: 16-32.

Ichino, M., and J. Sklansy. 1985. The relative neighborhood graph for mixed feature variables. *Pattern Recognition,* **18** (2): 161-167.

Ichon, A. 1973. *La religión de los totonacas de la sierra* (translated by José Arenas). Mexico: Instituto Nacional Indigenista.

Ishibuchi H., N. Yamamoto, T. Murata, and H. Tanaka. 1994. Genetic algorithms and neighborhood search algorithms for fuzzy flowshop scheduling problems. *Fuzzy Sets and Systems,* **67**: 81—100.

Ivy, R. L. 1995. The restructuring of air travel linkages in the new Europe. The Professional Geographer, **47** (3): 280-288.

Jackson, P. 1989. *Maps of Meaning.* London: Unwin Hyman.

Jaromczyk, J. W., and G. T. Toussaint. 1992. Relative neighborhood graphs and their relatives. *Proceedings of the IEEE,* **80** (9): 1502-1517.

Jaromczyk, J. W., and M. Kowaluk. 1987. A Note on relative neighborhood graphs. In *Proceedings of the Third Annual Symposium on Computational Geometry*, 233-241. Waterloo, Canada.

Jaromczyk, J. W., and M. Kowaluk. 1991. Constructing the relative neighborhood graph in 3-dimensional Euclidean space. *Discrete Applied Mathematics,* **31**: 181-191.

Jaromczyk, J. W., M. Kowaluk, and F. Yao. (forthcoming). An Optimal Algorithm for Constructing B-Skeletons in l_p Metric. SIAM Journal of Computing.

Jarvis, R. A. 1973. On the identification of the convex hull of a finite set of points in the plane. *Information Processing Letters,* **2**: 18-21.

Jarvis, R. A. 1977a. Computing the shape hull of points in the plane. *Proceedings of the IEEE Computing Society. Conference on Pattern Recognition and Image Processing,* 231-241.

Jarvis, R. A. 1978. Shared nearest neighbour maximal spanning trees for cluster analysis. *Proceedings of the 4th. Joint Conference on Pattern Recognition,* 308-313, Kyoto, Japan.

Jarvis, R. A., and E. A. Patrick 1973. Clustering using a similarity measure based on shared nearest neighbours. *IEEE Transactions on Computing,* series C, **22**: 1025-1034.

Jen T-Y, and P. Boursier. 1994. A model for handling topological relationships in a 2D environment. In *Advances in GIS Research 1.* Proceedings of the Sixth International Symposium on Spatial Data Handling, eds. T. C. Waugh, and R. G. Healey, 73-88. London: Taylor & Francis.

Jiménez Badillo, D. 1998. *Ofrendata: Aplicación de un sistema de base de datos para controlar una colección arqueológica.* Mexico: Instituto Nacional de Antropología e Historia (INAH), Colección Textos Básicos y Manuales.

Jiménez Badillo, D., and D. Chapman. 2002. An application of proximity graphs in archaeological spatial analysis. In *Contemporary themes in archaeological computing,* eds. D. Wheatley, et. al., 90-99. Southampton: University of Southampton, Oxbow Books.

Jiménez F. and J. L. Verdegay. 1996. Interval multiobjective solid transportation problem via genetic algorithms. *Proceedings of the Sixth International Conference on Information Processing and Management of Uncertainty in Knowledge Based Systems (IPMU'96),* 787—792. Granada, Spain.

Jones, K., and J. Simmons. 1987. *Location, location, location. Analyzing the retail environment.* Toronto: Methuen & Co.

Kansky, K. J. 1963. *Structure of transport networks: Relationships between network geometry and regional characteristics.* Chicago: University of Chicago, Department of Geography, Research Papers 84.

Katajainen, J. 1988. The region approach for computing relative neighbourhood in the l_p metric. *Computing,* **40**: 147-161.

Katajainen, J. and O. Nevalainen. 1986a. Computing relative neighbourhood graphs in the plane. *Pattern Recognition*, **19** (**3**): 221-228.

Katajainen, J., and O. Nevalainen. 1986b. An almost naive algorithm for finding relative neighbourhood graphs in l_p metrics. *Informatique Theórique et Applications (Theoretical Informatics and Applications)*, **21** (**2**): 199-215.

Katajainen, J., O. Nevalainen, and J. Teuhola. 1987. A linear expected-time algorithm for computing planar relative neighbourhood graphs. *Information Processing Letters*, **25**: 77-86.

Kendall, D. G. 1981. The statistics of shape. In *Interpreting Multivariate Data*, ed. V. Barnett, Chichester: John Wiley & sons.

Kendall, D. G. 1990. Random Delaunay simplexes in R^m. *Journal of Statistical Planning and Inference*, **25**: 25-234.

Kennedy, J. M., and C. Ware. 1978. Illusory contours can arise in dot figures. *Perception*, 191-194.

Kershaw, K. A. 1964. *Quantitative and dynamic ecology.* London: E. Arnold.

King, L. J. 1969. *Statistical analysis in geography.* Englewood Cliffs, New Jersey: Prentice Hall.

King, L. J. 1984. *Central place theory.* Beverly Hills, California: Sage Publications, Scientific Geography Series, Volume 1.

Kinklenberg, B. 1997. Location-allocation on networks. Published on the Internet at: http://www.geog.ubc.ca/courses/klink/g370_472.html

Kintigh, K. W., and A. J. Ammerman. 1982. Heuristic approaches to spatial analysis in archaeology. *American Antiquity*, **47**: 31-63.

Kirkpatrick, D. G., and J. D. Radke 1985. A framework for computational morphology. In *Computational Geometry*, ed. G. Toussaint, 217-248. North Holland: Elsevier Science Publishers.

Kus, S., and V. Raharijaona. 1990. Domestic space and the tenacity of tradition among some Betsileo of Madagascar. In *Domestic architecture and the use of space. An interdisciplinary cross-cultural study,* ed. S. Kent, 21-33. Cambridge: Cambridge University Press, New Directions in Archaeology.

Lagopolous, A. P. 1993. Postmodernism, geography, and the social semiotics of space. *Environment and Planning Series D: Society and Space*, **11**: 255-278.

Lankford, P. M. 1969. Regionalization: theory and alternative algorithms. *Geographical Analysis*, **1**: 196-212.

Lattuada, R., and J. F. Raper. 1995. Application of 3D Delauney triangulation algorithms in geoscientific modelling. In *Proceedings of GIS Research, UK 95.*, 150-153, Newcastle.

Lea, A., and J. Simmons. 1995. *Location-allocation for retail site selection.* Toronto: Ryerson Polythecnic University, The Centre for the Study of Commercial Activity.

Lee, D. T. 1980. Two dimensional Voronoi diagrams in the l_1-metric. *Journal of the Association for Computer Machinery,* **27**: 604-618.

Lee, D. T. 1985. Relative neighborhood graphs in the l_1-metric. *Pattern Recognition*, **18**: 327-332.

Lee. D. T., and F. P. Preparata. 1977. Location of a point in a planar subdivision and its applications. *SIAM Journal of Computing*, 594-606.

Lefebvre, H. 1991. *The production of space*, (translated by D. Nicholson-Smith from the original in French). Blackwell Publishers.

Lefkovitch, L. P. 1984). A nonparametric method for comparing dissimilarity matrices, a general measure of biogeographical distance, and their applications. *American Nature*, **123**: 484-499.

Lefkovitch, L. P. 1985. Further nonparametric tests for comparing dissimilarity matrices based on the relative neighbourhood graph. *Mathematical Biosciences*, **73**: 71-88.

León Portilla, M. 1958. *Ritos, sacerdotes y atavíos de los dioses.* Mexico: Universidad Nacional Autónoma de México.

León Portilla, M. 1978. *MéxicoTenochtitlan: Su espacio y tiempo sagrados.* Mexico: Instituto Nacional de Antropologia e Historia.

León Portilla, M. ed. 1985. *Tonalámatl de los pochtecas (Códice mesoamericano 'Fejérváry-Mayer').* Mexico: Celanese Mexicana.

Lévi-Strauss, C. 1963. *Structural anthropology.* New York: Basic Books.

Lock, G., and T. Harris. 1992. Visualizing spatial data: the importance of geographic information systems. In *Archaeology and the information age. A global perspective,* eds. P. Reilly, and S. Rahtz, 81-96. London: Routledge.

López Austin, A. 1973. Hombre-dios: religión y política en el mundo náhuatl. Mexico: UNAM.

López Austin, A. 1983. Nota sobre la fusión y la fisión de los dioses en el panteón mexica. *Anales de Antropología,* **20**: 75-87.

López Austin, A. 1987. The masked god of fire. In *The Aztec Templo Mayor,* ed. E. H. Boone, 257-291. Washington D. C.: Dumbarton Oaks Research Library and Collection.

López Austin, A. 1989. *Cuerpo humano e ideología. Las concepciones de los antíguos nahuas,* 2 vols., *third edition.* Mexico: Universidad Nacional Autónoma de México, (translated as *Human body and ideology,* 2 vols., transl. T. Ortiz de Montellano, and B. Ortiz de Montellano. Salt Lake City: University of Utah Press, 1988).

López Austin, A. 1990. *Los mitos del tlacuache: Caminos de la mitología mesoamericana.* Mexico: Alianza Editorial Mexicana.

López Austin, A. 1993. El Árbol cósmico en la tradición mesoamericana. *Iichiko intercultural,* 5: 47-66.

López Austin, A. 1994. *Tamoanchan y Tlalocan.* Mexico: Fondo de Cultura Económica, (translated as *Tamoanchan, Tlalocan: Places of mist,* transl. B. Ortiz de Montellano, and T. Ortiz de Montellano. Colorado: University Press of Colorado, 1997).

López Austin, A. 1995. La religión, la magia y la cosmovisión. In *Historia antigua de México,* vol. 3: 419-458, ed. L. Manzanilla, and L. López Luján. Mexico.

López Austin, A., and J. García Quintana. 2000. Glossario. In *Historia general de las cosas de la Nueva España,* B. Sahagún, 1237-1353. Mexico: Secretaría de Educación Pública, Colección Cien de México.

López Luján, L. 1989. *La recuperación mexica del pasado teotihuacano.* Mexico: INAH/GV editores/Asociación de Amigos del Templo Mayor, Colección de Divulgación.

López Luján, L. 1994. *The offerings of the Templo Mayor of Tenochtitlan.* Colorado: University Press of Colorado.

López Luján, L. 1998. *Anthropologie religieuse du Templo Mayor, Mexico: La Maison des Aigles.* Ph. D. Thesis, University of Paris-X, Nanterre, Paris, France (forthcoming *La Casa de las Águilas: Un Ejemplo de Arquitectura Sacra Mexica* (2 Vols.). Mexico: Instituto Nacional de Antropología e Historia, Mesoamerican Archive, Princeton University, Mexican Fine Arts Museum Center, Chicago).

Lösch, A. 1936. *The economics of Location.* London: John Wiley & sons.

Lowe, J. C., and S. Moryadis. 1975. *The geography of movement.* Prospect Heights, Illinois: Waveland Press.

Mardia, D. M., R. Edwards, and M. L. Puri. 1977. Analysis of central place theory. *Bulletin of the International Statistical Institute,* 47: 93-110.

Mardia, K. V. 1989. Shape analysis of triangles through directional techniques. *Journal of the Royal Statistical Society, Series B,* 51 (3): 449-458.

Marquina, I. 1960. *El Templo Mayor de México.* Mexico: Instituto Nacional de Antropología e Historia.

Marr, D. 1976. Early processing of visual information. *Philosophical Transactions of the Royal Society of London*, **275 (945)**: 483-524.

Marshall, R. J. 1991. A review of methods for the statistical analysis of spatial patterns of disease. *Journal of the Royal Statistical Society,* Series A, **154**: 421-441.

Mateos Higuera, S. 1998. *Enciclopedia gráfica del México antiguo*, 4 vols., second edition. Mexico: Secretaría de Hacienda y Crédito Público.

Matos Moctezuma, E. 2000. *Los Aztecas.* Mexico: CONACULTA and Jaca Books.

Matos Moctezuma, E. 1988b. *Ofrendas.* Mexico: Hewlett Packard.

Matos Moctezuma, E. 1979. El proyecto Templo Mayor: Objetivos y programas. In *Trabajos arqueológicos en el centro de la Ciudad de México (antología),* ed. E. Matos Moctezuma, 13-26. Mexico: Instituto Nacional de Antropología e Historia.

Matos Moctezuma, E. 1982. *El Templo Mayor: Excavaciones y estudios.* Mexico: Instituto Nacional de Antropología e Historia.

Matos Moctezuma, E. 1986. *Vida y muerte en el Templo Mayor.* Mexico: Ediciones Océano.

Matos Moctezuma, E. 1988. *The Great Temple of the Aztecs: Treasures of Tenochtitlan.* London: Thames and Hudson.

Matula, D. W., and R. R. Sokal. 1980. Properties of Gabriel graphs relevant to geographic variation research and the clustering of points in the plane. *Geographical Analysis*, **12**: 205-222.

Maus, A. 1984. Delaunay triangulation and the convex hull of points in expected linear time. *BIT*, **24**: 151-163.

Medek, V. 1981. On the boundary of a finite set of points in the plane. *Computer Graphics and Image Processing*, **15**: 93-99.

Medina, J.R., and V. Yepes. 1993. Optmization of touristic distribution networks using genetic algorithms. *SORT,* **27(1)**, 95-112.

Medvedkov, Y. V. 1967. An application of topology in central place analysis. *Papers of the Regional Science Association,* **20**: 77-84.

Morris, W. ed. 1992. *The American heritage dictionary of the English language, third edition,* Boston: Houghton Mifflin Company.

Moser, C. 1973. *Human decapitation in ancient Mesoamerica.* Washington D. C.: Dumbarton Oaks Research Library and Collection.

Mukhopadhyay, A. 2000. Output-sensitive algorithm for computing B-Skeletons. *Computing*, **65 (3)**: 285-289.

Nagao, D. 1985. *Mexica buried offerings: A historical and contextual analysis.* BAR International Series, **235**. Oxford: BAR.

Nájera, M. I. 1987. *El don de la sangre en el equilibrio cósmico. El sacrificio y el autosacrificio sangriento entre los antiguos mayas.* Mexico: Universidad Nacional Autónoma de México.

Nicholson, H. B. 1971. Religion in Pre-Hispanic Central Mexico. In *Handbook of Middle American Indians, Vol. 10. Archaeology of Northern Mesoamerica, Part 1*, eds. G. F. Ekholm, and I. Bernal, 395-446. Austin, Texas: University of Texas Press.

Niedergeli, J., and K. H. Hinrichs. eds. 1993. *Algorithms and data structures with applications to graphics and geometry.* Englewood Cliffs, New Jersey: Prentice Hall.

O'Callaghan, J. F. 1975. An alternative definition for neighbourhood of a point. *IEEE Transactions on Computing*, Series C, **24**: 1121-1125.

O'Rourke, J. 1982. Computing the relative neighborhood graph in the l_1 and l_∞ metrics. *Pattern Recognition,* **15 (3)**: 189-192.

O'Rourke, J., H. Booth, and R. Washington. 1987. Connect-the-dots: A new heuristic. *Computer Vision, Graphics, and Image Processing,* **39**: 258-266.

Okabe, A., and M. Aoyagi. 1991. Existence of equilibrium configurations of competitive firms on an infinite two-dimensional space. *Journal or Urban Economics,* **29**: 349-370.

Okabe, A., and A. Suzuki. 1987. Stability of spatial competition for a large number of firms on a bounded two dimensional space. *Environment and Planning,* Series A, **19**: 1067-1082.

Okabe, A., B. Boots, and K. Sugihara. 1992. *Spatial tessellations. Concepts and applications of Voronoi diagrams,* first edition. Chichester: John Wiley & sons.

Okabe, A, B. Boots, and K. Sugihara. 2000. *Spatial tessellations. Concepts and applications of Voronoi diagrams,* second edition. Chichester: John Wiley & sons.

Olariu, S. 1989. A simple linear-time algorithm for computing the RNG and MST of unimodal polygons. *Information Processing Letters*, **31**: 243-248.

Olmedo Vera, B., and C. González González. 1986. *Presencia del estilo Mezcala en el Templo Mayor: Una clasificación de piezas antropomorfas.* Thesis submitted in partial fulfilment of the requirements for the degree of *Licenciado en Arqueología* (i.e. Bachelor in Archaeology). Mexico: Escuela Nacional de Antropología e Historia, Mexico.

O'Rourke, J. 1994. *Computational geometry in C.* Cambridge: Cambridge University Press.

Páztor, L. 1994. Partition based point pattern analysis methods for investigation of spatial structure of various stellar populations. In *Astronomical data analysis software and systems III*, eds. D. R. Crabtree, R. J. Hanisch, and J. Barnes, 5 pp. ASP Conference Series, **61**.

Pernus, F. 1988. The Delaunay triangulation and the shape hull as tools in muscle fibre analysis. *Pattern Recognition Letters,* **8**: 197-202.

Pielou, E. C. 1957. The effect of quadrat size on the estimation of the parameters of the Neyman's and Thomas's distributions. *Journal of Ecology* **45**: 31-47.

Ponce de León, A. 1982. Fechamiento arqueoastronómico en el altiplano de México, Mexico: Departamento del Distrito Federal.

Preparata, F. P., and M. I. Shamos. 1985. *Computational geometry: An introduction.* New York: Springer Verlag.

Preparata, F. P., and S. J. Hong. 1977. Convex hulls of finite sets of points in two and three dimensions. *Communications of the ACM*, **20 (2)**: 87-93.

Radke, J. D. 1982. *Pattern recognition in circuit networks.* Ph.D. Thesis, Department of Geography, University of British Columbia.

Radke, J. D. 1988. On the shape of a set of points. In *Computational morphology, ed.* G. T. Toussaint, 105-136. North Holland: Elsevier Science Publishers.

Rao, S. V. 1998. *Some studies on beta-skeletons.* Ph.D. Thesis, Department of Computer Science and Engineering, Indian Institute of Technology, Kanpur, India.

Ripley, B. D. 1981. *Spatial statistics.* Chichester: John Wiley & sons.

Ritchey, T. 2003. *Modelling complex socio-technical systems using morphological analysis.* Text Adapted from an Address to the Swedish IT Commission, Stockholm, December, 2002. Published on the Internet at: http://www.swemorph.com/tutorial

Robison, L. 1999. *Database programming with Visual C++ 6.* SAMS, Teach Yourself Series, Indianapolis.

Rohlb, F.J. 1973. Hierarchical clustering using the minimum spanning tree. *The Computer Journal,* **16**: 93-95.

Rosenberg, B., and D. J. Langridge. 1973. A computational view of perception. *Perception:* 415-424.

Sack, R. D. 1980. *Conceptions of space in social thought.* London: Macmillan.

Sahagún, B. 1950-1969. *Florentine Codex. General history of the things of New Spain*, 12 vols., translated and edited by C. E. Dibble, and A. J. O. Anderson. Salt Lake City: University of Utah Press.

Sahagún, B. 1956. *Historia general de las cosas de la Nueva España.* 4 vols., ed. A. M. Garibay. Mexico: Editorial Porrúa.

Sahagún, B. 2000. *Historia general de las cosas de la Nueva España*, 3 vols., introduction, paleography, glossay and notes by A. López Austin, and J. García Quintana. Mexico: CONACULTA, Colección Cien de México.

Saito, T., J-I. Toriwaki, and S. Yokoi. 1991. Properties of extended digital alpha-hull with applications to shape feature analysis of a figure set. *Forma,* **6**: 9-25.

Samet, H. 1991. *The design and analysis of spatial data structures.* Reading, Massachussetts: Addison Wesley.

Sanaei-Nejad, S. H., and H. A. Faraji-Sabokbar. n/d. Using location-allocation models for regional planning in GIS environment. Published on the Internet at: http://www.gisdevelopment.net/application/nrm/overview/nrm01pf.htm

Schaeffer, F. K. 1953. Exceptionalism in geography: A methodological examination. *Annals of the Association of American Geographers*, **43**: 226-249.

Schulze, N. 1997. *La ofrenda 20 del Templo Mayor de Tenochtitlan: un análisis económico.* Summary of a Master Degree Thesis, 22 pp. Germany: Hamburg University, Germany, (copy in the archives of Museo del Templo Mayor, Mexico).

Sedgewick, R. 1992. *Algorithms in C++.* Reading Massachussetts: Addison-Wesley.

Seler, E. 1988. *Códice Borgia*, 2 vols. Mexico: Fondo de Cultura Económica.

Sendov, B. 1991. Planar neighborhood graphs without cycles. *Comptes Rendus de l'Academie Bulgare des Sciences*, **44** (4): 23-25.

Shamos, M. I. and D. Hoey. 1975. Closest-point problems. *Proceedings of the 16th Annual IEEE Symposium on Foundations of Computer Science,* 151-162.

Shieh, Y-N. 1985. K. H. Rau and the economic law of market areas. *Journal of Regional Science,* **25** (2): 191-199.

Silverman, B. W. 1986. *Density estimation.* London: Chapman and Hall.

Simonsen, K. 1991. Towards an understanding of the contextuality of mode of life. *Environment and Planning, Series D: Society and Space*, **9**: 417-431.

Simonsen, K. 1996. What kind of space in what kind of social theory?. *Progress in Human Geography,* **20** (4): 494-512.

Singh, R. K., A. Tropsha, and I.I. Vaisman. 1996. Delaunay tessellation of proteins: Four body nearest neighbor propensities of amino acid residues. *Journal of Computer Biology.*

Singh, R. L., and R. P. B. Singh. 1975. Shape analysis in rural settlement geography: Qualitative v. quantitative approach. In *Readings in Rural Settlement Geography, ed.* : R. L. Singh, 444-452. Varanasi, India: National Geographical Society of India.

Singh, R. P. B. 1976. A note on the transformation of village shapes into Thiessen polygons and hexagons. *Geographical Review of India*, **38**: 50-53.

Sneath, P. H. A., and R. R. Sokal. 1973. *Numerical taxonomy: The principles and practice of numerical classification.* San Francisco, California: W. H. Freeman.

Sokal, R. R., and P. H. A. Sneath. 1963. *Principles of numerical taxonomy.* San Francisco, California: W. H. Freeman.

Soustelle. 1969. *Los cuatro soles. Origen y ocaso de las culturas.* Madrid: Ediciones Guadarrama.

Spranz, B. 1973. Los dioses en los códices mexicanos del grupo Borgia. Una investigación iconográfica. Mexico: Fondo de Cultura Rconómica.

Stiteler, W. M., and G. P. Patil. 1971. Variance-to-mean ratio and Morisita's index as measures of spatial patterns in ecological populations. In *Statistical Ecology,* Vol. 1, ed. G. P. Patil, Pennsylvania: Pennsylvania State University.

Stoyan, D., and H. Hermann. 1986. Some methods for statistical analysis of planar random tessellations. *Statistics*, **17** (3): 407-420.

Stoyan, D., and H. Stoyan. 1990. Exploratory data analysis for planar tessellations: Structural analysis and point process models. *Applied Stochastic Models and Data Analysis,* **6**: 13-25.

Stoyan, D., W. S. Kendall, and J. Mecke 1995. *Stochastic geometry and its applications,* second edition. New York: John Wiley & sons.

Su, T.-H., and R.-C. Chang. 1990. The k-Gabriel graphs and their applications. *Proceedings of the International Symposium SIGAL '90,* 66-75.

Su, T.-H., and R.-C. Chang. 1991a. Computing the constrained relative neighborhood graphs and constrained Gabriel graphs in Euclidean plane. *Pattern Recognition,* **24** (3): 221-230.

Su, T.-H., and R.-C. Chang. 1991b. Computing the K-relative neighborhood graphs in Euclidean Plane. *Pattern Recognition*, **24** (3): 231-239.

Su, T.-H., and R.-C. Chang. 1991c. On constructing relative neighborhood graphs in Euclidean K-dimensional spaces. *Computing*, **46**: 121-130.

Supowit, K. J. 1983. The relative neighborhood graph, with an application to minimum spanning trees. *Journal of the Association for Computing Machinery*, **30** (3): 428-448.

Tamassia, R. 1993. An introduction to Voronoi diagrams. *Lecture notes for a course on computational geometry.* www address:

Tambiah, S. J. 1969. Animals are good to think and good to prohibit. *Ethnology,* **7-8 (4)**: 423-459.

Thomas, R.W. 1977. *Introduction to quadrat analysis.* Concepts and techniques in modern geography 12, Norwich: Geo Abstracts.

Thompson, J. Eric S. 1975. *Historia y religión de los Mayas.* Mexico: Siglo XXI Editores.

Tichey, F. 1978. El calendario solar como principio de ordenación del espacio para poblaciones y lugares sagrados. *Comunicaciones,* **15**: 153-164.

Tichey, F. 1981. Order and relationship of space and time in Mesoamerica: Myth or reality. In *Mesoamerican sites and world-views*, ed. E. P. Benson, 217-245. Washington, D. C.: Dumbarton Oaks Research Library and Collections.

Tinkler, K. J. 1977. *An introduction to graph theoretical methods in geography.* Concepts and techniques in modern geography 14. Norwich: Geo Abstracts.

Tinkler, K. J. (1979). Graph theory. *Progress in Human Geography,* **3**: 85-116.

Toussaint, G. T. 1978. The use of context in pattern recognition. *Pattern Recognition,* **10**: 189-204.

Toussaint, G.T. 1980a. The relative neighbourhood graph of a finite planar set. *Pattern Recognition,* 12: 261-268.

Toussaint, G.T. 1980b. Comment to the article: 'Algorithms for computation of relative neighborhood graph' by R. B. Urquhart, *Electronic Letters*, **16 (22)**: 860-861.

Toussaint, G.T. 1980c. Pattern recognition and geometric complexity. In *Proceedings of the Fifth International Conference on Pattern Recognition,* 1324-1347.

Toussaint, G. T. 1980d. Decomposing a simple polygon with the relative neighborhood graph. In *Proceedings of the Allerton Conference*, 20-28.

Toussaint, G. T. 1985a. *Computational geometry.* Amsterdam, North-Holland: Elsevier Science Publishers.

Toussaint, G. T. 1985b. Computational geometry and morphology. In *Proceedings of the First Symposium on Science and Form* (Tsukuba, Japan), 395-403.

Toussaint, G. T. 1988. A graph-theoretical primal sketch. In *Computational Morphology,* ed. G. T. Toussaint, 229-261. Amsterdam, North-Holland: Elsevier Science Publishers.

Toussaint, G. T. 1991. Some unsolved problems on proximity graphs. In *Proceedings of the First Workshop on Proximity Graphs,* eds. D. W. Dearholt, and F. Harary, Memoranda in Computer and Cognitive Science MCCS-91-224. New Mexico: New Mexico State University, Computer Research Laboratory.

Toussaint, G.T., and R. Menard. 1980. Fast algorithms for computing the planar relative neighbourhood graph. In *Proceedings of the Fifth Symposium of Operations Research,* (Kolhn), 425-428.

Toussaint, G.T., B.K. Bhattacharya, and R.S. Paulsen. 1984. The application of Voronoi diagrams to non-parametric decision rules. *Proceedings of Computer Science and Statistics, 16th Symposium on the Interface,* Atlanta, Georgia.

Tropsha, A., R. K. Singh, I. I. Vaisman, and W. Zheng. 1995. Statistical geometry analysis of proteins: Implications for inverted structure prediction. In *Biocomputing,* eds. L. Hunter, and T. E. Klein, 614-623. Singapore: World Scientific.

Tsung-Pao Fang. 1995. Delaunay triangulation in three dimensions. *IEEE Computer Graphics and Applications,* **15** (**5**): 62-69.

Tukey, J. 1977. *Exploratory spatial data analysis.* Reading, Massachussetts: Addison-Wesley.

Unwin, D. J. 1981 *Introductory spatial analysis.* London: Methuen & Co.

Unwin, D. J. 1994. Cartography, ViSC and GIS. *Progress in Human Geography,* **18** (**4**): 516-522.

Unwin, D. J. 1996. GIS, spatial analysis and spatial statistics. *Progress in Human Geography,* **20** (**4**): 540-551.

Upton, G., and B. Flingeton. 1985. *Spatial data analysis by example. Volumen 1: Point pattern and quantitative data.* Chichester: John Wiley & sons.

Urquhart, R. 1980. Algorithms for computation of relative neighborhood graph. *Electronic Letters,* **16** (**14**): 556-557 (includes a comment by G. T. Toussaint, **16** (**22**): 860-861).

Urquhart, R. 1982. Graph theoretical clustering based on limited neighbourhood sets. *Pattern Recognition,* **15** (**3**): 173-187.

Urquhart, R. 1983. Some properties of the planar Euclidean relative neighbourhood graph. *Pattern Recognition Letters,* **16**: 317-322.

Urueta Flores, C. 1990. *Presencia del material mixteco dentro del Templo Mayor.* Thesis submitted in partial fulfilment of the requirements for the degree of Licenciado en Arqueología (i.e. Bachelor in Archaeology), Escuela Nacional de Antropología e Historia, Mexico

Velázquez Castro, A. 1999. *Tipología de los objetos de concha del Templo Mayor de Tenochtitlan.* Mexico: Instituto Nacional de Antropología e Historia.

Velázquez Castro, A. 2000. *El simbolismo de los objetos de concha encontrados en las ofrendas del Templo Mayor de Tenochtitlan.* Mexico: Instituto Nacional de Antropología e Historia, Colección Científica 403.

Vincent, P. J., J. M. Howarth, J. C. Griffiths, and R. Collins. 1976. The detection of randomnes in plant patterns. *Journal of Biogeography,* **3**: 373-380.

Vincent, P. J., J. M. Howarth, J. C. Griffiths, and R. Collins. 1977. Urban settlement patterns and the properties of the simplicial graph. *The Professional Geographer,* **29**: 21-25.

Vincent, P. J., R. Collins, J. Griffiths, and J. Haworth. (1983). Statistical geometry of geographical point patterns. *Geographia Polonica,* **45**: 109-127.

Vogt, E. Z. 1983. *Ofrendas para los dioses. Análisis simbólico de rituales zinacantecos,* (translated by S. Mastrangelo). Mexico: Fondo de Cultura Económica.

Winning, H. von. 1987. *La iconografía de Teotihuacan. Los dioses y los signos, 2 vols.* Mexico: Universidad Nacional Autónoma de México, Instituto de Investigaciones Estéticas.

Von Thünen, J.H. 1826. *Der isolierte staat in beziehung auf landwirtschaft un nationalokonomie,* Stuttgart, Gustav Fisher, (translated by C. M. Wartenburg, with an introduction by P. Hall, *The isolated state,* Oxford, Pergamon, 1966).

Voronoï, G. 1908. Nouvelles applications des paramtres continus a la theorie des formes quadratiques. Deuxieme Mémoire: Recherches sur les parallélloedres primitifs. Second partie. Domaines de formes quadratiques correspondant aux différent types de parallélloedres primitifs. *Journal für die Reine und Angewandte Mathematik,* **136**: 67-181.

Weber, A. 1909. *Über den standort der industrien.* Tubingen: Erster Teil, (translated by C. J. Friedrich, *Theory of the location of industries.* Chicago: Chicago University Press, 1957).

West, D. S., and B. von Hohenbalken. 1984. Spatial predation in Canadian retail oligopoly. *Journal or Regional Science,* **24**, (**3**): 415-427.

Whallon, R. Jr. 1973. Spatial analysis of occupation floors I: Application of dimensional analysis of variance. *American Antiquity,* **38**: 266-278.

Whallon, R. Jr. 1974. Spatial analysis of occupation floors II: The application of nearest neighbor analysis. *American Antiquity,* **39**: 16-34.

Wigner, E. and F. Seitz. 1933. On the constitution of metallic sodium. *Physical Review,* **43**: 804-810.

Wilson, A. G., and R. J. Bennett. 1985. *Mathematical methods in human geography and planning.* Chichester: John Wiley & sons.

Wilson, R. J. 1996. *Introduction to graph theory,* fourth edition. Essex: Longman.

Worboys, M. F. 1995. *GIS: A Computing perspective.* London: Taylor & Francis, London.

Yao, A. C-C. 1982. On constructing minimum spanning trees in K-dimensional spaces and related problems. *SIAM Journal of Computing*, **11**: 721-736.

Zahn, C. T. 1971. Graph-theoretical methods for detecting and describing gestalt clusters. *IEEE Transactions on Computers, Series* C, **20** (1): 68-86.